Novel high phosphate low fluoride containing bioactive glasses for hard and soft tissue repair

By

Jie Liu

Submitted in partial fulfilment of the requirements of the Degree of Doctor of Philosophy

Institute of Dentistry, Bart's and the London School of Medicine and Dentistry, Queen Mary University of London

April 2016

Statement of originality

I, Jie Liu, confirm that the research included within this thesis is my own work or that where it has been carried out in collaboration with, or supported by others, that this is duly acknowledged below and my contribution indicated. Previously published material is also acknowledged below.

I attest that I have exercised reasonable care to ensure that the work is original, and does not to the best of my knowledge break any UK law, infringe any third party's copyright or other Intellectual Property Right, or contain any confidential material.

I accept that the College has the right to use plagiarism detection software to check the electronic version of the thesis.

I confirm that this thesis has not been previously submitted for the award of a degree by this or any other University.

The copyright of this thesis rests with the author and no quotation from it or information derived from it may be published without the prior written consent of the author.

Signature:

Date:

Publications and awards

Journal publications

LIU, J., RAWLINSON, S. C., HILL, R. G. & FORTUNE, F. 2016a. *Fluoride incorporation in high phosphate containing bioactive glasses and in vitro osteogenic, angiogenic and antibacterial effects*. Dent Mater. (doi: 10.1016/j.dental.2016.07.003)

Liu J, Rawlinson SCF, Hill RG, Fortune F. *Strontium-substituted bioactive glasses in vitro osteogenic and antibacterial effects*. Dental materials. 2016;32:412-22.

A. D'Onofrio, N. Kent, S. Shahdad, R. Hill, J. Liu, S. Rawlinson. *Development of a novel Strontium containing injectable bone substitute for dental applications.* Clin. Oral Impl. Res. 25 (Suppl. 10), 2014

Fu CG, Liu J, Xia HB. *The biological characteristics of Osteopotin and its role in bone reconstruction*. Journal of Clinical Stomatology, 2012 Nov, 28(8):506-507. (*in Chinese*)

Conference publications

J. Liu, S.C.F. Rawlinson, R. Hill, F. Fortune. *Increased bioactivity in fluoride and high phosphate containing glasses and stimulation of VEGF production in MC3T3-E1 osteoblast-like cells.* Oral presentation at the 63rd, Annual General Meeting of the BSODR, 2015. Cardiff, UK.

J. Liu, S.C.F. Rawlinson, R. Hill, F. Fortune. *Novel Low Fluoride High Phosphate Bio-glasses And In Vitro Effects.* Oral presentation at IADR 93nd General Session, 2015. Boston, Massachusetts, USA.

J. Liu, S.C.F. Rawlinson, R. Hill, F. Fortune. *High phosphate, strontium-substituted bioactive glasses to enhance osteogenesis*. Presented at BORS 2014. Bath, UK

J. Liu, R. Hill, S.C.F. Rawlinson, F. Fortune. *A comparison of high phosphate bioactive glass properties in cell culture media and Tris buffer*. Presented at BORS 2014. Bath, UK

J. Liu, R. Hill, S.C.F. Rawlinson, F. Fortune. *New low fluoride, high phosphate bioactive glasses*. Presented at BORS 2014. Bath, UK

A. D'Onofrio, R.G. Hill, S. Shahdad, N.W. Kent, S. Rawlinson, and J. Liu, *Development of novel strontium containing bioglass cements for dental*

applications. Presented at IADR 92nd General Session, 2014. Cape Town, South Africa.

Manuscripts under review or in preparation

J. Liu; A. Senusi; F. Fortune, *Fatigue and quality of sleep in Behcet's Disease patients* (*in preparation*)

Awards

British Society of Dental Research (BSODR)/Johnson & Johnson bursary, 2015

Odontology section of Royal Society of Medicine (RSM) Award, 2015

Queen Mary, University of London conference studentship, 2015

The Armourers and Brasiers' Company conference grants, 2015

China Scholarship Council (CSC)/Queen Mary University of London Joint PhD scholarships, 2012

Acknowledgements

The writing of this dissertation has been the greatest endeavour so far in my life. It could not have been possible without support from many people.

First and foremost, I would like to thank my supervisors Professor Farida Fortune and Dr Simon Rawlinson for their inspiration, encouragement, patience and guidance throughout this project. I also must acknowledge and extend my gratitude to Professor Robert Hill, who so kindly provided me invaluable help for the bioactive glass studies. I acknowledge the support of my funding agencies, China Scholarship Council (CSC) and Queen Mary University of London.

I would also like to thank all the members in the department of dental physical sciences for their help with the bioactive glass studies. To all the lovely people in the centre for clinical and diagnostic oral sciences of Blizard Building, thank you for the help in cellular and bacterial experiments, and most importantly, I had wonderful time here.

I would like to thank my examiners, Professor Kevin Seymour and Dr Richard Cook, for the time they spent reading my thesis and during examination. Your constructive criticism was important and helpful.

A special thanks to all my family especially my parents and parents in-laws in China. Lastly, but definitely not least, this journey would not be a success without the two most important people in my life, my husband, Shi and my 21-month old son, Gelan (yes, you were born in November 2014 just after I entered the 3rd year of my PhD!). Thank you for all your love, patience and sacrifice.

Abstract

Bioactive glasses undergo dynamic changes *in vivo* to produce an apatite layer permitting a strong bond with living tissues including both bone and soft tissues, and their compositions can be modified and tailored. The aim of this project was to generate high phosphate low fluoride containing bioactive glasses and explore their bioactivity and biological performances *in vitro*.

Bioactive glasses (0-7% F^- content, constant 6.33% P_2O_5 in Mol.%) were produced and the particles immersed in Tris Buffer solution or cell culture medium (α-MEM) to determine apatite formation and ion (Ca, P, Si and F) release. Bioactive glass conditioned medium was used to treat pre-osteoblasts MC3T3-E1 for cytotoxicity, pre-osteogenic and pro-angiogenic responses, and to human oral fibroblasts and epithelial cells for proliferation. Antibacterial ability was explored by incubating supra- and sub-gingival bacteria with bioactive glass particulates.

Rapid apatite formation was observed in F^- containing bioactive glasses after only 2 h immersion in Tris buffer solution, while it was not detectable until 72 h in the F^- free bioactive glass. Alkaline phosphatase activity, cell number, collagen formation, bone-like mineral nodules and osteogenic gene expression of MC3T3-E1 cells were significantly promoted in low F^- bioactive glass (P6.33F1) conditioned medium. MC3T3-E1 VEGF gene expression was increased, and protein production was dose-dependently promoted with F^- containing bioactive glass conditioned medium, which also promoted human oral fibroblast proliferation, but suppressed

epithelial cell numbers. After incubation with glass particulates, the growth of *L. casei*, *S. mitis*, *A. actinomycetemcomitans* and *P. gingivalis*, was significantly inhibited; the antibacterial activity being dependent on the F^- content of the bioactive glasses.

As a potential bone graft substitute *in vivo*, such novel bioactive glasses would be expected to stimulate bone formation and overcome problems associated with infection and the poor vascularisation in large bone graft sites. Additionally, they could reduce the need for further clinical intervention, and in particular, will be advantageous for the periodontal soft tissue regeneration.

Table of contents

List of figures

List of tables

Abbreviation

ALP	Alkaline phosphatase
α-MEM	alpha-Minimum Essential Medium
CK5	Cytokeratin 5
Col1a1	Type I collagen
CPS	Capsular polysaccharide
DMEM	Delbecco modified Eagle’s medium
DMSO	Dimethylsulfoxide
Dsg3	Desmoglein-3
FAp	Fluorapatite
FBS	Fetal bovine serum
FTIR	Fourier Transform Infrared Spectroscopy
GAPDH	Glyceraldehyde-3-phosphate dehydrogenase
GTR	Guided tissue regeneration
HA	Hydroxylapatite
HCA	Hydroxylcarbonate apatite
ICP-OES	Inductively coupled plasma-optical emission spectrometry
LPS	Lipopolysaccharide
MAS NMR	Magic angle spinning nuclear magnetic resonance
NC	Network connectivity

NHOF	Normal human oral fibroblast
OCP	Octacalcium phosphate
OPG	Osteoprotegerin
OPN	Osteopontin
PBS	Phosphate-buffered saline
PDL	Periodontal ligament
ρNP	ρ-nitrophenyl
qPCR	Quantitative polymerase chain reaction
RANKL	Receptor activator of nuclear factor kappa-B ligand
SBF	Simulated body fluid
TRAP	Tartrate-resistant acid phosphatase
VEGF	Vascular endothelial growth factor
VEGFR	Vascular endothelial growth factor receptor
XRD	X-ray diffraction

Chapter 1 Literature review

For clarity, the literature reviewed in this thesis is organized from four parts to reflect the structure as well as rationale of this project. Part one provides the background information of periodontium, including soft and hard tissues. Literature presented in parts two and three provides the knowledge of periodontitis pathogenesis and periodontal regeneration. In summary, the above three sections describe the biological basis of bone grafts for periodontal defective bone repair, as well as rationale for the experimental chapters. Finally, part four focuses on the theory of bioactive glass. Specifically, the effects of phosphate and fluoride on bioactive glass structure and bioactivity as well as effects on bone biology are discussed.

1.1 Periodontium

As depicted in Fig. 1.1, the healthy periodontium comprises gingiva (overlaying epithelium and underlying connective tissues), periodontal ligament (PDL), cementum and alveolar bone (Nanci and Bosshardt, 2006). A healthy periodontium can provide tissue seals at the cervical portion of teeth, preserve the position of teeth inside the alveolar socket of maxilla and mandible, provide support to the teeth during mastication and protect the dentin and provide nourishment to teeth (Nanci and Bosshardt, 2006).

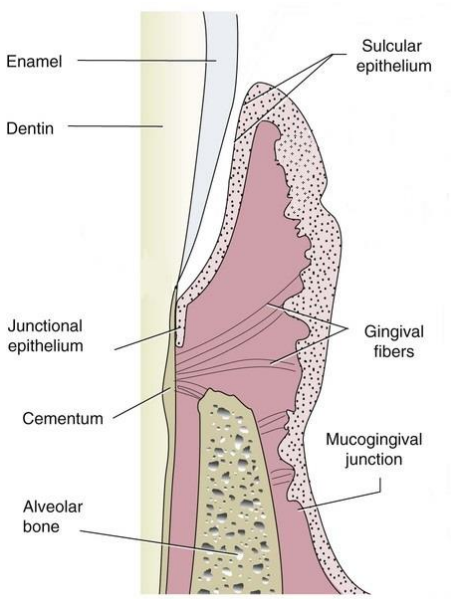

Figure 1.1 Schematic representation of the periodontium

(Taken from: http://pocketdentistry.com/2-periodontium-anatomic-characteristics-and-host-response/)

1.1.1 Gingiva

Gingiva is made up by overlying epithelium (defined as junctional, sulcular and mucogingival epithelium depends on their sites) and the underlying gingival fibres (connective tissues).

The oral gingival epithelium is the lining of the oral cavity surface being subject to wear and tear, with a deeper lamina propria (connective tissue) underneath and a basement membrane in–between (Fig. 1.2A). Histologically, oral gingival epithelium is stratified and consisted of four layers, from the bottom to superficial, namely the stratum basal (basal layer), stratum spinosum (prickle cell layer), stratum granulosum (granular layer) and the stratum corneum as shown in Fig. 1.2B.

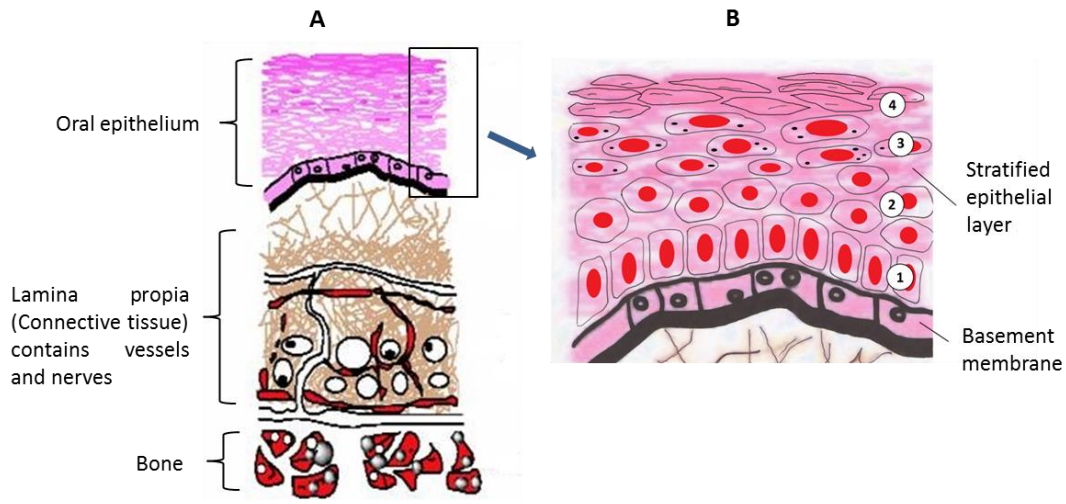

Figure 1.2 Schematic illustration of the oral mucosa layers

1: Stratum basal

2: Stratum spinosum

3: Stratum granulosum

4: Stratum corneum

(Adapted from: http://meddic.jp/lamina_propria_mucosae
and http://am-medicine.com/2014/07/oral-potentially-malignant-disorders.html)

Epithelial cells, the predominant cells in epithelium, are metabolically active and able to react to external stimulus by producing numerous cytokines, adhesion molecules, growth factors and enzymes. More importantly, they can generate a family of potent antimicrobial peptides for immunity protection against bacterial infection (Bartold et al., 2000). Other cells such as, Langerhans cells, melanocytes and Merkel cells also can be found in the basal layer of epithelium to provide immunity protection and Merkel cells form epidermal complexes named Merkel cell–neurite, which is considered to be involved in mechano-perception (Bartold et al., 2000, Horch et al., 1974).

Based on the location and composition, oral gingival epithelium can be categorized into three different types. Firstly, the mucogingival epithelium is continuous from the mucogingival junction to the gingival crest. Then, extending from the tip of gingival crest to cover the lateral wall of the sulcus is the sulcular epithelium (Schupbach and Glauser, 2007). Junctional epithelium is enclosed from the bottom of the gingival sulcus to the alveolar bone crest and provides the junction between the gingiva and the tooth by an epithelial attachment, which is a structural complex consisting of a basal lamina-like structure that is adherent to the tooth surface by hemi-desmosomes of the superficial cell layer (Nanci and Bosshardt, 2006). This structure forms an efficient barrier against periodontal pathogens and their products. It also acts as an important initiator, regulator and mediator of the host immune response against bacteria (Bartold et al., 2000).

Epithelium has a notable capacity to regenerate following injury. Within hours of gingival injury, epithelial cells from the wound margins commence migration to cover the exposed connective tissue surface under locally released stimulation factors such as epidermal growth factor, platelet-derived growth factor A and B, fibronectin and other cytokines (Green et al., 1997). Epithelial migration will continue along the surface of tooth root until collagen fibres are encountered, which is called epithelialization and explains the formation of a ‘‘long junctional epithelium’’ (Bartold et al., 2000). As epithelium migrates at a much faster rate than the formation of new connective tissue attachment to the root surface, excluding or

delaying rapid re-epithelialization forms an essential requirement to achieve periodontal regeneration.

The gingival connective tissue, also known as lamina propria, is underlying epithelium and consisting largely of collagen fibres (about 60% by volume), fibroblasts (5%), vessels, nerves, and matrix (about 35%) (Vignoletti et al., 2014, Newman et al., 2011). Type I collagen is the main collagen and preferentially organized into denser fibrils to provide the tensile strength to the gingival tissue, while type III collagen appears to be preferentially localized as thinner fibres in a reticular pattern near the basement membrane. Fibronectin, osteonectin, vitronectin, elastin and tenascin are also distributed throughout the gingival connective tissues (Steffensen et al., 1992).

Fibroblasts of mesenchymal origin play a major role in the development, maintenance and repair of gingival connective tissues. Their principal function is to synthesize and maintain the extracellular matrix components of the connective tissue. Fibroblasts are sensitive to changes in the local environment and will respond to a variety of stimuli, either endogenous (such as growth factors, cytokines and other inflammatory mediators), or exogenous (such as bacterial challenges and mechanical forces) (Bartold et al., 2000). Macrophages, mast cell, endothelial cells, polymorphonuclear leucocytes, lymphocytes and plasma cells are also present in this connective tissue.

The gingival connective tissue serves primarily to protect the tooth root surface and alveolar bone from the external oral environment. In addition,

it aids in the support and fixation of teeth within their alveolar housing and provides adequate support for the epithelial tissues.

1.1.2 Periodontal ligament

The periodontal ligament (PDL) is a specific connective tissue, which is highly cellular and vascular, situated between the cementum covering the tooth root and the bone that forms the socket wall (Nanci and Bosshardt, 2006). It is primarily composed of bundles of Type I collagen fibres namely alveolar crest fibres, horizontal fibres, oblique fibres, periapical fibres and interradicular fibres, according to their anatomic locations. The PDL is a physically small, but functionally important tissue. It forms a meshwork of interconnected fibres rather than a stretch cable-like form to support the teeth in their sockets and at the same time to permit them to withstand the considerable forces of mastication. It has the capacity to act as a sensory receptor necessary for the proper positioning of the jaws during mastication and the feelings such as pain and pressure and also to provide nutrition to the bone and the cementum (Bartold et al., 2000). In addition, the PDL is also a cell reservoir to permit tissue homeostasis, repair, and regeneration. Besides the principle fibroblasts, other cells including osteoblasts, osteoclasts, epithelial cells, rests of malassez, monocytes and macrophages, undifferentiated mesenchymal cells, cementoblasts and odontoclasts are also present (Nanci and Bosshardt, 2006).

1.1.3 Cementum

Anatomically, cementum is an integral part of the tooth firmly attached to the radicular dentin, however, it is a functional component of the periodontium (Grzesik and Narayanan, 2002). The main function is to serve as the site of attachment for PDL to the root surface (Bosshardt and Selvig, 1997). The composition of cementum is considered similar to that of bone (Saygin et al., 2000). It comprises approximately 45-50% inorganic matrix in which mainly hydroxyapatite and 50-55% organic component including collagen and non-collagenous proteins such as Type I collagen, bone sialoprotein and osteopontin (Saygin et al., 2000). Cementoblasts, cementoclasts and fibroblasts are found in cementum and responsible for the cementum formation while the regeneration of cementum in periodontal defects can be achieved by cells originating from the PDL.

1.1.4 Alveolar bone

Alveolar bone provides primary support for the teeth and constantly undergoes remodelling depending on functional stimuli. The macrostructure of alveolar bone can be considered as the thickened inner and outer dense cortical plate with less dense trabecular bone sandwiched in between. There are numerous small canals in the alveolar walls through which vessel and nerve branches can enter to supply teeth. Like other bones, alveolar bone also consists of bone matrix and bone cells.

1.1.4.1 Bone cells

There are three distinct types of bone cells: the matrix producing osteoblasts, tissue resorbing osteoclasts and osteocytes.

Osteoblasts, responsible for the synthesis and secretion of bone matrix, with characteristic morphology of protein synthesizing cells, including abundant rough endoplasmic reticulum and prominent Golgi apparatus, as well as various secretory vesicles (Florencio-Silva et al., 2015). Thus, they can regulate the mineralization process such as synthesizing tightly packed collagen to provide lattices for the growth of hydroxyapatite crystals (Kirsch, 2012). They also secrete a number of proteins such as osteocalcin, osteopotin and bone sialoprotein linked to the mineralization and maturation of bone matrix (Florencio-Silva et al., 2015).

Osteocytes are non-proliferative, terminally differentiated cells of the osteoblast lineage and reside within the bone matrix and in newly formed osteoid (Noble, 2008). They are distributed throughout the bone matrix and extensively interconnected, thus, osteocytes probably sense bone deformation and regulate osteoclast/osteoblast functions through mechanosensor action (Seeman and Delmas, 2006, Bonewald and Johnson, 2008).

Osteoclasts are derived from monocyte lineage cells and attracted to bone surfaces to fuse and form multinucleated cells to complete bone resorption (Boyce, 2013). Osteoclasts also play other roles, such as, they can regulate osteoblast precursors differentiation and, drive the hematopoietic stem cells move from the bone marrow to the bloodstream; they are also

involved in immune responses including cytokine secretion to affect their own functions and other cells in inflammatory and neoplastic processes affecting bone (Boyce et al., 2009).

1.1.4.2 Bone matrix

Organic component:

The organic matrix of bone, gives tensile strength, is secreted by osteoblasts and constitutes about 10% bone volume (Posner and Beebe, 1975). It mainly consists of collagenous proteins (up to 85-90%), which are predominantly type I collagen and some type III and V collagens (Clarke, 2008). The organic matrix also contains some non-collagenous proteins including proteoglycans, glycosylated proteins and other growth factors such as bone morphogenic proteins, osteocalcin, osteonectin, and bone sialoprotein, which contribute in bone mineralization, and remodelling (Buck and Dumanian, 2012).

Inorganic component:

The inorganic bone matrix, constitutes 90% of overall bone volume, gives stiffness to resist compression and, is considered to be the main mineral store in humans. It contains 99% of the body's calcium, 85% of the phosphorous and 40-60% of the magnesium and sodium (Buck and Dumanian, 2012). Hydroxyapatite [$Ca_{10}(PO_4)_6(OH)_2$] is the main component in inorganic matrix, with small amounts of carbonate, magnesium and acid phosphate (Clarke, 2008).

Bone remodelling is a dynamic process involving continuous removal of discrete packets of old bone, replacement of these packets with newly

synthesized matrix, and subsequent mineralization of the matrix to form new bone (Kini and Nandeesh, 2012). It is dominated by osteoclasts and osteoblasts to maintain normal physiological structure and mineral content (Das and Crockett, 2013). The bone remodelling process is composed of four sequential phases, named osteoclast activation, bone resorption, reversal phase and new bone formation, in which the remodelling sites may develop randomly but also are targeted to areas that require repair (Clarke, 2008).

1.2 Periodontitis

Periodontitis is defined by the American Academy of Periodontology (AAP) as 'Inflammation of the supporting tissues of the teeth. Usually, it is a progressively destructive change leading to loss of bone and periodontal ligament. It is an extension of inflammation from gingiva into the adjacent bone and ligament' (Barbato et al., 2015). Up to 15% of adults in the UK are estimated to have severe periodontitis, with different degrees of bone loss needing treatment (NRAS, 2014). In the FY2003 Fact Sheet, the American Association for Dental Research reports that '48% of adults aged 35 – 44 years of age have inflammation of the gingiva (gingivitis), and 22% destructive periodontal disease – a major cause of tooth loss' (Nanci and Bosshardt, 2006).

As depicted in Fig. 1.3 below, periodontitis causes irreversible damage to the supporting tissues and affects all parts of the periodontium including the gingiva, PDL, cementum and alveolar bone. This eventually leads to the loss of teeth (Bostanci and Belibasakis, 2012).

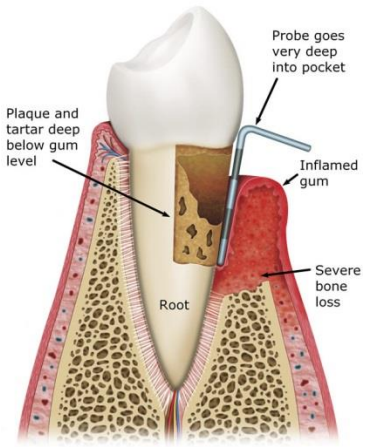

Figure 1.3 Schematic representation of periodontitis.

(Taken from: http://www.streetlanedentalimplants.co.uk/gumdisease.html)

Periodontitis can be classified into chronic and aggressive periodontitis (Armitage, 2004). Chronic periodontitis is the most common form with the following characteristics: prevalence mainly in adults; slow to moderate progression rate of periodontium destruction; major role of local factors such as plaque; smoking and emotional stress can also affect the disease characteristics; association with systemic diseases such as diabetes. Aggressive periodontitis occurs in a severe and rapidly progressing form and most often affects young adults aged 25-30 years old. It particularly affects first molars and incisors with rapid loss of clinical attachment and bone destruction and lacks of association with systemic diseases (Brigido et al., 2014, Dentino et al., 2013).

In periodontitis, the initiation and progression of periodontium destruction is related to the presence and development of a subgingival biofilm containing specific bacteria and the major pathogens including *Aggregatibacter actinomycetemcomitans (A. actinomycetemcomitans*) and *Porphyromonas gingivalis (P. gingivalis)* have been identified (Algate et al., 2015, Dentino et al., 2013). The severity and progression of periodontitis is also influenced by host factors such as genetics and oral hygiene, together with environmental factors such as smoking and diet (Jonasson and Rythen, 2016, Page et al., 1997).

A strong correlation has been established between *P. gingivalis* and periodontal disease activity in adults (Duncan, 2003). As a keystone pathogen for periodontitis, this Gram-negative anaerobe species is a late colonizer in bacterial plaque, however, it can rapidly and actively invade gingival sulcus epithelial cells, and potentially the underlying soft and hard

tissues. *P. gingivalis* can survive, replicate and disseminate from cell to cell through actin cytoskeleton bridges, and affect cell-cycle pathways after intracellular invasion (Bostanci and Belibasakis, 2012). It can block the epithelial cell interleukin-8 (IL-8) response to other oral bacteria, suggesting that the host may not detect the presence of local bacterial colonization and cannot direct leukocytes to remove them (Darveau, 2009), resulting in the rapid establishment and growth of other species found in subgingival biofilms. These properties may be among the reasons that *P. gingivalis* is so frequently associated with active tissue destruction (Page et al., 1997).

A. actinomycetemcomitans, previously known as *Actinobacillus actinomycetemcomitans*, has been frequently associated with the initiation and progression of aggressive periodontitis from longitudinal studies of both humans and animals (Fine et al., 2010). It is found in 90% of localised aggressive periodontitis and 30-50% of severe adult periodontitis (Raja et al., 2014). *A. actinomycetemcomitans* is a Gram-negative, non-motile, facultative anaerobic coccobacillus bacterium producing a variety of virulence factors to modulate the host immune system, inducing tissue destruction and inhibiting tissue repair. *A. actinomyctemcomitans* produces two important exotoxins named cytolethal distending toxin (CDT) and leukotoxin to cause death of the host tissues by blocking cell proliferation and inducing cell death (Fine et al., 2010, Raja et al., 2014, Johansson, 2011, Haubek and Johansson, 2014), In addition, leukotoxin is demonstrated to induce a substantial pro-inflammatory effect in human endothelial cells (Haubek and Johansson, 2014). *A.*

actinomyctemcomitans also can produce lipopolysaccharide (LPS) to induce the expression of membrane IL-1 in macrophages, enabling them to promote bone resorption *in vitro* (Henderson et al., 2003). In addition, *A. actinomyctemcomitans* has been reported to produce a number of, as yet unidentified, proteins with cell cycle-inhibitory activity to cause T cell apoptosis and to inhibit osteoblast proliferation and bone collagen synthesis (Raja et al., 2014, Fives-Taylor et al., 1999).

1.3 Periodontal regeneration

The ultimate goal of periodontal therapy is the regeneration of the original architecture and function of the periodontal complex including both soft (gingiva, periodontal ligament) and hard (bone, cementum) tissues (Ivanovski et al., 2014). The initial phase is aimed to eliminate infection and inflammation by removing root surface plaques and to control the bacterial infection by an effective oral hygiene programme (Garrett, 1996). However, regenerative procedures such as guided tissue regeneration (GTR) are required to regenerate the lost periodontal tissues in some cases.

Wound healing involves migration, adhesion, proliferation and differentiation of several cell types (Grzesik and Narayanan, 2002). The healing of damaged tissues depends upon two crucial factors: the availability of appropriate cell types and the presence or absence of cues and signals necessary to recruit and stimulate these cells (Polimeni et al., 2006). Due to the complex structure of periodontium, the healing outcome of periodontal regeneration will be determined by the biological environment where this healing takes place (Vignoletti et al., 2014). Fig. 1.4 represents the possible healing patterns of a periodontal wound. The healing results are dependent on the three possible cell types that predominate that wound site. The over- and down-growth of epithelial cells results in a long junctional epithelium characterized by a thin epithelium extending apically interposed between the root surface and the gingival connective tissue (Fig. 1.4 A). The excessive proliferation of connective tissues may result in connective tissue adhesion (Fig. 1.4 B). With the

over predominance of bone cells, there is root resorption and even ankyloses (Fig. 1.4 C). Therefore, as shown in Fig. 1.4 D, a regenerated periodontium develops with the ingress of periodontal ligament (PDL), perivascular cells from the bone and appropriate growth of epithelium, connective tissues and cementum (Polimeni et al., 2006).

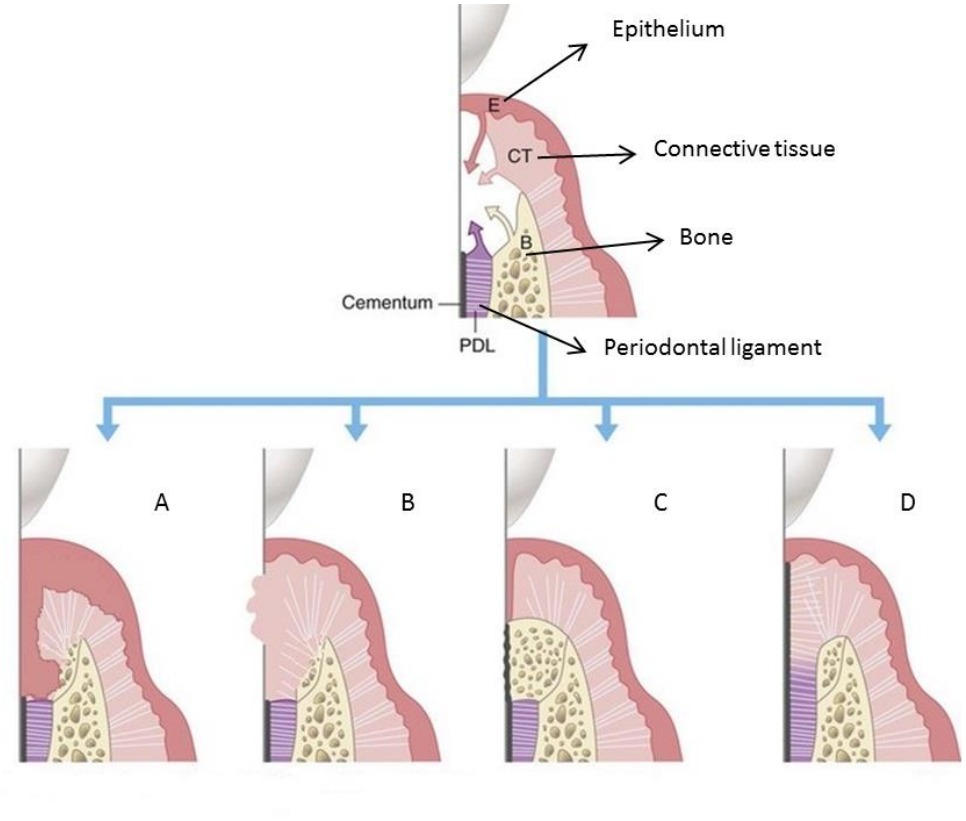

Figure 1.4 Possible healing patterns for a periodontal wound

(Adapted from http://www.dr-tlc.com/services/bone-grafting/ and http://pocketdentistry.com/61-periodontal-regeneration-and-reconstructive-surgery/)

Conventional periodontal therapies such as open flap debridement provide a critical access to detoxify root surfaces and arrest the disease process, thus, establishing an improved periodontal form favours tissue regrowth (Sam and Pillai, 2014). However, if the periodontal defect is deep and broad, it could be left empty and filled with the fast-growing epithelial cells

to form long-epithelium which prevents the bone and PDL cells to refill the pocket. Therefore, based on the above solid biologic principal, GTR technique was proposed by Melcher to selectively guide cell proliferation and tissue expansion within the tissue compartments (Melcher, 1976). It uses a membrane which covers the periodontal defect to isolate the defective area from overlying soft tissue, thus blocking fast growing soft tissue cells from invading the area and allowing cells from PDL and bone to repopulate the defective area as represented in Fig. 1.5 below (Ivanovski et al., 2014, Karring, 2000). A Cochrane review has compared the application of GTR and open flap debridement for the treatment of intra-bony defects, GTR was found to improve the relevant clinical parameters including attachment gaining, pocket depth reduction, and more gaining in hard tissue probing at re-entry (Bartold et al., 2016).

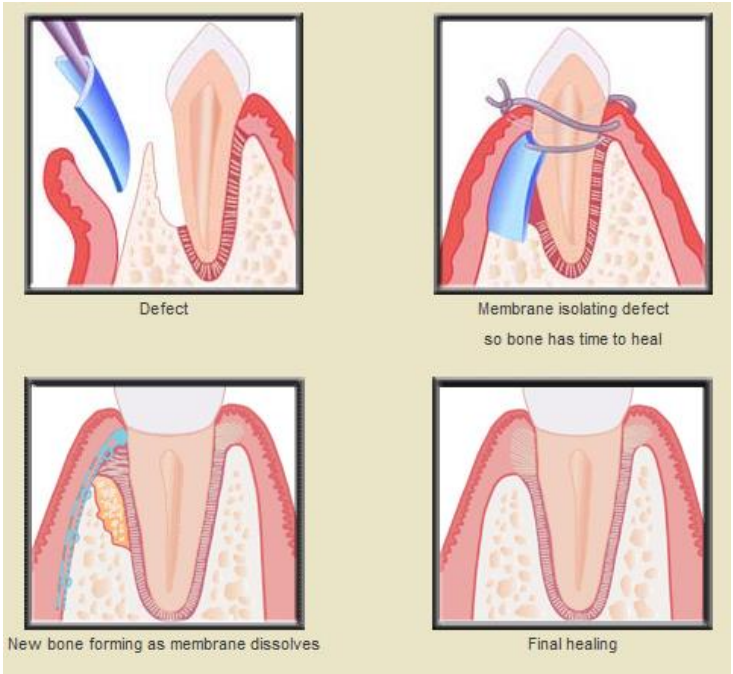

Figure 1.5 The procedure of guided tissue regeneration.

(Taken from: http://www.davidlkresedds.com/bone-and-tissue-regeneration)

There are two types of GTR membranes consisting of non-resorbable and resorbable barrier materials. The non-resorbable membranes have suitable mechanical properties to maintain the space necessary for new bone and periodontal attachment to occur (Ivanovski et al., 2014). However, a significant limitation is that a second surgical procedure is required to remove the non-resorbable barrier membrane generally four to six weeks after the surgery (Wolff and Mullally, 2000). Therefore, there has been significant interest and development of biodegradable GTR membranes which would be biologically degraded in order to negate the risk of an additional surgical procedure. The resorbable barriers mainly consist of synthetic polymers such as lactide/glycolide copolymers and natural barrier materials include those made from collagen, calcium sulphate or enamel matrix proteins (Wolff and Mullally, 2000). Due to the non-supportive structure and low mechanical properties of those resorbable materials, they are prone to collapse and adhere to what they cover, thereby losing the ability to maintain space for periodontal tissue regeneration and as a result, graft materials are often required to support those resorbable barriers (Darby, 2011). In addition, if the periodontal defect is broad, deep and complex, the effectiveness of membrane alone is limited.

Therefore, to promote more effective periodontal regeneration, the combination of bone grafts to support the membranes was developed and reported in numerous studies such as, in supra-alveolar and two wall infra-bony (missing buccal wall) defect models of periodontal regeneration, the additional use of a grafting material gave superior histological results of

bone repair to barrier membranes alone (Palmer and Cortellini, 2008). For Class II furcation defects, the addition of a bone replacement graft to the GTR procedure resulted in improved vertical probing depth reduction and attachment gain (Wolff and Mullally, 2000, Ivanovski, 2009). A Cochrane, PubMed-MEDLINE and Scopus databases study also found that the combined GTR technique with filling material and membranes obtained a greater success rate both in 4-wall lesions and in through-and-through lesions (Sanchez-Torres et al., 2014). In addition, in periodontal defects such as lesions with more than 5mm depth, lower teeth, apicomarginal and through-and-through lesions which have the worst healing prognosis, the application of bone grafting materials seem to be more necessary to maintain the space for cell repopulation and to act as osteoinductive or osteoconductive materials for the formation of host bone (Bashutski and Wang, 2009, Sanchez-Torres et al., 2014).

Autografts are considered as the ‘gold standard’, but significant drawbacks including extra painful harvest surgery, donor site morbidity and inadequate supply limit their clinical utilization. Allografts are another alternative, but sterilization process to minimize disease transmission and eliminate immunogenic factors destroys all osteogenic cells and organic factors. Xenografts are from nonhumans with sufficient supply but with greater antigenicity, more sterile processing is required and results in obviously reduced osteoinductive properties. (Lareau et al., 2015, Shibuya and Jupiter, 2015, Jakob et al., 2012, Bhatt and Rozental, 2012, Zimmermann and Moghaddam, 2011).

Therefore, the above limitations have driven the research community to investigate alternatives that incorporate the use of synthetic bone graft substitutes to improve periodontal regeneration such as simplifying the periodontal surgery process without using or minimal the GTR technique.

Jones *et al.* suggested some general criteria for an ideal bone-graft substitute (Jones et al., 2006, Jones et al., 2007): the scaffold needs to act as a template for new bone growth; resorb at the same rate as the bone is repaired, produce degradation products that are non-toxic and can be excreted easily by the body; is biocompatible and promotes cell adhesion and activity, stimulating new bone growth (osteogenesis); bond directly to the host bone, creating a stable interface; exhibit mechanical properties matching those of the host bone; can be produced into required shapes to match the irregular bone defect; has the potential to be produced commercially and sterilised to meet international standards for clinical use. Furthermore, natural bone is highly vascularized, therefore, an ideal scaffold also needs to form blood vessels to actively support nutrient, oxygen and waste transport (Bose et al., 2012). In the periodontal bony defect treatment, surrounding soft tissue reestablishment including epithelium and periodontal ligament is also required. Being an antibacterial agent to eliminate the active disease and avoid infection during or after the surgery is another important requirement.

Bioactive glasses are amorphous and biocompatible products composed of silicate, calcium, sodium and phosphorus, and are both osteocnductive and osteoionductive (Kurien et al., 2013, Nandi et al., 2010). When immersed in solution or embedded *in vivo,* they undergo ion-exchange

rapidly with the surrounding fluids to form a film of apatite layer on the surface. This layer allows bioactive glasses to bond strongly to living tissues including both bone and soft tissues and creates an enriched osteoconductive environment (Wilson et al., 1981). Active degradability is also a desired property depends on bioactive glass morphology, surface area, implantation site and composition and type (Jones, 2013). Furthermore, whether bioactive glasses take an active role in stimulating angiogenesis is also a topic of much discussion (Gorustovich et al., 2010, Keshaw et al., 2005, Day, 2005, Jones, 2013). The most important and outstanding advantage for the bioactive glass is that the chemical composition can be modified and tailored according to the specific requirements, such as to be osteoinductive, angiogenic, antibacterial and maybe to guide the periodontal soft tissue growth to improve the periodontal regeneration (Gorustovich et al., 2010, Keshaw et al., 2005, Day, 2005, Bhatt and Rozental, 2012).

1.4 Bioactive glass

1.4.1 Glass formation

A glass is defined as a vitreous state and considered to be an extremely undercooled liquid (Vogel et al., 2012). It is conventionally produced by cooling the molten liquid. As the liquid temperature decreases, its viscosity quickly increases to prevent atoms rearranging themselves into a crystalline form, as the crystalline material consists of regular and repeating units, while glassy solids have randomly arranged atoms without long-ordered patterns.

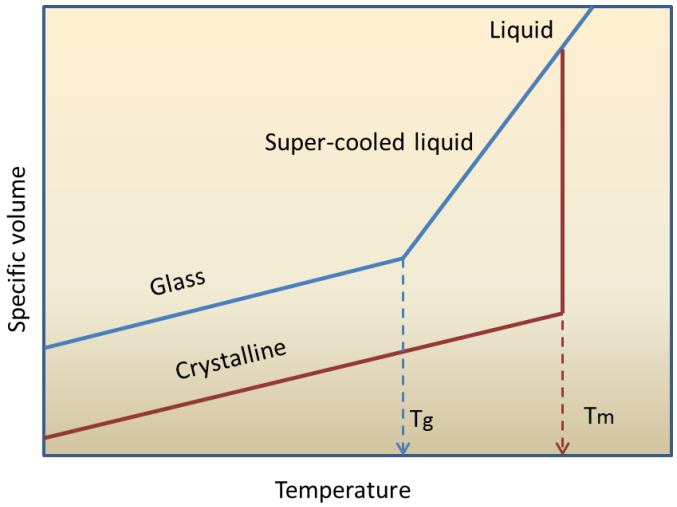

Figure 1.6 Temperature and specific volume correlation of a glass formation

Fig. 1.6 above represents the correlation of liquid, glass and crystalline states in a diagram of temperature-specific volume (volume/unit mass). If the normal molten liquid is cooled slowly, it will start to crystallize when the temperature reaches its melting point (T_m) followed by a sudden decrease in the specific volume as the crystallization occurs. In contrast, when the molten liquid is cooled quickly below its T_m, it will move into a super-

cooled state and being accompanied by a continuous specific volume change over a wide temperature range and finally transits to the glass state. The glass state-changing temperature is known as transition temperature (T_g), which is related to the energy required to break and reform covalent bonds in glasses. In silicate glasses, the T_g is not fixed and depends mainly on the glass composition, which means a more disrupted glass network with fewer covalent bonds will decrease the T_g.

1.4.2 Glass structure

In 1932, Zachariasen proposed a random network theory to explain the roles of different elements throughout a glass structure, and how they interact with each other (Zachariasen, 1932). This model can be applied to various glasses and will be described with a focus on oxide silicate glasses, especially bioactive glasses.

As represented in Fig. 1.7 below, in a two-dimensional network, the bond lengths within the polyhedra and bonding angles between the adjacent polyhedra distinguish glasses (vitreous) from crystals. In vitreous silica, there are no two atoms structurally equivalent and the atoms as well as polyhedra are arranged in an irregular manner, suggesting a glass network is not periodic or symmetrical, while the crystalline silica leads to a periodic structure. If in three-dimensional network model, oxygen atoms form tetrahedra to surround the silicon atoms and the relative orientation of two tetrahedra with a common corner will be the same throughout the entire crystalline silica. In other words, the angle between the bonds from an oxygen atom to the two neighbouring silicon atoms is the same for all

oxygen atoms. However, in vitreous silica the bond angle varies from oxygen to oxygen atom (Zachariasen, 1932).

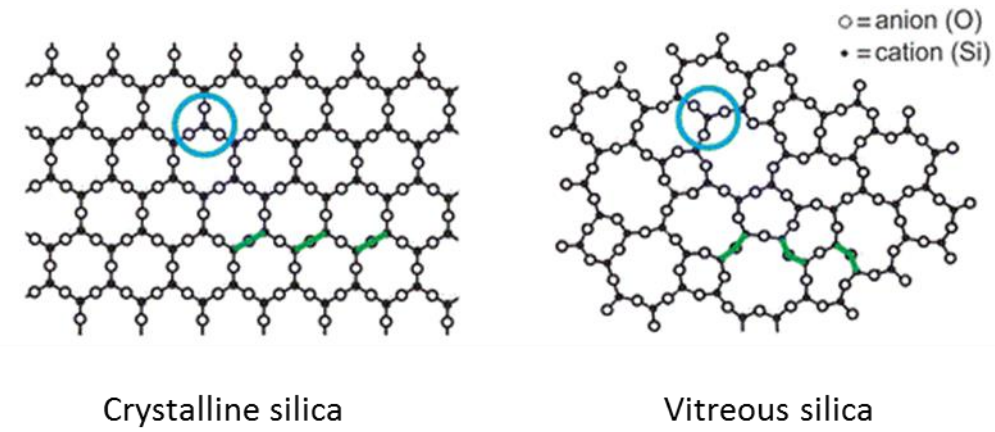

Figure 1.7 Illustrations of the structural differences between crystalline and vitreous silica. Both crystalline and vitreous structures exhibit the same building unit, marked with blue circles, but different angles between these units marked with green lines (Burson et al., 2015).

Zachariasen classified the oxides in a glass into three groups according to their roles on the glass structure (Zachariasen, 1932).

Network formers: Oxides that have the capacity to form glasses, such as SiO_2, are known as network formers. They are considered as the backbone of a glass. For example, silicate glasses are comprised of silicon polyhedra which are coordinated by oxygen atoms throughout the structure. Network forming silicon atoms are connected together via oxygen atoms known as bridging oxygen atoms (Si-O-Si) and are also co-ordinated with non-bridging oxygen atoms ($Si\text{-}O^-$) which do not link two silicon atoms together, but carry a negative charge instead. Fig. 1.8 below depicts network former atoms covalently linked with bridging and non-bridging oxygen atoms.

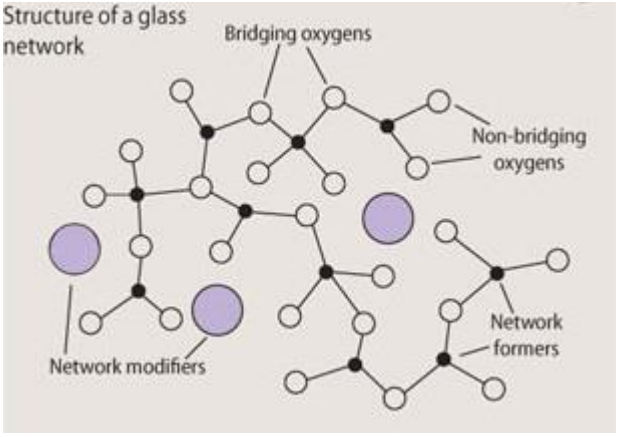

Figure 1.8 The structure of two-dimensional glass network

(Taken from: http://www.rsc.org/education/eic/issues/2006nov/glassbones.asp)

Network modifiers: Cations like Na^+ and Ca^{2+} are unable to form a continuous three-dimensional network on their own. They act to weaken the glass network by creating non-bridging oxygen atoms, to reduce the glass stability and make it more reactive. As represented in Fig. 1.9 below, when network modifier Na_2O/CaO is introduced into a silica glass, the bridging oxygen Si-O-Si bonds are broken down, and two non-bridging oxygen $Si\text{-}O^-$ bonds are formed. Then the two negative charges on the non-bridging oxygens are compensated by Na^+/ Ca^{2+} cations.

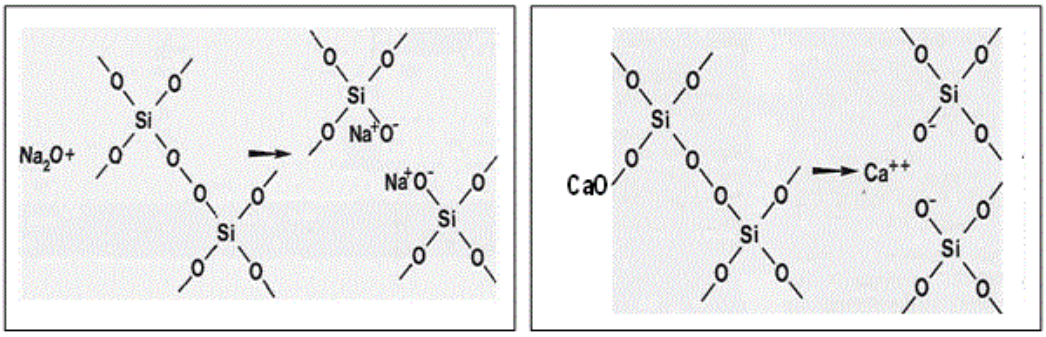

Figure 1.9 Illustration of the reaction between silica tetrahedral unit and sodium/calcium oxide (Taken from: https://digitalfire.com/4sight/education/the_chemistry_physics_and_manufacturing_of_glaze_frits_340.html)

Intermediate oxides: Intermediate oxides cannot form glasses on their own, but they can take part in the network to reinforce or weaken the glass network structure. Elements such as Al, Zn, Ti and Pb could behave as intermediate oxides. Fig. 1.10 below represents the aluminium oxide, Al_2O_3, as an intermediate oxide in a silicate glass network, where the AlO_4 tetrahedral groups can replace the SiO_4 tetrahedra.

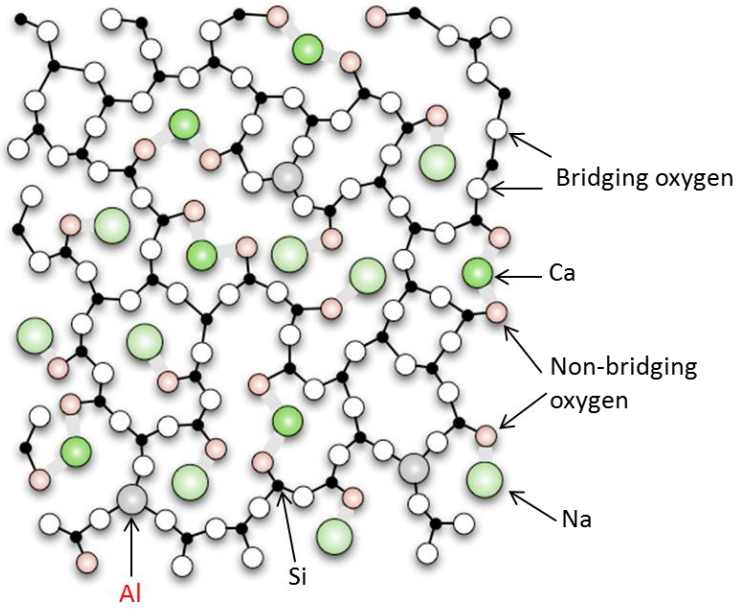

Figure 1.10 Aluminium in a silicate glass as intermediate oxide

(Taken from: http://www.chemguideforcie.co.uk/section4/learningfg.html)

Some studies found that the decreased glass transition temperature was caused by the addition of network modifiers as they disrupted bridging oxygens and opened up the glass structure (Elgayar et al., 2005, Angell, 1983, Angell, 1986). Therefore, this random network theory can be applied to explain or predict various glass properties. It can be envisaged that different numbers of bridging oxygen atoms per silicon atom can cause vast changes in the structure of the glass network. Due to the possible

variation in the number of bridging oxygen and non-bridging oxygen atoms in silicon tetrahedra, the structure of glasses is best described using the Q^n notation. It is used to describe the structure and quaternary/tetrahedral coordination of the glass network forming units. In other words, 'Q' stands for quaternary and 'n' is the number of bridging oxygen atoms per tetrahedron (Kavouras et al., 2008). This is represented in Fig. 1.11 below,

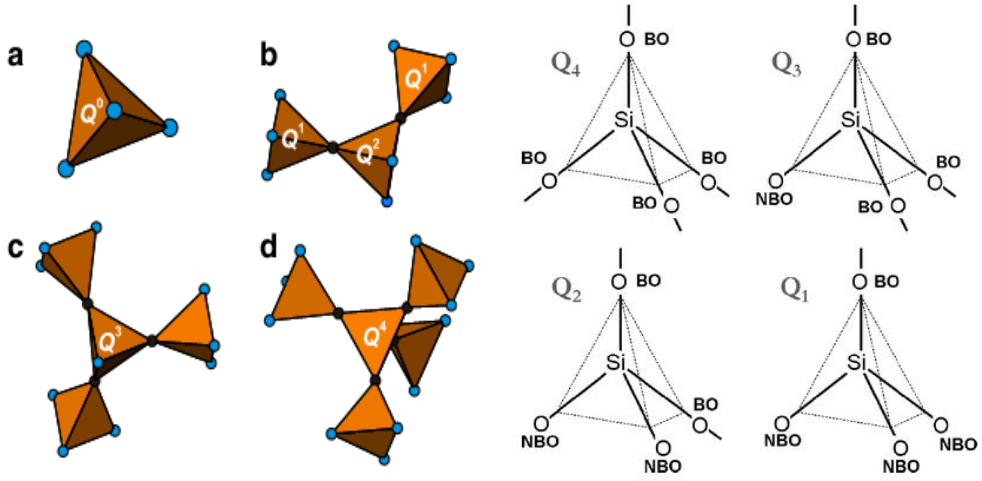

Figure 1.11 Illustration of the Q^n nomenclature for tetrahedrally coordinated silicate glass 'BO' refers to bridging oxygen atoms, 'NBO' refers to non-bridging oxygen atoms (Kavouras et al., 2008)

- Q^0 refers to a single isolated unit without any bridging oxygen atom.
- In the Q^1 structure, there is one bridging oxygen and three non-bridging oxygens in two silicon tetrahedra. It means the network former in the glass is structured so the individual units are dimers.
- In the Q^2 structure, there are two bridging oxygens and two non-bridging oxygens, which mean the network former forms long chains or possibly rings.
- In the Q^3 structure, there are three bridging oxygens and one non-bridging oxygen, which means a sheet or even a three-dimensional structure is formed.

- While in the Q^4 structure, four bridging oxygens are formed without any non-bridging oxygen. It implies three-dimensional networks.

The Q^n structure has a significant influence on the properties of the final glass. Generally, it is considered that the lower the Q structure, the higher the glass solubility. Recently, some researchers have developed a formula to deduce the average number of bridging oxygen atoms per silicon atom in bioactive glasses and apply this to theoretically determine the structure of new glass compositions, which will be discussed in section 1.4.6.

1.4.3 Bioactive glass history

The first bioactive glass was discovered in 1960s by Professor Larry L. Hench and the widely known composition, 45S5 Bioglass® (46.1 % SiO_2, 26.9% CaO, 24.4% Na_2O and 2.6% P_2O_5 in Mole), has been in clinical use since 1985 (Hench, 2006, Hench, 1988).

The development of bioactive glass was for the production of new biomaterials, and unlike the metallic and plastic materials, would not be rejected by the body. Research started in 1968 and was based on a simple hypothesis that as hydroxyapatite (HA) is the main mineral phase of bones and teeth, if there is a material that can form an HA layer on its surface, then it may not be rejected by the body, compared with the other metallic and plastic materials used at the time (Hench, 2006).

Initial research disclosed that bioactive glasses with composition of 45% SiO_2, 24.5% Na_2O, 24.5% CaO, 6% P_2O_5 (in weight) can bond to bone in an animal model and *in vitro* tests showed that the bioactive glasses developed an HA layer in a test solution which did not any contain calcium

or phosphate ions (Hench et al., 1971). The further work suggested that HA crystals were bonded to collagen fibrils layers, which were produced at the interface by osteoblasts. Therefore, a strong and firmly bonded interface was created through the chemical bonding of the HA layer to soft connective tissues as well as bone (Wilson et al., 1981). Toxicology and biocompatibility studies were also carried out to establish safety for bioactive glass products (Wilson et al., 1981). Later, in a monkey periodontal defect model, bone regeneration was sufficiently rapid by bioactive glass particulates while the encapsulation of the site by epithelial tissues was prevented (Wilson and Low, 1992).

In 1985, the first Bioglass® device cleared for commercial clinical use was a replacement for the middle ear bone to treat conductive hearing loss. It was from the ability of bioactive glass bonding with soft tissue (tympanic membrane) as well as bone tissue. The second marketed Bioglass® device was the Endosseous Ridge Maintenance Implant (ERMI®) to support labial and lingual plates in natural tooth roots and to provide a more stable ridge for denture construction following tooth extraction (Hench, 2016). Later, more commercial products were marketed such as PerioGlas to treat periodontal infra-bony defects, NovaBone as general orthopaedic bone grafting in non-load bearing sites and NovaMin for the dentinal hypersensitivity treatment (Hench, 2016, Hench and Thompson, 2010, Hench, 2015, Hench and Jones, 2015).

1.4.4 Bioactive glass structure

In 45S5 Bioglass®, SiO_2 plays the role of network former while Na_2O and CaO act as network modifiers. As shown in Fig. 1.8 and 1.9 previously,

the Na^{+} bonds with one non-bridging oxygen atom, while the 2+ charge Ca^{2+} atom forms bonds with two non-bridging oxygen atoms. This suggests that network modifiers, with different charges and ionic radii, will have significantly different effects on the structure of the bioactive glass and its properties.

However, the effect of P_2O_5 on bioactive glass structure is controversial. Previously, it was believed that phosphorus formed Si-O-P bonds to act as a part of the silicate network. However, several recent studies have shown the phosphate, instead of entering the silicon glass network, in fact separates to form an orthophosphate $(PO_4)^{3-}$ phase, which will be discussed in detail later in section 1.4.7. (Pedone et al., 2010, O'Donnell et al., 2008b, O'Donnell et al., 2008a, O'Donnell et al., 2009)

Based on Raman measurements and model studies, West and Hench suggested that ring systems may exist in the silica glass structure (West and Hench, 1995). Later, researchers explored the Q^n structure of 45S5 bioactive glass structure by X-ray and neutron diffraction with Reverse Monte Carlo Modelling and MAS NMR spectra, they found that the host silica network was consisted of chains and rings of Q^2 Si (67.2%) SiO_4 tetrahedra with some cross-linked with Q^3 Si (22.3%) species and a low quantity of Q^1 Si (10.1%) species as well (Pedone et al., 2010, FitzGerald et al., 2007, Lockyer et al., 1995), which is in relatively good agreement with the Q structure of the silica glasses.

1.4.5 Bioactive glass bioactivity

The dissolution is important to understand the bioactive glass bioactivity, which is considered the time to form apatite. The bioactive glass implants bonding ability depends on the surface reactions. It is generally presumed that for a composition to be bioactive, a layer of apatite must precipitate on the implant surface. The ability of the glass to release ions for forming apatite will determine their bioactivity. The mechanism that was proposed by Hench *et al* in 1971 has been accepted as the degradation mode of bioactive glasses (Hench et al., 1971). As represented in Fig. 1.12 below, there are five stages including three main processes: ion exchange, dissolution and precipitation (Hill, 1996, Peitl et al., 2001).

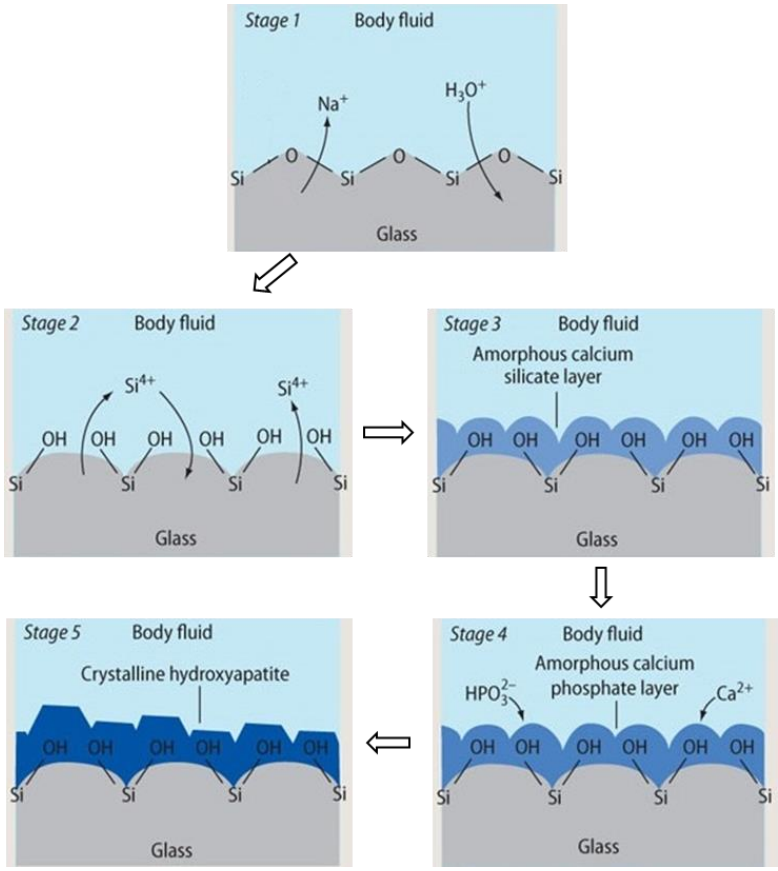

Figure 1.12 Schematic diagram of bioactive glass degradation

(Taken from: http://www.rsc.org/Education/EiC/issues/2006Nov/GlassBones.asp)

Stage 1: Na^+ atoms, from the glass, exchange with H^+ or H_3O^+ from the surrounding solution.

$$Si\text{-}O\text{-}Na^+ + H^+ + OH^- \longrightarrow Si\text{-}OH + Na^+ (solution) + OH^-$$

Rapid ion exchange occurs easily at the surfaces of bioactive glasses since Na^+ ions are network modifiers with weak bonds to glass networks. The consumption of solution H^+ results in the solution pH increase.

Stage 2: Soluble silica is released in the form of $Si(OH)_4$ and Si-OH (silanols) forms at the glass-solution surface.

$$2(Si–O–Si) + 2(OH^-) \longrightarrow SiOH + OH\text{-}Si$$

The rising solution pH and free hydroxyl ions (OH^-) allows for the catalysed alkaline hydrolysis of the network bonds Si-O-Si, resulting in the soluble silica release into solution in the form of $Si(OH)_4$ and Si-OH (silanols) forms at the glass-solution interface.

Stage 3: A SiO_2 rich layer with condensation and polymerization is formed on the surface.

$$2(Si–OH) + 2(OH–Si) \longrightarrow Si–O– Si–O– Si–O– Si–O$$

The hydrated silica (Si–OH) formed on the glass surface undergoes rearrangement by polymerization and condensation of neighbouring silanols and using out alkalis and alkaline earth cations, resulting in the formation of a silica rich gel layer.

Stage 4: Breakage of the silicate network opens the glass network which allows Ca^{2+} and PO_4^{3-} groups to migrate from bioactive glasses through the SiO_2 rich layer to the glass surface. Consequently, a $CaO\text{-}P_2O_5$ rich

film is formed on top of SiO_2 rich layer. This is followed by the growth of this amorphous layer via incorporation of soluble calcium and phosphate ions from the solution.

Stage 5: The amorphous $CaO\text{-}P_2O_5$ film undergoes crystallization by incorporating OH^- and CO_3^{2-} or F^- ions from the solution to form a mixed hydroxyl-carbonate apatite layer (HCA).

Stage 6: If the bioactive glass is inserted *in vivo* or cultured with cells, it will be incorporated with collagen produced by osteoblasts or fibroblasts and form bone with the agglomeration and chemical bonding of biological moieties within the growing HCA layer.

To conclude, the Hench mechanism gives an explanation to the bioactive glass's degradation process including how the ion exchange, subsequent apatite layer forms and even further bone formation *in vivo*. It also indirectly suggests that increasing the solubility of the glass would increase the rate of apatite formation, as the exchange of Na^+ ions at the surface of the glass initiates the bioactive glass degradation process. However, this mechanism gives no consideration on how glass composition influences apatite formation. Numerous studies demonstrate that there is a large difference in the rates of apatite formation when the glass composition is altered. O'Donnell *et al*. reported that increasing the bioactive glass phosphate content significantly accelerated apatite formation in SBF, as phosphate resides in a separated orthophosphate phase in the bioactive glass structure (O'Donnell et al., 2009, O'Donnell et al., 2008a, O'Donnell et al., 2008b). Hill suggests that for apatite formation the surrounding solution must become super-saturated with PO_4^{3-} and

Ca^{2+} ions, therefore altering the glass composition to maximize this (increasing CaO relative to Na_2O and increasing P_2O_5 content) would give a more rapid formation of apatite (Hill, 1996). Therefore, the effects of glass structure and compositions on bioactivity need to be further discussed as it is essential for designing new compositions with improved bioactivity.

1.4.6 Network connectivity

As discussed in section 1.4.4, the glass Q^n structure has a significant influence on the bioactive glass properties. Therefore, network connectivity (NC), defined as the average number of bridging oxygen atoms per silicon atom in bioactive glasses, is applied to theoretically deduce and predict the structure, reactivity, solubility, as well as the bioactivity of new bioactive glass compositions (Towler et al., 2002, Hill, 1996). For instance, for a glass with an average of two bridging oxygen atoms per silicon atom would give a NC of 2.0, three bridging oxygen atoms per silicon atom would correspond to a NC of 3.0 and so on. Therefore,

- NC of 4.0 refers to Q^4 structures like pure silica glasses (SiO_2)
- NC of 3.0 refers to Q^3 structures mainly consisted by three-dimensional structures
- NC of 2.0 refers to Q^2 structures with chains or rings of infinite molar mass
- NC < 2.0 refers to Q^1 structures varying from finite molar mass to a single unit

For the bioactive phospho-silicate glasses, Hill states that they may be regarded as inorganic polymers of oxygen cross-linked by silicon atoms (Hill, 1996). In his assumption, silicon existed as a Si^{4+} ion surrounded by four oxygens in a tetrahedral configuration. Phosphorus existed as a P^{5+} ion in the glass network and was present as PO_4 tetrahedra, in which one of the four oxygens was double bonded to the central P^{5+} ion. Therefore, the network connectivity was calculated using the following equation in the molar concentrations:

$$NC = 2 + \frac{[(2 \times \mathrm{SiO2}) + (2 \times \mathrm{P2O5})] - [(2 \times \mathrm{CaO}) + (2 \times \mathrm{Na2O})]}{\mathrm{SiO2} + (2 \times \mathrm{P2O5})}$$

However, there are flaws in this equation as it assumes that phosphate exists as part of the glass network with formation of Si-O-P bonds, which is no longer believed to be the case due to studies on the effects of phosphate to bioactive glasses (Hill and Brauer, 2011, O'Donnell et al., 2008b, O'Donnell et al., 2008a, O'Donnell et al., 2009, Aguiar et al., 2008, Mercier et al., 2011). It is pointed out that phosphate in bioactive glass exclusively exists as separated orthophosphate regardless of composition. Therefore this equation has been updated to account for the role of phosphate in the glass in the modified network connectivity (NC').

$$NC' = 2 + \frac{(2 \times \mathrm{SiO2}) - [(2 \times \mathrm{CaO}) + (2 \times \mathrm{Na2O}) - (6 \times \mathrm{P2O5})]}{\mathrm{SiO2}}$$

If the network connectivity equations are applied to 45S5 glass, a NC of 1.9 and a NC' of 2.1 can be achieved. However, FitzGerald *et al*. explored the 45S5 glass structure by ^{29}Si MAS-NMR studies and they found 45S5 glass consisted mainly of chains and rings of Q^2 SiO_4 tetrahedra, with

some degree of cross linking Q^3 units (FitzGerald et al., 2007), which is in excellent agreement with the NC' of 2.1. It shows that the concept of network connectivity can be used to supply information for the structure of glasses and can be used as a design tool for developing new glass compositions.

Edén *et al*. (Edén, 2011) suggested that a NC range between 2.0 and 2.6 was optimum for bioactivity (with NC<1.8 and NC>2.7 being described as unfavourable for increased crystallisation tendency), while the NC model by Hill (Hill, 1996) recommended an NC close to 2.0 (i.e., a silicate chain structure) and <2.4. As mentioned before, glasses with a NC of 2.0 are two-dimensional chains or rings, while the structures begin to develop into three-dimensional networks as the NC increases above 2.0. Furthermore, as described in the Hench dissolution mechanism, the glass bioactivity depends on the dissolution process at the bioactive glass surface, which allows for the apatite formation. In the two-dimensional chains, there would be a larger surface area exposure for the glass to carry out these surface dissolution processes with the living tissue. Therefore, a two-dimensional chain with loose structure and being easier to be broken down would be far more effective than the three-dimensional network. Fig. 1.13 below represents the relationship between bioactivity and NC.

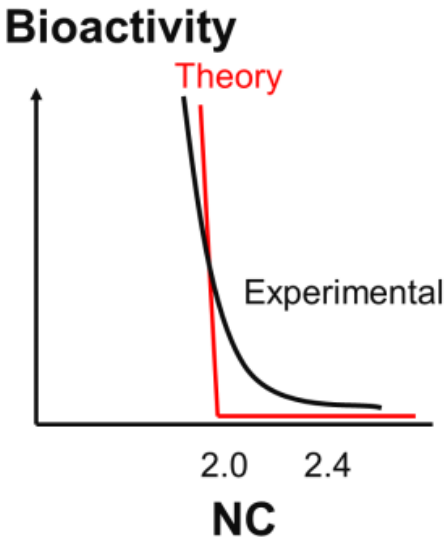

Figure 1.13 The relationship between bioactivity and network connectivity

Theoretically, the glass bioactivity changes drastically around a NC of 2.0 corresponding to Q^2 chains mentioned above. Experimentally, Hill *et al.* investigated the bioactivity by testing the apatite formation time of Magnesium (Mg) substitution bioactive glasses with NC increased from 2.17 to 2.41 in SBF (Hill and Brauer, 2011). It was found that bioactivity dropped gradually as in Fig. 1.14 below, rather than the theoretical sharp cut off in Fig. 1.13 above.

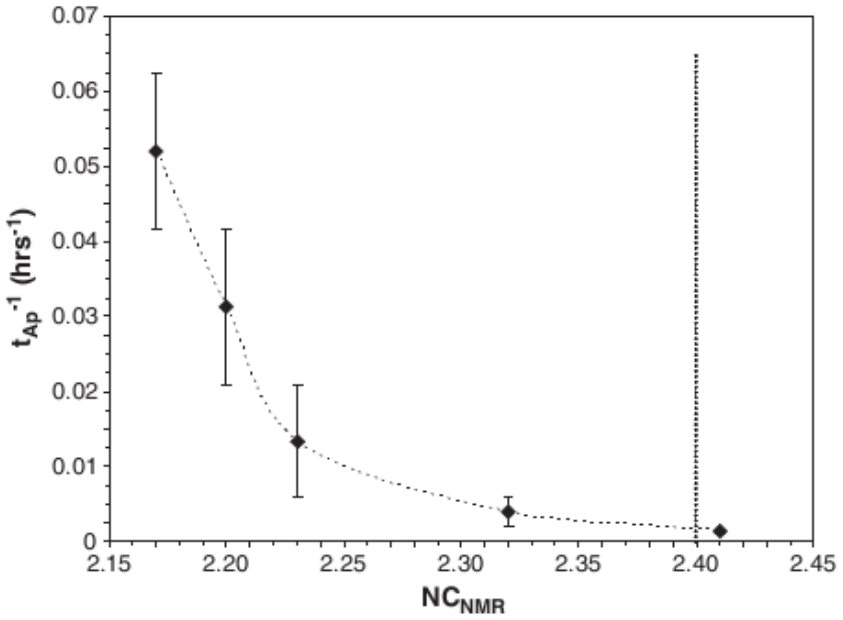

Figure 1.14 Bioactivity (defined as t_{Ap}^{-1} where t_{Ap} is the time of first apatite formation in SBF detected by XRD) of glasses vs. NC (Hill and Brauer, 2011)

In order to determine the level of glass bioactivity using this NC model, it is critical to have a structural understanding of each species within the glass. Without such knowledge, assessing the bioactive behaviour of a specific glass composition is extremely problematic. Watts *et al*. designed a series of glasses with Mg substitution, which was thought to act as a network modifier and the glass NC kept at 2.13 (Watts et al., 2010). However, ^{29}Si MAS NMR investigations showed that the actual NC increased from 2.13 to 2.41 with increasing Mg substitution. This was due to that Mg in fact acts as an intermediate, which partially enters the silicate network (forming Si-O-Mg bonds) and consumes cations to keep charge balance. It induced a more cross-linked silicate network and increased the actual NC. Therefore, in the following sections, the effects of phosphate and fluoride on bioactive glasses will be discussed.

1.4.7 Effects of phosphate

Biologically, phosphate is involved in various activities such as membrane integrity, energy metabolism, intracellular signalling and skeletal mineralization (Michigami, 2013). In the Hench degradation model, phosphate plays a vital role in bioactive glass bioactivity by forming a $CaO\text{-}P_2O_5$ rich bilayer after the leaching of Na^+ from the glass (Hench et al., 1971). This surface promotes the formation of apatite, necessary for bone tissue attachment to an implant.

Lebecq *et al*. carried out a systematic *in vitro* study on phosphorus-free glasses ($SiO_2\text{-}CaO\text{-}Na_2O$ system) and the phosphorus-containing glasses ($SiO_2\text{-}CaO\text{-}Na_2O\text{-}P_2O_5$) (Lebecq et al., 2007). Phosphate was introduced into glasses with unchanged Si/Ca and Si/Na ratios. For comparison purpose, the Bioglass® 45S5, which contains 2.6 Mol. % P_2O_5, was also studied. All the glass cylinders were embedded in epoxy resin with one unprotected surface and subsequently were immersed in SBF to observe the surface HCA layer formation. As depicted in Table 1-1, although all the glasses formed an HCA layer, the formation time was different. Phosphorus-containing glasses formed the HCA layer more rapidly, and as the P_2O_5 content increased, the HCA formation time significantly decreased.

Table 1-1 HCA formation time for phosphorus-free and phosphorus-containing glasses (Lebecq et al., 2007)

Glass Name	Mol.% of P_2O_5	HCA formation Time
A3	0	3-4 days
P2A3	2	14h
45S5	2.6	12h
P6A3	6	6h

To summarise, phosphate is necessary for the apatite formation in bioactive glasses and is also important for various biological activities. The following sections will further discuss the effects of phosphate on bioactive glass structure, bioactivity and bone biology.

1.4.7.1 Phosphate effects on bioactive glass structure

O'Donnell *et al*. investigated the structural role of phosphate in soda-lime-phosphosilicate glasses based on the 45S5 glass composition and glasses studied by Elgayar *et al.* (O'Donnell et al., 2008a, O'Donnell et al., 2008b, Elgayar et al., 2005). Two series of glasses were produced. In series I, P_2O_5 was added to the glass with a fixed Na_2O:CaO ratio (1.00:0.87). In series II, P_2O_5 was introduced while the amounts of Na_2O and CaO were adjusted to charge balance for a suspected orthophosphate (PO_4^{-3}) species being formed. Series I is a simple substitution of phosphate for silica to explore if phosphate would enter the glass network as a network former through the formation of 'Si-O-P' type bonds. Series II investigates whether phosphate would form a second and separate orthophosphate phase. Thus, the aim behind the work was to

investigate how phosphate exists in the glass structure. The glass compositions are listed below in Table 1-2.

Table 1-2 Glass compositions for series I (fixed Na_2O:CaO = 1:0.87) and II (charge balanced) (O'Donnell et al., 2008a)

ID	Mol.%				NC	NC'
	SiO_2	Na_2O	CaO	P_2O_5		
Series I						
ICIE1	49.46	26.38	23.08	1.07	2.04	2.13
ICSW2	47.84	26.67	23.33	2.16	2.00	2.18
ICSW3	44.47	27.26	23.85	4.42	1.92	2.30
ICSW5	40.96	27.87	24.39	6.78	1.83	2.44
ICSW4	37.28	28.52	24.95	9.25	1.75	2.62
Series II						
ICSW1	51.06	26.10	22.84	0.00	2.08	2.08
ICSW6	48.98	26.67	23.33	1.02	2.00	2.08
ICSW7	47.07	27.19	23.78	1.95	1.92	2.08
ICSW8	43.66	28.12	24.60	3.62	1.79	2.08
ICSW10	40.71	28.91	25.31	5.07	1.67	2.08
ICSW9	38.14	29.62	25.91	6.33	1.56	2.08

Network connectivity (NC) assuming P_2O_5 enters the glass network while modified network connectivity (NC') assuming isolated orthophosphate units

The glass structure was investigated using ^{29}Si and ^{31}P MAS-NMR, and the results are summarized in Table 1-3 below. In series I, the ^{31}P MAS-NMR spectra illustrate a chemical shift range of 8.4 to 10 ppm with an approximate constant linewidth of around 9 ppm, which corresponds to an orthophosphate structure, suggesting that phosphorus is in an orthophosphate environment. When the phosphate content increases, the ^{29}Si MAS-NMR spectra peak asymmetry became more evident and chemical shifted from -78 ppm to -81 ppm, in which the resonance at -78 ppm can be assigned to a Q^2 species and the peak at -86 ppm can be assigned to a Q^3 species. It suggests that on increasing the phosphate

content, more Na and Ca ions are required to charge balance the orthophosphate, therefore removing them from their network modifying role within the silicate network and increasing the polymerisation causing more Q^3 units to form, agreeing with the results that the NC' value increased greatly above 2.00 as the phosphate content increased.

Table 1-3 ^{29}Si and ^{31}P MAS-NMR peak positions and full width half maximums (FWHM) for glasses in series I and series II (O'Donnell et al., 2008a)

Glass	^{31}P peak (ppm)	^{31}P FWHM (Hz)	^{29}Si peak (ppm)	^{29}Si FWHM (Hz)
Series I				
ICIE1	8.4	873	-78.0	516
ICSW2	10.0	721	-79.0	683
ICSW3	9.5	721	-78.5	592
ICSW5	9.0	737	-80.0	584
ICSW4	9.0	793	-81.0	695
Series II				
ICSW6	10.7	745	-78.0	524
ICSW7	10.9	745	-78.0	516
ICSW8	10.5	769	-78.0	505
ICSW10	10.5	745	-78.0	469
ICSW9	10.9	745	-78.0	505

However, in series II, all the ^{31}P MAS-NMR spectra had a single resonance at about 10.5 ppm with a FWHM consistent with that of an orthophosphate environment (9 ppm). The ^{29}Si spectra were highly symmetrical with a single resonance centred around -78 ppm with line widths between 12 and 13 ppm in the ^{29}Si MAS-NMR spectra. The results here demonstrate that the P_2O_5 introduced into the glass exists as a separate orthophosphate phase rather than acts as network former. It also suggests that when designing a glass which incorporates P_2O_5, it should be assumed to exist as orthophosphate and therefore should be charge-

balanced. This is in agreement with other NMR and molecular dynamics (MD) work on the influence of P_2O_5 in SiO_2-Na_2O-CaO-P_2O_5 bioactive glasses (Mercier et al., 2011, Tilocca and Cormack, 2007).

Subsequently, the same authors used more conventional characterization techniques to assess physical properties, including density, thermal expansion coefficients (TEC), glass transition temperature (T_g), crystallisation temperature (T_c) and heat treated glass structure, which are important for processing promising compositions (O'Donnell et al., 2008b). Experimental values and theoretical calculated values from glass network connectivity based on glass composition were compared to validate the above MAS-NMR spectroscopy findings and further confirm the structural role of phosphate in bioactive glasses.

X-ray diffraction was applied to confirm the glassy nature of all investigated bioactive glasses. The results showed all glasses, except glass ISCW4 from series I, were amorphous. It suggests that there may be a maximum P_2O_5 addition content without glass crystallising as glass ISCW4 has the highest P_2O_5 content of all glasses at 9.25 Mol.% (O'Donnell et al., 2008b).

1.4.7.2 Phosphate effects on bioactive glass bioactivity

Bioactivity studies were carried out by O'Donnell *et al*. based on using the same two series of glasses in simulated body fluid (SBF) (Kokubo and Takadama, 2006) *in vitro* (O'Donnell et al., 2009). Glass particles with diameter < 38 μm were soaked in SBF for up to 21 days and subsequently solution pH was measured while filtered and dried glass particles were

analysed HCA layer formation by X-ray diffraction (XRD) and Fourier Transform Infrared Spectroscopy (FTIR).

In the Hench degradation model, bioactive glasses are well known to cause a pH rise upon immersion in aqueous solutions as released Na^+ exchange with H^+ or H_3O^+ from the surrounding solution, resulting in the OH^- being left. An alkali environment favours apatite deposition, but can negatively affect the surrounding tissue *in vivo.* In the study of O'Donnell *et al.* (O'Donnell et al., 2009), the results of pH change showed that, in both series of glasses, the pH increased after glass dissolution. However, as the P_2O_5 content increased, the solution shifted close to 7.3, which is optimal and advantageous in physiological fluid for apatite deposition. It could be explained that the amount of released phosphate from the glass would buffer the solution alkalinity caused by the sodium and calcium ions. At the same time, the large amount of basic ions (Na and Ca) release buffered the acidic pH caused by phosphate.

All glasses showed apatite formation after 21 days in SBF. However, the crystalline apatite formation speed was different. Table 1-4 below summarised the time for crystalline apatite formation. Generally, apatite formation was faster as the P_2O_5 content increased in both series, which indicated that in the studied glass compositions, P_2O_5 content was even more important than NC of the silicate phase for bioactivity.

Table 1-4 Time for crystalline apatite formation observed by splitting of the FTIR P–O bending mode at around 550 cm^{-1}(sample ICSW4 partially crystalline) (O'Donnell et al., 2009, Delia S. Brauer, 2008).

Glass	Mol.% P_2O_5	Time
Series I		
ICIE1	0.00	1 week
ICSW2	2.16	2 days
ICSW3	4.42	16 h
ICSW5	6.78	16 h
ICSW4	9.25	1 day[a]
Series II		
ICSW6	1.02	2 days
ICSW7	1.95	2 days
ICSW8	3.62	16 h
ICSW10	5.07	16 h
ICSW9	6.33	16 h

[a] Sample partially crystalline

On further comparison of glass ICSW9 (6.33% P_2O_5) from series II against 45S5 Bioglass® (2.6% P_2O_5), in FTIR spectra represented in Fig 1.15 below, it can clearly be seen that after 24h in SBF, the apatite formed far more rapidly on the ICSW9 glass with intense, narrow, split peaks in the 550 cm^{-1} region, whereas the phosphate peak can hardly be resolved from the background in 45S5, which further confirmed the important role of phosphate in glass bioactivity.

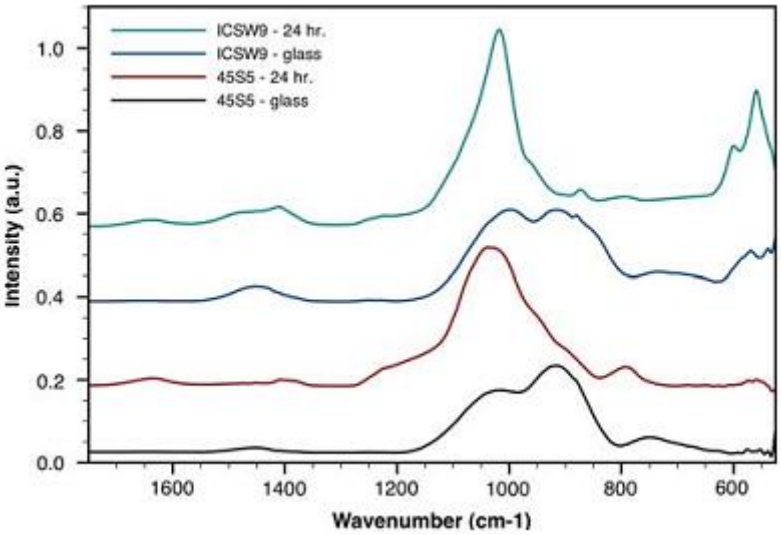

Figure 1.15 Comparison of ICSW9 and 45S5 Bioglass® by FTIR after 24 h in SBF (O'Donnell et al., 2009)

Furthermore, a crystallite size analysis, obtained from the XRD peak width and position using the Scherrer equation, showed that the size of the apatite crystallites were possibly decreased with phosphate content in series II bioactive glasses after 21 days immersion in SBF, but the total amount of crystals clearly increased evidenced from the increase in the areas of the features in the XRD and FTIR data associated with HCA crystallinity (O'Donnell et al., 2009). This result is promising, suggesting that those biomimetic crystalline apatite particles with smaller or even nano-sizes will have greater protein absorption and may encourage osteoblast attachment and proliferation *in vivo*.

1.4.7.3 Phosphate effects on bone biology

As phosphorus is present mainly in the form of HPO_4^{2-} and $H_2PO_4^-$ in serum instead of free phosphorus, it will be referred to as phosphate in this section. In human adults, phosphate is in a balance through the renal

reabsorption and intestinal absorption. Approximately 85% of the total phosphate distributes in bone in the form of hydroxyapatite crystals deposited in the bone matrix. Intracellular phosphate is around 15% of the total amount and only 0.1% phosphate is present in the extracellular fluids (Murray J. Favus, 2006), as showed in Fig. 1.16 below.

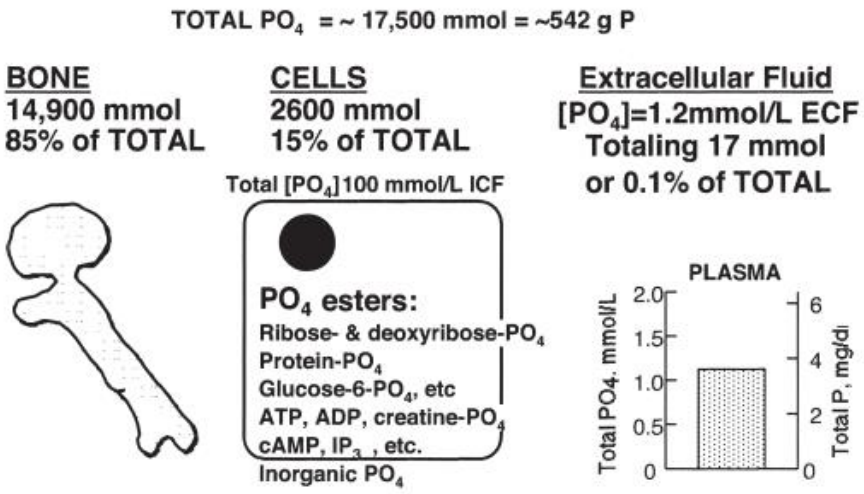

Figure 1.16 Phosphate distribution in human adults (Murray J. Favus, 2006)

Phosphate plays a vital role and is essential in the biological mineralization, which is an ongoing process accomplished by the function of osteoblasts and osteoclasts and inorganic ions calcium and phosphate, which are main components of hydroxyapatite mineral, $Ca_{10}(PO_4)_6(OH)_2$ (Beck, 2003).

Although phosphate is a necessary component of hydroxyapatite and only 0.1% exists in the extracellular fluids, it regulates various cellular functions in the skeleton and extraskeletal tissues (Michigami, 2013). In the mineralization process, active osteoblasts deposit a collagenous extracellular matrix, accompanied by the activation of related genes such as alkaline phosphatase (ALP), osteocalcin, and osteopontin. Beck *et al*.

found that a decrease in extracellular phosphate production resulted in a decreased expression of osteopontin (Beck et al., 1998). Then, they further demonstrated that osteopontin expression was strongly regulated at the RNA level in response to elevated extracellular phosphate levels (Beck et al., 2000). In addition, the same authors later pointed out that the ability of phosphate to induce osteopontin gene expression relied on the function of the phosphate transport system. The extracellular phosphate must be transported into the cell to exert its effect on osteopontin, so that the actual response is mediated by the rise in the intracellular phosphate level (Beck, 2003). Later, a range concentration of inorganic phosphate, 4-10 mM, was used to treat osteoblast cell line MC3T3-E1 to identify the effects of increased phosphate to osteoblastic differentiation. Beck *et al*. found that genes of osteoblast-related extracellular factors such as collagens, periostin, and decorin were down regulated by increased phosphate. While genes for transcription factors that may be important in the later stages of osteoblast development because in which the environment is high in phosphate were up regulated (Beck et al., 2003). Similar results were also published by other researchers (Conrads et al., 2004, Conrads et al., 2005, Hacchou et al., 2007, Ito et al., 2013, Kanatani et al., 2003, Muller et al., 2011, Usui et al., 2010). To summarise, it is indicated that extracellular phosphate acts as a specific signal that regulates the gene expression in osteoblastic cells and it is of importance to maintain the proper phosphate concentration in the extracellular environment.

1.4.8 Effects of fluoride

The addition of fluoride into bioactive glasses provides a wide range of advantages based on the characteristics of fluoride itself and the potential of forming fluorapatite ($Ca_{10}(PO_4)_6F_2$). Fluoride is well known to inhibit bacterial enzymes, prevent dental decay by inhibiting dentine and enamel demineralisation as well as enhancing remineralization (Brauer et al., 2009). It is also known to increase bone density, which results in the interest of treatment for osteoporosis (Chachra et al., 2008). Fluorapatite (FAp) is an apatite phase that is found in teeth and bones (Mojumdar et al., 2004). In oral environment, FAp has better stability and lower degradation being more acid resistant in comparison to HA, and can inhibit caries. Through occluding the dentinal tubule surfaces, fluoride can reduce tooth sensitivity (Al-Noaman et al., 2013). For these reasons, incorporation of fluoride into bioactive glasses is of great interest for the development of dental and orthopaedic applications.

1.4.8.1 Fluoride effects on bioactive glass structure

The structural role of fluoride was explored by Brauer *et al.* (Delia S. Brauer, 2008). CaF_2 was incorporated into bioactive glasses in increasing amounts, while the ratio of all other components was kept constant based on the assumption that the added fluoride species will effectively charge balance itself and will not use up network modifiers. The theoretical NC was calculated assuming fluorine complexes calcium (NC_1) or fluorine forms non-bridging fluorine attached to silicon (NC_2). The experimental glass compositions are represented in Table 1-5 below.

Table 1-5 Synthetic glass composition in Mol.% and theoretical network connectivity

Glass	SiO_2	P_2O_5	CaO	Na_2O	CaF_2	NC_1	NC_2
A	49.47	1.07	23.08	26.38	0.00	2.13	2.13
B	47.00	1.02	21.93	25.06	5.00	2.13	1.49
C	44.52	0.96	20.77	23.74	10.00	2.13	0.78
D	42.05	0.91	19.62	22.42	15.00	2.13	-0.01
E	39.58	0.86	18.46	21.10	20.00	2.13	-0.90

NC_1 calculated assuming fluorine complexes calcium, NC_2 calculated assuming fluorine forms non-bridging fluorines attached to silicon (Delia S. Brauer, 2008)

In ^{29}Si MAS NMR spectra, there was a peak at about -80 ppm corresponding to Q^2 Si units and a shoulder at about -92 ppm indicating the presence of a small number of Q^3 Si units, which was in good agreement with NC calculated to be 2.13, assuming fluorine was binding to calcium, rather than forming non-bridging fluorine attached to silicon. Furthermore, there was no change in peak position with increasing CaF_2 addition, which suggested that formation of Si–F bonds did not occur as the authors regarded, otherwise peaks would move to less negative chemical shift (towards 0 ppm) if there was formation of Si–F bonds in the glass (Delia S. Brauer, 2008). Lusvardi *et al*. also investigated bioactive glasses belonging to the Na_2O-CaO-P_2O_5-SiO_2 system and modified by CaF_2 substitution for CaO and Na_2O alternatively (Lusvardi et al., 2008). The results of molecular dynamics simulations also showed that fluoride was almost exclusively bonded to modifier cations (Ca and Na), and no appreciable amount of Si-F bonds were detected. Similar results are reported by other researchers (Al-Noaman et al., 2012, Pedone et al.,

2012). This indeed shows that adding CaF_2 whilst maintaining the ratio between pre-existing components will not alter the silicate structure.

In the ^{19}F MAS NMR spectra by Brauer *et al.*, peaks were found from -135 ppm to -120 ppm, as the CaF_2 content increased from 5 Mol.% in glass B to 20 Mol.% in glass E (Table 1-5). Generally, peaks at about -220 ppm and -108 ppm correspond to sodium and calcium fluoride, respectively (Hill et al., 2005). Thus, these signals between -135 and -120 ppm were assigned to mixed sodium/calcium fluoride species. However, it is controversial whether there is a preference for F^- bond to calcium or sodium (Stebbins and Zeng, 2000, Christie et al., 2011, Brauer et al., 2009, Lusvardi et al., 2008). Stebbins and Zeng *et al*. presented results for sodium-, potassium-, calcium-, lanthanum- and mixed cation silicate glasses, containing 1-2 wt.% fluoride through ^{19}F NMR experiments (Stebbins and Zeng, 2000), in which, they observed a preference for fluoride to bond to modifiers with higher field strengths, which is defined as the ion valence divided by the square of the bond length to its oxygen neighbour when six-coordinated. Thus, they suggested a preference for F-Ca (the Ca field strength is 0.33) over F-Na (the Na field strength is 0.19) interactions in F-containing bioactive glasses. However, the NMR study, Car-Parrinello molecular dynamics (CPMD) simulations and molecular dynamics simulations based on SiO_2-Na_2O-CaO-P_2O_5-CaF_2 bioactive glasses by other researchers suggested that almost all fluoride atoms were associated with both sodium and calcium, and no preference for fluoride to coordinate to either Na or Ca was observed (Christie et al., 2011, Brauer et al., 2009, Lusvardi et al., 2008).

Furthermore, the glass transition temperature (T_g) decreased with increasing CaF_2 content, compared with fluoride-free glasses (Brauer et al., 2009, Al-Noaman et al., 2012, Delia S. Brauer, 2008). This was explained due to the fact that fluorine was complexing calcium. As represented in Fig. 1.17 below, in fluorine-free glass, Ca^{2+} ions bind to silicate anions by electrostatic forces and the Ca^{2+} ions act as ionic bridges between two non-bridging oxygens. When CaF_2 is added, hypothetical CaF^+ species are added to the silicate ions, which reduce the electrostatic forces between non-bridging oxygens considerably and results in a decrease in Tg.

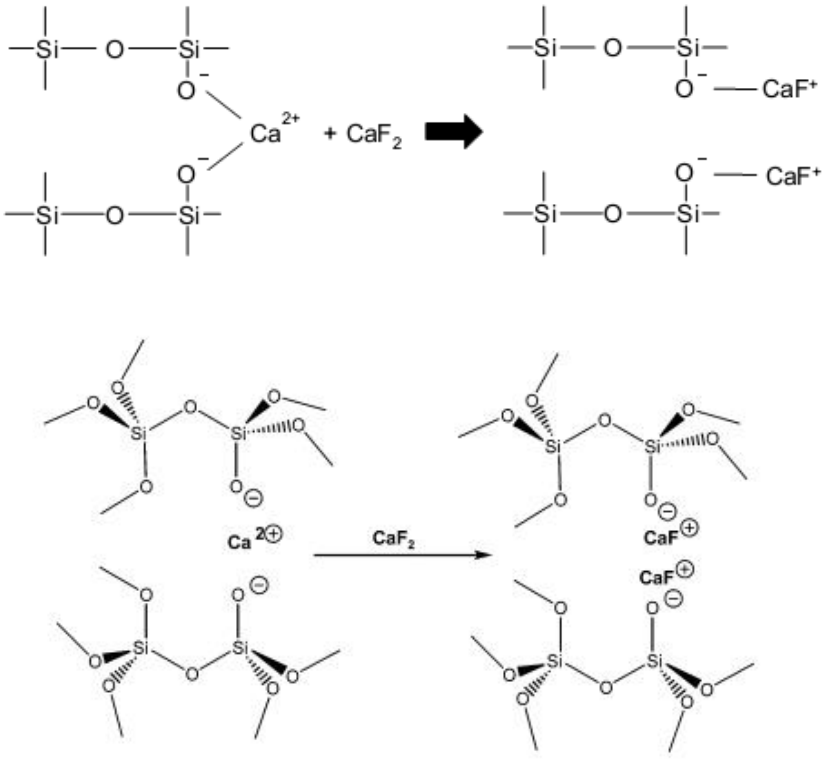

Figure 1.17 Illustration of the hypothetical effect of CaF_2 addition on silicate network (Brauer et al., 2009, Delia S. Brauer, 2008)

To summarise, fluoride is readily incorporated into bioactive glasses. It is complexed with calcium and sodium rather than forming Si-F bonds, which

results in decreasing the compactness of the glass network. By keeping the ratio of network former to network modifier constant when adding CaF_2, the silicate structure and network connectivity will not be altered.

1.4.8.2 Fluoride effects on bioactive glass bioactivity

Bioactivity studies were also carried out by Brauer *et al*. using similar bioactive glasses with more extensive fluoride incorporation (Table 1-6) in SBF (Brauer et al., 2010).

Table 1-6 Synthetic glass composition in Mol.% and theoretical network connectivity (NC)

Glass	SiO_2	P_2O_5	CaO	Na_2O	CaF_2	NC
A	49.47	1.07	23.08	26.38	0.00	2.13
B	47.12	1.02	21.98	25.13	4.75	2.13
C	44.88	0.97	20.94	23.93	9.28	2.13
D	42.73	0.92	19.94	22.79	13.62	2.13
E	40.68	0.88	18.98	21.69	17.76	2.13
F	36.83	0.80	17.18	19.64	25.54	2.13
G	33.29	0.72	15.53	17.75	32.71	2.13
H	44.88	0.97	44.87	0.00	9.28	2.13

It was found that the solution pH increased during the first 3 d immersion and then kept constant over the remaining 2 weeks of the experiment. However, as a function of CaF_2 content in glasses (Fig. 1.18 below), increased fluoride incorporation resulted in a solution pH decrease from 8.03 to 7.83 after immersing for 1 w. Similar results were reported by Al-Noaman *et al*. in Tris buffer solution (CaF_2 content was 0-13% in Mole) (Al-Noaman et al., 2012).

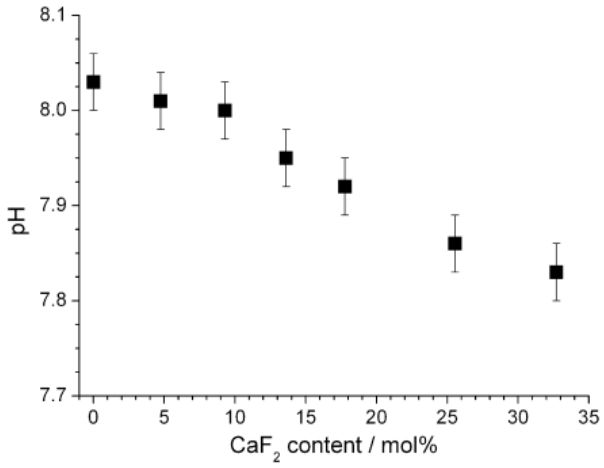

Figure 1.18 pH of SBF vs. CaF_2 content in the glasses at 1 week immersion (Brauer et al., 2010)

As the above pH rise was less pronounced with increasing fluoride content and formation of apatite is strongly pH dependent (Lu and Leng, 2005b), the authors expected that the apatite deposition in SBF would decrease with increasing fluoride content in the glass. However, after 1 week immersion in SBF, all glass compositions showed apatite formation with characteristic peaks at approximately 560 cm^{-1} in FTIR spectra in comparison to the spectrum of the unreacted glass. And the characteristic phosphate peak was more pronounced with increasing fluoride content (Brauer et al., 2010). This suggests that additions of fluoride affect apatite formation in SBF.

Lynch *et al*. carried out work on multi-component bioactive glasses (SiO_2-P_2O_5-CaO-CaF_2-SrO–SrF_2-ZnO-Na_2O-K_2O) with increasing CaF_2+SrF_2 content (0 - 32.7 Mol.%), and found that the fluoride-containing bioactive glasses formed apatite as early as 6 h, while the fluoride-free control did not form apatite within 7 days (Lynch et al., 2012). It also suggests fluoride addition significantly improved apatite formation of the bioactive glasses.

As the XRD patterns of hydroxyapatite (JCPDS 09-432), fluorapatite (15-876), carbonated hydroxyapatite (JCPD 19-272) and carbonated fluorapatite (JCPDS 31-267) are very similar, Brauer *et al*. applied ^{19}F MAS–NMR to further clarify fluoride contents in the glass result in formation of FAp rather than HCA (Brauer et al., 2010). After SBF treatment for 2 weeks, all fluoride containing glasses showed a prominent feature between -101 and -107 ppm, which were assigned as an overlap between fluorapatite (-103 ppm) and fluorite (-108 ppm). Furthermore, Rietveld analysis was used to plot the results for relative amounts of crystal phases, and it is found that sigmoidal curves of increasing relative amounts of fluorite with increasing CaF_2 content in the glass, while the relative amount of apatite decreased. It can be explained that there are low phosphate contents (1.07 Mol.% or less) in this series, which favours formation of CaF_2 rather than apatite, as there is an excess of calcium and fluoride ions but not enough phosphate.

It is attractive in the glass B (lowest CaF_2 content, 4.75% in Mole), as the XRD traces represented in Fig. 1.19 below, the apatite peaks at 1 week were even less pronounced than at 3 days, which was explained by the researchers that due to a lower initial pH of the SBF (7.24 instead of 7.27) and the solution pH was at around 8.05 at 3 days, dropped to 8.0 at 1 week and increased to 8.05 again at 2 weeks. The authors then suggested that this glass composition was very susceptible to slight pH changes and formation of apatite in SBF is strongly pH dependent (Brauer et al., 2010).

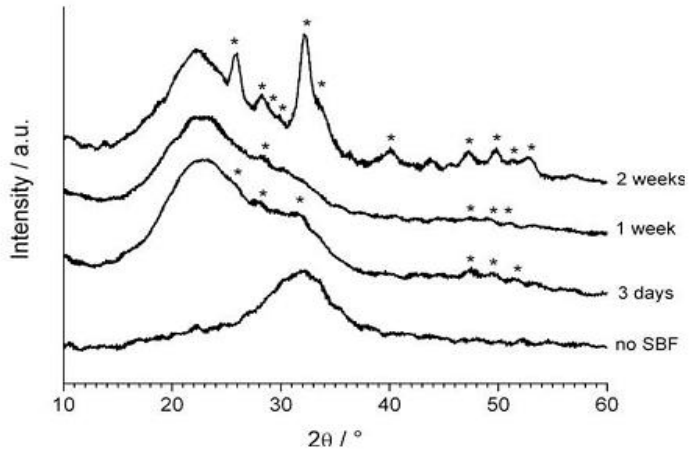

Figure 1.19 XRD patterns of untreated glass B (bottom) and after immersion in SBF for 3 days, 1 week and 2 weeks. Crystal phase in XRD pattern is apatite (*) (Brauer et al., 2010)

However, Shah *et al*. later investigated the dissolution behaviour of a series of fluoride-containing bioactive glasses (0, 4.75%, 9.28% and 17.76% CaF_2 contained) under physiologically relevant conditions of low pH (acetate-buffered MEM, pH was adjusted to 4.80) (Shah et al., 2014a). It was found that despite the pH remaining below 6 throughout the study, bioactive glasses partially dissolved and formed fluorapatite with the fluoride incorporation and subsequent release, which suggested that these fluoride containing bioactive glasses also formed apatite even at low pH conditions.

Later, in order to further explore the effects of surrounding solution characteristics such as pH, composition and presence of proteins on glass dissolution and apatite formation, Shah *et al*. investigated the dissolution behaviour of a fluoride-containing bioactive glass in different solutions as showed in Table 1-7 below (Shah et al., 2014b). After immersion for 1 w, surprisingly, apatite formation was the fastest in acetate buffered MEM (A-MEM), which had the lowest pH among the four solutions. It is known that

an alkaline environment favours apatite formation (Lu and Leng, 2005a), therefore, Shah *et al*. suggested that a high pH is not necessary for the formation of FAp as it is considered to be more stable at low pH conditions than HAp or HCA.

Table 1-7 Compositions of investigated solutions (HEPES refers to 4-(2-hydroxyethyl)-1-piperazinee-thanesulfonic acid) (Shah et al., 2014b)

Test medium	Stock MEM	Buffer	Serum	Final pH
Acetate medium (A-MEM)	Carbonate free (CF-MEM)	20 mL, sodium acetate buffer solution, pH 4.6	None added	4.80
HEPES medium (H-MEM)	Carbonate free (CF-MEM)	20 mL, 1 M HEPES buffer solution	None added	6.60
HEPES carbonate medium (HC-MEM)	Carbonate supplemented (CS-MEM)	20 mL, 1 M HEPES buffer solution	None added	7.40
HEPES serum medium (HS-MEM)	Carbonate supplemented (CS-MEM)	20 mL, 1 M HEPES buffer solution	100 mL fetal bovine serum	7.30

In addition, the authors also found that presence of carbonate resulted in formation of calcite (calcium carbonate). The apatite formation was significantly delayed by the existence of serum proteins (Shah et al., 2015). These results suggest that in exploring bioactivity of a material, the solution composition and properties are important and need to be taken into consideration, in particular when studying the bioactive glasses in culture.

1.4.8.3 Fluoride effects on bone biology and microbiology

Fluoride, an element that occurs naturally in the human diet, is found in water sources, daily foods and also biologically available in the human body and approximately 99% fluoride of the total body content is retained in the bones (Aaseth et al., 2004). The physiological concentration in saliva is about 1 µM (Dogan et al., 2002).

Generally, fluoride interacts with mineralized tissues in a biphasic manner (Chachra et al., 2008, Aaseth et al., 2004). At low doses, it is passively incorporated into the minerals such as bone and teeth to form FAp, which has better stability than the mineral HA against dissolution. This has promoted the application of fluoridated water to reduce dental caries incidence. At low dose fluoride is mitogenic and plays positive effects to bone cells, improve the mineralized tissue amount and structure as well as the interface between the collagen and mineral, which is the principle for fluoride use in osteoporosis treatment. High dose fluoride induces occurrence of skeletal and dental fluorosis, which is characterized by debilitating skeleton and increased fracture risk as well as marked mottling and discoloration in the teeth and even increased wear in the enamel.

Several clinical trials demonstrated the positive effect of fluoride salts on bone mass in osteoporosis (Caverzasio et al., 1998, Riggs et al., 1990, Bernstein and Cohen, 1967, Bernstein and Guri, 1963, Epker, 1967, Menczel, 1964). Its actions on bone appear to be mediated at several levels.

For bone matrix, fluoride is incorporated into bone mineral during the dynamic bone remodelling process. The hydroxyl group (OH^-) in hydroxyapatite ($Ca_{10}(PO_4)_6(OH)_2$) is replaced by fluoride to form fluorapatite ($Ca_{10}(PO_4)_6F_2$), which makes the crystal lattice more compact and stable (Grynpas, 1990). It was highlighted that the fluoride substitution for hydroxyl group would not be completed in therapeutic fluoride concentrations, the replacement was only about a third of the hydroxyl ions (Boivin et al., 1989). Research carried out by Moreno *et al*. demonstrated that a mixture of FAp and HA would be more stable against dissolution than either component individually (Moreno et al., 1977). However, extensive substitution of hydroxyl groups with fluoride is required to generate skeletal fluorosis, when the bone deposits exceed a threshold of about 0.6% of bone ash, which is characterized by an augmentation in trabecular bone volume with a parallel increase in osteoid volume, often leads to recurrent bone fractures, or micro-fractures (Aaseth et al., 2004).

For bone cells, Farley *et al*. firstly reported the direct effects of fluoride on osteoblastic cell activity (Farley et al., 1983). In micro-molar concentrations (2.5-25 μM), fluoride increased the proliferation and alkaline phosphatase activity of bone cells derived from chick embryonic calvaria. Similar results were reported in human bone cells as well (Wergedal et al., 1988). However, negative results were reported later (Kopp and Robey, 1990, Chavassieux et al., 1993). Kopp and Robey tested the effect of fluoride, in doses ranging from 10^{-6} to 10^{-3} M, on first passage human osteoblastic bone cells derived from collagenase-treated

trabecular bone fragments. No promotion on cell proliferation was detected. It was explained that fluoride did not act *in vitro* upon differentiated osteoblastic bone cells derived from adult human patients, which was confirmed by the study carried out by Kassem *et al*. (Kassem et al., 1994). The effects of NaF were compared on more differentiated human osteoblast-like (hOB) cells derived from trabecular bone explants and on osteoblast committed precursors derived from human bone marrow, human marrow stromal osteoblast-like (hMS(OB). It was found that NaF at concentration of 10^{-5} M increased proliferation, alkaline phosphatase activity, pro-collagen type I and osteocalcin levels of hMS(OB) cells but not hOB cells. Wider fluoride concentrations were investigated by Qu *et al.* via using caprine (goat) osteoblasts (Qu et al., 2008). They found NaF at concentrations of 10^{-8} to 10^{-5} M promoted cell proliferation, ALP activity and mineralization, whereas at 10^{-4} to 10^{-3} M it suppressed cell proliferation and induced apoptosis. These results suggest that fluoride may act differently to various osteoblastic cells, depending upon concentration (micro-molar to milli-molar) and cell types and source (animal and site). As to the mechanisms of fluoride action on osteoblastic cells, Huo *et al*. suggested that BMP/Smad signalling pathway was involved in the fluoride-induced promotion of osteoblastic cell viability and differentiation (Huo et al., 2013). By examining the effect of NaF concentrations (10^{-6} - $5x10^{-4}$ M) on osteoblast proliferation, cell cycle, apoptosis, oxidative stress, and the level of insulin-like growth factor-I (IGF-I), Wang *et al*. found that all the tested fluoride concentrations inhibited osteoblast proliferation and arrested cell cycle at S phase, which

was attributed to decreased IGF-I expression and increased oxidative stress damage (Wang et al., 2011). Similar results were reported by Yang *et al.* and they linked the increased fluoride-induced osteoblastic apoptosis to altered expression of Bcl-2 family members, which are key regulators of the mitochondrial response to apoptotic signals and control the release of pro-apoptotic proteins (Yang et al., 2011). Ren *et al*. reported that in osteoblast-like MC3T3-E1 cells, NaF affected the OPG/RANKL/RANK system, which is important in maintaining the balance between bone formation and resorption (Ren et al., 2011).

For osteoclasts, Okuda *et al*. analysed the effects of NaF on the activity of isolated rabbit osteoclasts via culturing cells on thin slices of bone and quantifying osteoclastic resorption by counting the resorption lacunae number and measuring their surface area and depth using scanning electron microscope (SEM) (Okuda et al., 1990). It was found that NaF at modest concentrations of 0.5-1.0 mM was inhibitory. Similar results were reported in osteoclasts isolated from chick long bones with a NaF concentration at 15 mg/L (approximately 0.8 mM) (Taylor et al., 1989). Biphasic effects of fluoride on osteoclasts have been reported as well (Taylor et al., 1990). It was found that NaF at concentration of 15-30 mg/L inhibited osteoclast activity, while at low dose (approximately 1 mg/L), NaF promoted osteoclast function. Recently, in an *in vivo* model revealed that fluoride at concentrations, 5 and 50 ppm in drinking water, slowed the rat alveolar bone repair (Fernandes et al., 2012). For the molecular mechanism of fluoride to osteoclasts, Pei *et al*. revealed the nuclear factor

of active T cells c1 (NFATc1) and its downstream genes may be involved (Pei et al., 2012).

While NaF may increase bone mass, it is pointed out that the newly formed bone appears to lack normal structure and strength (Carter and Beaupre, 1990, Riggs et al., 1990, Sogaard et al., 1994, Everett, 2011). Studies of 15 osteoporosis patients with sodium fluoride therapy, Aaron *et al*. found a marked increase in trabecular bone volume (43%), which was attributed to an increase in trabecular thickness (46%) rather than strut number. There were no significant changes in the trabecular bone surface, number and the ratio of bone volume/trabecular width after fluoride treatment (Aaron et al., 1991). Similar observations were found in rats as well (Sogaard et al., 1995, Turner et al., 1995). These results suggest that fluoride increases the bone mass but may reduce bone quality.

Besides the ability to form FAp, to reduce demineralisation as well as enhance re-mineralization and to bring positive effects on bone, fluoride is also known for highly effective anti-microbial properties (Burke et al., 2006, Bradshaw et al., 1990). It affects bacterial metabolism through a spectrum of actions with fundamentally different mechanisms (Marquis, 1995, Marquis et al., 2003). Firstly, fluoride can act directly as a bacterial enzyme inhibitor, such as inhibiting the glycolytic enzyme enolase in an irreversible manner. In addition, fluoride can bind directly to heme then inhibits the heme-based peroxidases of bacteria. Another action involves the formation of metal-fluoride complexes, most commonly AlF^{4-}, which interact with bacterial proton-translocating F-ATPase and nitrogenase enzymes, mimicking phosphate to form complexes with ADP at the

enzyme reaction centres and resulting in bacterial activity inhibition. In the cariogenic dental plaque, fluoride weak-acid character is the most pertinent action. It enhances the bacterial membrane permeability to protons and compromises the F-ATPases function in exporting protons, thereby inducing cytoplasmic acidification and acid inhibition of glycolytic enzymes (Marquis, 1995). Therefore, it is an important player to reduce the bacterial acid tolerance. Marquis *et al.* found that fluoride at levels as low as 0.1 mM can cause complete arrest of glycolysis by intact cells of *S. mutans* (Marquis, 1995). Overall, the antibacterial effects of fluoride appear to be complex, involving both direct and indirect actions on bacteria.

Fluoride is widely used to modify biomaterials. *In vitro* and *in vivo* studies were carried out by Cooper *et al*. and they found fluoride ion modification of the TiO_2 grit - blasted surface enhanced osteoblastic differentiation and interfacial bone formation (Cooper et al., 2006). Another fluoride implant study revealed that after 8-weeks' healing, at the bone - implant interface, the pull-out, volumetric bone mineral density and osteoblast gene expression such as osteocalcin, runx2 and collagen type I gene expression were higher in fluoride implants, while the inflammation markers (TNF-a and IL-6) and osteoclast gene expression (TRAP) decreased (Monjo et al., 2008). In another fluoride containing bioactive glass study, they showed promotion in osteoblast proliferation, differentiation and mineralization as well (Gentleman et al., 2013). F surface-modified titanium specimens significantly inhibit the growth of both *P. gingivalis* and *A. actinomycetemcomitans* compared with the polished

titanium (Yoshinari et al., 2001). Rostami *et al.* investigated the antibacterial ability of bioactive glasses and they found the fluoride containing ones had significant antibacterial activity against *E. coli*, *P. aeruginosa* and *S. aureus*, which are responsible for most infections, while the fluoride-free bioactive glass samples did not show any antibacterial activity (Rostami et al., 2015).

Therefore, combining the positive effects of fluoride on bioactive glass structure and bioactivity, in particular, on bone formation and being antibacterial, it is rational and of importance to develop low fluoride containing bioactive glasses. During the bioactive glass synthesis, fluoride is incorporated mainly in the form of CaF_2, as apatite contains Ca^{2+} and it is suggested that the surrounding solution must become super-saturated with PO_4^{3-} and Ca^{2+} ions for rapid apatite formation (Hill, 1996). Thus, the addition of CaF_2 not only brings fluoride but also calcium, in which the biological performance of released Ca^{2+} cannot be ignored.

In a normal individual, Ca^{2+} in the blood is maintained at consistent levels (~1.4 mM) (Hofer, 2005). Changes in extracellular Ca^{2+} concentrations affect osteoblast function, bone remodelling and contribute to systemic calcium homeostasis including the intracellular calcium, which is a ubiquitous second messenger responsible for numerous cellular processes such as fertilization, mitosis, neuronal transmission, muscle contraction and relaxation, gene transcription and cell death (Valério et al., 2007). Such as, human osteoblast-like cells showed different responses of the intracellular calcium concentration to changes of the extracellular calcium concentration (Habel and Glaser, 1998). Foetal rat calvarial cells

were treated with a narrow range of Ca^{2+} concentrations ($CaCl_2$, 0.5–3 mM) and responded in a time- and concentration-dependent manner including the promotion of differentiation and mineralized bone nodule formation (Dvorak et al., 2004). When designing calcium phosphate-based scaffolds for bone tissue engineering, Liu *et al*. suggested that cellular Ca^{2+} level must be taken into consideration, as they found that the ALP activity, Type I collagen formation and osteocalcin mRNA expressions reached the highest level with a 1.8 mM Ca^{2+} concentration, however, the above cellular activities were significantly decreased as the Ca^{2+} concentration rose from 1.8 to 7.2 mM (Liu et al., 2009). Valerio *et al*. also reported that after treatment with a range of Ca^{2+} concentrations (100-500 mg/L), the rat osteoblast cellular viability was not altered up to 300 mg/L (7.5 mM) and decreased thereafter (Valerio et al., 2004). Thus, combining the benefits of other ions such as silicon, bioactive glass (BG60S) ionic products with a released Ca^{2+} concentration around 50 mg/L significantly increased osteoblast proliferation, in addition, the Ca^{2+} from BG60S dissolution triggered further mobilization of intracellular Ca^{2+} and may alter osteoblast glutamate release, which is important in neurotransmitter in mechano-sensitivity (Valério et al., 2007, Valerio et al., 2009). Therefore, although calcium is important in bioactive glass structure and apatite formation, it is biological performance also needs to be considered.

1.5 Hypothesis and aims

Synthetic biomaterials are an alternative clinical strategy for autografts to repair the defective bone tissues. To obtain a favourable biological outcome, ideally these synthetic grafts should emulate the chemical and physical structure of the native bone tissue, as well as being osteoinductive for the bone-forming cells, angiogenic for the vessel growth, display antibacterial ability and be non-toxic for the surrounding tissues. Due to the complex structure of periodontium, a GTR technique with combined bone grafts and bioresorbable membranes is applied for periodontal regeneration, to block the fast growing soft tissue cells from invading the defective area and allowing cells from PDL and bone to repopulate the periodontal defects (Ivanovski et al., 2014, Karring, 2000).

Bioactive glasses have been widely studied for their specific clinical applications due to their significant advantages such as promoting HA layer on their surface and bonding with the surrounding living tissues including both bone and soft tissues, being osteoinductive and degradable, in addition, their compositions can be modified and tailored depend upon the requirement.

Therefore, the strategy adopted in this work in order to achieve the above requirements was to consider the effect of bioactive glass compositions on material properties and biological performances, especially the effect on periodontal soft tissues to guide favouring unimpeded healing and improve periodontal regeneration such as simplifying the periodontal surgery process without using or minimal the GTR technique.

The aim of this thesis is to understand modified chemical compositions (high P_2O_5 content and varied low fluoride addition) on characteristic properties of a base bioactive glass (SiO_2-P_2O_5-Na_2O-CaO), including pH change, ion release and apatite formation in Tris Buffer solution. Novelty and contribution to knowledge is gained through relating the observed bioactivity change in Tris buffer with the results in cell culture medium and, investigating the effects of modified bioactive glass conditioned medium on pre-osteoblast cells (osteogenic and angiogenic responses), human fibroblasts and epithelial cells. An investigation of the bioactive glass antibacterial potential on both supra- and sub-gingival pathogens is also presented.

1.5.1 Objectives

1) To document the effects of fluoride on pre-osteoblasts (MC3T3-E1), human oral fibroblasts and epithelial cells

2) To design and produce bioactive glasses with high phosphate and varied low fluoride content (P_2O_5 content will be kept constant at 6.33%, while F will increase from 0% to 7% in Mole)

3) To experimentally characterise the bioactive glass properties in Tris Buffer solution and cell culture medium (α-MEM), including pH change, apatite formation and Ca, Si, P, Na and F release

4) To assess the cytotoxicity of bioactive glass conditioned medium

5) To further assess the effect of bioactive glass conditioned medium (72 h immersion) on cellular response, including osteogenic and angiogenic

potential in pre-osteoblasts and proliferation in human oral fibroblasts and epithelial cells

6) To quantify the antibacterial activity of bioactive glass particulates on supra- and sub-gingival pathogens

1.5.2 Thesis outline

Relevant background literature is discussed in Chapter 1, including periodontium, periodontitis, periodontal regeneration and bioactive glass theory, in which the effects of phosphate and fluoride on bioactive glasses and bone biology are discussed. The aims as well as outline of this thesis are also presented in Chapter 1.

Chapter 2 represents the experimental work and techniques. Chapters 3 - 6 focus on the *in vitro* results of the novel low F^-/high P_2O_5 bioactive glasses. The rate of pH change, apatite formation and ion release in both Tris buffer solution and cell culture medium (α-MEM) are assessed in Chapter 3. Whether this bioactive glass could be used to regulate local bone turnover and potentially alleviate problems such as osteoporosis and complex bone defects, an investigation of the effects of F^- and bioactive glass conditioned medium on pre-osteoblasts (MC3T3-E1), including osteogenic and angiogenic responses is represented in Chapter 4. To further explore the potential application for periodontal soft tissue regeneration, the cytotoxicity and proliferation of F^- and bioactive glass conditioned medium on human oral fibroblasts and epithelial cells are reported in Chapter 5. Chapter 6 assesses the antibacterial activity of bioactive glass particulates on supra- and sub-gingival pathogens.

The overall project conclusions and recommended future work are discussed in Chapter 7.

Appendix at the end provides more knowledge of bone biology and oral microorganism.

Chapter 2 Materials and methods

2.1 Diagram of experimental plan

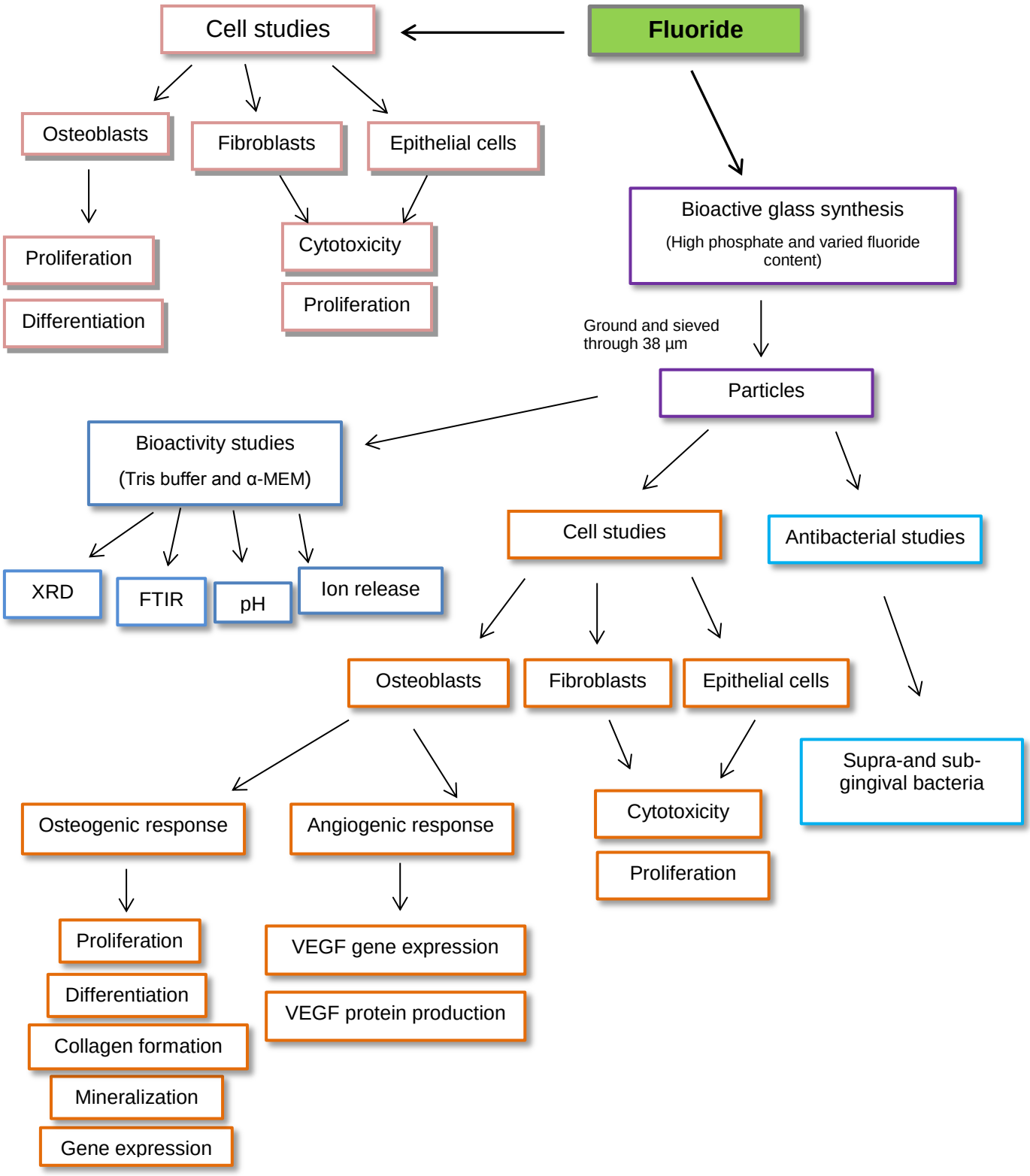

2.2 Cell culture

2.2.1 Cell lines and culture conditions

2.2.1.1 Osteoblast cell line

MC3T3-E1 is a pre-osteoblast cell line established from mouse calvaria with osteogenic potential to differentiate into osteoblasts and osteocytes and, has been demonstrated to form calcified bone tissue *in vitro* (Wang et al., 1999, Jeong and Jeong, 2016). In this study, MC3T3-E1 cells were maintained in alpha-Minimum Essential Medium (α-MEM) supplemented with 10% fetal bovine serum (FBS), 1% antibiotic (penicillin and streptomycin), 1% L- glutamine (all from Invitrogen, UK) and incubated at 37 ºC, 5% CO_2 atmosphere. Medium were changed every 3 days to maintain cell cultures.

2.2.1.2 Epithelial cell line

The A431 cell line is used as an epithelial cell model derived from an epidermoid carcinoma in the vulva of an 85-year old female. These cells are morphologically similar to normal differentiated squamous epithelial cells (Brown et al., 2014). They were cultured in an incubator at 37 ºC, 10% CO_2 atmosphere in Delbecco modified Eagle's medium (DMEM) with 10% FBS, 1% antibiotic and 1% L-glutamine.

Recently, human oral epithelial primary cells have been marketed from a commercial company (Celprogen, USA). They are derived from oral cavity epithelia tissue and were cultured in an incubator at 37 ºC, 10% CO_2

atmosphere with extra-cellular matrix pre-coated flasks in specific medium, human oral epithelial cell culture complete medium (Celprogen, USA).

2.2.1.3 Fibroblasts

NHOF-1 is a fibroblast strain prepared from human normal oral mucosa tissue samples by Professor E Ken Parkinson group (Queen Mary University of London) (Lim et al., 2011). They were cultured in an incubator at 37 ºC, 10% CO_2 atmosphere in DMEM with 10% FBS, 1% antibiotic and 1% L-glutamine.

2.2.2 Cell passage

At 80-90% confluence, cells were passaged and split in a ratio of 1:3. After two washes with phosphate-buffered saline (PBS), 2 ml trypsin/EDTA (Lonza, UK) was added to cells grown in T75 plastic tissue culture flasks. Cells were incubated at 37 ºC with trypsin/EDTA for approximately 5 min until completely detached from the flasks. Once cell attachment was dissociated, 8 ml growth medium containing serum was added, in which the serum was required to deactivate the proteolytic activity of trypsin. Cell suspension was then transferred to a conical centrifuge tube and centrifuged at 800 rpm for 5 min to pellet cells. The supernatant was carefully removed and cells were re-suspended in fresh growth medium supplemented with 10% FBS. An aliquot of the cell suspension was seeded into new flasks containing growth medium.

2.2.3 Cryopreservation and recovery of cell stocks

For cryopreservation, cells were grown to 80-90% confluence as previously described in cell passaging. However, in this case the cell

pellets were re-suspended in Freeze down medium (FDM) (10% DMSO in FBS). Aliquots of 1 ml suspensions were transferred to 2.5 ml cryovial and frozen down to -80 ºC in a freezing container filled with Isoproponal. Cells were stored at -80 ºC for 48 h before transferred to liquid nitrogen for long-term storage. The use of FDM and Isoproponal filled freezing container is to ensure temperature reduces in a controlled manner (1 ºC/min), which protects cells against intracellular and extracellular ice formation and dehydration occur during the freeze down stage of cryopreservation.

For the recovery of frozen aliquots, cryovials were removed from liquid nitrogen and immediately placed in a 37 ºC water bath until completely thawed. Then vials were cleaned with 70% Industrial methylated spirit (IMS) and cell suspension aliquots were added to culture medium and transferred to conical centrifuge tube. Cells were centrifuges for 5 min at 800 rpm to pellet the recovered cells. The supernatant was carefully removed and cells were re-suspended in fresh growth medium supplemented with 10% FBS in T75 flasks.

2.3 Cellular response to F^- concentrations

2.3.1 Osteoblasts

2.3.1.1 Cell differentiation by quantitative alkaline phosphatase (ALP) activity assay

Alkaline phosphatase (ALP) is a membrane enzyme localized to the outer surface of cells through a phosphatidylinositol-glycolipid anchor (Harrison et al., 1995). In bone, it is produced by osteoblasts and deposited in matrix (Christenson, 1997). During the bone formation phase, ALP is produced in

extremely high amounts and considered as an indicator of early stage osteoblast differentiation (Whyte MP, 1983).

An enzyme histochemical assay with good analytical sensitivity is widely used for ALP activity measurement *in vitro* (Lee et al., 2013, Ma et al., 2013b, Sun et al., 2013), in which ALP converts ρ-nitrophenyl phosphate into soluble yellow coloured ρ-nitrophenyl (ρNP) (Fig. 2.1). Afterwards, the intensity of yellow coloured reaction product ρNP is quantified by measuring the absorbance at 405 nm.

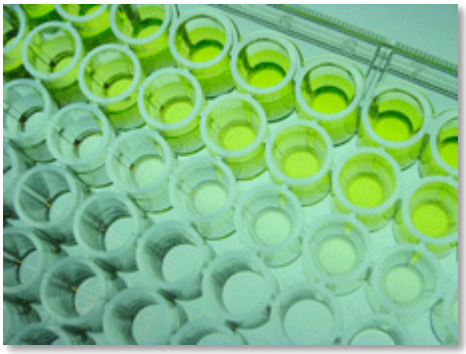

Figure 2.1 The soluble yellow coloured reaction product ρNP

A standard curve (Fig. 2.2), demonstrates a linear relationship between absorbance and known amounts of ρNP, is used to determine the quantity of ρNP generated by ALP in the cells. Then ALP activity of the test samples can be calculated and expressed as nmol/ml/min (Lim et al., 2014):

$$ALP\ activity\ (nmol/ml/min) = A / V / T$$

Where:

A is amount of ρNP generated by samples (in nmol).

V is volume of sample added in the assay well (in ml).

T is reaction time (in minutes)

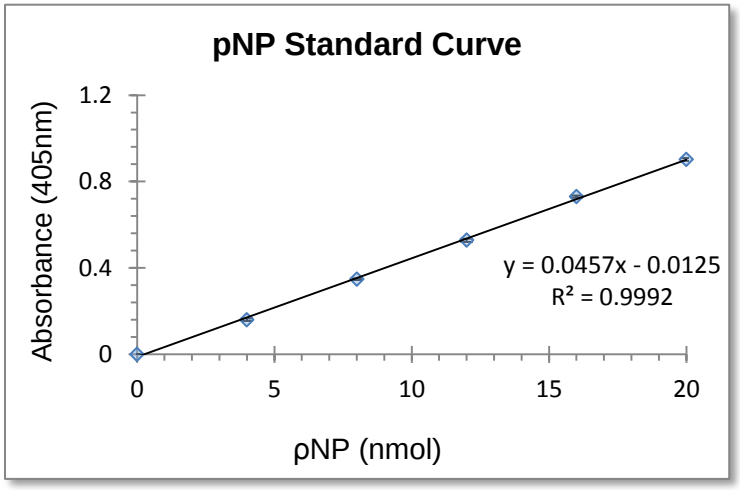

Figure 2.2 ρNP standard curve. The standard curve is constructed by adding 0, 4, 8, 12, 16 and 20 nmol pNP standard solution in a 96-well plate. Tris-buffer and 0.5 M NaOH are added to bring a final volume of 200 µl in each well. Absorbance is measured at 405 nm. Each marker represents mean ± S.E.M of eight independent experiments.

To investigate the effects of fluoride on MC3T3-E1 differentiation, cells were seeded at a density of 3000 cells/cm^2 in 96-well plates and allowed to attach for 24 h in α-MEM containing 2% FBS. Then cells were treated for 4, 7 and 10 days with various concentrations of NaF (F- concentrations: 0, 0.1, 1, 1.9, 9.5, 19ppm) (Sigma, UK) supplemented to the growth medium, which consisted of α-MEM with 5% FBS.

At each time point, medium was removed and cells were washed twice with PBS. After that, wells were emptied and plates inverted on tissue paper before being stored in the freezer until all samples collected. Cells were lysed through a freezing and thawing process and reacted with a solution of 2.5 mg/ml 4-Nitropheyl phosphate disodium salt hexahydrate in Tris buffer solution with 1 mM $MgCl_2$ (pH = 9.5, all from Sigma, UK) for 40 min in 37 $^{\circ}$C. 0.5 M NaOH was used to stop the reaction and the intensity of yellow colour reaction product was quantified by measuring the

absorbance at 405 nm and ALP activity of the test samples were calculated and expressed as nmol/ml/min. For each experimental group, ten wells were assessed under the same condition.

2.3.1.2 Cell proliferation by quantitative DNA content assay

Determining DNA quantity with the fluorochrome bisbenzimidazole (Hoechst 33258) is a well-established, simple, sensitive and inexpensive method to estimate mononuclear cell number. (Rago et al., 1990). It is based on the increased fluorescence intensity of the fluorochrome Hoechst 33258 upon binding cellular DNA. The reaction is highly specific and other cellular components such as RNA and proteins do not cause significant fluorescence intensity change.

In this assay, it is vital to make the fluorochrome come into contact with the cellular DNA. Labarca *et al.* found that higher fluorescence yield was observed in the presence of high salt concentrations, which may be caused by improved DNA dissociation, resulting in more DNA binding site exposure for the binding of dye (Labarca and Paigen, 1980). Therefore, incubation with hypotonic distilled water and freezing are used to lyse cells and produce a relatively homogenous crude cell extracts. Afterwards, the fluorochrome bisbenzimidazole (Hoechst 33258) in a high salt TNE buffer (10 mM Tris, 1 mM EDTA, 2 M NaCl, pH 7.4) is added to the lysed cells in 96-well plates, which are measured for the fluorescence intensity at 355 nm emission and 460 nm excitation on a plate reader. This allows accurate determination of cell number by comparing fluorescence intensity

with an established standard curve, which is a linear correlation between fluorescence intensity and the cell number over a broad range (Fig. 2.3).

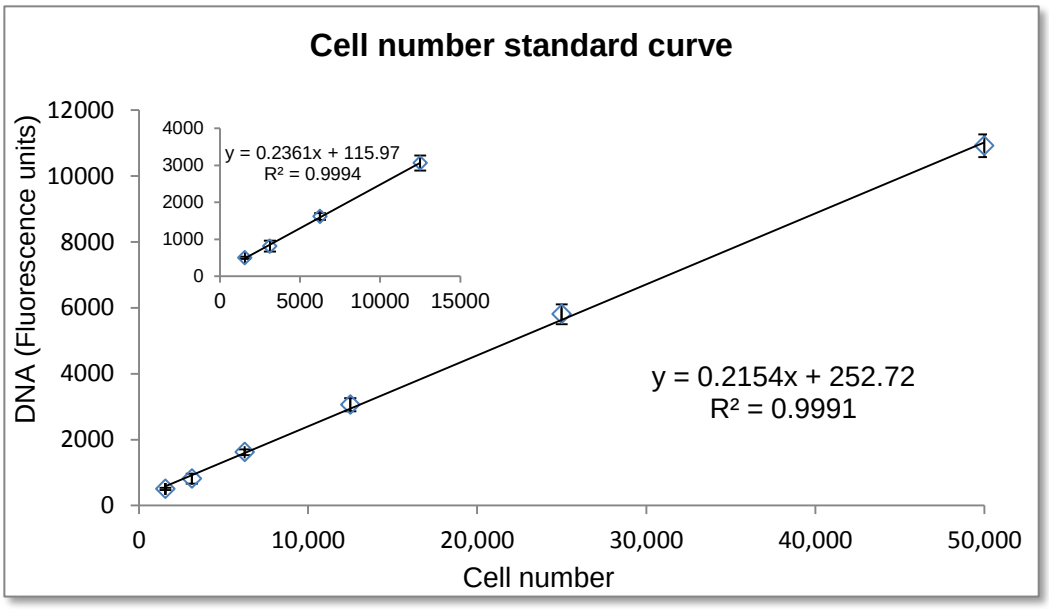

Figure 2.3 Cell number standard curve for MC3T3-E1 cells. 1500-50,000 cells, using Hoechst 33258 after lysis by brief incubation in distilled water and freezing. Insert shows a second cell standard assay for 1000-10,000 cells. Fluorescence is expressed as arbitrary units. Each marker represents mean ± SE of eight independent experiments

For the effects of fluoride on MC3T3-E1 proliferation, cells were treated as those in the differentiation (ALP) assay. At each time point, medium was removed and cells were washed twice with PBS, emptied by inversion and then stored at -20 $^{\circ}$C freezer. After 24 h, wells were incubated with 100 µl deionized water at room temperature for 2 h and returned to the freezer for another 24 h. This progress ruptured the cells and released DNA. Subsequently, the reactive mixture was made by adding fluorochrome bisbenzimidazole (Hoechst 33258) to TNE buffer buffer (10 mM Tris, 1 mM EDTA, 2 M NaCl, pH 7.4) in a volume ratio of 1:50. 100 µl reactive mixture was added to each well and the product fluorescence intensity was measured in the plate reader. The accurate cell number was

determined by comparing fluorescence intensity with the known cell number standard curve. For each experimental group, ten wells were assessed for each same condition.

2.3.2 Epithelial cells and oral fibroblasts

2.3.2.1 Cytotoxicity by MTT assay

MTT assay is a technique for measuring the living cells activity to determine the cytotoxicity of drugs at different concentrations *in vitro* (van Meerloo et al., 2011, Plumb, 2004, Carmichael et al., 1988, Ciapetti et al., 1993, Marks et al., 1992).

Viable cells with active metabolism convert the yellow tetrazolium MTT (3-[4, 5-dimethylthiazol-2-yl]-2, 5 diphenyl tetrazolium bromide) into a purple coloured formazan product, while the dead cells do not have this ability. Then the purple formazan crystals can be solubilised in DMSO and the formazan concentration is detected by measuring absorbance spectra using a plate reader at 570 nm. Thus, colour formation is considered as a useful and accurate marker of the viable cells and the increase or decrease in cell viability could be detected by measuring the absorbance at 570 nm with validity in various cell lines (Mosmann, 1983). However, the exact cellular mechanism of MTT reduction into formazan is not well understood. Some researchers attributed it to the mitochondrial activity as mitochondrial dehydrogenases of viable cells cleave the tetrazolium ring, yielding purple formazan crystals (Riss et al., 2004, van Meerloo et al., 2011).

Thus, to investigate the toxicity of F^- concentrations on epithelial cells and fibroblasts, A431 and NHOF-1 were seeded at a density of 3000 cells/cm^2 in 96-well plates and allowed to attach for 24 h in DMEM containing 2% FBS. Then cells were treated for 1, 3 and 5 days with various concentrations of NaF (F^- concentrations: 0, 0.1, 1, 1.9, 9.5, 19 ppm).

At each time point, medium was removed and cells were washed twice with PBS. 30 µl MTT solution (5 mg/ml in PBS) was added to each well and the cells were incubated in 37 ºC for 4 h. After that, DMSO was added to dissolve the formed formazan crystals (100 µl/well). The intensity of purple colour reaction product was quantified by measuring the absorbance spectra at 570 nm in a plate reader. The final data was normalised with the control and presented in percentages.

2.3.2.2 Cell proliferation

A431 and NHOF-1 were treated with NaF concentrations (F^-: 0, 0.1, 1, 1.9, 9.5, 19 ppm) for 4 d, 7 d and 10 d. Then the cell number was investigated as previously done for MC3T3-E1 cells.

2.3.2.3 Assessing validity of human oral epithelial primary cells

As the purchased human oral epithelial primary cells were recently marketed from a commercial company (Celprogen, USA) and there was no publication, the specific epithelial cell markers were tested by immunostaining before using them in the later experiments.

Cytokeratin 5 (CK5) is a cytoplasmic intermediate filament protein specifically expressed in epithelial cells from stratified squamous

epithelium including oral mucosa. Desmoglein-3 (Dsg3) is a transmembrane glycoprotein component of desmosomes, which are cell-cell junctions between epithelial cells. Therefore, CK5 and Dsg3 were chosen as two specific markers for the human oral epithelial primary cells.

Cells were seeded on coverslips and 24 h later, they were washed twice with PBS and fixed with 4% formaldehyde for 10 min. Then the cells were permeabilized with 0.1% Triton X-100 in PBS for 2 min followed by the washing in PBS (5min x 2). For fluorescence staining, non-specific binding was prevented by blocking buffer for 30 min followed by incubation with target specific primary antibodies (kindly provided by Dr. Hong Wan, QMUL) diluted in blocking buffer for 1 h at room temperature. Cells were then washed three times with washing buffer and incubated in secondary antibodies (kindly provided by Dr. Hong Wan) for 1 h at room temperature. After two washes with washing buffer, cells were incubated with DAPI (kindly provided by Dr. Hong Wan) for 10 min for nuclear counter-stain. After a final wash with washing buffer, coverslips were mounted on slides using ProLong® Gold anti-fade liquid mount (Invitrogen, UK) and sealed with clear nail varnish. Coverslips were imaged using Leica DM5000 epi-fluorescence microscope.

Blocking buffer

- 10% goat serum in washing buffer

Washing buffer

- 0.2% Tween 20 in PBS

2.4 Bioactive glass design and synthesis

2.4.1 Rationale

Bioactive glasses have been used to repair bone defects. However, recent studies by Monfoulet *et al*. revealed that a rapid pH rise, and subsequent deleterious effects on resident cells, during application is a major problem with the current bioactive glass bone grafts such as the traditional 45S5 composition (Monfoulet et al., 2014).

As discussed previously in the literature review (O'Donnell et al., 2008b, O'Donnell et al., 2008a, O'Donnell et al., 2009), the high phosphate content glasses, not only promote apatite formation, but also reduce the rate and extent of the pH rise, which may reduce the damage brought by a rapid pH rise, to the cells in the local environment and improve osseointegration. Furthermore, the higher phosphate content will enable the development of products with higher surface areas without running into the pH problems of the currently available bioactive glasses that use a coarse particle size. The finer particle size/ increased surface area will result in faster glass dissolution creating an environment in which HA and hopefully, bone can be more rapidly formed.

Fluoride is of interest for the treatment of osteoporosis, with significant antibacterial ability and, is readily incorporated into bioactive glasses via complexing with calcium and sodium in glass network (Brauer et al., 2009, Brauer et al., 2012). However, it plays negative role at high sustained doses such as the inducing of skeletal and dental fluorosis. For the *in vitro* cell research, high doses of fluoride (10^{-4} to 10^{-3} M) suppressed osteoblast

proliferation, differentiation and can even induced apoptosis (Qu et al., 2008). But Mneimne *et al*. reported, fluoride even at low content (4.53% in mole) significantly promoted apatite formation after immersion in Tris buffer solution (Mneimne et al., 2011)

Therefore, the aim of this aspect for the project was to develop bioactive glasses with high phosphate and low fluoride content to reduce the rapid pH rise problem in current bioactive glass bone grafts, to form crystallite apatite *in vitro* within a short time period and to promote efficient osseointegration.

2.4.2 Bioactive glass design and compositions

The bioactive glasses produced in this research were based on the previous glass (O'Donnell et al., 2008a) with the highest phosphate content and with a gradual fluoride addition in this study (Table 2-1).

Table 2-1 Bioactive glass compositions. Compositions in Mol.%

NC fixed at 2.08

Glass	SiO_2	Na_2O	CaO	P_2O_5	CaF_2
P6.33F0	38.14	29.62	25.91	6.33	0
P6.33F1	37.59	29.38	25.70	6.33	1.00
P6.33F3	36.57	28.85	25.25	6.33	3.00
P6.33F5	35.55	28.33	24.79	6.33	5.00
P6.33F7	34.53	27.81	24.33	6.33	7.00

P6.33F0 named ICSW9 in previous publications (O'Donnell et al., 2008b, O'Donnell et al., 2008a, O'Donnell et al., 2009)

2.4.3 Bioactive glass synthesis

Bioactive glasses in the system SiO_2-P_2O_5-CaO-Na_2O-CaF_2 were prepared by the melt-quench route. Briefly, mixtures of analytical grade SiO_2 (Prince Minerals Ltd, UK) P_2O_5, Na_2CO_3, $CaCO_3$ and CaF_2 (all from Sigma Aldrich, UK) were weighed in the appropriate amounts to give a batch size of 200 g. The batch was mixed thoroughly and placed in a platinum/rhodium crucible and melted at 1360 $^{\circ}$C for 1 hour in an electrically heated furnace (Lenton EHF 17/3). After melting, the glass was quenched rapidly into deionized water to prevent crystallization and phase separation. The resulting frit was washed with ethanol then dried in a drying cabinet overnight.

100 g of the dried frits were then ground in a vibratory Gyro Mill (Glen Creston, UK) for 2 x 7 minutes and sieved for 60 minutes in a sieve shaker (Retsch ,VS1000, Germany) to obtain below and above 38 μm particles. The size of the particles and the grinding time was kept constant in order to maintain control over the particle size distribution. Particles with a size under 38 μm were used in this study.

2.5 Bioactive glass characterization

X-ray diffraction (XRD) is an useful tool for the investigation of material structure (Bear and Selby, 1956, Carlstrom and Engfeldt, 1954, Culity, 1956, Trautz, 1955). When an x-ray beam hits an atom, the electrons around the atom start to oscillate with the same frequency as the incident beam does. Diffracted x-rays with interference to one another are generated when they leave the sample. This phenomenon is called x-ray diffraction. Hence, a diffracted x-ray may be described as a beam composed of a large number of scattered rays mutually reinforcing one another. However, if the atoms are in a crystal with regular arrangements, constructive interference will be developed in a very few directions. The waves will be in phase and there will be well defined x-ray beams leaving the sample, which could be collected and interpreted to produce a pattern with some featured regions of intensity in characteristic sharp peaks at specific analysis of 2θº, which can be used to identify the crystalline components of the sample. However, in amorphous materials, such as bioactive glasses which have randomly arranged atoms, destructive interference in almost all directions will occur, which are out of phase and there are no resultant strong coherent beams energy leaving the solid sample. Thus, there are no sharp peaks with amorphous materials, only broad diffuse humps are present.

For the aims of this study, XRD was used to determine that whether synthetic bioactive glasses were amorphous or partially crystalline, whether the quenching process in deionized water initiated the reaction between bioactive glasses and water to form crystalline phase, and to

identify the different crystalline phases in bioactive glasses after immersion in different solutions.

Here, 100 mg of each bioactive glass composition was studied using an X Pert Pro X-ray diffractometer (Panalytical, the Netherlands) with flat plate θ/θ geometry and Ni-filtered Cu-Kα radiation (Kα1= 1.540598 and Kα2= 1.5444260Å) at 45 kV/40 mA. The pattern was taken in the 2θ range of 5º to 70º with a step size of 0.0334º (2θ) and a step time of 2.0 seconds. The experiments were run at 25 ºC.

2.6 Bioactive glass bioactivity study

2.6.1 Tris buffer solution preparation

Tris buffer solution, free of Ca^{2+} and PO_4^{3-} ions with a pH 7.3, is an excellent medium to assess bioactive glass dissolution and apatite forming capacity (Shah et al., 2014b).

For a 2 L batch of Tris buffer solution, 15.090 g tris-(hydroxymethyl) aminomethane (Sigma–Aldrich) was slowly dissolved in 800 ml deionised water, with the addition of 44.2 ml 1 M HCl and the solution was left in a shaking incubator at 37 °C overnight. Then the pH was adjusted to 7.3 by adding small amounts of 1 M HCl followed by the solution transferred to a 2 litre flask where the total volume was adjusted to 2 L by adding deionised water.

2.6.2 Dissolution study

75 mg bioactive glass powder was weighed on a scale (±0.1 mg) and then transferred into a 50 ml Falcon tube with 50 ml Tris buffer solution. The bioactive glass powder in solution was kept in an orbital shaking incubator at 37 °C with an agitation rate of 60 rpm for 2, 8, 24, 72 and 168 hours. For each experimental group, three samples were assessed under the same conditions.

At each time point, tubes were removed from the incubator with the pH immediately measured by a pH electrode (Oakton Instruments, Nijkerk, the Netherlands) to analyse the pH change resulting from reaction of the bioactive glasses. Then samples were filtered with filter paper (4-13 micron pore size retention). The filtrate was collected in 50 ml Falcon

tubes and stored in a fridge at 4 °C. Remaining solid powders were stored in petri dishes in a 37 °C drying cabinet to dry overnight and were collected the following day.

2.6.3 Solution characterisation

Inductively coupled plasma-optical emission spectrometry (ICP-OES) is a powerful tool for the presence and quantity of elements. Within the technique, the sample solution is converted to an aerosol, enters the central tube of the plasma and exposed to radio frequency then it evaporates and breaks down into atoms. Due to the high temperature (10,000K) of the plasma, a large proportion of the atoms are ionized by losing its most loosely bound electron. Then the detector will receive an ion signal in proportion to the concentration of the ion. The concentrations of the samples can be determined through calibration with the reference standard. ICP-OES is highly sensitive with good precision, reproducibility and multi-element determinations for different elements including P and Si could be performed simultaneously. (Amadasi et al., 2013, Wang et al., 2013b).

However, for the fluoride, ICP-OES is not applicable. A fluoride selective electrode is a type of ion selective electrode sensitive to the concentration of the fluoride ion. It consists of a sensing element bonded into an epoxy body. When the sensing element is in contact with a fluoride containing solution, an electrode potential develops across the sensing element. Therefore, the first step is the calibration of the instrument, in which, the potentials of fluoride standard solutions are measured. By plotting the

measured potential values as a function of the fluoride ion concentration, the calibration line can be obtained, which is expected to be straight as showed in Fig. 2.4 below. In the next step, potentials in the tested solutions will be measured. Using the calibration straight line, the fluoride concentration in the samples can be calculated.

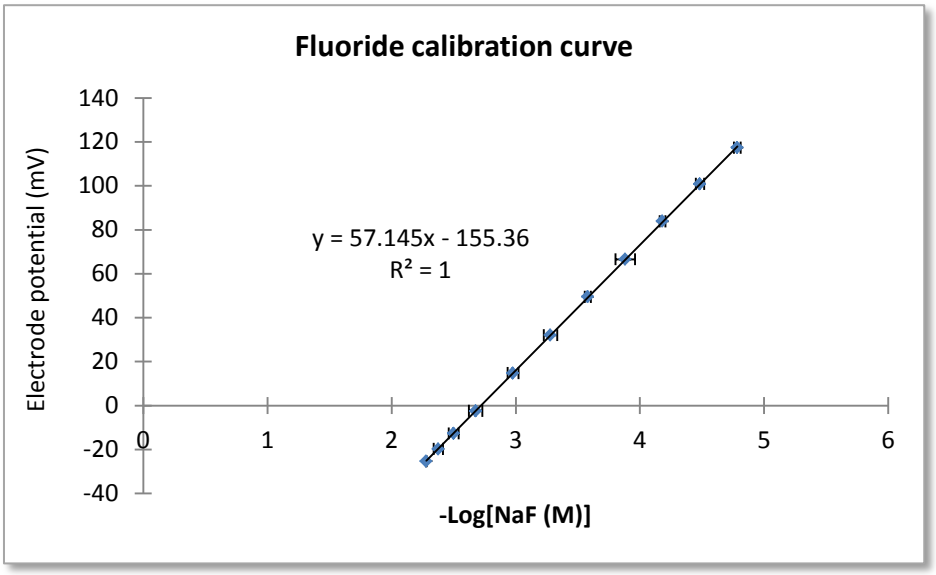

Figure 2.4 Typical fluoride calibration curve. The standard curve is constructed by measuring the electrode potential of NaF concentrations (100-0.3125 ppm). Each marker represents mean ± S.E.M of three independent experiments.

Therefore, in this study, the remaining solutions were analysed by both ICP-OES and fluoride ion selective electrode to examine the solutions from the bioactivity studies. ICP-OES (Varian Vista-PRO, Varian Ltd., Oxford, UK) was used to detect concentrations of silicon, calcium, sodium, and phosphorus in solution. All samples were diluted 1:10 with distilled water then stabilized and digested with the addition of 1% nitric acid. Fluoride selective electrode (Orion 9609BNWP with Orion pH/ISE meter

710, both Thermo Scientific, Waltham, MA, USA) was used to measure fluoride levels with calibration standards.

2.6.4 Solid characterisation

Once the dried glass particles from the dissolution studies were collected, they were analysed by XRD (same conditions and instrument as described earlier) and FTIR (Fourier Transform Infrared Spectroscopy, Spectrum GX, Perkin-Elmer, Waltham, MA, USA; data collected from 1600 cm^{-1} to 500 cm^{-1}) to look primarily for apatite formation.

FTIR, is sensitive to the mid-region electromagnetic spectrum (4000-200 cm^{-1}), and is an effective method to determine the molecule structures with their characteristic absorption of infrared radiation. Essentially, the energy associated with infrared beams are absorbed or transmitted by sample molecules. Then the rest energy can be detected and presented in a spectral plot against wavelength to create a fingerprint of the sample by identifying the molecular bond types.

2.7 Cytotoxicity of bioactive glass conditioned medium

2.7.1 Preparation of bioactive glass conditioned medium

Cell culture medium more closely reflects the composition of the physiological environment and could be used to investigate cellular response to bioactive glass dissolution behaviour. Thus, 75 mg fine bioactive glass particles from each composition was immersed in 50 ml α-MEM or DMEM with 1% antibiotic (penicillin and streptomycin) and kept in a shaker (60 rpm) at room temperature for 2, 8, 24 and 72 h.

At each time point, the samples were centrifuged (800 rpm, 5 min) to separate the solution and solid. Solution was then filtered with filters (0.2 micron pore size) for sterilization. Filtrate was further supplemented with 1% L- glutamine and 5% FBS for α-MEM and 2% FBS for DMEM and stored in a fridge at 4 °C for cell treatment. The schematic representation of the bioactive glass conditioned medium preparation is showed in Fig. 2.5.

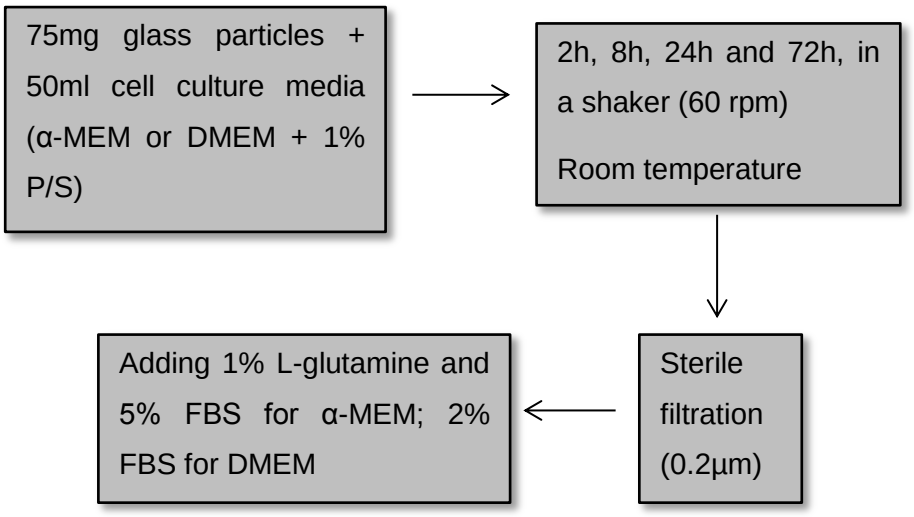

Figure 2.5 Schematic representation of the bioactive glass conditioned medium preparation

2.7.2 Cytotoxicity by MTT assay

MC3T3-E1, A431 and NHOF-1 cells were seeded at a density of 3000 cells/cm^2 in 96-well plates and allowed to attach for 24 h. To assess whether cells could survive in bioactive glass conditioned medium, cells were treated for 1, 3 and 5 days with the bioactive glass conditioned medium (all bioactive glasses immersed in medium for 2, 8, 24 and 72 h). For each experimental group, six samples were assessed under the same condition. At each time point, cytotoxicity was investigated by MTT assay as previously completed.

2.8 Cellular response to 72 h bioactive glass conditioned medium

75 mg fine bioactive glass particles from each group was immersed in 50 ml α-MEM or DMEM with 1% antibiotic and kept in a shaker (60 rpm) at room temperature for 72 h.

Solution was collected and sterilized as previously reported. The remaining solid powders were washed with 70% ethanol then stored in fume cupboard to dry overnight and collected the following day.

2.8.1 Medium characterisation

The filtered solutions were analysed by both ICP-OES and a fluoride selective electrode to detect silicon, calcium, phosphorus and fluoride concentrations in bioactive glass conditioned medium.

2.8.2 Solid characterisation

Once the dried powders from the dissolution studies were collected, they were analysed by FTIR (Spectrum GX, Perkin-Elmer, Waltham, MA, USA; data collected from 1600 cm^{-1} to 500 cm^{-1}) and XRD (same conditions and instrument as described earlier) to look primarily for apatite formation.

2.8.3 Osteoblasts

2.8.3.1 Cell differentiation in bioactive glass conditioned medium

Filtered bioactive glass conditioned medium was further supplemented with 1% L- glutamine and 5% FBS and stored in a fridge at 4°C for cell treatment. MC3T3-E1 cells were treated for 7, 14 and 21 days with 72 h bioactive glass conditioned medium.

At each time point, medium was removed and cells were collected for ALP activity assay as described previously. For each experimental group, ten wells were assessed for each condition.

2.8.3.2 Cell proliferation in bioactive glass conditioned medium

Experimentally, cells were treated as in the cell differentiation assay. At each time point, medium was removed and cells were collected for DNA content assay as described previously. For each experimental group, ten wells were assessed for each condition.

2.8.3.3 Type I collagen formation in bioactive glass conditioned medium

Type I collagen is the most abundant structural protein in the human body and is a critical component of bone extracellular matrix to form the structural scaffolding for bone. Picro-Sirius red, an anionic dye, specifically binds strongly within the tertiary groove of collagen I fibrils and is well-established to highlight collagen formation (Junqueira et al., 1979).

In this study, bioactive glass conditioned medium was further supplemented with 5mM β-glycerophosphate and 50 µg/ml L-ascorbic acid (Sigma, UK) to make 'osteogenic medium'.

MC3T3-E1 cells were treated for 2, 3 and 4 weeks with bioactive glass conditioned osteogenic medium. After 10 min fixation in 2.5% glutaraldehyde at 4 ºC and three times deionized water wash, monolayers were incubated in 0.1% Sirius red F3B in 1.3% saturated aqueous solution of picric acid (all from Sigma, UK) for 1 h at room temperature. Cultures were then washed twice with 0.5% acidified water and three times in

deionized water to remove the unincorporated dye. After photographing the stained cultures, Type I collagen formation was quantified by measuring the concentration of Sirius red stain incorporated in cell-mediated matrix (Kliment et al., 2011, Houghton et al., 1996). Briefly, the dye was extracted using a mixture of 0.1 M NaOH and absolute methanol (1:1, all from Sigma, UK) and incubated for 30 min at room temperature. 200 µl aliquots of solution and dye were transferred to a 96-well plate and measured the absorbance at 570 nm. For each experimental group, three wells were assessed for each condition.

2.8.3.4 Mineralization in bioactive glass conditioned medium

Biomineralization, mediated by osteoblastic cells, is believed to accumulate calcium and inorganic phosphate which are regarded as nucleating agents for the formation of hydroxyapatite ($Ca_{10}(PO_4)_6(OH)_2$), the main inorganic component of bone.

Alizarin red S (Sodium Alizarine sulfonate, $C_{14}H_7NaO_7S$) is used to qualitatively identify calcium deposition by cells of an osteogenic lineage or in tissue sections (Bertoni et al., 2009, Verma et al., 2010). It can form an Alizarin red S-calcium complex in a chelation process. However, this reaction is not strictly specific for calcium, since magnesium, manganese, barium, and strontium may interfere, but these elements usually cannot reach the sufficient concentration to interfere with the staining (Lievremont et al., 1982). Furthermore, as Stanford *et al*. (Stanford et al., 1995) reported, Alizarin red S staining is particularly versatile based on that the dye could be extracted from the stained monolayer and readily assayed

for quantification. This sensitive method is based on cetylpyridinium chloride incubation followed by absorbance reading at 570 nm.

In this study, for the detection of bone nodule formation, MC3T3-E1 cells were treated as those in the Type I collagen formation assay, at each time point, medium was removed and cells were washed twice with PBS and fixed in 2.5% glutaraldehyde at 4ºC for 10min. Then excess deionized water wash was carried out prior to addition of 200 µl of 40 mM Alizarin Red S (pH 4.1) per well. The plates were incubated at room temperature for 40 min and washed three times with deionized water after aspiration of the unincorporated dye.

For quantification of staining, Alizarin Red S was extracted from the monolayer by incubation in 10% (w/v) cetylpyridinium chloride (CPC, Sigma, UK) in 10 mM sodium phosphate, pH 7.0, for 30 min at room temperature. The dye was then removed and 100 µl aliquots were transferred to a 96-well plate prior to absorbance reading at 570 nm. For each experimental group, three wells were assessed for each condition.

2.8.3.5 Osteogenic gene expression in bioactive glass conditioned medium by relative quantitative polymerase chain reaction (qPCR)

mRNA Extraction

RNeasy mini kit (Qiagen, UK) was used to extract mRNA from cells according to the manufacture's protocol. Briefly, MC3T3-E1 cells were treated with bioactive glass conditioned medium for 1 d, 4 d, 7 d, 14 d and 21 d in 6-well plates. At each time point, cells were disrupted by Buffer

RLT (350 µl/well) followed by addition of 1 volume 70% ethanol to homogenize the lysate. Then the cell lysis sample was transferred to an RNeasy spin column placed in a collection tube and centrifuged for 15 s at 16,000 x g to let the mRNA bind to the RNeasy membrane. To wash the spin column membrane, 350 µl Buffer RW1 was added, centrifuged and the flow-through was discarded. In order to further eliminate the DNA contamination in mRNA samples, RNase-Free DNase set (Qiagen, UK) was used here. The incubation mix (10 µl DNase I with 70 µl Buffer RDD) was added directly to the RNeasy spin column membrane where mRNA binding, and placed in room temperature for 15 min. Then, the DNase I was removed by a second wash with Buffer RW1. 500µl Buffer RPE was added to the RNeasy spin column with a 15 s centrifugation. Then 500 µl Buffer RPE was added again with a 2 min centrifugation to dry the column membrane, ensuring that no ethanol was carried over during RNA elution, which may interfere with downstream reactions. The RNeasy spin column was placed in a new collection tube and 30 µl RNase-free water was added directly to the spin column membrane with a 1 min centrifugation to elute mRNA. The purity of the isolated RNA was determined through measuring the optical density (OD) value (*A260/A280*) using the NanoDrop™ 1000 Spectrophotometer (Thermo Scientific, UK).

cDNA synthesis

After mRNA extraction, cDNA synthesis was carried out by reverse transcription reactions in 0.2 ml PCR tubes, each reaction contained the following using the transcriptor first strand cDNA synthesis kit (Roche, UK):

- 5xbuffer 4.0 µl
- dNTP 2.0 µl
- Random+OligoDT primers 0.8 µl
- RNasin 0.4 µl
- Reverse Transcriptase 0.4 µl
- mRNA 13 µl

Reverse transcription reactions were performed using a thermos-cycler block at 42 ºC for 30 min, 85 ºC for 5 min and 4 ºC for 5 min. The resulting cDNA was diluted in 40 µl RNase-free water and stored in -20 ºC.

Relative quantitative polymerase chain reaction (qPCR)

Generation of PCR products can be detected by measurement of the SYBR Green I fluorescence signal. As SYBR Green I could intercalate into the double stranded DNA helix and its fluorescence is greatly enhanced upon binding to DNA due to conformational changes.

Here, Glyceraldehyde-3-phosphate dehydrogenase gene (GAPDH) was used as a reference gene. All primers used in this study are listed as in table 3-2 below.

Table 2-2 Sequences of primer pairs used for qPCR analysis

Name	Primers 5' – 3'
GAPDH	Forward ATTGTCAGCAATGCATCCTG
	Reverse ATGGACTGTGGTCATGAGCC
OPN	Forward GAGATTTGCTTTTGCCTGTTTG
	Reverse TGAGCTGCCAGAATCAGTCACT
Col1a1(Type I collagen)	Forward CATGTTCAGCTTTGTGGACCT
	Reverse GCAGCTGACTTCAGGGATGT
VEGF	Forward CAGGCTGCTGTAACGATGAA
	Reverse GCTTTGGTGAGGTTTGATCC

Reactions in 96-well plates were set up and each well contained the following:

- 2x SYBR Green I Master mix 5 µl
- 5 uM F/R Primer 1 µl
- dH2O 3 µl
- template (cDNA) 2 µl

Once the loaded plate was sealed with a Roche sealing film and centrifuged for 30 s at 3000 rpm. The qPCR was carried out in LightCycler 480 qPCR system (Roche) using the following protocol:

- Denaturation (Hot Start) 95°C 5 min
- Amplification (45 cycles)

Melting	95°C	10s
Annealing	60°C	6s
Extension	72°C	6s
Acquisition	76°C	1s

- Melting Analysis

Melting	95°C	30s
Cooling/annealing	65°C	30s
Gradual heating + acquisition	65 to 99°C	
Cooling/termination	40°C	5s

The relative gene expression level was determined by comparing against the reference gene and normalised by the control group (normal cell culture medium treatment). Therefore, final data presented as mean fold change ± SE with respect to the control. For each experimental group, three samples were assessed under the same condition.

2.8.3.6 Angiogenesis gene expression and protein production in bioactive glass conditioned medium by qPCR and Western blot

The VEGF gene expression was performed as previously done and the primers used are represented in table 3-2.

Western blot

MC3T3-E1 cells were treated in bioactive glass conditioned medium or NaF concentrations (F^- concentrations: 0, 0.1, 1.9 and 9.5ppm) in 10 cm tissue culture dish for 7 d, 14 d and 21 d. At each time point, cell culture dish was placed on ice and cells were washed with ice-cold PBS. Then cell lysates were extracted using RIPA lysis buffer with freshly added Protease Inhibitors (Roche, UK) and collected with the aid of cell scrapers. Lysates were transferred into pre-cooled micro-centrifuge tubes, sonicated

for 30 s on ice and centrifuged at 16,000 × g for 20 min in 4 ºC. Then the supernatant was transferred into new tubes and the protein concentration was determined by *DC* protein assay (Bio-Rad, UK). Briefly, 5 µl of each test sample was loaded into a 96-well plate alongside a set of bovine serum albumin standards (BSA, 0, 0.08, 0.16, 0.3125, 0.625, 1.25, 2.5, 5, 10 µg/ml) to which 25 µl of Reagent A^+ (solution A + solution Dc, 50:1) followed by 200 µl of Reagent B were added. The blue colour was allowed to develop for 15 min at room temperature followed by the measurement of sample absorbance using a plate reader. Absorbance of each sample and standard was obtained at a wavelength of 650 nm. The protein concentration of tested samples was calculated from the standard curve generated from the BSA standards. As in all Western blots, equal protein amounts of samples were loaded into gels in this study, the lysates were diluted with deionized water to keep the same protein concentration. 4x Laemmli sample buffer (Bio-Rad, UK) which contains blue dye to assist gel loading was added to the lysates followed with boiling at 100 ºC for 5 min then -20 ºC storage.

An equal amount of total protein was loaded into each lane of the 10% NuPAGE® Bis-Tris gel (Thermo scientific, UK) alongside molecular weight marker (full range rainbow marker, Invitrogen). The gel ran at 121 V for 90 min at room temperature.

Then the electrophoretic transfer of protein from gels to polyvinyl difluoride (PVDF) membrane (Thermo scientific, UK) was carried out at 35 V for 90 min at 4 ºC. The PVDF membranes were then subjected to blocking of non-specific sites by incubation with blocking buffer for 1 h at room

temperature. Membranes were cut to divide the target protein area and the loading control then incubated with primary antibodies (anti-VEGF antibody (1:2000, Abcam), anti-Cyclophilin B antibody (1:6000, Abcam)) diluted in blocking buffer overnight at 4 ºC. After three washes (3 × 5 min) in TBST (see below), the membranes were incubated with secondary antibody (Goat anti-Rabbit IgG (H+L) Secondary Antibody (1:2000, Thermo scientific, UK)) for 1 h at room temperature. Finally, after three washes in TBST the membranes were subjected to the Enhanced Chemiluminescence (ECL) plus western blotting detection system (Amersham) to detect target proteins and recorded using hypersensitive ECL film (GE healthcare Bio-science).

RIPA buffer

- 150mM NaCl
- 1.0% NP-40
- 0.5% sodium deoxycholate
- 0.1% sodium dodecyl sulfate (SDS)
- 50 mM Tris-HCl

  pH 8.0

Running buffer (Invitrogen)

- NuPAGE® MES SDS running buffer (20x)

1x Transfer buffer

- 25mM Tris base
- 190mM glycine
- 20% methanol

1xTBST

- 0.1% Tween 20
- 20mM Tris base
- 150mM NaCl

  pH 7.5

Blocking buffer

- 5% (w/v) non-fat dry milk

Western blot analysis

The exposed films from Western blots were scanned using a flatbed scanner with a minimum of 600 dpi and the bands density of blots was determined using Image J 1.49 (downloaded from: http://imagej.nih.gov/ij/index.html). As shown in Fig. 3.8A, a set of blot bands, shows bands densities of VEGF expression in MC3T3-E1 cells after treatment with bioactive glass conditioned medium, were selected and analysed together. This selection was then identified as the first lane (Analyse>Gels>Select first lane) followed by 'Plot lanes' (Analyse>Gels>Plot lanes) to generate a 'Western demo plot' (Fig. 3.8B). The lanes were then divided using the line tool to allow for the area of each peak to be determined separately (Fig. 3.8C). Using the 'Wand tool' each peak was selected to generate a band area with values (Fig. 3.8D, E). The peak values were then exported to an Excel spreadsheet where all values were normalised against the loading control (Cyclophilin B). The normalised band densities were expressed relative to the control and final data presented as mean fold change ± SE with respect to the control. For each experimental group, three samples were assessed for each condition.

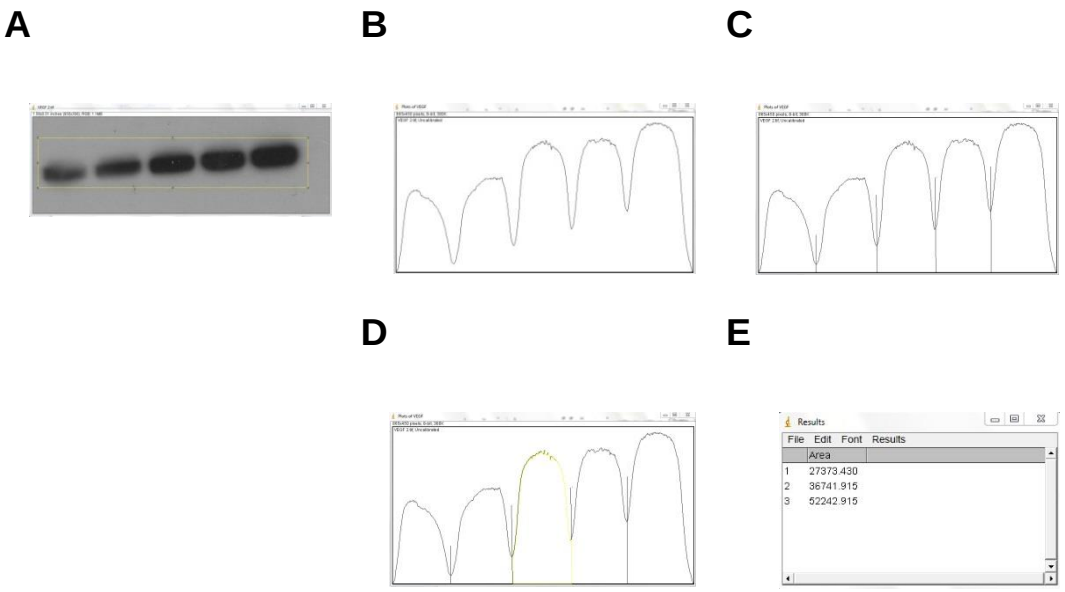

Figure 2.6 Western blot analysis using Image J (A) Bands selected for analysis. (B) Bands density plotted with Image J. (C) Bands separated by lines to allow for quantification of each peak. (D) Bands area selection. (E) Quantification of each peak.

2.8.4 Epithelial cells

A431 cells were treated in 72 h bioactive glass conditioned medium for 4, 7 and 10 d. At each time point, medium was removed and cells were collected for DNA content assay as described previously. For each experimental group, ten wells were assessed under the same condition.

2.8.5 Oral fibroblasts

NHOF-1 cells were treated in 72 h bioactive glass conditioned medium for 4, 7 and 10 d. DNA content assay was carried out as described previously. For each experimental group, ten wells were assessed under the same condition.

2.9 Antibacterial studies

alamarBlue® is a cell viability assay reagent quantitatively measuring the cell proliferation particularly in bacteria and, it contains the cell permeable, non-toxic and weakly fluorescent blue indicator dye called resazurin (Bio-Rad, 2015). Resazurin acts as an oxidation-reduction indicator to undergo colorimetric change in response to cellular metabolic reduction. The reduced form called resorufin is pink with high fluorescent and, the measured fluorescence intensity is proportional to the number of living cells respiring (Bio-Rad, 2015). Therefore, by detecting the level of oxidation during respiration, alamarBlue® is widely used as a direct indicator to quantitatively measure cell viability in numerous antibacterial studies (Collins and Franzblau, 1997, Carpenter et al., 2012, Scherr et al., 2012, de Paula e Silva et al., 2013, Gemechu et al., 2013, Katawera et al., 2014).

In this study, typical supra-gingival bacteria, *L. casei* and *S. mitis*, sub-gingival bacteria, *A. actinomycetemcomitans* and *P. gingivalis* (kindly gifted by Professor Rob Allaker, QMUL), were grown in brain heart infusion agar plates (Fisher Scientific, UK) for 48 h at 37 °C under aerobic or anaerobic conditions. Then the log phase cultures were harvested and the bacterial concentrations were measured with absorbance reading at 595 nm.

Bioactive glass particulates were sterilized by autoclaving (dry cycle) at 121 °C for 15 min. Then the bioactive glass particulate suspensions in brain heart infusion broth at concentrations of 1.25, 2.5, 5, 10 and 20 mg/ml were made and plated in 96-well plates (100 µL/well). The bacteria

(10^6 to 10^7 CFU/mL) were added subsequently (100 µL/well). Therefore, the final bioactive glass particle working concentrations were 0.625, 1.25, 2.5, 5 and 10 mg/mL. Sodium Fluoride (NaF) concentrations (2, 1, 0.5, 0.25, 0.125 and 0 mM) in brain heart infusion broth were used to treat bacteria as well to investigate the antibacterial effects of F^-.

After incubation under aerobic or anaerobic conditions for 0, 2, 4 and 8 h, 20 µl alamarBlue (Bio-Rad, UK) was added to each well and incubated for 1 h according to the manufacture's protocol. Then the plates were centrifuged for 10 min at 4000 rpm and 100 µl aliquots were transferred to new black 96-well plates, to measure the Fluorescent Intensity at 590 nm emission and 560 nm excitation. Percent inhibition of bacterial growth was then defined as 1 - (mean fluorescence of test wells / mean fluorescence of negative control well) × 100% (Carpenter et al., 2012, Collins and Franzblau, 1997). For each experimental group, four wells were assessed under the same condition.

2.10 Statistical analysis

The elemental analysis was carried out with three samples per group. Cell assay data with bioactive glass conditioned medium are presented as means ± standard deviations. qPCR and western blot assay were performed with three samples per group and bacterial studies were four replicates. Comparisons of cell assay data were made using a one-way analysis of variance (ANOVA). Significance is indicated when $P \leq 0.05$.

Chapter 3 The bioactivity of high phosphate and fluoride containing bioactive glasses

3.1 Introduction

For bioactive glasses, the term ‘bioactivity’ refers to the ability and rate of apatite formation, which is necessary for surrounding tissues and cells to attach to the implanted bone grafts. As discussed previously in the literature review (O’Donnell et al., 2008b, O’Donnell et al., 2008a, O'Donnell et al., 2009), phosphate is present largely as an orthophosphate phase in bioactive glasses, which potentially promotes glass bioactivity leading to an increase of the apatite formation rate. Furthermore, higher phosphate content can reduce the rate and extent of local pH rise, which will reduce the deleterious effects brought by high alkalinity, on resident cells in the local environment (Monfoulet et al., 2014). Therefore, higher phosphate content may enable the development of products with higher surface areas without running into the pH problems. The finer particle size with increased surface area will result in faster glass dissolution creating an appropriate environment in which apatite and later bone can be more rapidly formed.

The use of fluoride in bioactive glasses is of interest because of its effects in the treatment of osteoporosis and outstanding antibacterial ability. Fluoride is readily incorporated into bioactive glasses via complexing with

calcium and sodium, instead of forming of Si–F bonds in glass network (Brauer et al., 2009, Brauer et al., 2012). Furthermore, Mneimne *et al*. found that addition of fluoride into low phosphate containing bioactive glasses significantly promoted apatite formation after immersion in Tris buffer solution (Mneimne et al., 2011). However, at high sustained doses, fluoride plays negative role leading to skeletal and dental fluorosis. Using *in vitro* cell research, high doses of fluoride (10^{-4} to 10^{-3} M) supresses osteoblast proliferation, differentiation and can even induce apoptosis (Qu et al., 2008).

Bioactive glasses apatite formation is investigated *in vitro* in solutions such as SBF and Tris buffer. Tris buffer solution, free of Ca^{2+} and PO_4^{3-} ions with a pH 7.3, is an excellent medium to assess bioactive glass dissolution and apatite forming capacity (Shah et al., 2014b). A simulated body fluid (SBF), a solution with ion concentrations close to that of human blood plasma, was firstly proposed by Kokubo *et al*. in the 1990s and later widely applied by biomaterial scientists to evaluate the bioactive glasses and ceramics bioactivity *in vitro* and to predict the apatite formation ability *in vivo* (Kokubo et al., 1990, Kokubo and Takadama, 2006). However, tests in SBF are found to produce false positive and false negative results (Bohner and Lemaitre, 2009) and an apatite layer was formed in SBF but no direct bone bonding *in vivo* (Walsh et al., 2003, Theiss et al., 2005, Apelt et al., 2004). For most potential dental and orthopaedic biomaterials, cellular biocompatibility *in vitro* and animal studies are routinely investigated. Cell culture medium with proteins and amino acids more

closely reflects the appropriate composition of the physiological environment, therefore, it is considered as a more *in vivo* like model.

Therefore, the aim of this Chapter is to assess the amorphous structure of the synthesised high phosphate and low fluoride containing bioactive glasses, monitor change in pH with dissolution, investigate apatite formation and ion release both in Tris buffer solution and cell culture medium.

3.2 Results

3.2.1 Bioactive glass characterization

Obtaining an amorphous structure in the prepared bioactive glasses is important, since crystallization significantly reduces bioactivity. Through the XRD traces here (Fig. 3.1 below), all the prepared glasses in this study exhibited broad halos without sharp peaks, which is the typical feature of an amorphous structure. It indicates that all the bioactive glasses prepared during the course of this work do not contain a crystalline phase to any significant extent and the quenching process in deionized water did not initiate the reaction to form crystalline phase.

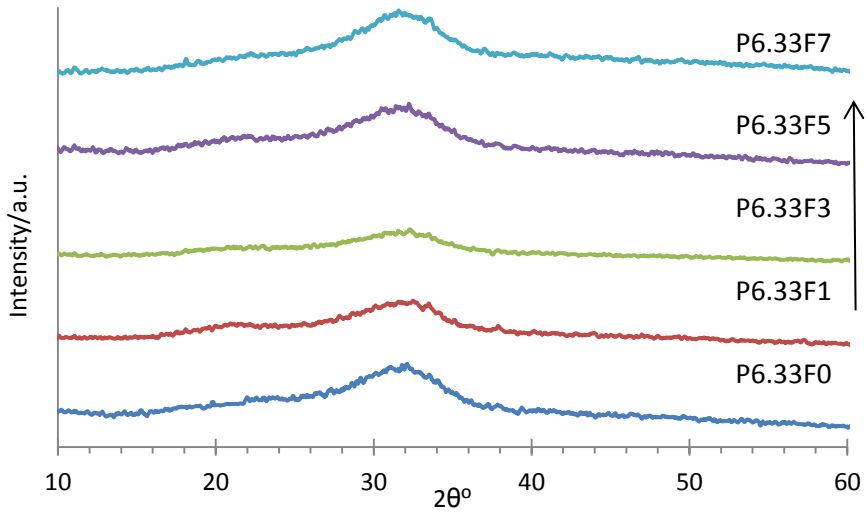

Figure 3.1 XRD traces of all the initial glasses. (P6.33F0 indicates a bioactive glass contains 6.33 Mol.% phosphate and 0 Mol.% fluoride)

3.2.2 Bioactive glass bioactivity study in Tris buffer solution

3.2.2.1 pH change

Fig. 3.2 below shows the variation in pH as a function of incubation time for bioactive glasses from P6.33F0 to P6.33F7 after immersion in Tris buffer solution. All the bioactive glasses in this work clearly showed a pH rise within the first 2 h of immersion and a further but very slight increase in pH between 2 h and 72 h. For fluoride containing bioactive glasses P6.33F1 to P6.33F7, the pH stayed constant for the rest of the experiment (72 h to 168 h), while the pH in the fluoride free bioactive glass P6.33F0 was still rising slightly at 168 h. It is also observed the addition of fluoride to bioactive glasses (P6.33F1 to P6.33F7) increased the final pH level slightly by around 0.07 to 0.14 pH.

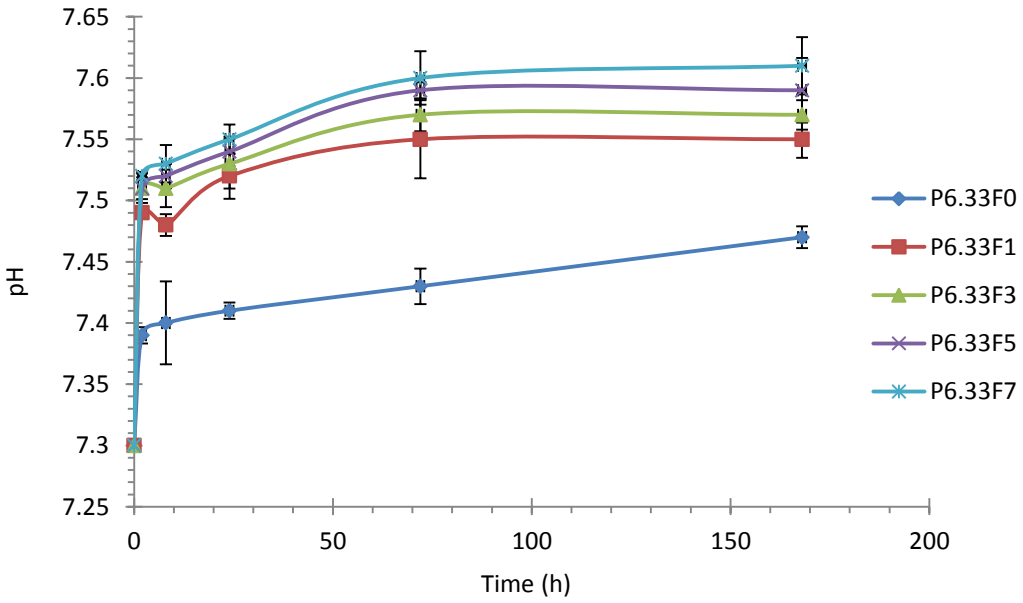

Figure 3.2 pH change of Tris buffer solution according to the incubation time. 75 mg fine bioactive glass particles were immersed in 50 ml Tris buffer for different periods followed by an immediate pH measurement. Data is represented as mean ± SE. n=3. (P6.33F0 indicates a bioactive glass contains 6.33 Mol.% phosphate and 0 Mol.% fluoride)

Fig 3.3 illustrates the pH change as a function of fluoride content in the bioactive glasses. When fluoride was added from 0 to 7 Mol.% into the high phosphate bioactive glass, solution pH rose gradually but slightly and reached the highest value in the 7 Mol.% fluoride added glass after 8 h, 24 h and 168 h immersion.

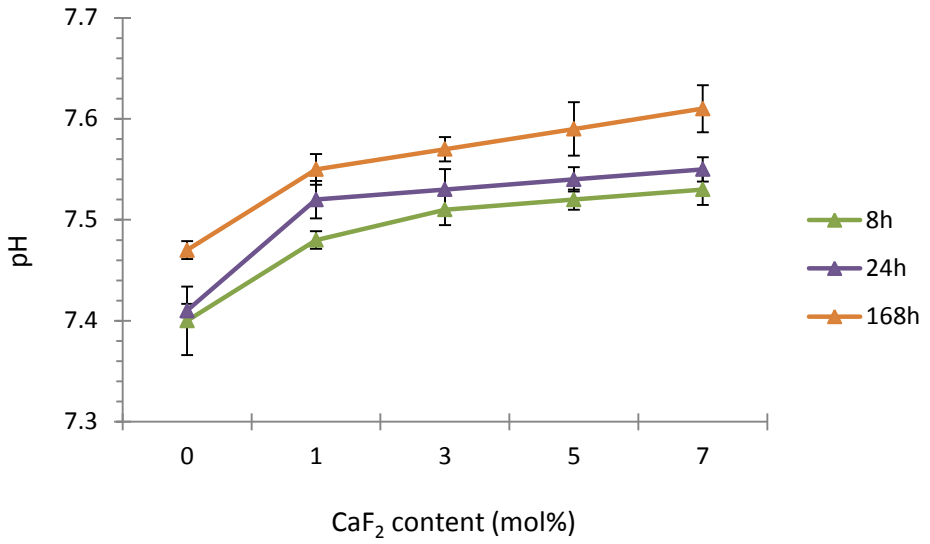

Figure 3.3 pH change of Tris buffer solution according to the CaF_2 content in the bioactive glasses. 75 mg fine bioactive glass particles were immersed in 50 ml Tris buffer for different periods followed by pH measurement. Data is represented as mean ± SE. n=3. (P6.33F0 indicates a bioactive glass contains 6.33 Mol.% phosphate and 0 Mol.% fluoride)

3.2.2.2 Apatite formation

As depicted in Fig. 3.4 and Fig. 3.5 below, fluoride added to the bioactive glass compositions resulted in significant changes in the XRD traces and FTIR spectra after immersion in Tris buffer solution for 8 h, compared with the high phosphate but fluoride free bioactive glass.

The XRD traces, patterns of hydroxyapatite (JCPDS 09-432), fluorapatite (15-876), carbonated hydroxyapatite (JCPD 19-272) and carbonated

fluorapatite (JCPDS 31-267) all overlap (Brauer et al., 2010). Therefore, the pattern of 'apatite' in the XRD traces is referred to here.

After 8 h immersion in Tris buffer solution (Fig. 3.4), the typical apatite peaks at 26º, 32–34º, 47º, 50º and 52º 2θº appear in traces for the fluoride containing bioactive glasses. These peaks become intense and more clearly pronounced as the fluoride content increased from 1 to 7 Mol.%. For the bioactive glass P6.33F0, the XRD pattern shows a small peak at around 28.5º 2θ (starred), which may indicate the presence of a small amount of calcite ($CaCO_3$).

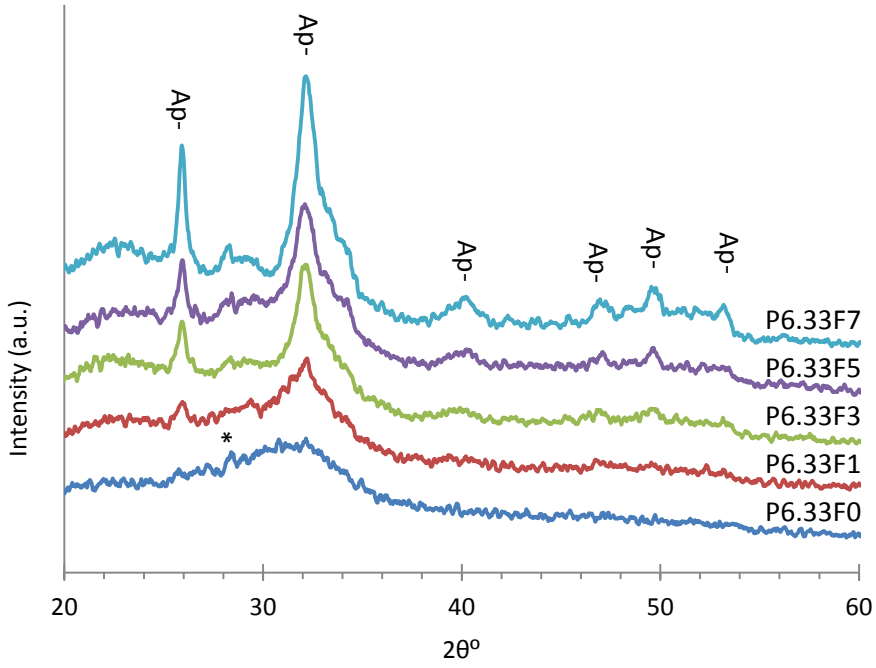

Figure 3.4 XRD traces for bioactive glasses immersed in Tris buffer solution for 8 h. 75 mg fine bioactive glass particles were immersed in 50 ml Tris buffer for 8 h followed by a separation of solution and glass powder. Then the dried powders were tested using XRD. (P6.33F0 indicates a bioactive glass contains 6.33 Mol.% phosphate and 0 Mol.% fluoride)

After immersion in Tris buffer solution for 8 h, the FTIR spectra shows the sharpening of the Si-O-Si stretching band at about 1030 cm^{-1} in the fluoride added bioactive glasses P6.33F1 to P6.33F7 (Fig. 3.5). At the

same time, new bands appeared at around 800 cm^{-1}, which were assigned to Si-O-Si bond vibration between two adjacent SiO_4 tetrahedra as described previously for SBF-treated glasses (Brauer et al., 2010). These changes indicate the formation of a silica-gel surface layer after leaching of Na^+ ions and formation of Si-OH groups in this ion-depleted glass.

A split band at approximately 560-600 cm^{-1}, is the most characteristic region for apatite and other orthophosphates. After immersion in Tris buffer for 8 h in this study, a single band in this region appeared in the high phosphate and fluoride free bioactive glass (P6.33F0), suggesting the presence of a disordered apatite or amorphous calcium phosphate. Characteristic split bands at 560 and 600 cm^{-1} appeared in the fluoride containing bioactive glasses P6.33F1 to P6.33F7, suggesting that adding fluoride significantly accelerates ordered and well crystallised apatite formation.

Bands at about 870 cm^{-1} in the fluoride containing bioactive glasses after immersion in Tris buffer for 8 h indicate the presence of carbonate substitution in the formed apatite. It is pointed out that this carbonate band is usually considered as an indication for carbonate being incorporated into the apatite, resulting in the formation of HCA, rather than stoichiometric HA (Lu and Leng, 2005b). Furthermore, further broad CO_3^{2-} bands are present in the region starting from 1410 cm^{-1} indicating a B-type substitution (i.e. carbonate replacing a phosphate group), rather than an A-type substitution (i.e. carbonate replacing a hydroxyl group), which

would be shifted to higher wave numbers, starting from 1460 cm^{-1} (Brauer et al., 2010).

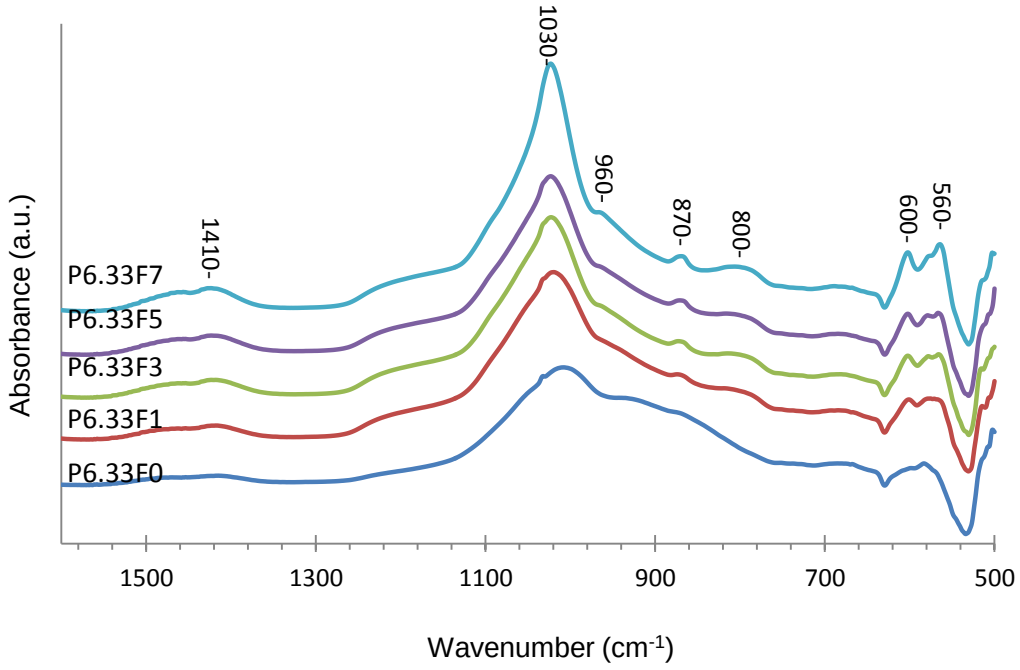

Figure 3.5 FTIR spectra for bioactive glasses immersed in Tris buffer solution for 8 h. 75 mg fine bioactive glass particles were immersed in 50 ml Tris buffer for 8 h followed by a separation of solution and glass powder. Then the dried powders were tested using FTIR. (P6.33F0 indicates a bioactive glass contains 6.33 Mol.% phosphate and 0 Mol.% fluoride)

In Fig. 3.6 and Fig. 3.7 below, the XRD traces and FTIR spectra of bioactive glass P6.33F1 (1 Mol.% CaF_2) showed significant changes after immersion in Tris buffer in comparison to the pattern and spectrum of the unreacted bioactive glass (0h). As early as 2 h on exposure in Tris buffer solution, a small apatite peak at 26º 2θº appeared in the XRD trace. As immersion time increased, these typical apatite peaks at 26º and 32–34º 2θº become larger in intensity and more clearly pronounced. It is consistent in the FTIR spectra: disappearance of the NBO (non-bridging oxygens, $Si–O^-$ $alkali^+$) band at 920 cm^{-1}, sharpening of the Si–O–Si

stretch band at about 1030 cm^{-1}, new bands appeared at about 800 cm^{-1} and a single band at 560-600 cm^{-1} indicates the presence of non-apatitic or amorphous calcium phosphate was observed after 2 h immersion. As immersion time increased to 8 h, characteristic split band at 560 and 600 cm^{-1} appeared indicative of calcium phosphate crystallites.

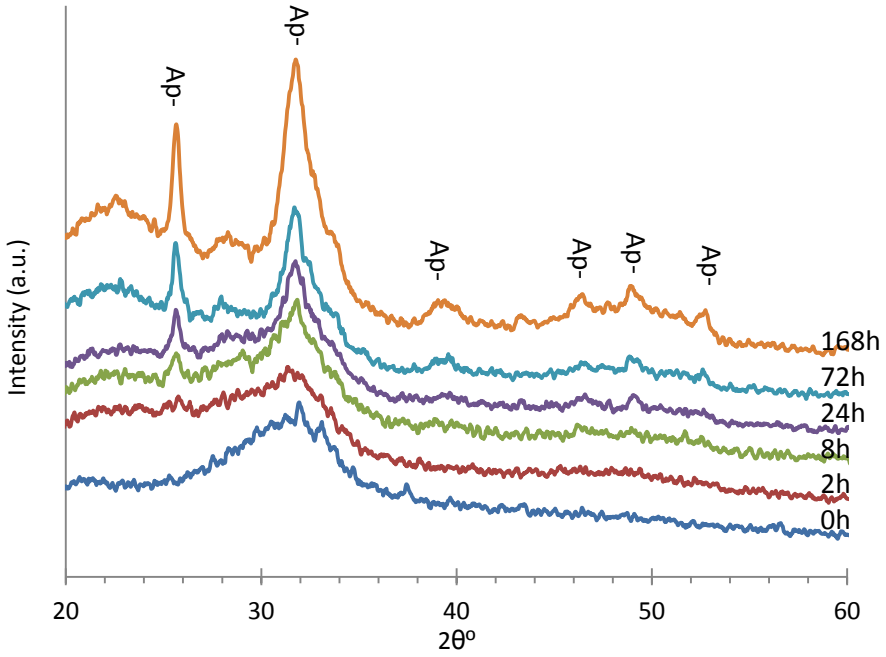

Figure 3.6 XRD traces for bioactive glass P6.33F1 with different immersion time in Tris buffer solution. 75 mg fine bioactive glass particles (P6.33F1) were immersed in 50 ml Tris buffer for different experimental periods followed by a separation of solution and glass powder. Then the dried powders were tested using XRD.

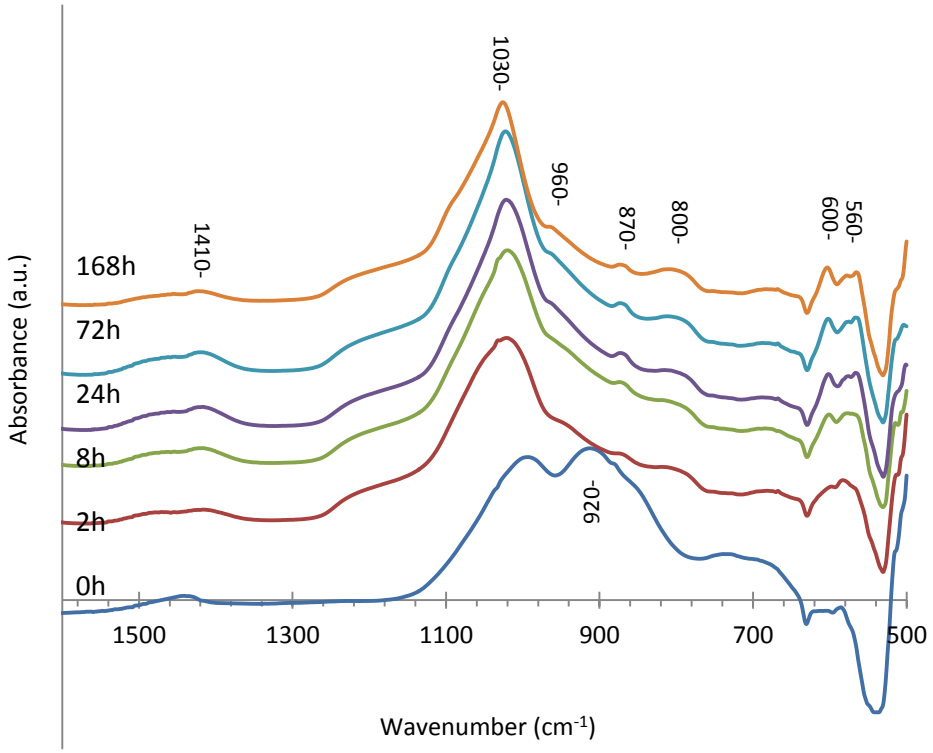

Figure 3.7 FTIR spectra for bioactive glass P6.33F1 with different immersion time in Tris buffer solution. 75 mg fine bioactive glass particles (P6.33F1) were immersed in 50 ml Tris buffer for different experimental periods followed by a separation of solution and glass powder. Then the dried powders were tested using FTIR.

For the apatite formation in the high phosphate but fluoride free bioactive glass P6.33F0 as showed in Fig. 3.8 below, there was no significant changes after immersion in Tris Buffer for 2 to 24 h in comparison to the XRD pattern of the unreacted bioactive glass (0 h). Small peaks at around 28.5° 2θ° (arrowed) after 8 h and 24 h immersion may indicate the presence of a small amount of calcite ($CaCO_3$) instead of apatite. Typical apatite peaks at 26° and 32–34° 2θ° did not appear in the XRD traces until 72 h immersion and a small peak at 26° 2θ° (starred) appeared in the 24 h pattern, which indicates that apatite of bioactive glass P6.33F0 began to form after 24 to 72 h immersion in Tris buffer solution. However, other

typical apatite peaks at 47º, 50º and 52º 2θº did not pronounce clearly even after immersion for 168 h.

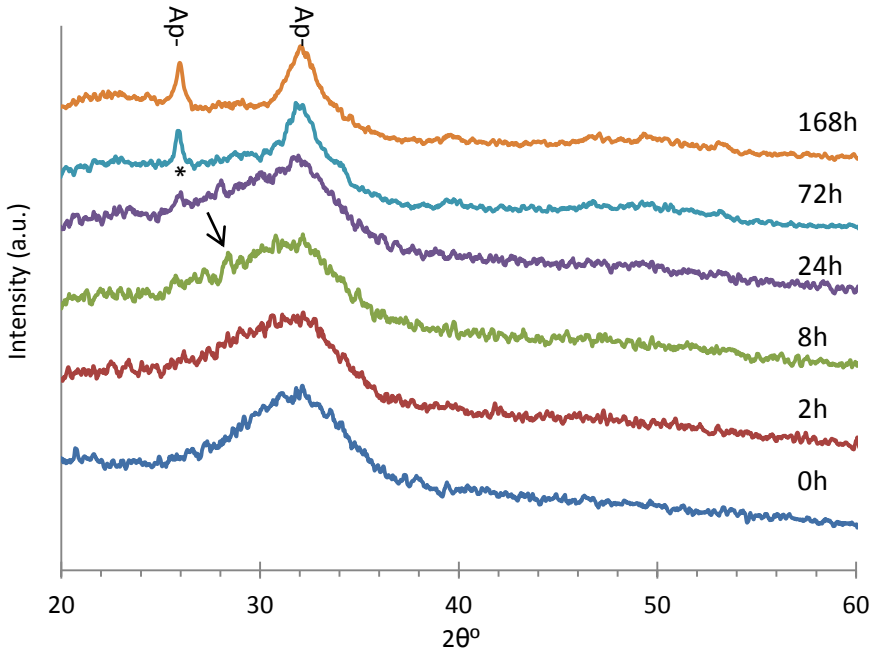

Figure 3.8 XRD traces for bioactive glass P6.33F0 with different immersion time in Tris buffer solution. 75 mg fine bioactive glass particles (P6.33F0) were immersed in 50 ml Tris buffer for different experimental periods followed by a separation of solution and glass powder. Then the dried powders were tested using XRD.

Fig. 3.9 below represents the FTIR spectra of bioactive glass P6.33F0 after immersion in Tris buffer. In comparison with the untreated bioactive glass (0 h), disappearance of the non-bridging oxygens ($Si–O^-$ $alkali^+$) band at 920cm^{-1} and sharpening of the Si–O–Si stretch band at about 1030 cm^{-1} were observed after 2-8 h immersion. As immersion time increased to 24 h, new bands appeared at about 800 cm^{-1} and a single band at 560-600 cm^{-1} indicates the presence of non-apatitic or amorphous calcium phosphate. Characteristic split band at 560 and 600 cm^{-1} indicative of calcium phosphate crystallites appeared at immersion periods of 72 to 168 h. These data indicate that the rate of apatite formation in Tris

buffer solution was significantly accelerated by the fluoride addition (as low as 1 Mol.%).

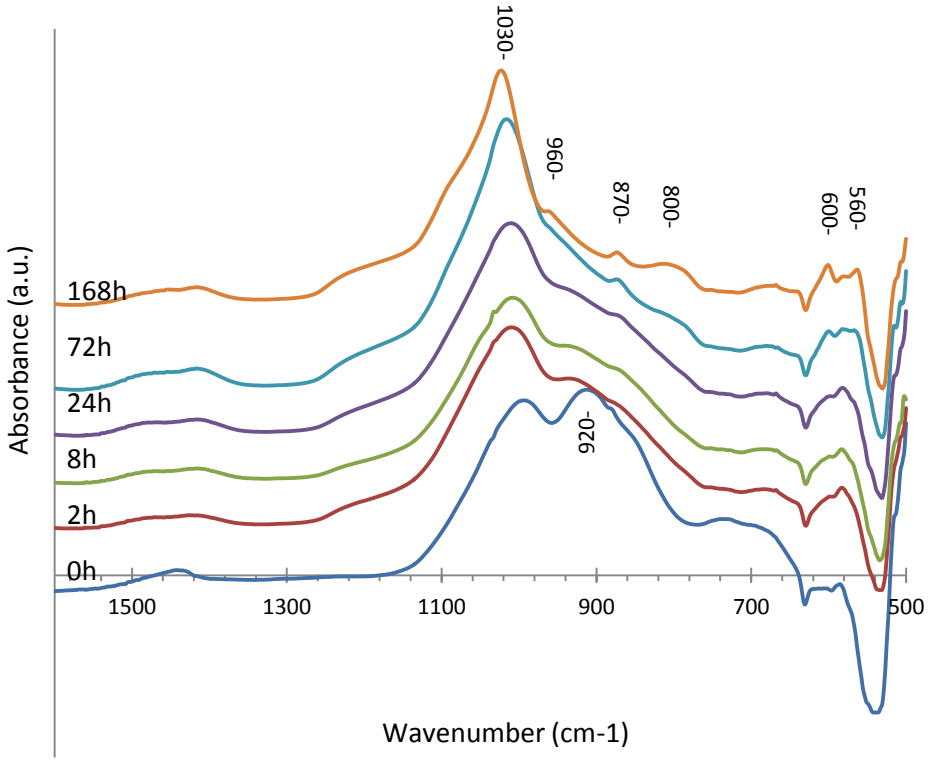

Figure 3.9 FTIR spectra for bioactive glass P6.33F0 with different immersion time in Tris buffer solution. 75 mg fine bioactive glass particles (P6.33F0) were immersed in 50 ml Tris buffer for different experimental periods followed by a separation of solution and glass powder. Then the dried powders were tested using FTIR.

3.2.2.3 Ion release

The Ca and P concentrations in Tirs buffer reached a maximum after 2 h immersion and then dropped drastically from 2 h to 8 h (Fig. 3.10A, C below), which is consistent with the results of XRD and FTIR: that apatite formed in the fluoride added bioactive glasses after 2 h to 8 h immersion and consuming Ca and P in the process.

In bioactive glass compositions, calcium content (derived from CaO and CaF_2) increased gradually as the fluoride content increased from 0% to

7%. For the released Ca concentration change as a function of F content in the bioactive glasses (Fig. 3.10B), after 2 h immersion in Tris buffer, released Ca concentrations rose as F content increased. However, at the later time points from 8 h to 168 h, the released Ca concentration dropped slightly from bioactive glasses P6.33F0 to P6.33F3, then increased when bioactive glass fluoride content increased from 3% to 7%.

Compared with the fluoride containing bioactive glasses, released P concentration of high phosphate but fluoride free bioactive glass P6.33F0 was much higher after 8h (Fig. 3.10C), which indicates incorporation of fluoride promotes phosphate consumption and may result in the acceleration of apatite formation.

P6.33F1, as the lowest fluoride containing bioactive glass in this study, shows some amorphous calcium phosphate formation in the XRD and FTIR patterns after 8 h exposure in Tris buffer. It may explain why the P concentration of P6.33F1 was a little higher than those in the other fluoride added bioactive glasses at the time point of 8h (Fig. 3.10C).

Although the phosphate content was kept constant in all the bioactive glass compositions, the released P concentrations were variable as a function of bioactive glass F content (Fig. 3.10D). At 2 h, the released P concentrations dropped as bioactive glass F content increased from 0-3%. Then it increased from P6.33F3 to P6.33F7 bioactive glasses. However, from 8 h to 168 h immersion in Tris buffer, the released P concentration dropped sharply between the bioactive glasses with 0% fluoride and 1% fluoride, followed with a gradual decrease when the fluoride content increased from 1% to 3% and kept relatively constant at low

concentrations close to 0ppm when the bioactive glass F content increased from 3% to 7%. It indicates that with the high phosphate content in the bioactive glasses, small amount fluoride addition may significantly increase the apatite formation rate evidenced by phosphate consumption.

The fluoride concentrations increased significantly after 2 h immersion in Tris buffer solution in all the investigated bioactive glasses. In the low fluoride containing bioactive glasses, P6.33F1 and P6.33F3, F concentrations decreased gradually from 2 h to 168 h. However, when bioactive glass fluoride content increased from 5% to 7%, the solution fluoride was relatively constant.

Silicon concentrations peaked after 2 h immersion and then kept relative constant in the remaining experimental time. Na concentrations increased sharply in the first 2h immersion and then underwent a further gradual increase in the rest experimental period.

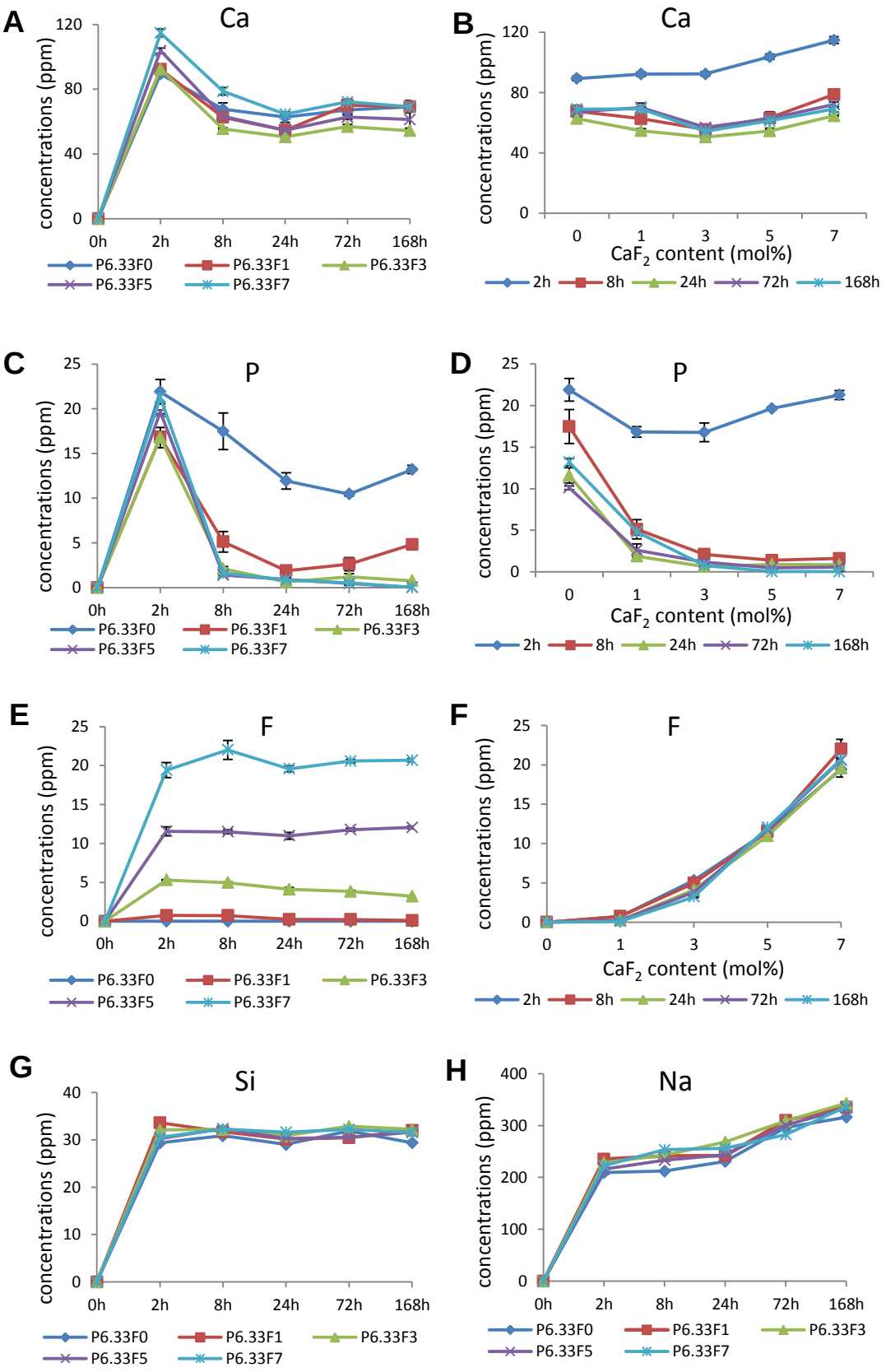

Figure 3.10 Elemental concentrations in Tris buffer vs incubation time and CaF_2 content. 75 mg fine bioactive glass particles were immersed in 50 ml Tris buffer for different experimental periods followed by a separation of solution and glass powder.

Then the filtrates were diluted 1:10 and the elemental concentrations were measured by ICP-OES and a fluoride ion selective electrode. Data was represented as mean ± SE. n=3. (P6.33F0 indicates a bioactive glass contains 6.33 Mol.% phosphate and 0 Mol.% fluoride)

3.2.3 Bioactive glass bioactivity study in cell culture medium

3.2.3.1 Apatite formation

After 72 h immersion in α-MEM, there was no difference between the untreated and treated bioactive glasses in the XRD traces (Fig. 3.11 below). All the treated bioactive glasses showed similar patterns and no typical apatite peaks were observed. A small peak at around 28.5º 2θº appeared in glass P6.33F5, which may indicate the presence of a small amount of calcite ($CaCO_3$) instead of apatite.

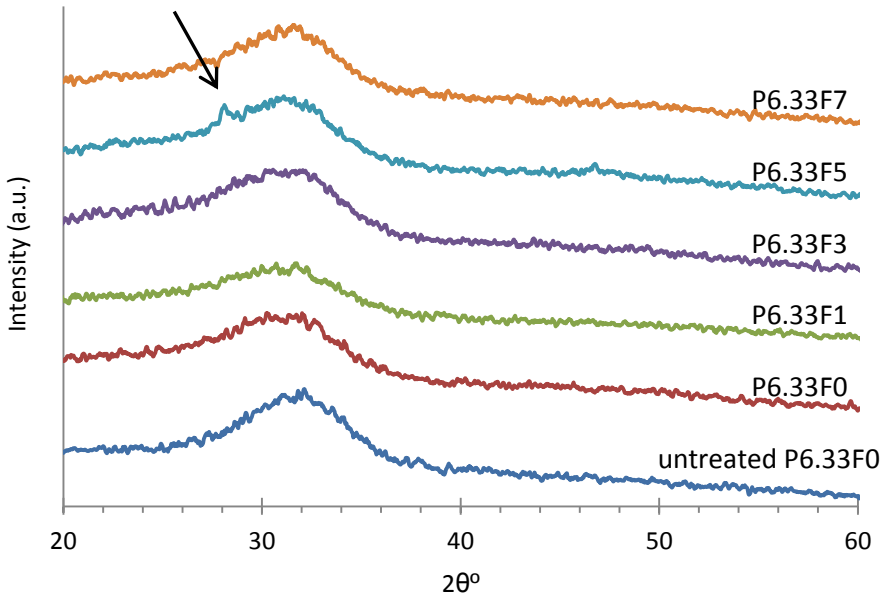

Figure 3.11 XRD traces for bioactive glasses immersed in α-MEM for 72 h. Bioactive glass particulates were immersed in α-MEM then the solution and solids were separated after 72 h. The dried powders were investigated by XRD. (P6.33F0 indicates a bioactive glass contains 6.33 Mol.% phosphate and 0 Mol.% fluoride)

In the FTIR spectra, compared with the untreated bioactive glass with a non-bridging oxygen band at 920 cm^{-1}, all the treated bioactive glasses showed disappearance of 920 cm^{-1} band and the sharpening of the Si-O-Si stretch band at about 1030 cm^{-1} (Fig. 3.12 below). It indicates the formation of a silica-gel surface layer after leaching of Ca^{2+} and Na^{+} ions and formation of Si-OH groups. In all the treated bioactive glasses, a single P-O band was observed at around 570 cm^{-1} and suggests an amorphous or disordered crystalline apatite formation (Jones et al., 2001, Shah et al., 2014b). Furthermore, in the F containing bioactive glasses, new bands at about 870 cm^{-1} and further broad bands starting from 1410 cm^{-1} indicating carbonate replaced phosphate in the formed apatite.

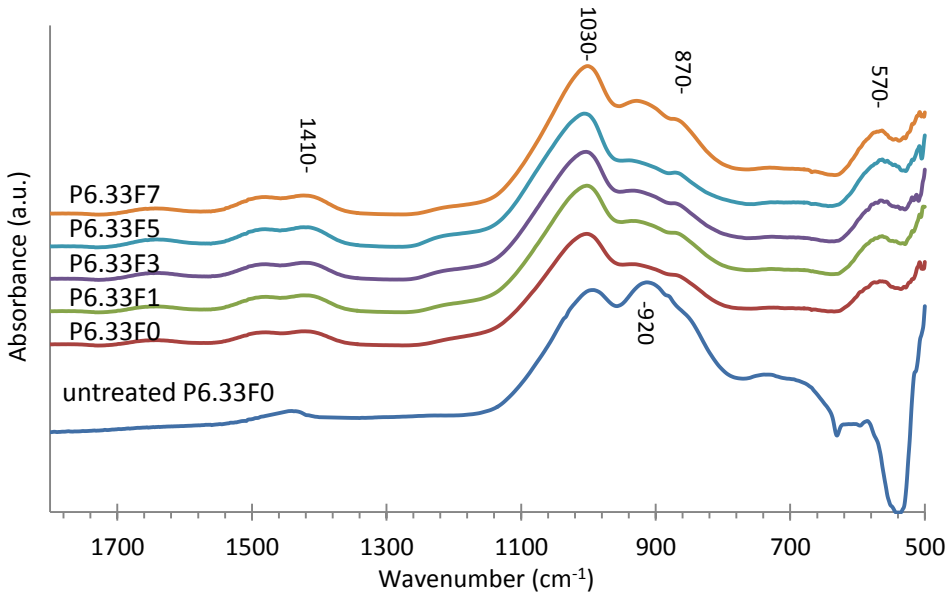

Figure 3.12 FTIR spectra for bioactive glasses immersed in α-MEM for 72 h. Bioactive glass particulates were immersed in α-MEM then the solution and solids were separated after 72 h. The dried powders were investigated by FTIR. (P6.33F0 indicates a bioactive glass contains 6.33 Mol.% phosphate and 0 Mol.% fluoride)

3.2.3.2 Ion release

After 72 h immersion in α-MEM, solution calcium concentrations increased slightly as bioactive glass fluoride content increased from 0% to 7% (Fig. 3.13 below). In the fluoride free and low fluoride containing bioactive glasses (P6.33F0, P6.33F1 and P6.33F3), solution calcium concentrations dropped slightly in comparison with that in the α-MEM. However, for the high fluoride containing bioactive glass, P6.33F7, calcium concentrations were significant higher than that in α-MEM.

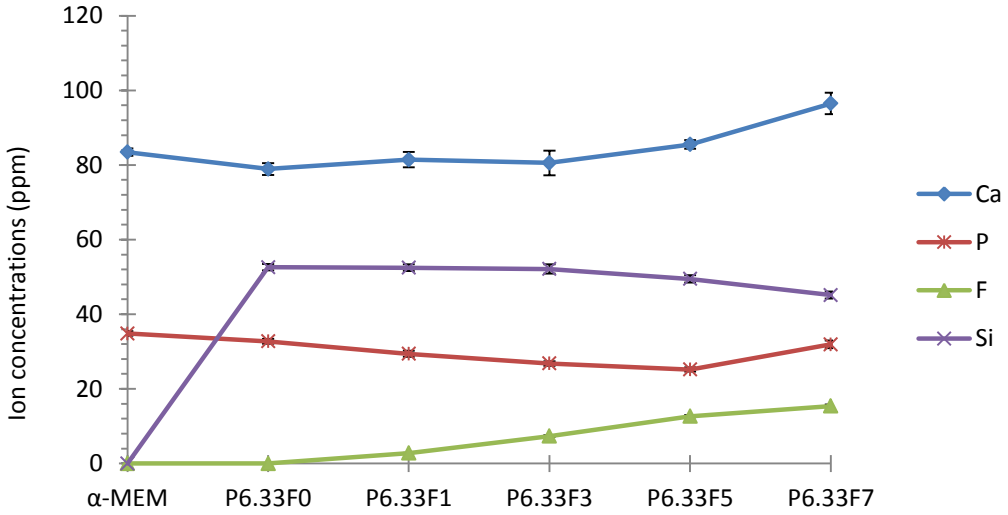

Figure 3.13 Elemental concentrations in α-MEM for 72 h. 75 mg fine bioactive glass particles were immersed in 50 ml α-MEM for 72h followed by a separation of solution and solids. Then the filtrates were diluted 1:10 and the elemental concentrations were measured by ICP-OES and a fluoride ion selective electrode. Data was represented as mean ± SE. n=3. (P6.33F0 indicates a bioactive glass contains 6.33 Mol.% phosphate and 0 Mol.% fluoride)

Phosphate concentration in all the bioactive glass compositions was constant, however, the released concentrations in all the glass groups were little lower than that in the α-MEM and dropped gradually as the

bioactive glass fluoride content increased from 0% to 5% and slight increase was observed in P6.33F7 group.

The α-MEM is silicon and fluoride free (Lonza, London, UK), F concentrations in the medium increased gradually as the bioactive glass fluoride content increased from 0% to 7% during 72 h immersion. Silicon concentrations in the α-MEM was the greatest in the P6.33F0 group and dropped slightly as the glass fluoride content increased. It is consistent with the bioactive glass composition that the glass silicon content decreased as the glass fluoride levels increased (Table 2-1).

3.3 Discussion

It is believed that increasing the P_2O_5 content in the bioactive glass enhances the reactivity of the bioactive glass, as the phosphate is often regarded to exist as a separate phase within the glass which is considerably more soluble than the silicate phase. When the bioactive glass is placed into solution the phosphate phase rapidly dissolves releasing ions (PO_4^{3-}, Ca^{2+} and Na^{+}) and apatite forms quickly (O'Donnell et al., 2009, O'Donnell et al., 2008b, O'Donnell et al., 2008a). However, it is found that, in Tris buffer solution, the formation of apatite occurred even more rapidly with the addition of fluoride (as low as only 1 Mol.%). Numerous experimental studies have reported that octacalcium phosphate (OCP), is a precursor phase, that is involved in apatite formation *in vitro* (Aoba, 1997, Iijima, 2001, Johnsson and Nancollas, 1992, LeGeros et al., 1989, Siew et al., 1992, Tseng et al., 2006). Eanes *et al.* demonstrated that the presence of fluoride eliminated the formation of the intermediate OCP phase (Eanes and Meyer, 1978), and that only 0.1–2 mg/L fluoride in the mineralization solution can promote the hydrolysis of OCP to apatite (Iijima and Moradian-Oldak, 2005, Fan et al., 2009). This may explain why even the 1% fluoride significantly accelerates apatite formation in Tris buffer solution in this study. Furthermore, fluoride can accelerate epitaxial growth of apatite crystals on the OCP precursor, changing the crystal morphology. Fan *et al.* found that as little as 1 mg/L fluoride promoted formation of needle-like nano-crystals on enamel. Such crystals are similar to native crystals in width and thickness and therefore have the potential

to possess similar mechanical properties (Fan et al., 2009, Fan et al., 2007).

In the ion exchange processes (Hench et al., 1971, Hill, 1996): Na^+ cations near the glass surface go into solution in exchange for H^+ ions from the solution (from dissociation of water into H^+ and OH^-), which results in the solution pH increase significantly after 2 h immersion in Tris buffer. As the immersion time increased to 72 h, the ion exchange reaction slowed down resulting in a more gradual pH rise. From 72 h onwards, ion exchange and apatite formation finished in the fluoride containing bioactive glasses therefore the pH tended to stabilize from 72 h to 168 h. However, in the high phosphate, but fluoride free bioactive glass P6.33F0, the speed of reaction and apatite formation was slower, which resulted in continuous pH rise after 72 h immersion. Furthermore, fluoride complexes with calcium and sodium rather than forming Si-F bonds, resulting in decreasing the compactness of the glass network, which may promote greater solubility and make the glass structure easier to break down.

As for the effect of fluoride content in the bioactive glass on the pH in aqueous solution, Brauer *et al*. and Mneimne *et al*. observed a decrease in solution pH as fluoride content increased (Brauer et al., 2010, Mneimne et al., 2011). It was explained that F^- ions can be exchanged for OH^- ions resulting in the removing of hydroxyl ions from solution. Therefore with increasing fluoride content in the bioactive glass, the pH rise was less pronounced. However, in this study, pH slightly increased (approximately 0.07 to 0.14) as fluoride content increased from 0% to 7%. This difference between the studies may be attributed to the differences between

bioactive glass compositions. Brauer *et al*. used glasses with low phosphate content (1.02%-0.72 Mol.%) and high fluoride content (4.75%-32.71 Mol.%) while Mneimne *et al*. designed high fluoride containing glasses with increased phosphate content, which was variable from 4.71% to 6.04 Mol.%. In this research, the bioactive glasses phosphate content was kept high and constant (6.33 Mol.%) while low fluoride concentration varies (1-7%), which may counterbalance the pH changes. In addition, as the total Ca content increased while the F content rose in this bioactive glass compositions, the large amount Ca would consume the acidic phosphate and result in minor pH increases between the F containing and F free bioactive glasses. It has been demonstrated that a high pH environment is favourable for apatite nucleation in SBF (Lu and Leng, 2005a), and Brauer *et al.* suggest that apatite formation was very susceptible to slight pH changes in fluoride containing bioactive glass composition (Brauer et al., 2010). Therefore, in this project, addition of low fluoride content slightly increases Tris buffer pH and may also contribute to the faster apatite formation.

Although the phosphate content was kept constant in all the bioactive glasses, interestingly, the released P concentrations were variable as a function of the fluoride content in the bioactive glasses. From 8 h to 168 h immersion, the solution P concentration dropped sharply between the bioactive glasses P6.33F0 and P6.33F1, followed by a gradual decrease when the fluoride content increased from 1% to 3% and kept relatively constant as it was increased to 7% (Fig. 3.10D). This indicates that the combination of high phosphate content in the bioactive glasses, and a

small amount fluoride may significantly promote the rate of apatite formation as evidenced from XRD and FTIR and, would explain the consumption of phosphate from solution. It is very interesting to notice that in 0-1% F bioactive glasses, especially phosphate free bioactive glass, released P concentrations increased slightly from 72 to 168 h immersion, which may be attributed to the B-type substitution in HA (carbonate replacing a phosphate group) evidenced in the previous FTIR spectra that further broad CO_3^{2-} bands are present in the region starting from 1410 cm^{-1}. However, in the fluoride containing bioactive glasses, formed fluoapatite was more stable than HA, and may resist the B-type substitution to some degree.

In this study, as F content increased from 0 to 7 Mol.%, the Ca content (from CaO and CaF_2) increased slightly and the Ca/P ratio was from 2.05 to 2.47 which is higher than the Ca/P ratio (1.67) of hydroxyapatite ($Ca_{10}(PO_4)_6(OH)_2$). It means that there was sufficient calcium for apatite formation, which may explain the released calcium concentrations in Tris buffer solution was kept at similar levels as a function of F content in bioactive glasses (Fig. 3.10B), unlike the significant variations observed in released P levels (Fig. 3.10D). However, the released Ca concentrations of P6.33F0 (with lowest Ca content in bioactive glass composition) were slightly higher than those in bioactive glasses P6.33F1 and P6.33F3 after 8 to 168 h immersion in Tris buffer, which may be attributed to accelerated apatite formation induced by fluoride that consumes calcium. When the F content increased from 3 to 7%, the released Ca concentrations were consistent with the Ca contents in bioactive glass compositions. However,

Brauer *et al*. (Brauer et al., 2010) observed a decrease in calcium concentration in SBF with increasing CaF_2 content in bioactive glass compositions after 1 w immersion. They attributed this to the formation of apatite and particularly, fluorite (CaF_2), as they decreased the P_2O_5 content from 1.02% to 0.72% when the CaF_2 increased from 4.75% to 32.71%. It may result in the use out of phosphate quickly to form apatite and large amounts of extra calcium and fluoride to form fluorite. Therefore, the higher F content in bioactive glasses, more Ca was consumed to form fluorite. However, in the bioactive glass compositions in this study, P_2O_5 content was 6.33% with low fluoride addition (0-7 Mol.%). It suggests that the released calcium was used to form apatite instead of fluorite, which explains the results of released Ca concentrations in Tris buffer solution as a function of F content in bioactive glasses

For the Si release into Tris Buffer solution, Brauer *et al.* previously suggested that apatite formed in SBF once Si had reached the solubility limit (around 60 ppm), as the formation of silica gel layer is regarded to aid the nucleation of apatite (Brauer et al., 2010). However, in this project, it is observed that the presence of silica-gel formation in FTIR for glass P6.33F3 after immersion in Tris buffer for 2 h, while the Si concentrations did not reach the solubility limit at this time point (around 30 ppm). It suggests that Si concentration in solution is less predictive of silica-gel and apatite formation as previously contested. These results are also confirmed by other researchers (Mneimne et al., 2011, Lusvardi et al., 2009). For the Na concentrations, it is known that in the ion exchange process apatite formation starts from the exchange of bioactive glass Na^+

with solution H^+, which results in the solution Na^+ concentration increasing drastically in the first 2 h immersion. The gradual increase during the remainder of the experiment may be attributed to the further release of small amounts of Na from the bioactive glasses.

Compared to Tris buffer solution testing, experiments with cell culture medium may provide a more *in vivo-like* model to examine how bodily fluids will interact with bioactive glasses. It is known that FTIR can give information on a range of structural changes during the dissolution and apatite crystallization process, such as changes to the silicate network. However, FTIR cannot unambiguously identify apatite as it can show the presence of crystalline orthophosphates. XRD allows for the identification of various phases such as apatite, calcite, or fluorite, but it is not suited to distinguish between different apatites, such as HA, HCA, or FAp when they are present as small crystallites (Shah et al., 2014b). After 72 h immersion in cell culture medium α-MEM, it is observed that a single band at approximately 570 cm^{-1} (Fig. 3.12), corresponding to the formation of an amorphous or disordered crystalline apatite such as OCP or amorphous calcium phosphate, which is considered as a precursor of apatite. O'Donnell *et al*. found that apatite formed in physiological solutions (SBF) in nanosized crystals (O'Donnell et al., 2009), which would not cause significant apatite peaks in XRD. Compared with the apatite formation in Tris buffer, the rate of formation is much slower in α-MEM. Sepulveda *et al.* attributed the delayed surface apatite formation in cell culture medium to the presence of proteins from serum (Sepulveda et al., 2002). In this study, however, serum was not added until the bioactive glass conditioned

α-MEM was used to treat cells, thus unable to interfere with the dissolution process. Magnesium (Mg), is involved in numerous metabolic pathways such as protein and nucleic acid synthesis, cell cycle, cytoskeletal integrity and bone remodelling (Diba et al., 2012, Staiger et al., 2006), is included in cell culture medium at a concentration of 0.8 mM. However, Mg^{2+} ion retards apatite formation, by adsorption onto crystal surfaces and blocking active growth sites, irrespective of whether Mg^{2+} ion originates from test medium or from the bioactive glass (Barrere et al., 2002, Dietrich et al., 2009, Ma et al., 2011). Mg^{2+} can inhibit crystallization of the formed amorphous apatite layer through entering the forming hydroxyapatite nuclei and reduce apatite crystal growth (Diba et al., 2012, Vallet-Regi et al., 1999). Jallot *et al*. firstly demonstrated the presence of Mg in the Ca–P rich layer, but the Mg substituted apatite may be Ca deficient, which is more soluble than stoichiometric apatite (Jallot, 2003). Although Mg^{2+} slows down apatite layer formation, it is found to increase the layer thickness (Vallet-Regi et al., 1999, Dietrich et al., 2009). The Mg-substituted hydroxyapatite materials were demonstrated to have excellent biocompatible and show greater osteoconductivity and higher material resorption (Ma et al., 2010). Furthermore, compared with the mechanism and kinetics of glass dissolution *in vivo*, this *in vitro* study differs. The continuous flow of physiological fluids promotes continuous glass dissolution, leading to thicker apatite layers *in vivo* (Sepulveda et al., 2002). Therefore, such high phosphate, low fluoride containing bioactive glasses may be useful to accelerate bone defect regeneration when applied *in vivo*.

3.4 Future work

It was found that apatite formation was significantly accelerated in bioactive glasses with addition of fluoride after immersion in Tris buffer solution. Whilst, FAp formation was reported in previous publications (Brauer et al., 2010, Mneimne et al., 2011), it is more acid resistant than hydroxyapatite, has better stability and slow of degradation kinetics (Al-Noaman et al., 2013). In this study, FAp could not be identified by XRD and FTIR. Therefore, ^{19}F MAS–NMR could be used to further explore whether FAp is generated by these bioactive glasses.

For the investigation of bioactive glass bioactivity in cell culture, apatite formation was delayed or nano-sized apatite formed, as we did not find significant apatite peaks by XRD. Therefore, in the next step the experimental period can be prolonged and, ^{19}F MAS–NMR can be used to further explore the bioactive glass bioactivity in cell culture medium.

In order to replicate the *in vivo* situation more closely, a perfusion system with a constantly refreshing medium environment can be designed and conducted to investigate the apatite formation.

Chapter 4 Osteoblast responses

4.1 Introduction

Osteoblasts, developed from the osteoblasts progenitor populations (periosteal and endosteal), are the main cells in the new bone formation process as they are responsible for the synthesis and secretion of bone matrix in mineralization.

Numerous *in vitro* and animal studies have demonstrated that fluoride can regulate bone-forming cell activities (Farley et al., 1983, Fernandes et al., 2012, Huo et al., 2013, Kassem et al., 1994, Okuda et al., 1990, Pei et al., 2012, Qu et al., 2008, Ren et al., 2011, Wang et al., 2011, Yan et al., 2009). Furthermore, F^- can be incorporated into bioactive glasses by complexing with calcium and sodium and F^- significantly accelerates the apatite formation in Tris buffer as represented in the last Chapter. FAp, which is more acid resistant, is formed upon immersion of fluoride containing glasses into SBF (Brauer et al., 2010). For these reasons, the addition of fluoride into bioactive glass with later local delivery at appropriate concentrations would be beneficial for bone forming cells in dental and orthopaedic applications. However, high levels of systemic fluoride are known to cause skeletal and dental fluorosis characterized by debilitating changes in the skeleton, and marked mottling and discoloration in the teeth (Chachra et al., 2008, Vestergaard et al., 2008) and caution must be applied.

For efficient osteogenesis, angiogenesis with vascular network development plays a crucial role, as bone-forming cells are highly metabolic requiring the supply of oxygen, nutrients and elimination of their byproducts. VEGF, released by osteoblastic and other cells (Spector et al., 2001, Zelzer and Olsen, 2005), can promote differentiation of local mesenchymal stem cells into endothelial cells and, subsequently activate the transmembrane VEFGR2 receptors in endothelial cells, which in turn activates several pathways responsible for angiogenesis during the new bone formation and has therapeutic value for bone applications (Weibing and Wang, 2014, Schliephake et al., 2015, Izuagie et al., 2015, Bose et al., 2013).

Therefore, the aim of this Chapter is to investigate the osteogenic and angiogenic responses of osteoblast MC3T3-E1 to F^- concentrations and conditioned medium derived from novel fluoride containing bioactive glasses.

4.2 Results

4.2.1 Cellular response to NaF concentrations

4.2.1.1 Cell proliferation and differentiation

To confirm the effects of fluoride at various concentrations on the proliferation and differentiation of MC3T3-E1, a bisbenzimidazole-chelation assay to assess DNA content by fluorescence intensity and an ALP-based assay generating a coloured reaction product measured spectrophotometrically were used.

For the F^- induced proliferation as showed in Fig. 4.1, compared with control group (0 ppm), the high fluoride concentrations, 9.5 and 19 ppm, suppressed MC3T3-E1 proliferation significantly in the whole experimental period. Other concentrations (0.1-1.9 ppm) showed increased levels in proliferation, but there was no statistical difference.

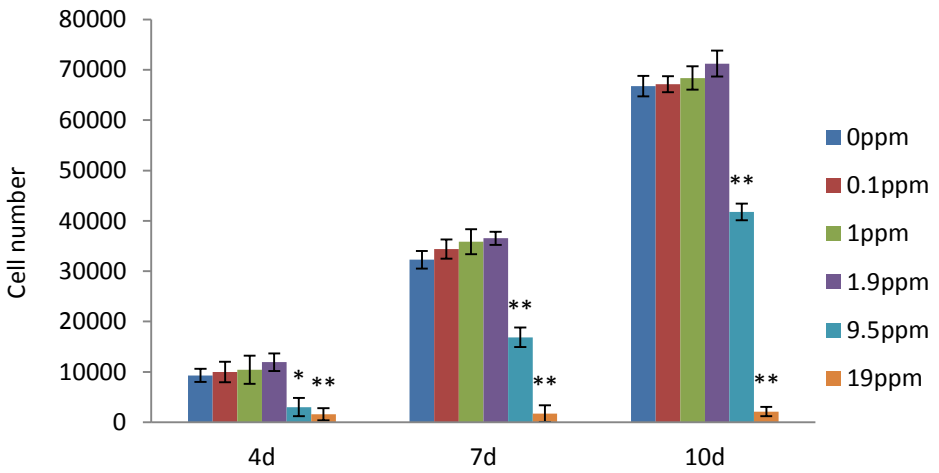

Figure 4.1 Effects of F^- concentrations on cell proliferation in MC3T3-E1. Cells were treated with fluoride at a range concentration for 1 d, 4 d, 7 d, and 10 d. After treatment, cell proliferation was estimated using a bisbenzimidazole-chelation assay to assess DNA content by fluorescence intensity. Results are indicated the cell number. Each bar represents mean ± SE of ten independent experiments. * *P* <0.05 or ** *P* <0.01, compared with 0 ppm group.

Fig. 4.2 represents the effects of F^- concentrations on MC3T3-E1 differentiation. It is found that 0.1 ppm F^- significantly promoted differentiation over the whole experimental period (4 d to 10 d). However, the high doses fluoride in this study (9.5 ppm and 19 ppm, equal to $5x10^{-4}$ and 10^{-3} M) suppressed MC3T3-E1 differentiation significantly. For the middle fluoride concentrations (1 ppm and 1.9 ppm), There were no significantly positive or negative effects on MC3T3-E1 differentiation.

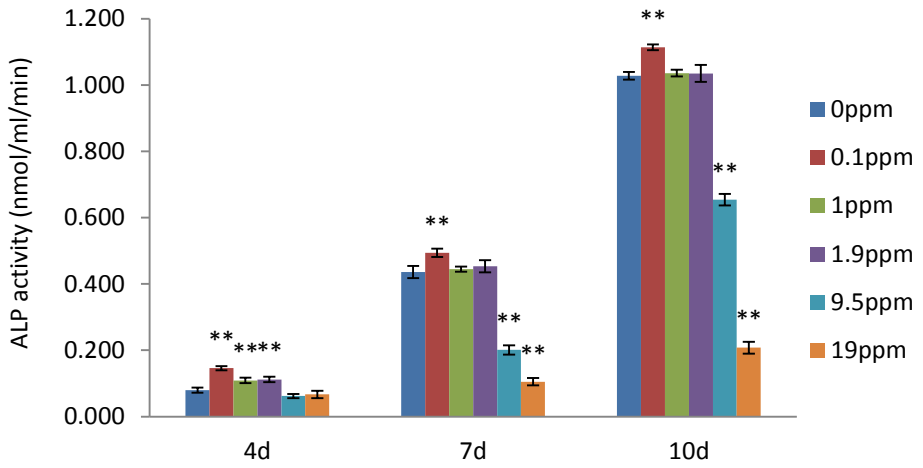

Figure 4.2 Effects of F^- concentrations on cell differentiation in MC3T3-E1. Cells were treated with fluoride at a range concentration for 1 d, 4 d, 7 d, and 10 d. After treatment, cell differentiation was estimated by using ALP assay. Results are indicated the ALP activity (nmol/ml/min). Each bar represents mean ± SE of ten independent experiments. * *P* <0.05 or ** *P* <0.01, compared with 0 ppm group.

4.2.2 Cytotoxicity of bioactive glass conditioned medium on osteoblasts

Compared with the control (normal medium without bioactive glass immersion), all the bioactive glass conditioned medium samples, except 7% F^- bioactive glass at 72 h, were not cytotoxic to the growth of MC3T3-E1 cells (Fig. 4.3 A, B, C, D). In the 72 h conditioned medium, levels of MTT reaction products were significantly higher in the bioactive glass

groups, 0-3% F content. However, this increase is small, and might be without meaning.

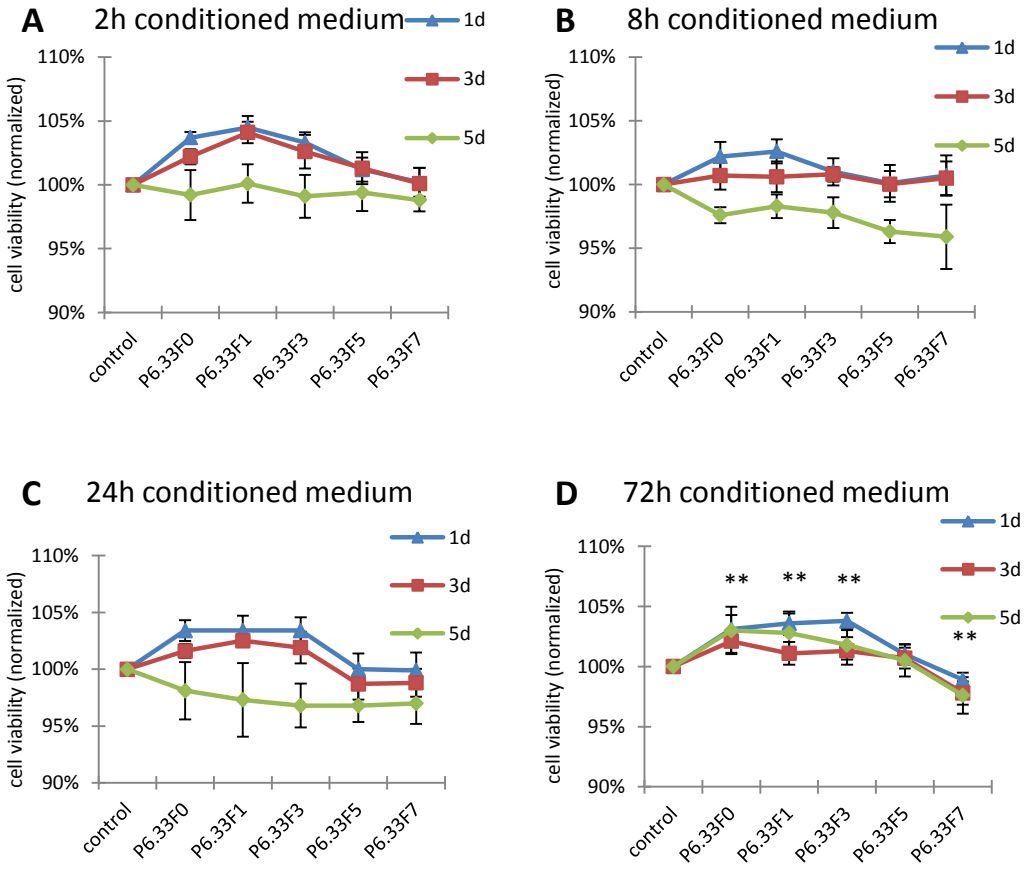

Figure 4.3 Cytotoxicity of bioactive glass conditioned medium on MC3T3-E1. Cells were treated with different conditioned medium (2 h, 8 h, 24 h and 72 h) for 1 d, 3 d and 5 d. After treatment, cytotoxicity was estimated using MTT assay. Results are indicated the normalized data. Each marker represents mean ± SE of six independent experiments. ** *P* <0.01, compared with control group. (P6.33F0 indicates a bioactive glass contains 6.33 Mol.% phosphate and 0 Mol.% fluoride)

4.2.3 Cellular response to 72 h bioactive glass conditioned medium

4.2.3.1 Total quantification of cells cultured in bioactive glass conditioned medium

MC3T3-E1 proliferation in 72 h conditioned medium varied depending on the bioactive glass composition (Fig. 4.4). Cell numbers were calculated

through an established calibration curve. The number of cells that survived was too few to be detected in the high F addition group (P6.33F7). However, significantly more cells were observed in P6.33F0 and P6.33F1 groups than non-conditioned medium (control) from 7 d to 21 d in culture. The cell number was significantly lower in the P6.33F5 group compared with the control group.

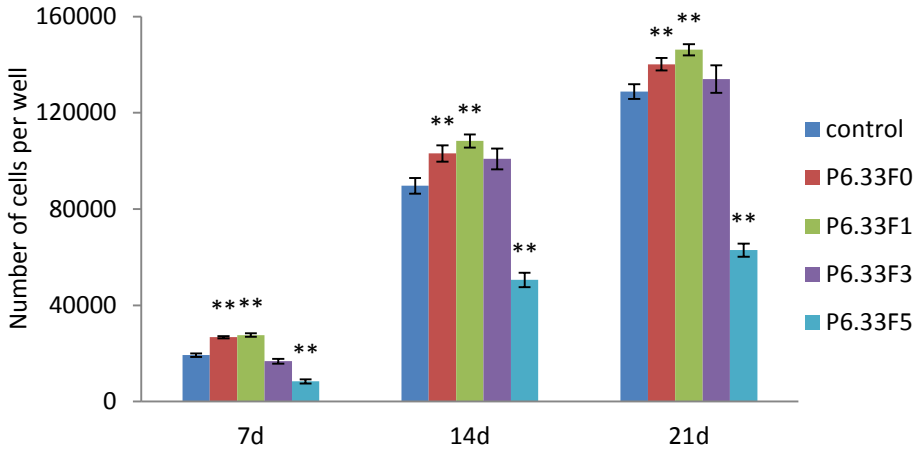

Figure 4.4 Effects of bioactive glass conditioned medium on cell proliferation in MC3T3-E1. Cells were treated in 72 h bioactive glass conditioned medium for 7 d, 14 d and 21 d. After treatment, cell proliferation was estimated using the bisbenzimidazole-chelation assay to assess DNA content by fluorescence intensity. Results are indicated the cell number. Each bar represents mean ± SE of ten independent experiments. * *P* <0.05 or ** *P* <0.01, compared with control group. (P6.33F0 indicates a bioactive glass contains 6.33 Mol.% phosphate and 0 Mol.% fluoride)

4.2.3.2 Alkaline phosphatase (ALP) activity in cells cultured in bioactive glass conditioned medium

After treating for 7 d, 14 d and 21 d in the bioactive glass conditioned medium, MC3T3-E1 cells in the P6.33F0 and P6.33F1 groups produced significantly higher ALP activity than those in the control. At the time points of 14 d and 21 d, ALP activity in P6.33F1 was significantly higher than that

in P6.33F0. While in the 5% F addition glass (P6.33F5), ALP activity was significantly suppressed (Fig. 4.5).

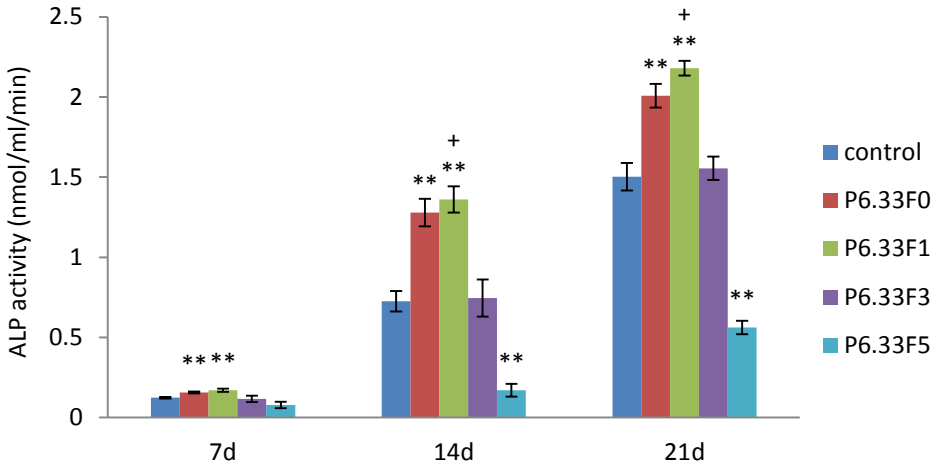

Figure 4.5 Effects of bioactive glass conditioned medium on cell differentiation in MC3T3-E1. Cells were treated with 72 h bioactive glass conditioned medium for 7 d, 14 d and 21 d. After treatment, cell differentiation was estimated using ALP assay. Results are indicated the ALP activity (nmol/ml/min). Each bar represents mean ± SE of ten independent experiments. * *P* <0.05 or ** *P* <0.01, compared with control group. + *P* <0.05, compared with P6.33F0. (P6.33F0 indicates a bioactive glass contains 6.33 Mol.% phosphate and 0 Mol.% fluoride)

4.2.3.3 Type I collagen formation in bioactive glass conditioned medium

Type I collagen formation was significantly promoted in P6.33F0 and P6.33F1 groups in comparison with that in control after 2 w, 3 w and 4 w culture (Fig. 4.6). At the time points of 2 w and 3 w, bioactive glass P6.33F1 induced more Type I collagen formation than P6.33F0. However, in the latest time point (4 w), it was significantly suppressed in 5% F addition group (P6.33F5).

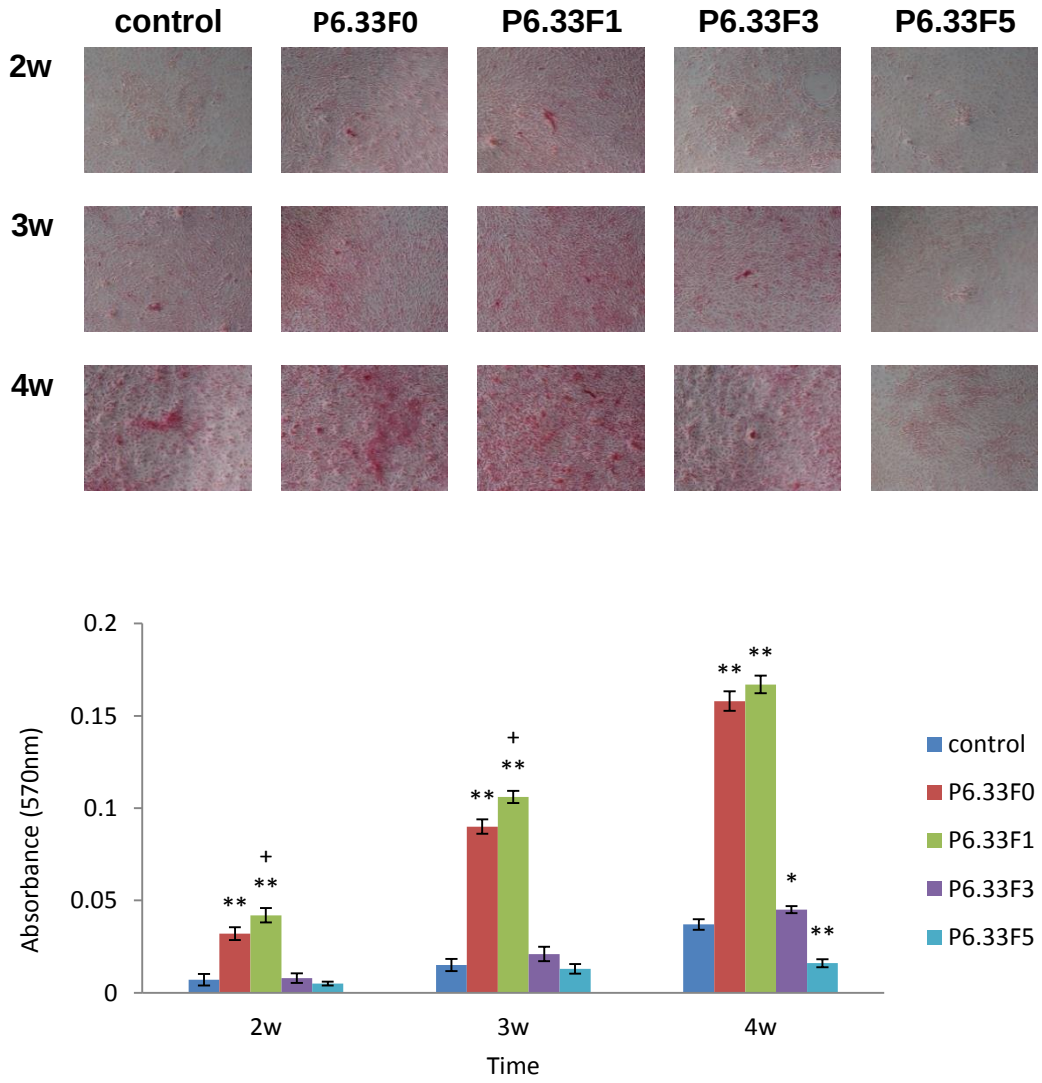

Figure 4.6 Qualitative and quantitative results of Type I collagen formation in MC3T3-E1. After treatment in bioactive glass conditioned medium for 2 w, 3 w and 4 w, cells were incubated with Picro-Sirius red for collagen staining then the dye was extracted by incubation with NaOH and methanol mix for quantitative analysis. Each bar represents mean ± SE of three independent experiments. * *P* <0.05 or ** *P* <0.01, compared with the control. + *P* <0.05, compared with P6.33F0. (P6.33F0 indicates a bioactive glass contains 6.33 Mol.% phosphate and 0 Mol.% fluoride)

4.2.3.4 Cell mineralization in bioactive glass conditioned medium

Fig. 4.7 represents the qualitative and quantitative results of MC3T3-E1 mineralization in bioactive glass conditioned medium. It was significantly promoted in the P6.33F0 and P6.33F1 groups, in comparison with the

control after 2 w, 3 w and 4 w culture. At 2 w and 3 w, mineralization in P6.33F1 was significantly higher than that in P6.33F0. For the P6.33F3 group, mineralization was significantly promoted in the later time points (3 w and 4 w). However, in the 5% F addition group (P6.33F5), mineralization was significantly suppressed in all the treatment periods.

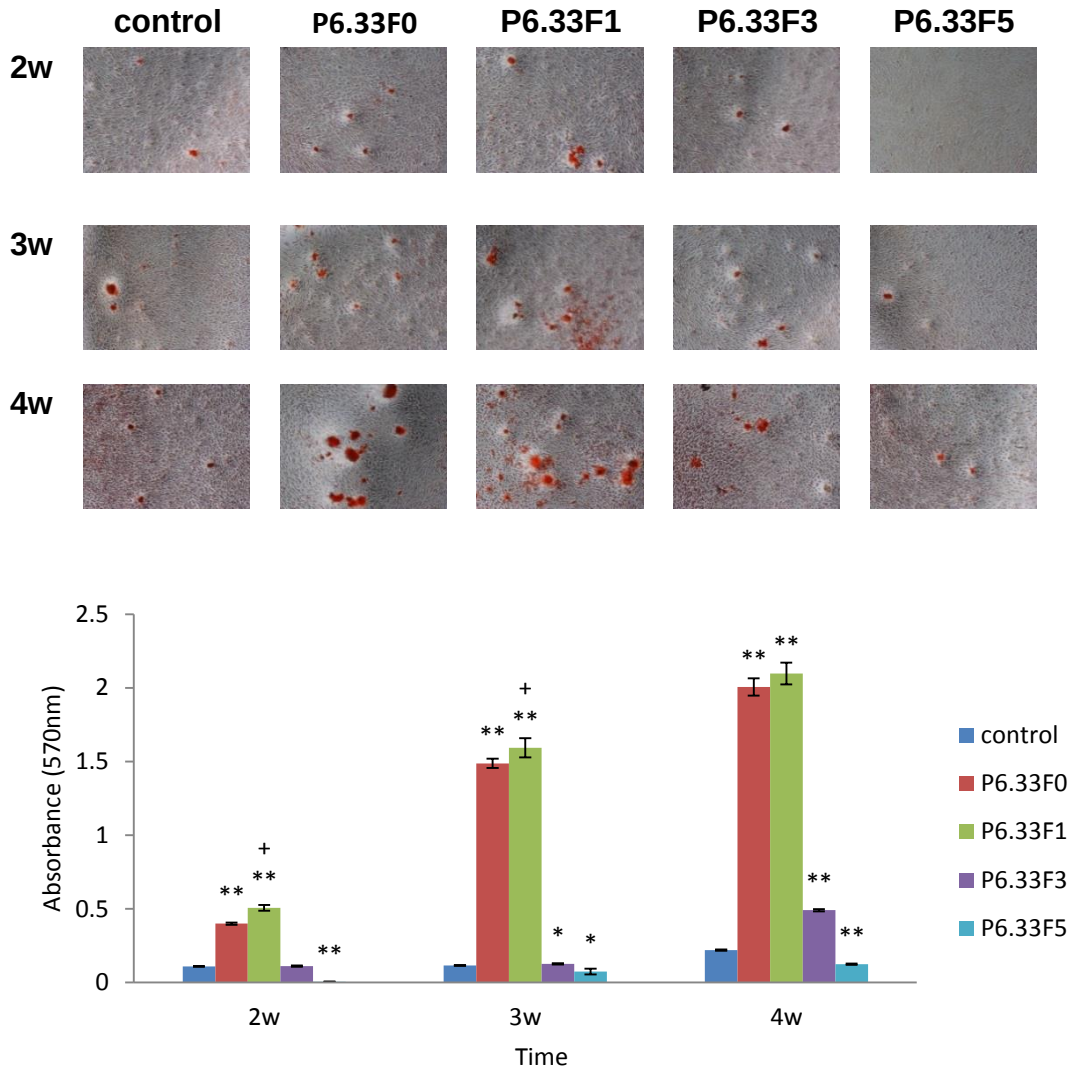

Figure 4.7 Qualitative and quantitative results of MC3T3-E1 mineralization in bioactive glass conditioned medium. After treatment in bioactive glass conditioned medium for 2 w, 3 w and 4 w, cells were incubated with Alizarin red S for bone nodule staining then the dye was extracted by incubation in 10% (w/v) cetylpyridinium chloride in 10 mM sodium phosphate for quantitative analysis. Each bar represents mean ± SE of three independent experiments. * P <0.05 or ** P <0.01, compared with the control. + P <0.05, compared with P6.33F0. (P6.33F0 indicates a bioactive glass contains 6.33 Mol.% phosphate and 0 Mol.% fluoride)

4.2.3.5 Osteogenic gene expression in bioactive glass conditioned medium

The expression of genes associated with osteogenesis, Col1a1 and OPN, were investigated as shown in Fig. 4.8. Gene expression increased in the P6.33F0 and P6.33F1 groups in comparison with those in the control from 1 d to 21 d. Furthermore, they were greater in P6.33F1 than those in the P6.33F0 through the whole experimental period. However, both Col1a1 and OPN gene expression significantly decreased in the P6.33F5 group.

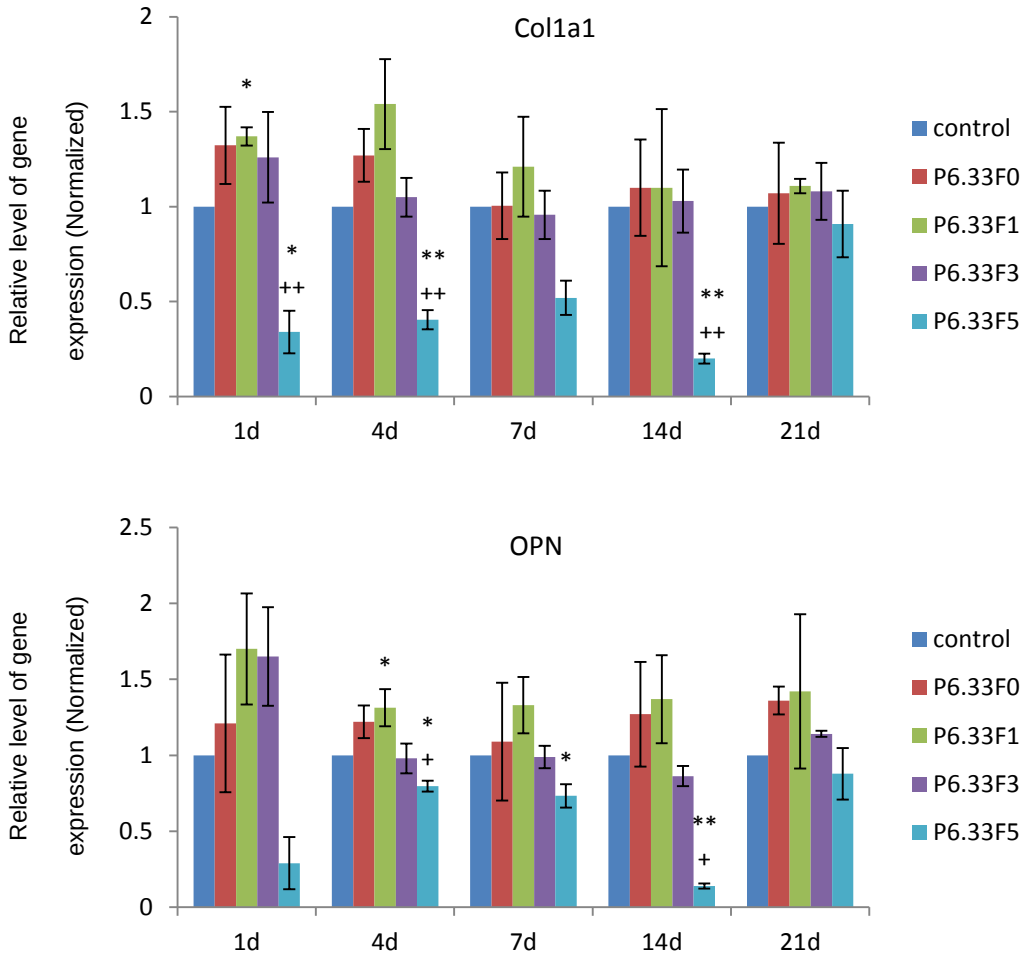

Figure 4.8 Expression of pre-osteogenic markers. After treatment in bioactive glass conditioned medium, cells were collected for mRNA extraction, cDNA synthesis followed by qPCR to quantify the OPN and Col1a1 gene expression in MC3T3-E1. Normalized by control and each bar represents mean ± SE of three independent experiments. * *P* <0.05

or ** *P* <0.01, compared with the control. (P6.33F0 indicates a bioactive glass contains 6.33 Mol.% phosphate and 0 Mol.% fluoride)

4.2.3.6 Angiogenic gene expression and protein production in bioactive glass conditioned medium and F^- concentrations

Compared with the control, VEGF gene expression was promoted by all the investigated bioactive glasses (P6.33F0 to P6.33F5) from 1 d to 21 d treatment (Fig. 4.9). When comparing the fluoride free glass (P6.33F0) and fluoride containing glasses (P6.33F1 to P6.33F5), the later exhibit greater levels of VEGF gene expression at the later time points of 14 d and 21 d.

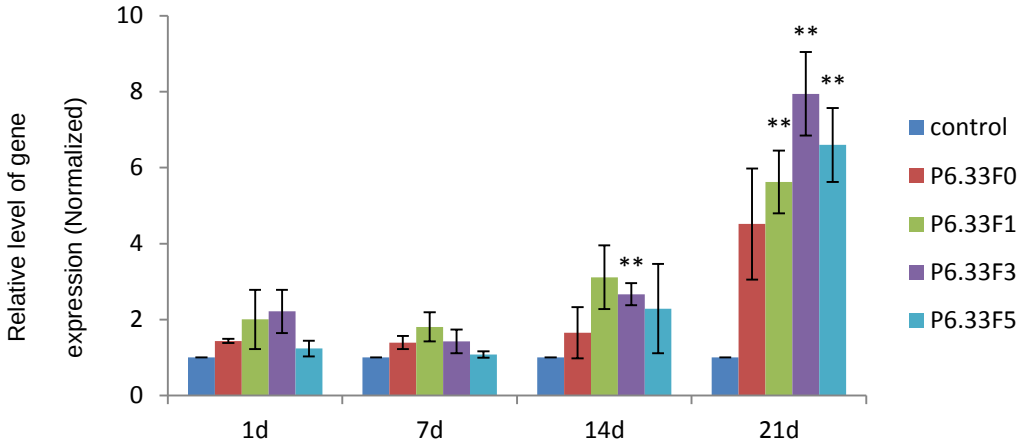

Figure 4.9 VEGF gene expression. After treatment in bioactive glass conditioned medium, cells were collected for mRNA extraction, cDNA synthesis followed by qPCR to quantify the VEGF gene expression in MC3T3-E1. Normalized by control and each bar represents mean ± SE of three independent experiments. * *P* <0.05 or ** *P* <0.01, compared with the control. (P6.33F0 indicates a bioactive glass contains 6.33 Mol.% phosphate and 0 Mol.% fluoride)

As for the VEGF protein production after treatment in bioactive glass conditioned medium (Fig. 4.10), no significant difference was observed between bioactive glass and control groups at 7 d. However, at 14 d and

21 d, greater VEGF protein production was observed in all the bioactive glass groups. Similar to the VEGF gene expression, the protein expression was also further promoted by the fluoride containing bioactive glasses than the fluoride free bioactive glass (P6.33F0).

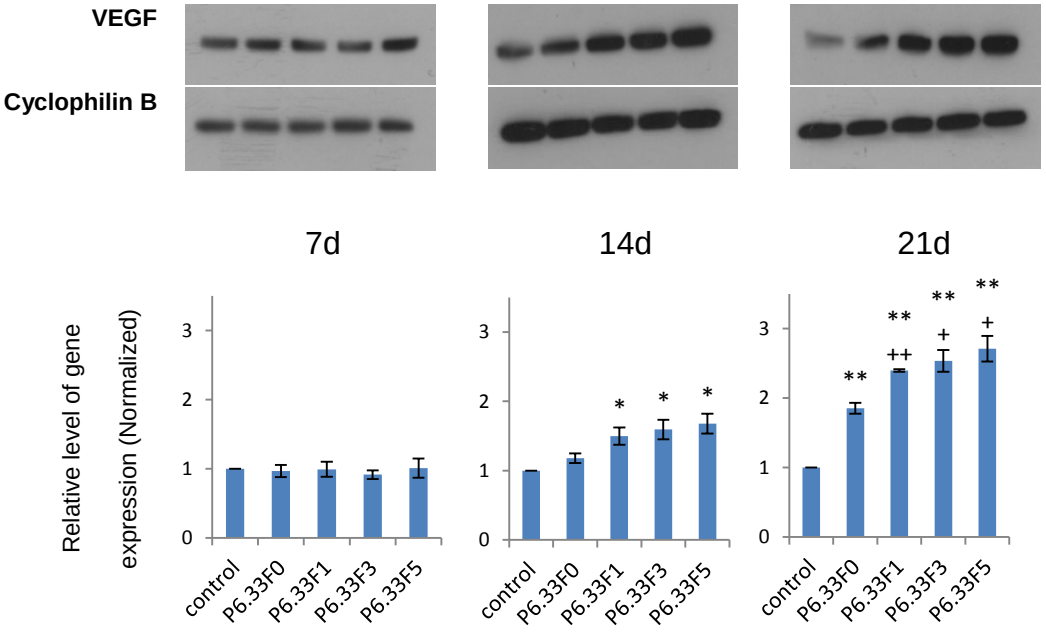

Figure 4.10 VEGF protein production by MC3T3-E1 in bioactive glass conditioned medium. After treatment in bioactive glass conditioned medium, cells were collected for protein extraction and the VEGF protein production was qualified using Western Blot and quantified by Image J. Normalized by the control and each bar represents mean ± SE of three independent experiments. * *P* <0.05 or ** *P* <0.01, compared with control group. + *P* <0.05, compared with P6.33F0 group. (P6.33F0 indicates a bioactive glass contains 6.33 Mol.% phosphate and 0 Mol.% fluoride)

The effects of F^- concentrations on VEGF protein production as showed in Fig. 4.11 below. After treating with NaF concentrations (F^- concentrations: 0 - 9.5 ppm) for 7 d, it is found that VEGF protein production was slightly promoted by all the fluoride groups and significantly higher in the 9.5 ppm group, in comparison with the control (0 ppm). However, at 14 d, there was no significant difference between control and fluoride groups. At 21 d, MC3T3-E1 cells treated by the normal medium (control) produced slightly

more VEGF protein than those treated by fluoride concentrations. But there was no statistical difference between them.

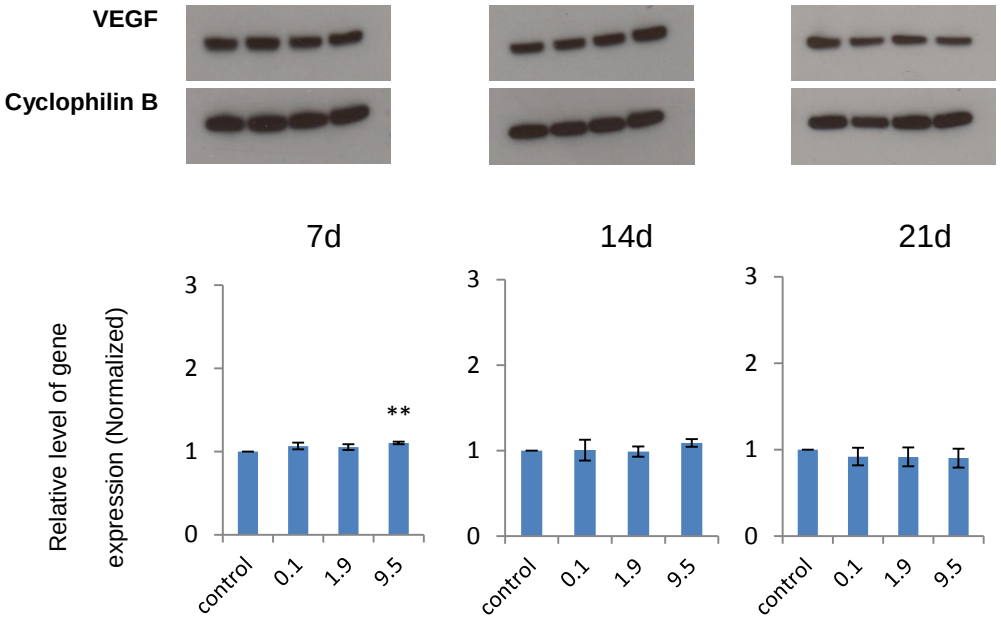

Figure 4.11 VEGF protein production by MC3T3-E1 in F^- concentrations. After treatment by NaF concentrations, cells were collected for protein extraction and the VEGF protein production was qualified using Western Blot and quantified by Image J. Normalized by the control and each bar represents mean ± SE of three independent experiments. * *P* <0.05 or ** *P* <0.01, compared with control group.

4.3 Discussion

Compared to Tris buffer solution testing, experiments with cell culture medium may provide a more *in vivo-like* model to examine how bodily fluids will interact with bioactive glasses. All potential dental and orthopaedic biomaterials are routinely investigated by cell culture for biocompatibility. Therefore, keeping the same conditions as for the Tris buffer experiments, bioactive glass conditioned medium was produced (immersed for 2 h, 8 h, 24 h and 72 h) and then used to treat MC3T3-E1 cells. It is found that the cell viability dropped as the treating time increased from 1 d to 5 d in the 2 h, 8 h and 24 h bioactive glass conditioned medium, which may attribute to the toxicity of high ion concentrations in the early immersed period (2 h, 8 h and 24 h). When the immersion time increased to 72 h, reactions between bioactive glass particles and surrounded solution tended stabilized, leading to the promoted cell viability in the 72 h bioactive glass conditioned medium.

Therefore, 72 h bioactive glass conditioned medium was used to investigate the bioactive glass composition on the MC3T3-E1 cell osteogenic responses including proliferation, ALP activity, Type I collagen formation, bone nodule formation and osteogenic gene expression. It was found that those osteogenic activities were promoted by the high phosphate, F free or low F addition bioactive glasses (P6.33F0 to P6.33F1) but significantly suppressed when the F content increased to 5-7%.

Inorganic phosphate plays a vital role and is essential for the biological mineralization, which is continual throughout life and is mainly achieved by

the function of osteoblasts, the activation of specific genes like ALP, osteopontin and osteocalcin and inorganic ions calcium and phosphate (Beck, 2003, Beck et al., 2003, Beck et al., 1998). Here, the high phosphate containing glasses resulted in the phosphate concentrations in bioactive glass conditioned medium kept similar to that in α-MEM (Fig. 3.13), avoiding consumption of cell culture medium phosphate to form apatite. In bioactive glasses, silicon acts as network former, and numerous studies have demonstrated its stimulatory effects on cellular activities, such as regulating the expression of key osteoblastic marker genes, cell cycle regulators and extracellular matrix proteins, stimulate new bone formation in animal models, inhibit osteoclast phenotypic gene expressions, osteoclast formation and bone resorption *in vitro*, although the exact mechanism is yet to be understood (Calvo-Guirado et al., 2014, Chadwick et al., 2014, Friederichs et al., 2015, Henstock et al., 2015, Manchon et al., 2015, Mladenovic et al., 2014, Odatsu et al., 2015). In this study, the released silicon concentrations into cell culture medium ranged from 45 to 52 ppm depending on the bioactive glass compositions. Therefore, when compared with the control (no bioactive glass) in this study, the promoted osteogenic responses including proliferation, ALP activity, Type I collagen formation, bone nodule formation and osteogenic gene expression in MC3T3-E1 osteoblastic cells by the high phosphate but fluoride free bioactive glass (P6.33F0) may be attributed to the effects of phosphate and silicon.

However, those activities were further increased in the P6.33F1 bioactive glass and significantly suppressed when the F content increased to 5-7%.

As discussed before in the literature review, fluoride interacts with mineralized tissues in a biphasic manner (Chachra et al., 2008, Aaseth et al., 2004). At low doses, it is passively incorporated into the minerals of both bone and teeth to form FAp, to improve the structure and amount of mineralized tissue, as well as the interface between the collagen and mineral during the treatment of osteoporosis. However, high doses of fluoride have undesirable effects including the occurrence of skeletal and dental fluorosis. Therefore, the MC3T3-E1 cells were treated with F^- concentrations and the findings are consistent with the literature that, both differentiation and proliferation were promoted in cells treated with low F^- concentrations (from 0.1 to 1.9 ppm) (Fig. 4.1-2). However, when F^- concentrations increased to 9.5 and 19 ppm, both activities were significantly suppressed. In the bioactive glass conditioned medium study, it was found that osteoblastic cell activities were significantly promoted in the low fluoride containing bioactive glass (P6.33F1), but suppressed when the fluoride content increased to 5-7%. From the results of the fluoride ion release into cell culture medium (Fig. 3.13), the fluoride concentration was 2.8 ppm (0.15 mM) in P6.33F1 group while up to 12-16 ppm (0.6-0.85 mM) in the 5-7% fluoride containing groups. It is consistent with the MC3T3-E1 cell responses in F^- concentrations. Similar results were also reported when human osteoblast-like Saos-2 cells were treated with different NaF concentrations (0-1.6 mM) for 72 h, Huo *et al.* found that 0.2 mM fluoride resulted in a higher proliferation and expression of osteoblast marker genes associated with the activation of the BMP/Smad pathway (Huo et al., 2013). In goat osteoblasts, low NaF concentrations

(under 0.01 mM) promoted proliferation, differentiation and mineralization while high concentrations (0.1-1 mM) showed negative effects (Qu et al., 2008). However, Wang *et al.* revealed that after treating with NaF concentrations (0.001 to 0.5 mM), primary mice osteoblast viability was inhibited in a dose- and time-dependent manner (Wang et al., 2011). Additionally, it was reported that only 0.01 mM NaF was required to reduce cell viability and promote apoptosis in the MC3T3-E1 cells, (Yang et al., 2011). This suggests the effects of fluoride on cells not surprisingly depend on the concentrations, time and cell type (primary cells or established cell line) (Everett, 2011). In this study, the bioactive glass P6.33F1 conditioned medium, with a released F^- concentration around 0.15 mM, significantly promoted the osteogenic responses of MC3T3-E1 cells.

For the angiogenic effects, we found that the VEGF gene expression and its protein production were both significantly promoted by the high phosphate but fluoride free bioactive glass P6.33F0 and further increased in the fluoride containing bioactive glass conditioned medium. Compared with the control, silicon and fluoride were released from bioactive glasses into medium. Silicon, aside from the potential osteogenic benefits as discussed before, several recent studies have noted that it may have angiogenic capabilities as well (Bose et al., 2013). Silicon containing bioactive glasses has been demonstrated to stimulate VEGF secretion and promote angiogenesis through *in vitro* and *in vivo* studies (Day, 2005, Gorustovich et al., 2010, Leu et al., 2009). In addition to bioactive glasses, utilizing a calcium silicate bioceramic resulted in VEGF expression in

human dermal fibroblasts, which was mainly induced by the presence of silicon (Li and Chang, 2013). Similarly, another study utilizing a calcium silicate in a rabbit femur defect was also able to demonstrate angiogenic effects (Wang et al., 2013a). Fielding *et al.* reported that neovascularization was increased up to three times with the incorporation of SiO_2 and ZnO into β-tricalcium phosphate scaffolds in an *in vivo* study (Fielding and Bose, 2013). Ca–Mg–Si-containing bioceramic enhanced angiogenesis of human aortic endothelial cells was reported by Zhai *et al*., and it was proposed that silicon ions might play an important role in the stimulation of angiogenesis (Zhai et al., 2012). However, very few publications discussed the effects of fluoride on angiogenesis. Through embedding different sponges into rabbit femur, Lalk *et al* (Lalk et al., 2013) found that MgF_2 coated sponges exhibited the highest vascularization in comparison with the CaP coating. Similar results were reported by Liu *et al.* (Liu et al., 2012) that the deposition of VEGF in the thyroid gland was significantly promoted through NaF water feeding in a rat model. Therefore, MC3T3-E1 cells were also treated with a range of F^- concentrations (0, 0.1, 1.9 and 9.5 ppm) for the VEGF protein production in this study. However, there was no significant difference between the control (0 ppm) and F^- concentration groups after 7 d, 14 d and 21 d treatment. Therefore, the improved angiogenesis on MC3T3-E1 cells after treatment with bioactive glass conditioned medium may be attributed to the combined effects of silicon and fluoride. A sufficient supply of blood and oxygen is a key and dependent factor for osteogenesis in bone healing (Nuss and von Rechenberg, 2008, Karageorgiou and Kaplan,

2005, Kuzyk and Schemitsch, 2011). The fluoride containing bioactive glasses exhibited angiogenic potential *in vitro* and could be used as bone substitutes with the expected promotion of VEGF gene expression and protein production *in vitro*.

4.4 Future plan

In this study, only Western Blot was used to measure the VEGF protein production inside of the MC3T3-E1 cells. In the future, the changed cell culture medium could also be collected to investigate whether the VEGF protein production is also secreted out of cells.

Chapter 5 Epithelial cell and fibroblast responses

5.1 Introduction

From Chapters 3 and 4, it is concluded that the high phosphate low fluoride containing bioactive glasses significantly accelerate apatite formation in Tris buffer solution and promote the osteogenic and angiogenic responses of MC3T3-E1 pre-osteoblast cells.

However, in periodontal bone defect treatment, the healing outcome will not only depend on the implanted biomaterials, apatite formation rate and osteoblast response, but also be determined by the surrounding soft tissues containing epithelial cells and fibroblasts (Vignoletti et al., 2014). Therefore, ideal strategies should be able to regenerate all damaged structures including the soft and hard tissues.

The effects of fluoride on periodontal soft tissues are contradictory. Some studies have reported that fluoride does not have any significant positive effects on the severity of gingival inflammation and periodontal pocket formation (Reddy and Grobler, 1988, Haikel et al., 1989), whereas others suggested that the intake of fluoride in drinking water lowered the incidence and severity of periodontal disease and was beneficial to the periodontal tissues (Anuradha et al., 2002, Kumar and John, 2011). In addition, Lutfioglu *et al.* demonstrated in a rabbit model that, excessive fluoride intake may affect the homeostasis of periodontal soft tissues by

altering their degradation and formation (Lutfioglu et al., 2012). However, most of these investigations were based on clinical assessments and animal studies, and there is little data on the mechanisms of fluoride dependent biological reactions in periodontal soft tissues.

Bioactive glasses have attracted more attention for their application in periodontal and implant therapy. Besides significant positive effects on bone cells and apatite formation, bioactive glasses also show benefits in soft tissue repair by increasing tissue strength (Gillette et al., 2001) and producing a transient reduction in the pro-inflammatory response to endotoxin (Rectenwald et al., 2002). Clinical research and animal studies show that bioactive glass prevent the apically directed growth of the junctional epithelium (Karatzas et al., 1999, Mengel et al., 2003, Mengel et al., 2006). However, there is insufficient data on the fluoride containing bioactive glasses and their effects on periodontal tissues and cells.

Therefore, this Chapter presents data to demonstrate the effects of fluoride concentrations and bioactive glass conditioned medium on epithelial cells and fibroblasts.

5.2 Results

5.2.1 Immunofluorescence for human oral epithelial primary cells

Human oral epithelial primary cells derived from human oral cavity epithelial tissue have recently been marketed, but there is no previous publication to validate them. Thus, CK5 and Dsg3 were chosen as two epithelial cell specific markers for validation. After 24 h culture followed by immunofluorescence staining as showed in Fig. 5.1, the cytoplasmic intermediate filament protein CK5, and Dsg3, a transmembrane glycoprotein component of cell-cell junction desmosomes, were clearly expressed by these human oral epithelial primary cells.

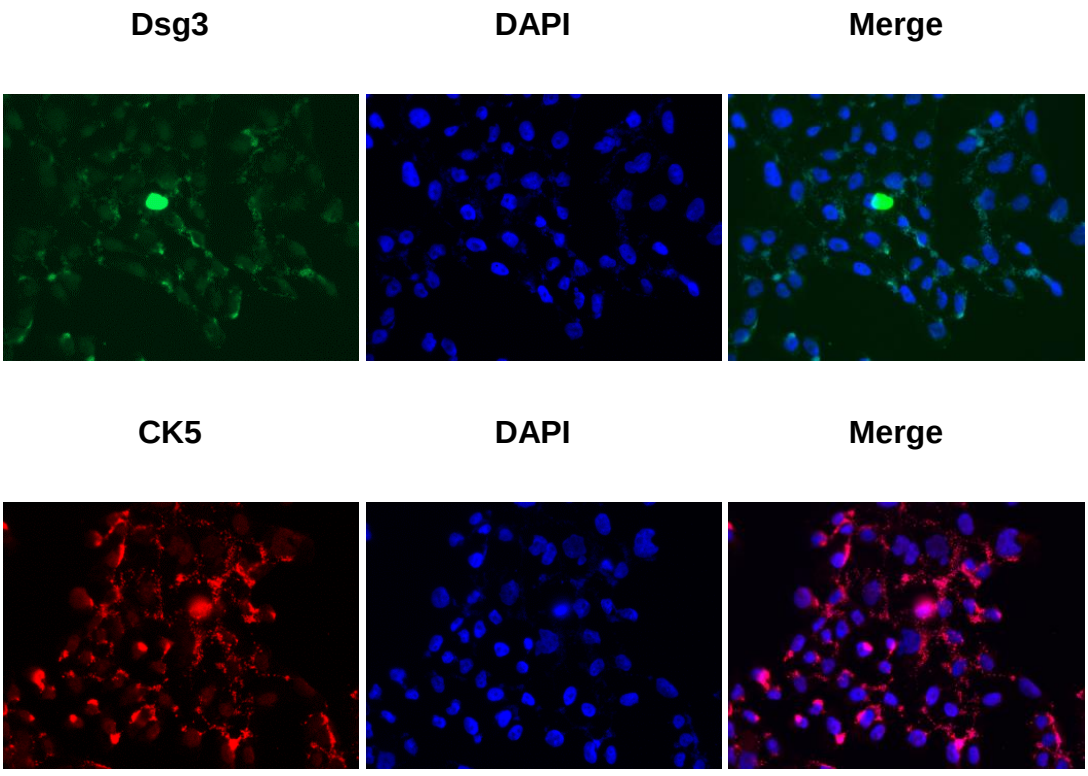

Figure 5.1 Expression of CK5 and Dsg3 in human oral epithelial primary cells assessed by fluorescence microscopy analysis. Cells were seeded at 70-80% confluence and were fixed by formaldehyde and immune-stained with the indicated antibodies. Nucleus and specific protein staining was merged using Image J.

DAPI is a specific stain for cell nuclei. However, significant cytoplasmic labelling was found between the cell nuclei as showed in Fig. 5.2 (arrowed), which may be mycoplasma contamination (discussed later). As those human oral epithelial cells are primary cells and they have limited number of passages for effective use (passage 3 and 4 are the most appropriate for experiments), the mycoplasma elimination kits are not applicable. Therefore, epithelial cell line A431 cells were used in the later experiments.

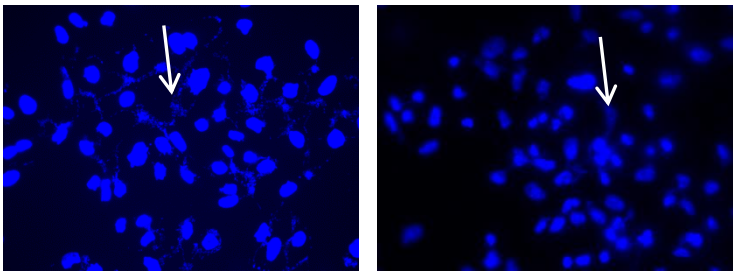

Figure 5.2 DAPI staining in human oral epithelial primary cells assessed by fluorescence microscopy analysis. Cells were seeded at 70-80% confluence and were fixed by formaldehyde and stained with DAPI.

5.2.2 Cellular response to NaF

5.2.2.1 Epithelial cells

For the cytotoxicity of fluoride on A431 cells, compared with the control group (0 ppm), all the investigated F^- concentrations (0.1 to 19 ppm) were not cytotoxic to the growth of A431 cells after 1 to 5 d treatment (Fig. 5.3), although the levels of MTT reaction products decreased slightly as the F^- concentrations increased.

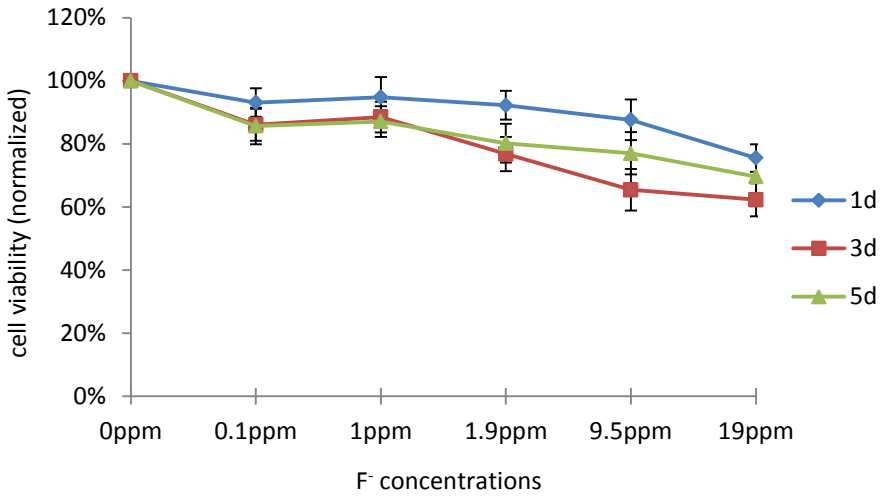

Figure 5.3 Cytotoxicity of F^- concentrations on A431 cells. Cells were treated with a range of NaF concentrations for 1 d, 3 d and 5 d. After treatment, cell viability was estimated using MTT assay. Results are indicated the normalized results. Each marker represents mean ± SE of ten independent experiments.

For the proliferation as showed in Fig. 5.4, the numbers of A431 cells in both control and experimental groups increased significantly as the treatment time increased from 4 d to 10 d. However, when compared with the control group (0 ppm), A431 cell proliferation was suppressed significantly as the F^- concentrations increased from 0.1 to 19 ppm during the whole experimental period.

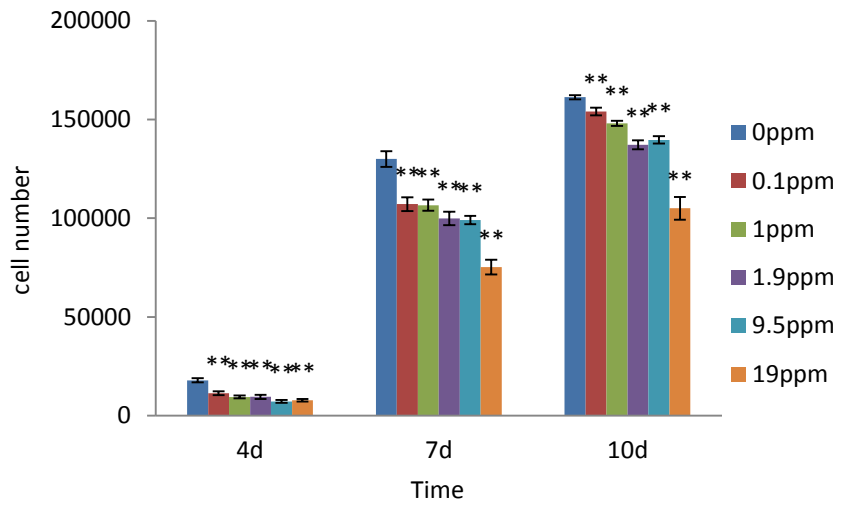

Figure 5.4 Effects of fluoride on cell proliferation in A431 cells. Cells were treated with F^- concentrations for 4 d, 7 d and 10 d. After treatment, cell proliferation was estimated using the bisbenzimidazole-chelation assay to assess DNA content by fluorescence intensity. Results are indicated the cell number. Each bar represents mean ± SE of ten independent experiments. * *P* <0.05 or ** *P* <0.01, compared with control group.

5.2.2.2 Fibroblasts

Compared with the control group (0 ppm), F^- concentrations from 1 to 19 ppm were not cytotoxic to the growth of NHOF cells after 1 to 5 d treatment (Fig. 5.5). In the 9.5 and 19 ppm F^- group, the levels of MTT reaction products were higher than that in the control. However, this increase is small, and not significantly greater.

For the F^- induced proliferation of NHOF cells as showed in Fig. 5.6, compared with control group (0 ppm), the high fluoride concentrations, 9.5 and 19 ppm, significantly increased NHOF cell numbers during the whole experimental period. Other lower concentrations (0.1-1.9 ppm) did affect NHOF cells proliferation.

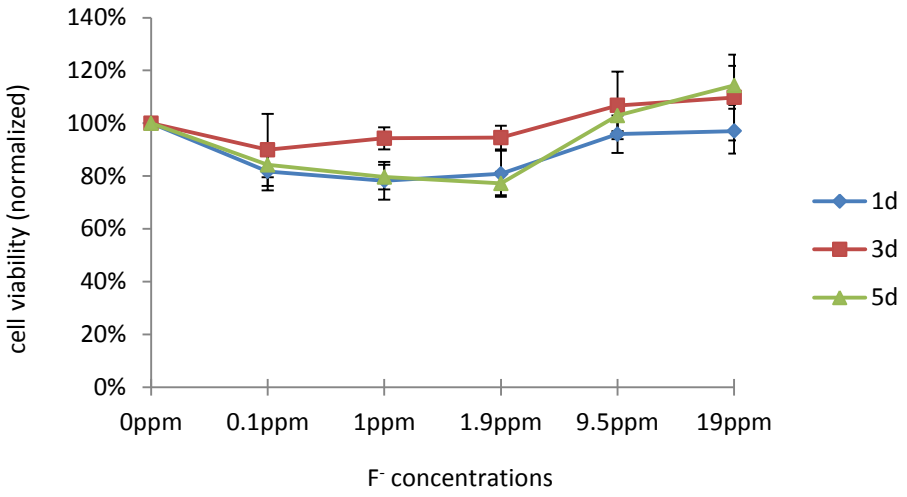

Figure 5.5 Cytotoxicity of F^- concentrations on NHOF cells. Cells were treated with a range of NaF concentrations for 1, 3 and 5 d. After treatment, cytotoxicity was estimated using MTT assay. Results are indicated the normalized results. Each marker represents mean ± SE of ten independent experiments.

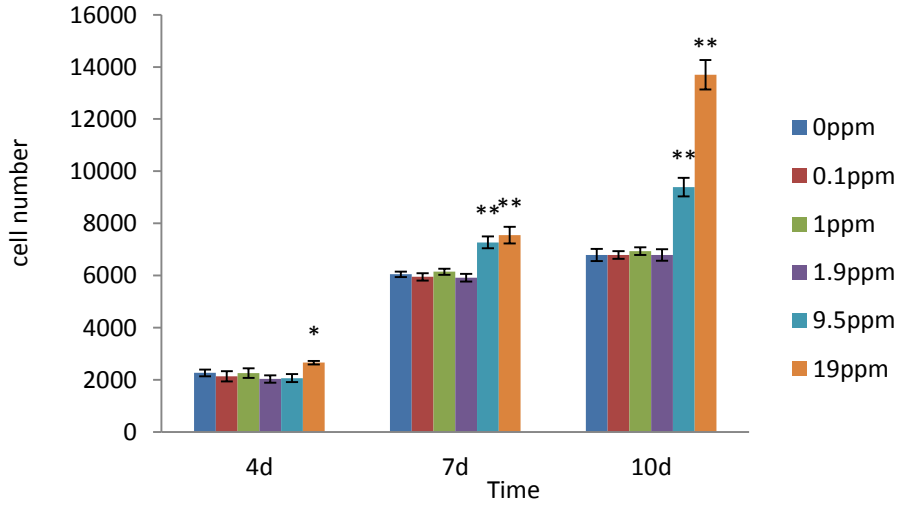

Figure 5.6 Effects of fluoride on cell proliferation of NHOF cells. Cells were treated with F^- concentrations for 4 d, 7 d and 10 d. After treatment, cell proliferation was estimated using the bisbenzimidazole-chelation assay to assess DNA content by fluorescence intensity. Results are indicated the cell number. Each bar represents mean ± SE of ten independent experiments. * P <0.05 or ** P <0.01, compared with control group.

5.2.3 Cellular response to bioactive glass conditioned medium

5.2.3.1 Epithelial cells

For the cytotoxicity of bioactive glass conditioned medium on A431 cells, compared with the control group (normal medium without bioactive glass immersion), all the investigated bioactive glass groups, except P6.33F7 bioactive glass, were not significantly cytotoxic to the growth of A431 cells from 1 to 3 d treatment (Fig. 5.7). However, when treatment time extended to 5 d, the growth of A431 cells was moderately inhibited by all bioactive glass conditioned medium.

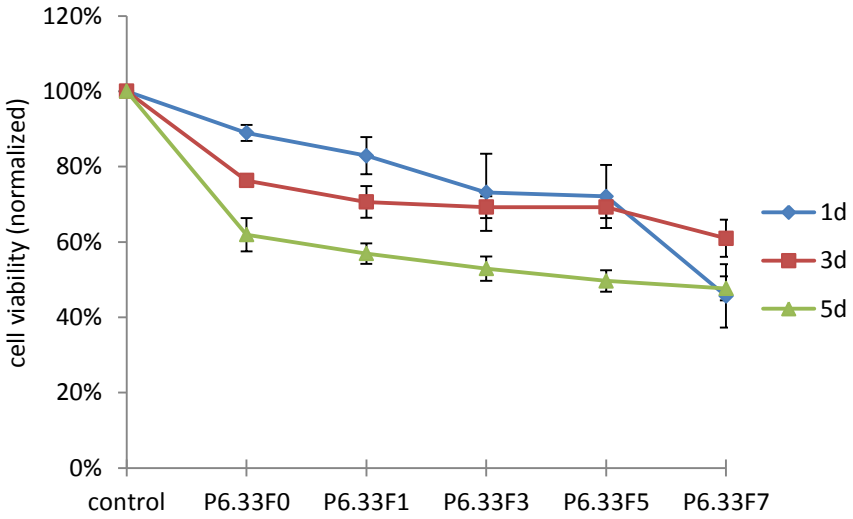

Figure 5.7 Cytotoxicity of bioactive glass conditioned medium on A431 cells. Cells were treated with bioactive glass conditioned medium for 1 d, 3 d and 5 d. After treatment, cytotoxicity was estimated using MTT assay. Results are indicated the normalized results. Each marker represents mean ± SE of ten independent experiments. (P6.33F0 indicates a bioactive glass contains 6.33 Mol.% phosphate and 0 Mol.% fluoride)

For the proliferation, as shown in Fig. 5.8, A431 cell numbers in experimental groups did not increase much as the treatment time increased from 4 d to 10 d. Compared with the control group, A431 cell

proliferation was significantly suppressed in the bioactive glass conditioned medium groups during the whole experimental period. When comparing the P6.33F0 and F containing bioactive glass groups, the later significantly further decreased A431 cell numbers after 7 d and 10 d treatment.

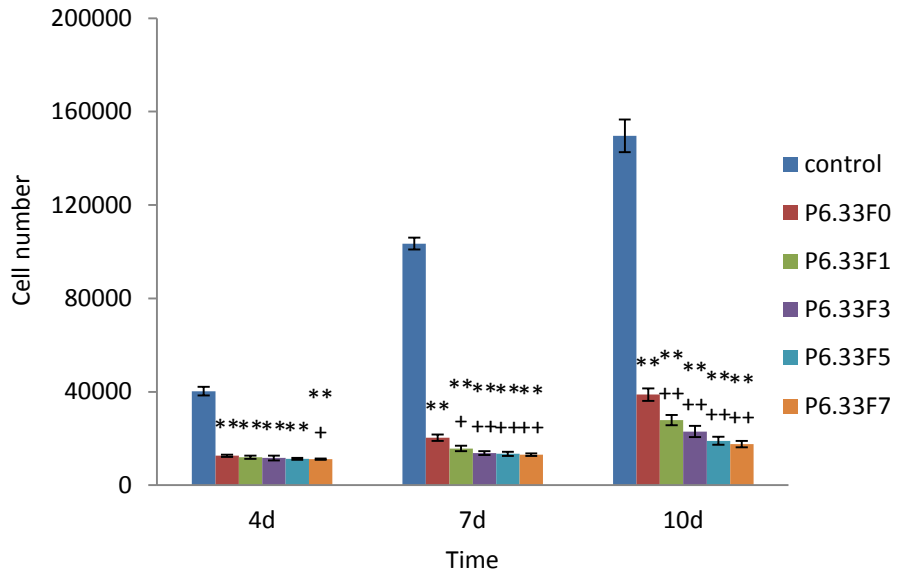

Figure 5.8 Effects of bioactive glass conditioned medium on cell proliferation in A431 cells. Cells were treated with bioactive glass conditioned medium for 4 d, 7 d and 10 d. After treatment, cell proliferation was estimated using the bisbenzimidazole-chelation assay to assess DNA content by fluorescence intensity. Results are indicated the cell number. Each bar represents mean ± SE of ten independent experiments. * *P* <0.05 or ** *P* <0.01, compared with control group. + *P* <0.05, compared with P6.33F0 group. (P6.33F0 indicates a bioactive glass contains 6.33 Mol.% phosphate and 0 Mol.% fluoride)

5.2.3.2 Fibroblasts

After treatment with the bioactive glass conditioned medium, the NHOF cell viability was not significantly affected, compared with the control (normal medium without bioactive glass immersion) (Fig. 5.9).

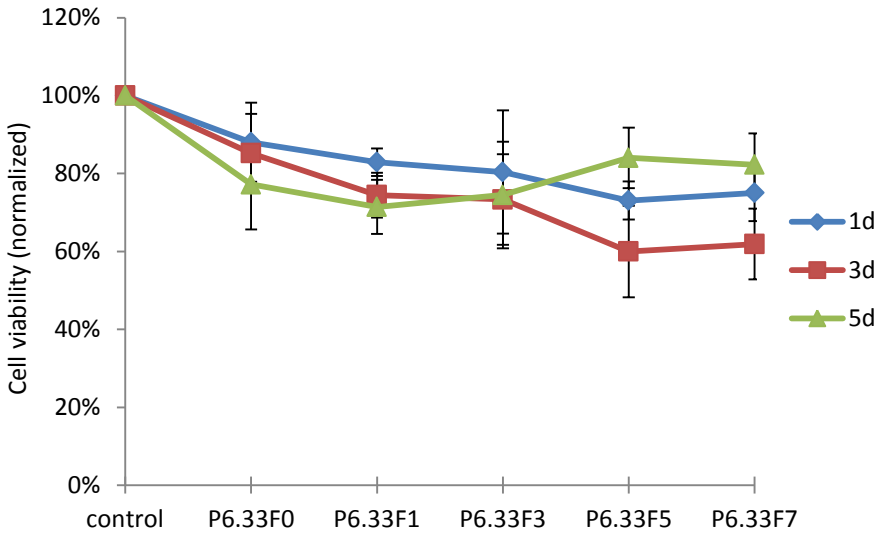

Figure 5.9 Cytotoxicity of bioactive glass conditioned medium on NHOF cells. Cells were treated with bioactive glass conditioned medium for 1 d, 3 d and 5 d. After treatment, cytotoxicity was estimated using MTT assay. Results are indicated the normalized results. Each marker represents mean ± SE of ten independent experiments. (P6.33F0 indicates a bioactive glass contains 6.33 Mol.% phosphate and 0 Mol.% fluoride)

For the effects of bioactive glass conditioned medium on NHOF cell proliferation (Fig. 5.10), compared with control group, the P6.33F5 and P6.33F7 groups significantly increased NHOF cell numbers during the whole experimental period, and at the early time point 4 d, both groups significantly induced more NHOF cell growth than that in the F free bioactive glass P6.33F0 group. For treatment time of 10 d, NHOF cell proliferation was significantly promoted by all the bioactive glass conditioned medium.

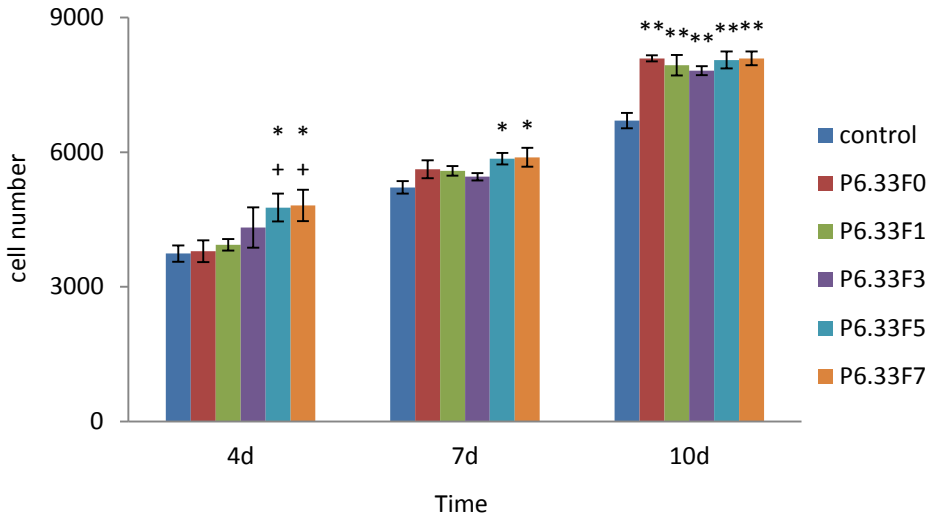

Figure 5.10 Effects of bioactive glass conditioned medium on cell proliferation in NHOF cells. Cells were treated with bioactive glass conditioned medium for 4 d, 7 d and 10 d. After treatment, cell proliferation was estimated using the bisbenzimidazole-chelation assay to assess DNA content by fluorescence intensity. Results are indicated the cell number. Each bar represents mean ± SE of ten independent experiments. * *P* <0.05 or ** *P* <0.01, compared with control group. + *P* <0.05, compared with P6.33F0 group. (P6.33F0 indicates a bioactive glass contains 6.33 Mol.% phosphate and 0 Mol.% fluoride)

5.3 Discussion

DAPI (4', 6-diamidino-2-phenylindole) is a blue-fluorescent nucleic acid stain that preferentially associates with the minor groove of double-stranded DNA, with a preference for the adenine-thymine clusters (Chazotte, 2011). When DAPI is bound to DNA, the fluorescence intensity will increase approximately 20-fold and its blue fluorescence stands out vividly against the green, yellow, or red fluorescent probes for other structures. Thus, it is a popular nuclear counterstain in multicolour fluorescent techniques. In this study, significant cytoplasmic DAPI labelling was found in the human oral epithelial primary cells. Most DNA is located in the cell nucleus, but a small amount can also be found in the mitochondria, which stays in cytoplasm. However, it is demonstrated that animal cells have a small mitochondria DNA (< 20 kb), which could not been detected without the usage of specific techniques (Dellinger and Geze, 2001). Therefore, in the human oral epithelial primary cells in this study, the detected cytoplasmic DAPI labelling can be attributed to mycoplasma contamination instead of mitochondria DNA in cytoplasm.

Mycoplasma is the simplest bacteria and smallest free-living organism (~100 nm in diameter) with extremely basic genomes, and therefore, it exists as a parasite exploiting host cells to fulfil its energy requirements and component biosynthesis. As the lack of a rigid cell wall around the cell membrane, mycoplasma is resistant to a number of common antibiotics used in cell culture, such as penicillin and streptomycin (InvivoGen, 2012). Mycoplasma can produce a variety of negative effects in the cultured eukaryotic cells they infect, such as altered levels of

protein, RNA and DNA synthesis, cellular metabolism alteration, induced chromosomal aberrations, cellular morphology and cytokine expression change, influence on signal transduction and *etc.* (Drexler and Uphoff, 2002). A microarray analysis revealed that mycoplasma altered the expression of hundreds of genes including those encoding for receptors, ion channels, growth-factors, and oncogenes (Miller et al., 2003). Therefore, another epithelial cell line A431 (morphologically similar to normal differentiated squamous epithelial cells and derived from an epidermoid carcinoma in the vulva) was used in this study instead of the mycoplasma contaminated human oral epithelial primary cells.

NaF concentrations (0.1 to 19 ppm, equal to 0.005 to 1 mM) did not demonstrate significant cytotoxicity to the A431 cells. However, cell proliferation was dose-dependently suppressed after 4 d to 10 d treatment. For lung epithelial cells A549, dose-dependent death was observed after exposure to 5-10 mM NaF, while low concentrations (0.25 - 3.73 mM) were not toxic (Refsnes et al., 2002, Refsnes et al., 2003, Ameeramja et al., 2015). In another study, with oral epithelial ROE2 cells, exposure to NaF concentrations (1, 2 and 4 mM) significantly and concentration-dependently decreased cell viability, while low concentrations (0.25 and 0.5 mM) did not affect cell viability and proliferation (Tabuchi et al., 2014). For the human skin epithelial cell line, HaCaT, NaF at high dose (5 mM) strongly inhibited proliferation and blocked terminal differentiation, which was visible by keratin expression and failure to assemble stratified layers, while low does (0.5 mM) did not inhibit cellular proliferation or affect the cell differentiation significantly

(Prado et al., 2011, Dogan et al., 2002). For a human gingival epithelial cell line Smulow-Glickman (S-G), toxicity was first observed at 1 mM NaF after 24 h exposure (Zuckerbraun et al., 1998). He and Chen *et al.* demonstrated that fluoride induced DNA damage, cell cycle changes and led to apoptosis in oral mucosal cells (He and Chen, 2006). However, Arakawa *et al.* reported that, in human primary gingival epithelial cells, lower NaF concentrations promoted proliferation with the peak at 50 μM, while the high levels (higher than 500 μM) drastically reduced cell proliferation (Arakawa et al., 2009). It means that effects of NaF on epithelial cells not only depend on the concentrations but also be determined by cell types under study. In this study with A431 cells, the investigated NaF concentrations (0.1 - 19 ppm, equal to 5 μM - 1 mM) were not significant cytotoxic, cell numbers increased significantly from 4 d to 10 d treatment although they were dose-dependently suppressed when compared with the control (0 ppm).

However, after incubation in bioactive glass conditioned medium, the A431 cell numbers did not increase greatly from 4 d to 10 d. In addition, when compared with the control, cell proliferation was significantly suppressed by bioactive glass conditioned medium and further decreased in the F containing groups. The effects of bioactive glasses on epithelium and epithelial cells are disputed. Ma *et al.* reported that the proliferation of GES-1 human gastric mucosa epithelial cells was significantly suppressed after 24 h treatment in 45S5 bioactive glass ionic dissolution, (Ma et al., 2013a). A study with intestinal epithelial cell line Caco-2 suggested that surfaces coated with bioactive glass did not cause any cytotoxic effect on

the epithelial cells, whereas the cell migration was inhibited (Moosvi and Day, 2009). In a monkey model, the implanted bioactive glasses (*Biogran*) showed a promising inhibition of junctional epithelium apical migration, while the junctional epithelium was observed to migrate up to the defect base in the control sites (coagulum filling) (Villaca et al., 2005). However, a clinical study revealed that a long junctional epithelium healing with minimal new connective tissue attachment to the teeth was observed after applying bioactive glass ceramic (Perioglas) to treat the intra-bony defects (Nevins et al., 2000). No significant difference in total epithelium extension was observed between the bioactive glass (Perioglas) and control (naturally filled with coagulum) groups in a dog bone defect model (Carvalho et al., 2011). Cetinkaya *et al.* reported that the proliferation of gingival epithelial cells was more prominent after applying bioactive glass to treat intra-bony defects (Cetinkaya et al., 2007). In this *in vitro* study, the fluoride containing bioactive glass conditioned medium did not strongly inhibit A431 epithelial cell viability, but the cell proliferation was significantly suppressed, and further decreased in the F containing groups, which may be attributed to the combined effects of fluoride and bioactive glasses.

In this study, NaF concentrations (0.1 to 19 ppm, equal to 0.005 to 1 mM) were not cytotoxic to fibroblasts NHOF and, 9.5 and 19 ppm fluoride significantly increased NHOF cell numbers during the whole experimental period. Fluoride was reported to be cytotoxic to fibroblasts at high concentrations: Dogan *et al*. observed that NaF strongly reduced the growth of mouse fibroblasts 3T3 at concentration of 10, 5 and 2.5 mM

(Dogan et al., 2002). For the human gingival fibroblast cell (CRL-2014), 1.5 mM fluoride induced significant cellular damage such as increased oxidative stress, inflammation, and apoptosis (Inkielewicz-Stepniak et al., 2014). In another study, NaF was observed to be cytotoxic to oral mucosal fibroblasts at concentrations of 4 mM or higher with inhibition of protein synthesis, mitochondrial function and depletion of cellular ATP, while no significant inhibition was found at concentrations lower than 2 mM (40 ppm) (Jeng et al., 1998). 5% fluoride varnish (*Duraflur*) was observed to significantly lower human gingival fibroblast cell viability (Parirokh et al., 2015). However, positive effects are initiated in fibroblasts by low fluoride doses: fluoride concentrations (0.0001 – 20 ppm) significantly increased the gene and protein levels of bone formation markers, core-binding factor α 1 (Cbfa1) and osteocalcin (OCN), in fibroblast cell line L929 (Duan et al., 2014). NaF concentrations (lower than 2 mM) were non-cytotoxic for human periodontal ligament fibroblasts (Chien et al., 2006). 0.002% NaF did not affect human gingival fibroblast viability and induced cell proliferation. In addition, NaF was demonstrated to increase resistance to the interleukin-1β-induced gingival inflammation in human gingival fibroblasts (Lee and Choi, 2015). Lochaiwatana *et al.* revealed that the human gingival fibroblast cell viability was significantly promoted after incubation with F varnish for 48 h (Lochaiwatana et al., 2015). A clear stimulation of cell proliferation and an enhancement of the mitochondrial respiratory activity were observed when fibroblasts (L929) were cultured with the fluoride surface-modified alloy and no significant change in apoptosis or viability rates was observed (Lozano et al., 2013). Using the

single cell gel (comet) assay with human skin fibroblasts, NaF (7 – 100 ppm) did not contribute to DNA damage (i.e. induce strand breakage in DNA) and did not affect cell viability (Ribeiro et al., 2006). In this study, the NaF concentrations (9.5 and 19 ppm, equal to 0.005 to 1 mM) were observed to promote NHOF cell proliferation. However, the NHOF cell numbers were significantly promoted after incubation in bioactive glass conditioned medium even in the P6.33F0 glass. A study with sub-epithelial myofibroblasts, CCD-18Co, suggested that surfaces coated with bioactive glass significantly increased secretion of basic fibroblast growth factor from myofibroblasts (Moosvi and Day, 2009). The addition of bioactive glasses into chitosan membranes were not cytotoxic to the periodontal ligament cells and significantly promoted the proliferation and cell metabolic activity (Mota et al., 2012). The presence of exposed bioactive glass particles enhances human gingival fibroblast proliferation on composite surfaces *in vitro* (Abdulmajeed et al., 2014). Bioactive glass modified ceramics promoted human periodontal ligament fibroblasts attachment and proliferation (Kontonasaki et al., 2007). In another study, it is found that both the bioactive glass/hydroxyapatite composites themselves and their extracts do not induce negative effects in murine fibroblasts BALB/3T3 viability and do not cause inhibition in cell growth (Bellucci et al., 2015). Surfaces coated with 45S5 Bioglass® or bioactive glass conditioned medium produced a significant increase in the secretion of VEGF and basic fibroblast growth factor (bFGF) from human fibroblasts (CCD18Co) (Day, 2005, Gerhardt et al., 2013, Keshaw et al., 2005), however, at higher bioactive glass concentrations and longer periods of

incubation on coated surfaces, cell proliferation was reduced (Day, 2005). Kubo *et al.* observed that although the bioactive glass decreased proliferation of periodontal-ligament fibroblasts, they increased the alkaline-phosphatase activity and the formation of nodules suggesting increased differentiation (Kubo et al., 1993, Kubo et al., 1995, Kubo et al., 1997). In addition, Commercial Bioglass^{TM} (45S5) conditioned medium even significantly promoted the osteogenic potential of human periodontal ligament fibroblasts (Varanasi et al., 2011). Therefore, with the combined effects of low fluoride and bioactive glass, proliferation of fibroblasts NHOF was significantly promoted in this study.

With the highest capacity of proliferation among periodontal tissues involved in wound healing, epithelial cells are the first cells to migrate to the site of injury, becoming a problem as they cause the formation of a long, non-keratinized junctional epithelium which prevents the migration of the cells from the periodontal ligament and alveolar bone. Therefore, in periodontal surgeries, the guided tissue regeneration (GTR) technique is widely applied by using a resorbable or non-resorbable membrane acting as a physical barrier against the migration of epithelial cells from the superficial soft tissue flap into the underlying grafted site. This procedure allows the necessary time for the cell repopulation of the periodontal ligament and adjacent alveolar bone, and will favour the regeneration of lost and damaged tissue (Kay et al., 1997). Periodontal ligament is a specialized connective tissue embedded between the cementum and the inner wall of the alveolar bone socket. It not only has an important role in supporting teeth and the homeostasis of periodontal tissues, but also

contributes to alveolar bone remodelling and tissue regeneration, since it contains a heterogeneous cell population including fibroblasts, cementoblasts, osteoblasts, and progenitor/stem cells, in which fibroblasts are the predominant cell type. Therefore, specific proliferation and migration of periodontal ligament cells, mainly fibroblasts, are crucial in successful periodontal tissue regeneration. In this study, bioactive glass conditioned medium was not cytotoxic to either epithelial cells or fibroblasts. In addition, epithelial cell numbers were significantly decreased while fibroblast proliferation was promoted, and the incorporation of fluoride into bioactive glasses brought greater effects. The mechanism of fluoride action is unknown as the wide variations of effective fluoride concentrations which suggest that different cell types react in a different way (Prado et al., 2011).

To conclude, the novel low fluoride high phosphate bioactive glasses *in vitro* promoted fibroblast growth and suppressed epithelial cells. *In vivo*, they may also block the epithelium migration and subsequent long junctional epithelium, stimulate the rapid re-establishment of periodontal ligament and allows for new bone formation without applying or minimal the guided tissue regeneration procedure.

5.4 Future plan

A migration test can be carried out using epithelial cells, to investigate whether those high phosphate low fluoride containing bioactive glasses can block the epithelial cell migration ability.

Angiogenic and osteogenic potentials can be explored for fibroblasts NHOF after treated with those high phosphate low fluoride containing bioactive glasses.

Chapter 6 Antibacterial study

6.1 Introduction

Oral alveolar bone resorption and tooth loss can be induced by periodontal disease, which is a bacterially induced inflammatory disease resulting in the destruction of soft and hard tooth-supporting (periodontal) tissues (Bostanci and Belibasakis, 2012). Peri-implantitis is also an inflammatory reaction associated with loss of supporting bone tissue around the dental implants and mainly caused by periodontal pathogens. Bacterial infections will hinder the repair of periodontal bone defects process and sometimes, lead to surgical failures, carry a financial consequence and reduce patient well being (Yuan et al., 2014). Some oral pathogens associated with periodontal disease have also been associated with dental implant and defect repair failure (van Winkelhoff et al., 2000). *Porphyromonas gingivalis* is highly associated with chronic periodontitis, and can be detected in up to 85% of the disease affected sites (Tribble et al., 2013). *Aggregatibacter actinomycetemcomitans* is mainly detected in aggressive periodontitis, a severe and rapidly progressing form that most often starts at an early age (Brigido et al., 2014). Dental caries is a chronic bacterial disease that induces demineralization and destruction of the hard tissue of teeth. However, caries can progress to affect the tooth pulp and spreads to the periodontal tissues and even the jaws (Featherstone, 2004). Oral bacteria *Lactobacillus* and *Streptococcus* are important in caries development, especially *Lactobacillus* which is found in root caries and

deep dentinal caries associated with pulpitis (Mitchell, 2011, Badet and Thebaud, 2008). More importantly, *Streptococcus mitis* has been demonstrated as a dental plaque pioneer colonizer, which initials the plaque formation and development. Therefore, ideal periodontal intra-bony defect regeneration needs to eliminate the active disease and the potential infection during or after surgery.

Fluoride is widely incorporated into dental restorative materials, besides the ability to form FAp and to reduce demineralisation as well as enhance re-mineralization, it is also known for anti-microbial properties (Burke et al., 2006). It can inhibit the tooth demineralizing dental plaque acid production of various oral pathogens such as *Streptococcus* and *Actinomyces* (Van Loveren, 2001, Kawashima et al., 2013). It also acts directly as an enzyme inhibitor, of the glycolytic enzyme enolase, to interfere with bacterial metabolism (Marquis, 1995). Another action involves the formation of metal-fluoride complexes, most commonly AlF^{4-}, which interact with bacterial F-ATPase and nitrogenase enzymes resulting in bacterial activity inhibition (Lellouche et al., 2009).

Therefore, the aim of this Chapter is to investigate the antibacterial effects of those novel fluoride containing bioactive glasses on supra- and sub-gingival bacteria growth.

6.2 Results

6.2.1 Effect on supra-gingival bacteria

In all the investigated bioactive glasses, the antimicrobial activity on *L. casei* was significantly dependent on the bioactive glass particulate concentrations after 4 h incubation (Fig. 6.1). However, for the *S. mitis*, the bactericidal effect stayed at appropriately 80% and did not change significantly as the bioactive glass concentrations increased from 0.625 mg/mL to 10 mg/mL, except the fluoride free bioactive glass P6.33F0, in which the percentage of growth inhibition promoted slightly.

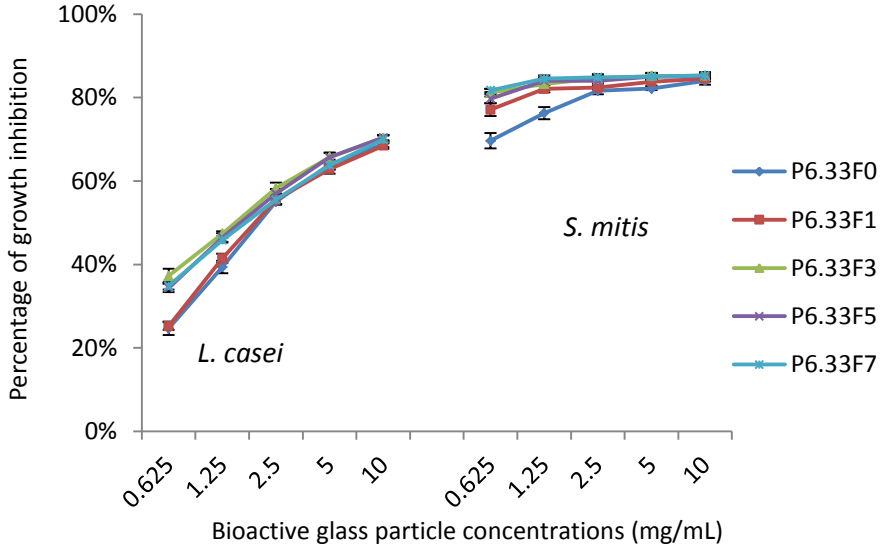

Figure 6.1 Growth inhibition percentage of *L. casei* and *S. mitis* after exposure to a range of bioactive glass particle concentrations for 4 h. *L. casei and S. mitis* were incubated under aerobic condition with a range of bioactive glass particulate concentrations (0-10 mg/mL) for 4 h. The growth inhibition percentage was detected using alamarBlue kit and normalized with negative control (no bioactive glass). Data is represented as mean ± SE of four independent experiments. (P6.33F0 indicates a bioactive glass contains 6.33 Mol.% phosphate and 0 Mol.% fluoride)

With different concentrations of bioactive glass particles and incubation time, the antimicrobial activity varied (Fig. 6.2). For *L. casei,* antimicrobial activity is changing as a function of treatment time, and bioactive glass concentrations. With 1.25 mg/mL particulates incubated for 2 h, no difference was observed between bioactive glasses. When the treatment time increased to 4 h and 8 h, the antibacterial activity increased as the bioactive glass F content increased (Fig. 6.2 A). If bioactive glass particle concentrations increased to 10 mg/mL as showed in Fig. 6.2 B, the bactericidal effect on *L. casei* significantly increased and was dependent on the treatment period. However, there was no difference between the F free and F containing bioactive glasses.

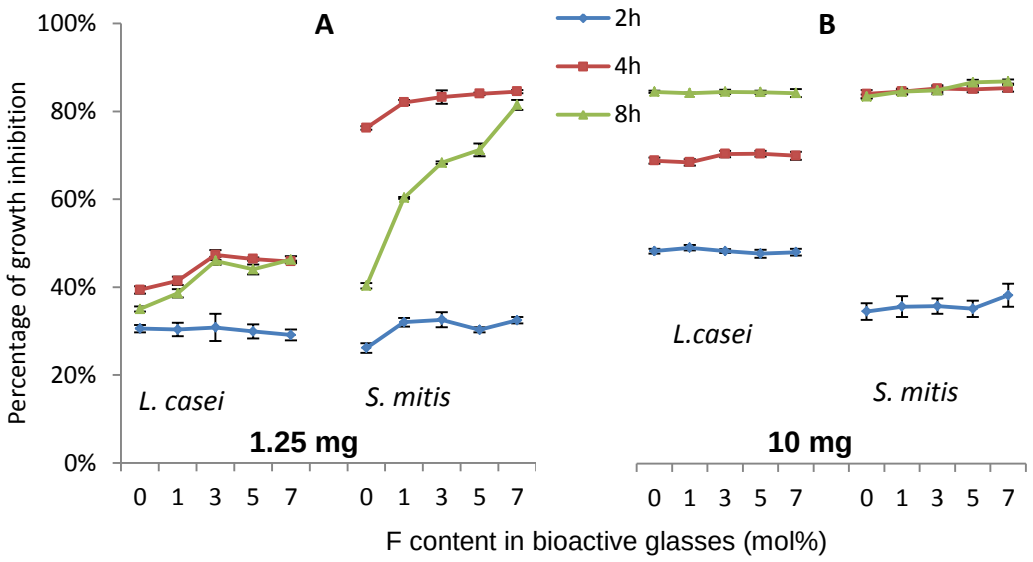

Figure 6.2 Growth inhibition percentage of *L. casei* and *S. mitis* after exposure to 1.25 mg/mL and 10 mg/mL bioactive glass particles. *L. casei and S. mitis* were incubated under aerobic condition with 1.25 mg/mL and 10 mg/mL bioactive glass particles for 2 h, 4 h and 8 h. The growth inhibition percentage was detected using alamarBlue kit and normalized with negative control (no bioactive glass). Data is represented as mean ± SE of four independent experiments.

For the *S. mitis* with 1.25 mg/mL particulates (Fig. 6.2 A), antimicrobial activity increased drastically as the treatment time increased from 2 h to 4 h but only slight increase was observed between the F free and F containing bioactive glasses and no difference between the F contents. However, the antibacterial activity dropped when incubation time increased to 8 h and it was significantly dependent on the bioactive glass F content, the higher bioactive glass F content, the greater *S. mitis* growth inhibition. When the particulate concentration increased to 10 mg/mL as represented in Fig. 6.2 B above, the bactericidal effect on *S. mitis* did not increase as much as that in the *L. casei*. It was the same at 4 h and 8 h, and no difference was observed between bioactive glasses.

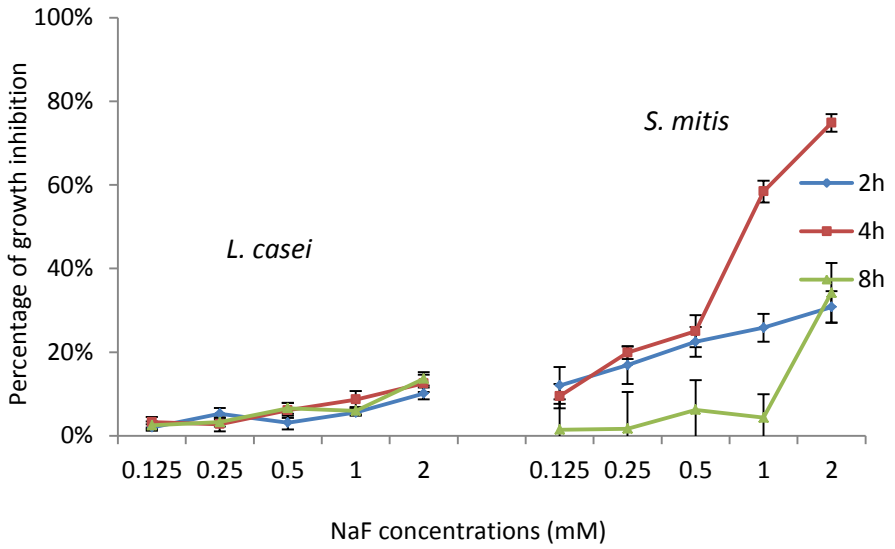

Figure 6.3 Growth inhibition percentage of *L. casei* and *S. mitis* after exposure to NaF concentrations. *L. casei and S. mitis* were incubated under aerobic condition with NaF concentrations (0 to 2 mM) for 2 h, 4 h and 8 h. The growth inhibition percentage was detected using alamarBlue kit and normalized with negative control (no NaF). Data is represented as mean ± SE of four independent experiments.

As the bioactive glass experiments questioned to role of fluoride, the effects of NaF concentrations on the viability of *L. casei* and *S. mitis* were

investigated (Fig. 6.3 above). It was found that fluoride did not show significant bactericidal effects on *L. casei*. However, the antimicrobial activity on *S. mitis* was clearly dependent on the F concentrations. The higher the F content the greater the bactericidal effect.

6.2.2 Effect on sub-gingival bacteria

For the sub-gingival bacteria, *A. actinomycetemcomitans* and *P. gingivalis*, the antibacterial activity on *P. gingivalis* was significantly dependent on the bioactive glass particulate concentrations after 4 h incubation in all the bioactive glasses (Fig. 6.4 below). For the *A. actinomycetemcomitans,* however, F free bioactive glass P6.33F0 showed very low bactericidal effects and no change was observed as the particle concentration varied. When the bioactive glass F content increased to 1-3%, antibacterial activity on *A. actinomycetemcomitans* significantly rose and was dependent on the particle concentrations. However, the particle concentration dependent effect decreased as the bioactive glass F content increased to 5% and 7%.

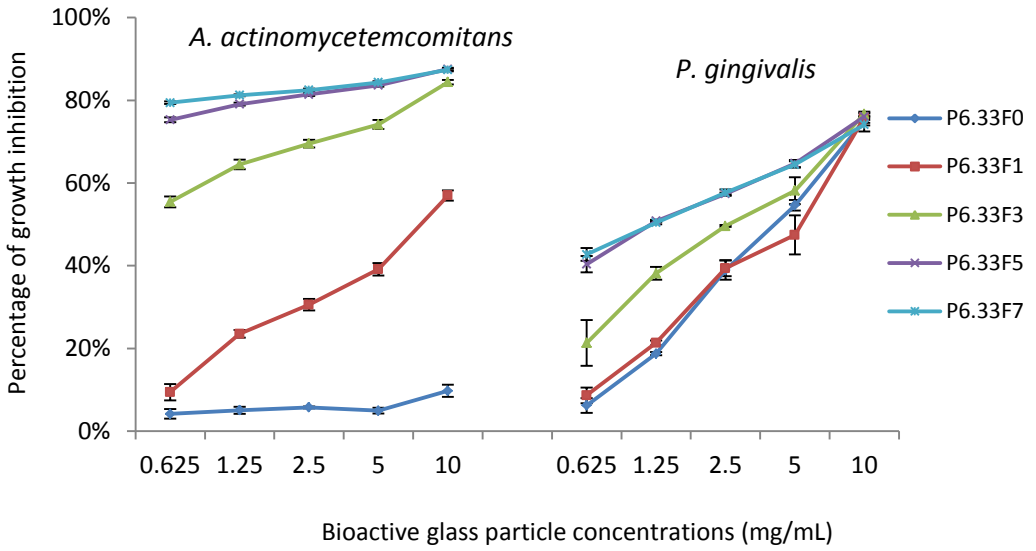

Figure 6.4 Growth inhibition percentage of *P. gingivalis* and *A. actinomycetemcomitans* after exposure to a range of bioactive glass particle concentrations for 4 h. *P. gingivalis* and *A. actinomycetemcomitans* were incubated under anaerobic condition with bioactive glass particle concentrations (0 to 10 mg/mL) for 4 h. The growth inhibition percentage was detected using alamarBlue kit and normalized with negative control (no bioactive glass). Data is represented as mean ± SE of four independent experiments. (P6.33F0 indicates a bioactive glass contains 6.33 Mol.% phosphate and 0 Mol.% fluoride)

With 1.25 mg/mL bioactive glass particulate treatment (Fig. 6.5 A), the antimicrobial activity on *A. actinomycetemcomitans*, from 2 h to 8 h incubation, increased slightly when bioactive glass F content increased from 0% to 1% followed by a drastic rise as bioactive glass F content increased to 5% and kept constant in the 5-7% F containing bioactive glasses. If bioactive glass particle concentration increased to 10 mg/mL as showed in Fig. 6.5 B, the total antibacterial effect on *A. actinomycetemcomitans* increased and rose significantly as the bioactive glass F content increased from 0% to 3%.

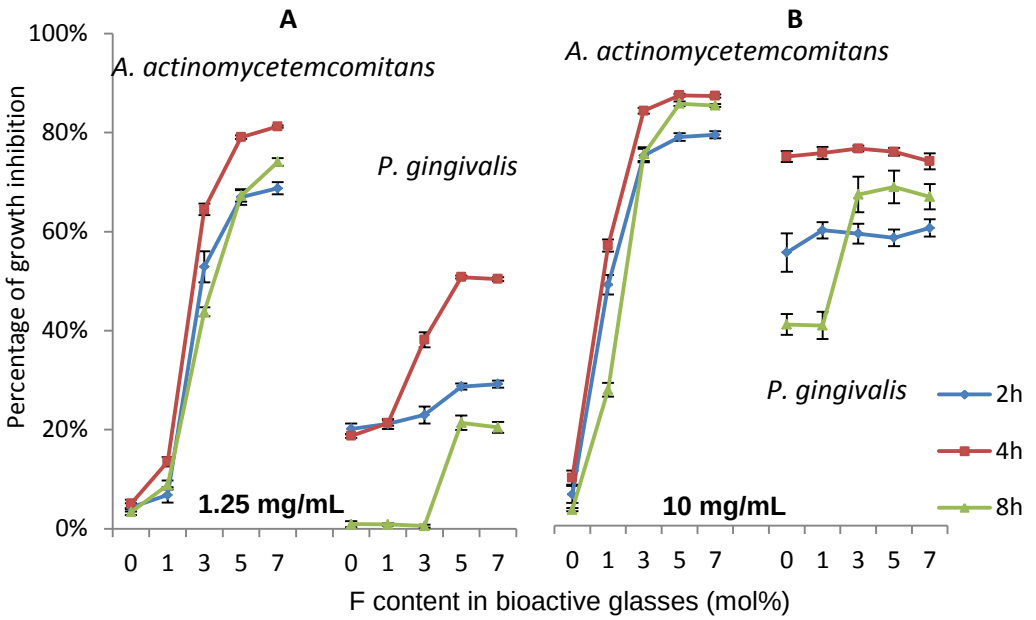

Figure 6.5 Growth inhibition percentage of *P. gingivalis* and *A. actinomycetemcomitans* after exposure to 1.25 mg/mL and 10 mg/mL bioactive glass particles, *P. gingivalis* and *A. actinomycetemcomitans* were incubated under anaerobic condition with 1.25 mg/mL and 10 mg/mL bioactive glass particles for 2 h, 4 h and 8 h. The growth inhibition percentage was detected using alamarBlue kit and normalized with negative control (no bioactive glass). Data is represented as mean ± SE of four independent experiments.

For the *P. gingivalis*, with 1.25 mg/mL bioactive glass particle treatment (Fig. 6.5 A), the antibacterial activity increased significantly as the bioactive glass F content increased from 1% to 5% after 4 h incubation. However, when increased to 8 h, the bactericidal effects in 0-3% F containing bioactive glass groups dropped close to 0 but still kept around 20% in the 5-7% F containing bioactive glasses. In Fig. 6.5 B, the antibacterial activity on *P. gingivalis* increased significantly when the particle concentration increased to 10 mg/mL and there was no difference between bioactive glasses after 2 h and 4 h incubation. However, when extended to 8 h, the bactericidal effects dropped in the 0-1% F bioactive

glasses and kept significantly higher in the 3-7% F containing bioactive glasses.

Both bacteria, *P. gingivalis* and *A. actinomycetemcomitans,* are viability sensitive to and dose dependent on the F concentrations (Fig. 6.6). However, the antimicrobial activity on *A. actinomycetemcomitans* was significantly higher than that on the *P. gingivalis.*

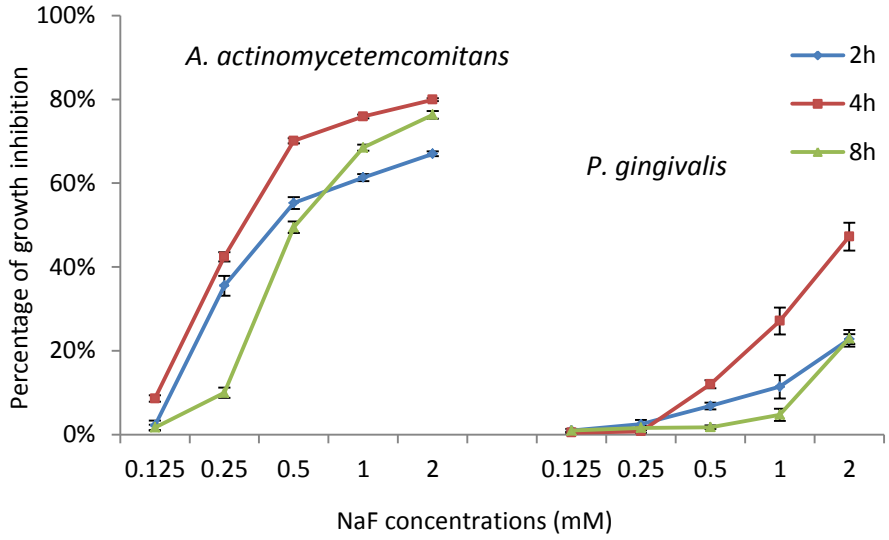

Figure 6.6 Growth inhibition percentage of *P. gingivalis* and *A. actinomycetemcomitans* after exposure to NaF concentrations. *P. gingivalis* and *A. actinomycetemcomitans* were incubated under anaerobic condition with NaF concentrations (0 to 2 mM) for 2 h, 4 h and 8 h. The growth inhibition percentage was detected using alamarBlue kit and normalized with negative control (no NaF). Data is represented as mean ± SE of four independent experiments.

6.3 Discussion

The pioneer colonizer *S. mitis* plays an important role in the establishment of dental plaque and *L. casei* is considered as a cariogenic bacterial species in numerous antibacterial studies. In addition, they also stay in saliva, which is a link between the different tissues and structures of the oral cavity (Mitchell, 2011, Badet and Thebaud, 2008). *P. gingivalis* is highly associated with the chronic periodontitis (Tribble et al., 2013) while *A. actinomycetemcomitans* is mainly detected in aggressive periodontitis, a severe and rapidly progressing form that most often starts at an early age (Brigido et al., 2014). Various degrees of bone loss are frequently encountered in periodontal diseases. In the treatment of bone defect repair following inserting of bone graft substitutes, there is a risk of bacterial colonization with the production of protein-specific adhesions on the surfaces of implanted materials, which may result in the failure of the implants (Coraca-Huber et al., 2014).

In this study, after incubation with bioactive glass particulates at a concentration of 1.25 mg/mL, the bactericidal effect on bacteria, including plaque pioneer colonizer *S. mitis* and periodontal pathogens *A. actinomycetemcomitans* and *P. gingivalis,* was increased significantly as the bioactive glass F content increased. It suggests the antibacterial effect was mainly from fluoride, which was confirmed by experiments in which bacteria were treated with NaF. It was found that the bacteria viability was sensitive to and dose-dependent on the F concentrations. Numerous studies have demonstrated the antimicrobial activity of fluoride (Naorungroj et al., 2010, Ogaard et al., 2001). A 30 min exposure test,

both *A. actinomycetemcomitans* and *P. gingivalis* exhibited a significant decrease of colony-forming units in a NaF concentration-dependent manner (Shimogishi et al., 2014). A 6-month clinical study found that the fluoride containing dentifrice resulted in a significant reduction in the number of anaerobic bacteria on both the dental implants and control teeth at 3 months (Sreenivasan et al., 2011). F surface-modified titanium specimens significantly inhibit the growth of both *P. gingivalis* and *A. actinomycetemcomitans* compared with the polished titanium (Yoshinari et al., 2001). Rostami *et al.* investigated the antibacterial ability of bioactive glasses and they found the fluoride containing ones had significant antibacterial activity against *E. coli*, *P. aeruginosa* and *S. aureus*, which are responsible for most infections, while the fluoride-free bioactive glass samples did not show any antibacterial activity (Rostami et al., 2015). Fluoride is also widely incorporated in dental vanish, mouth rinse and bonding products for its outstanding antibacterial ability (Pinar Erdem et al., 2012, Randall et al., 2014, Sajjan et al., 2013, Shinonaga et al., 2015, Slutzky et al., 2014, Wang et al., 2012, Wiegand et al., 2007, Yoshihara et al., 2001). It acts in multiple ways to affect the metabolism of cariogenic and other bacteria. Firstly, fluoride can bind directly to many enzymes such as heme-containing enzymes and metallo-enzymes to modulate and even interfere bacterial metabolism (Marquis, 1995). Fluoride also can form complexes with metals, such as aluminum or beryllium, and the metal-fluoride complexes are able to interact with a variety of enzymes, regulating phosphatases resulting in enzyme activity inhibition (Lellouche et al., 2009).

The role of *L. casei* is disputed. It can serve as a probiotic to promote and support a beneficial balance of microorganisms living in the human gastrointestinal tract (Probiotic, 2010). Teanpaisan *et al.* even found that *L. casei* was able to inhibit the growth of both periodontitis- and caries-related pathogens (Teanpaisan et al., 2011). However, in some antibacterial studies, *L. casei* is considered as a dental cariogenic bacterial species (Da Silva et al., 2012, Korkmaz et al., 2013, Pupo et al., 2014, Zhang et al., 2014). In this study, *L. casei* was found resistant to the NaF concentrations and the antibacterial activity did not change significantly as the bioactive glass F content increased.

Similar findings are also reported in other publications. For example, Bradshaw *et al.* reported that the growth of *S. mutans* was significantly reduced by 1mM NaF, which did not alter the viability of *lactobacilli* (Bradshaw et al., 1990). Clinically, the long-term use of fluoridated mouth rinses decreased the levels of *S. mutans* in saliva without affecting the levels of *lactobacilli* (Yoshihara et al., 2001). Arthur *et al.* also found that *Actinomyces*, *S. sanguinis* and *S. mutans* were more sensitive to fluoride than *L. casei* (Arthur et al., 2014). This suggests the antibacterial ability and sensitivity against fluoride depend on the bacteria types. In this study, *S. mitis*, *A. actinomycetemcomitans* and *P. gingivalis* were sensitive to NaF concentrations and the bactericidal effect was increased significantly as the bioactive glass F content increased.

However, even the base glass P6.33F0 in this study showed antibacterial activity against all the investigated bacteria. In particular, after incubation with bioactive glass particulates at a concentration of 10 mg/mL, the

growth of both supra-gingival bacteria *L. casei* and *S. mitis* was significantly inhibited, and there was no difference between different bioactive glasses. This suggests that the antibacterial effect was mainly from bioactive bioactive glass particles instead of fluoride. Several studies have demonstrated that bioactive glass (SiO_2–Na_2O–CaO–P_2O_5), without specific ions, has a clear growth-inhibitory effect against numerous aerobic and anaerobic clinically important pathogens (Coraca-Huber et al., 2014, Gergely et al., 2014, Lepparanta et al., 2008, Stoor et al., 1998, Fooladi et al., 2013). Bioactive glass S53P4 showed a clear antibacterial ability in the treatment of chronic osteomyelitis in clinical studies (McAndrew et al., 2013, Romano et al., 2014). Mortazavi *et al.* found the sol-gel-derived bioactive glass nanoparticles had antibacterial effects on aerobic bacteria like *E. coli*, *P. aeruginosa*, and *S. aureus* (Mortazavi et al., 2010). Munukka *et al.* reported that bioactive glasses had a broad spectrum of antibacterial effect on 29 clinically important bacterial species (Munukka et al., 2008). The antibacterial mechanism of bioactive glass in most studies is attributed to the alkaline nature of surface reactions with pH elevation. This is unfavorable for bacteria and is caused by the bioactive glass sodium release and increased osmotic pressure from ions (silicon, calcium, sodium and phosphate) dissolution, creating an hostile environment where the bacteria cannot adhere and subsequent proliferate that causes infections (Echezarreta-Lopez and Landin, 2013, Drago et al., 2013, Rahaman et al., 2014). TEM observation revealed that needle-like bioactive glass debris on bacterial surface interferes with bacterial structure, and indicates that debris from the bioactive glass particles may

be one of the reasons for destruction of cellular structure and bacterial death (Hu et al., 2009). Zehnder *et al.* found that the bactericidal effect of bioactive glasses correlated not only with the pH but also with high silicon ion levels in the supernatant (Zehnder et al., 2006).

Zhang *et al.* revealed that bioactive glasses without any special bactericidal ions showed strong antibacterial effects for a wide selection of aerobic bacteria but the antibacterial effects depended on glass composition and bacterial species (Zhang et al., 2010). In the treatment of dental caries, the release of therapeutic ions such as fluoride is of great importantance for the antibacterial activity of dental material (Marczuk-Kolada et al., 2006). Besides that, particle size also plays an important role in the antibacterial effect. Coraca-Huber *et al* reported that S53P4 bioactive glass <45 µm was more efficient against bacterial biofilm growth *in vitro* compared with glass particles of 0.5–0.8 mm (Coraca-Huber et al., 2014). This may be attributed to the increased glass surface area, facilitating faster and quantitatively superior release of alkali ions compared to the granular form (Gergely et al., 2014).

Furthermore, Allan *et al.* reported the 45S5 Bioglass® particulates exerted an antibacterial effect on certain supra- and sub-gingival oral bacteria and they even found the glass conditioned supernatants showed antibacterial properties as well (Allan et al., 2001). It demonstrated that direct contact between glass particulates and bacterial cells was not required to produce an antibacterial effect, which suggested that bacteria could be killed before they encounter the glass scaffold surface.

In this study, the bioactive glass particulates (<38 μm) with the incorporation of F showed a clear antibacterial effect against the plaque pioneer colonizer *S. mitis* and periodontal pathogens *A. actinomycetemcomitans* and *P. gingivalis*. This ability may be an important advantage for the successful osso-integration when these glasses are incorporated in bone graft substitutes and implanted in dental bone defects, as bacterial colonization has been suggested to be an important cause of implant failure.

6.4 Future plan

Besides dental bone defect repair, those high phosphate fluoride containing bioactive glasses can be incorporated into bone graft substitutes for the bone fracture and osteoporosis treatment. And, they can even be added to dental products such as bonding materials, fillings, toothpaste and mouth rinse for more applications. Therefore, the antibacterial activity of our novel bioactive glasses against some specific cariogenic pathogens and more common inflammation induced bacteria such as *E. coli* is worth investigating in the future.

Chapter 7 Concluding discussion

7.1 Concluding discussion

Autologous bone grafts are currently considered as the ‘gold standard’ to repair or regenerate defective bone tissue. However, significant drawbacks including extra painful harvest surgery, donor site morbidity, inadequate supply and even the risk of surgical complications limit their clinical utilization (Lareau et al., 2015, Shibuya and Jupiter, 2015, Jakob et al., 2012, Bhatt and Rozental, 2012, Zimmermann and Moghaddam, 2011).

Synthetic biomaterials are an alternative clinical strategy to repair the defective bone tissues. In order to obtain a favourable biological outcome, ideally these synthetic grafts should emulate the chemical and physical structure of the native bone tissue, as well as being osteoinductive for the bone-forming cells, angiogenic for the vessel growth, display antibacterial ability and be non-toxic for the surrounding soft tissues especially during the periodontal defective bone repair. Bioactive glasses have been widely studied for their specific clinical applications due to their significant advantages such as promoting HA layer on their surface and bonding with the surrounding living tissues, being osteoinductive and degradable. Therefore, the strategy adopted in this work in order to achieve the above requirements was to consider the effect of bioactive glass compositions on material properties and biological performances.

Relevant literature reviewed in Chapter 1, including periodontium, periodontitis and periodontal regeneration, as well as bioactive glasses (especially the effects of phosphate and fluoride). The objectives and outline for this project are listed at the end of Chapter 1. Chapter 2 presents the experimental work performed with the aim of designing novel and optimal bioactive glass compositions and investigating the biological performances including osteogenesis by bone nodule and Type I collagen formation, angiogenesis by VEGF gene and protein production, effects on periodontal soft tissues and antibacterial ability.

Results presented in Chapters 3-6 highlighted the significant effects of high phosphate and low fluoride addition to bioactive glasses. In particular, the bioactive glass fluoride content should be carefully considered since high fluoride influenced the viability of MC3T3-E1 cells. Promising improvements in the differentiation and proliferative rate of osteoblast precursor cells were seen in the low fluoride containing glass groups.

These results were followed by studies further concerning the effects of those novel bioactive glasses on osteogenesis such as mineralization, Type I collagen formation and gene expression, angiogenesis including VEGF gene expression and protein production, influences on oral soft tissues including epithelial cells and fibroblasts, and finally the ability to prevent bacterial growth. Overall, the composition with 1% fluoride addition significantly accelerated apatite formation in Tris buffer solution, promoted osteogenic and angiogenic markers in MC3T3-E1 cells, prevented the epithelial cells growth and displayed antibacterial ability. However, it is difficult to recommend an ‘optimised’ bioactive glass

composition from this *in vitro* study without conducting further experimental work as it differs from the *in vivo* environment. This chapter summarises the conclusions that can be drawn from the presented experimental findings.

7.1.1 Apatite formation

Increasing the P_2O_5 content in the glass enhances the reactivity of the glass, as the phosphate is often regarded to exist as a separate orthophosphate phase within the glass, which potentially promotes glass bioactivity leading to an increase of the apatite formation rate (O'Donnell et al., 2009, O'Donnell et al., 2008b, O'Donnell et al., 2008a). Furthermore, higher phosphate content can reduce the rate and extent of local pH rise induced by the bioactive glass dissolution, which may reduce the deleterious effects brought by high alkalinity, on resident cells in the local environment (Monfoulet et al., 2014). Therefore, higher phosphate content will enable the development of products with higher surface areas without running into the pH problems. The finer particle size with increased surface area will result in faster glass dissolution creating an appropriate environment in which apatite and later bone can be more rapidly formed. However, with increasing phosphate content, there is an increased tendency to obtain crystallised bioactive glasses instead of amorphous nature, since O'Donnell *et al.* found that when the P_2O_5 content reached to 9.25 Mol.%, the bioactive glass was crystallised. Therefore, based on the previous studies, 6.33 Mol.% phosphate was added as a high, but 'safe' concentration in this project.

It is found that in this project, in Tris buffer solution, the formation of apatite occurred even more rapidly with the addition of fluoride (as low as only 1 Mol.%), which may be attributed to:

(1) The presence of fluoride eliminated the formation of the intermediate octacalcium phosphate phase, which is a precursor phase involved in apatite formation *in vitro* (Aoba, 1997, Iijima, 2001, Johnsson and Nancollas, 1992, LeGeros et al., 1989, Siew et al., 1992, Tseng et al., 2006);

(2) Fluoride complexes with calcium and sodium rather than forming Si-F bonds, resulting in decreasing the compactness of the glass network, which may make the glass structure easier to break down and promote glass solubility and reactivity;

(3) Increasing fluoride content slightly increases Tris buffer pH, since a high pH environment is favourable for apatite nucleation in SBF (Lu and Leng, 2005a), and apatite formation was also very susceptible to slight pH changes in fluoride containing glass composition (Brauer et al., 2010).

As Tris buffer solution is free of Ca^{2+} and PO_4^{3-} ions with a pH 7.3, it is an excellent medium to assess bioactive glass dissolution and apatite forming capacity and therefore widely used by biomaterial researchers. However, experiments with cell culture medium can provide a more *in vivo-like* model to examine how bodily fluids will interact with bioactive glasses. Therefore, in this project, the apatite formation in cell culture medium (α-MEM) was also examined.

It is interesting to find that the reaction was significantly different in the two solutions. No significant apatite peaks were found in the XRD patterns after immersion in α-MEM, which may be attributed to the limitation of the technique since XRD allows for the identification of various phases such as apatite, calcite, or fluorite, but it is not sensitive enough to detect when they are present as small crystallites. It means small or nano-sized apatite may be formed after immersion in α-MEM but did not cause significant apatite peaks in XRD pattern, evidenced from the single band at approximately 570cm^{-1} in FTIR spectra (Fig 4.12), corresponding to the formation of an amorphous or disordered crystalline apatite such as OCP or amorphous calcium phosphate, which is considered as a precursor of apatite. If this is the real outcome, biomimetic nano-structured apatite would display better ability for the protein binding and encourage osteoblast attachment and proliferation.

7.1.2 Osteogenesis

For an ideal bone-graft substitute, besides the primary requirement to fill the defective site, form an apatite surface for bonding to the surrounding live tissues and provide scaffolding for the bone cells to adhere, proliferate and form extracellular matrix, it is also required to stimulate and activate bone-forming cells and promote growth factors production to accelerate new bone growth in the bony defect area.

Numerous *in vitro* and animal studies have demonstrated that fluoride can modulate bone-forming cell activities (Farley et al., 1983, Fernandes et al., 2012, Huo et al., 2013, Kassem et al., 1994, Okuda et al., 1990, Pei et al.,

2012, Qu et al., 2008, Ren et al., 2011, Wang et al., 2011, Yan et al., 2009). Addition of fluoride into bioactive glasses has been demonstrated to significantly accelerate the apatite formation in Tris buffer as represented in the Chapter 4. However, high levels of systemic fluoride are known to cause skeletal and dental fluorosis characterized by debilitating changes in the skeleton, and marked mottling and discoloration in the teeth (Chachra et al., 2008, Vestergaard et al., 2008) and caution must be applied.

As expected, the osteogenic responses of MC3T3-E1 cells including proliferation, ALP activity, Type I collagen formation, bone nodule formation and osteogenic gene expression were promoted by the high phosphate, low F addition glass (P6.33F1) but significantly suppressed when the F content increased to 5-7%, which can be attributed to the biphasic manner of fluoride interacts with mineralized tissues as discussed before in the literature review (Chachra et al., 2008, Aaseth et al., 2004).

However, it is interesting to find that in this study, compared with the control (no glass), the above osteogenic activities were also significantly promoted by the high phosphate but fluoride free glass (P6.33F0), which may be attributed to the effects of high phosphate and silicon. As phosphate plays a vital role and is essential in the biological mineralization and included as a basic element in the cell culture medium, in this study, the high phosphate containing glasses resulted in the phosphate concentrations in glass conditioned medium being kept similar to that in α-MEM (Fig. 4.13), avoiding of consumption of medium phosphate to form apatite. While numerous studies have demonstrated stimulatory effects of

silicon on cellular activities, such as regulating the expression of key osteoblastic marker genes, cell cycle regulators and extracellular matrix proteins, stimulating new bone formation in animal models, inhibiting osteoclast phenotypic gene expression, osteoclast formation and bone resorption *in vitro* although the exact mechanism is yet to be understood (Calvo-Guirado et al., 2014, Chadwick et al., 2014, Friederichs et al., 2015, Henstock et al., 2015, Manchon et al., 2015, Mladenovic et al., 2014, Odatsu et al., 2015).

7.1.3 Angiogenesis

For efficient osteogenesis, angiogenesis and vascular network development to provide a sufficient supply of blood and oxygen play a crucial role as bone-forming cells are highly metabolic requiring the supply of oxygen, nutrients and elimination of their by-products (Nuss and von Rechenberg, 2008, Karageorgiou and Kaplan, 2005, Kuzyk and Schemitsch, 2011). Therefore, the angiogenic potential of those novel high phosphate and low fluoride containing bioactive glasses was also investigated.

There is no doubt that the VEGF gene expression and its protein production were both significantly promoted by the high phosphate but fluoride free glass P6.33F0, since silicon released from bioactive glasses has been demonstrated to stimulate VEGF secretion and promote angiogenesis through *in vitro* and *in vivo* studies (Day, 2005, Gorustovich et al., 2010, Leu et al., 2009, Li and Chang, 2013, Wang et al., 2013a, Fielding and Bose, 2013, Zhai et al., 2012).

However, the VEGF gene expression and protein production were further promoted by the fluoride containing glasses, compared with the P6.33F0 glass. As there is no publication which directly discusses the effects of fluoride on VEGF production and only few animal studies indirectly suggest fluoride containing biomaterials may promote angiogenesis, then MC3T3-E1 cells were treated with a range of F^- concentrations (0, 0.1, 1.9 and 9.5ppm) for the VEGF protein production in this study. There was no significant difference between the control (0ppm) and F^- concentration groups after 7d, 14d and 21d treatment. Therefore, the improved angiogenesis on MC3T3-E1 cells after treatment with fluoride containing bioactive glasses may attribute to the combined effects of silicon and fluoride.

7.1.4 Effects on oral soft tissues

Periodontal intra-bony defects represent a major challenge as the ultimate goal is the regeneration of lost periodontal tissues including both the soft and hard. Therefore, a variety of clinical treatment modalities including the use of autogenous bone grafts and bone substitutes materials, barrier membranes and growth factors have been proposed to promote the periodontal tissue regeneration. In this way, the healing outcome will not only depend on the regeneration of the alveolar bone, but also be determined by the surrounding soft tissues to promote an adequate sealing by the gingival tissue which contains epithelial cells and fibroblasts (Vignoletti et al., 2014).

During the wound healing process, epithelial cells have the highest proliferation capacity and can be the first cells to migrate to the injury site. This becomes a problem as they form a long, non-keratinized junctional epithelium and will prevent the migration of the cells from the periodontal ligament and alveolar bone. Therefore, in periodontal surgeries, the guided tissue regeneration technique is widely applied by using a resorbable or non-resorbable membrane acting as a physical barrier against the epithelial cell migration, from the superficial soft tissue flap into the underlying graft site. This procedure allows the necessary time for the cell repopulation of the periodontal ligament and adjacent alveolar bone, and will favour the regeneration of lost and damaged tissue (Kay et al., 1997).

In this project, the bioactive glasses were not cytotoxic to the epithelial cell growth, compared with the control. However, they significantly suppressed the cell proliferation, which was further decreased by the fluoride containing bioactive glasses. It may be attributed to the combined effects of fluoride and bioactive glasses, since it also found that the epithelial cell proliferation was does-dependently suppressed after treating with NaF concentrations in this project.

Periodontal ligament is a specialized connective tissue embedded between the cementum and the inner wall of the alveolar bone socket. It not only has an important role in supporting teeth and the homeostasis of periodontal tissues, but also contributes to alveolar bone remodelling and tissue regeneration, since it contains a heterogeneous cell population including fibroblasts, cementoblasts, osteoblasts, and progenitor/stem

cells, in which fibroblasts are the predominant cell type. Therefore, specific proliferation and migration of periodontal ligament cells, mainly fibroblasts, are crucial in successful periodontal tissue regeneration.

In this project, fibroblast proliferation was significantly promoted by all the bioactive glasses after 10 d treatment, which also may be attributed to the combined effects of bioactive glass and fluoride, but mainly from bioactive glasses, since only the high NaF concentrations (9.5 and 19 ppm) were found to increase the fibroblast proliferation.

Therefore, if applied *in vivo* to repair the periodontal intra-bony defects, those high phosphate and low fluoride containing bioactive glasses potentially act to prevent the long, non-keratinized junctional epithelium growth, promote the periodontal ligament reestablishment and then to simplify the periodontal surgery process without using or minimal the guided tissue regeneration technique and increase the success of defective bone repair.

7.1.5 Antibacterial ability

For a successful periodontal bony defect treatment, besides the tissue regeneration, the first and important requirement is eliminating the active disease and avoiding infection during or after the surgery. To reach this goal, antimicrobial approaches are needed. As the use of systemic antibiotics can induce the development of bacterial resistance and may not be suitable for patients with some other diseases, local antibacterial application is an alternative option and, it is the best if the implanted graft substitutes themselves can be antimicrobial.

Fluoride is well known for the antibacterial ability, so as expected in this project, bioactive glasses showed strong prevention effects on the dental plaque pioneer colonizer *S. mitis* and cariogenic bacterial *L. casei*, and most importantly, they also significantly suppressed the growth of *P. gingivalis* and *A. actinomycetemcomitans,* which are highly associated with the chronic periodontitis and aggressive periodontitis respectively in numerous *in vitro* and *in vivo* studies.

However, it is noticeable that even the base glass P6.33F0 in this study showed antibacterial activity against all the investigated bacteria, in which condition the antibacterial effect was from bioactive glass particles instead of fluoride, the mechanism in which can be attributed to the alkaline nature of surface reactions with pH elevation in most studies. Therefore, with the combined antibacterial ability of bioactive glasses and fluoride, those high phosphate and low fluoride addition bioactive glasses will be advantageous in the periodontal bony defect treatment.

7.2 Conclusion

In summary, this project has shown that as a potential bone substitute, the high phosphate and low fluoride addition bioactive glasses resulted in significantly faster apatite formation in Tris buffer solution, and promoted osteoblast-like cell pre-osteogenic, pro-angiogenic responses, and prevented epithelial cell growth while promoted fibroblast proliferation, and significantly inhibited the growth of periodontal pathogens *in vitro*. Such novel bioactive glasses would be expected to stimulate bone formation and overcome problems associated with infection and the poor vascularisation in large bone graft sites and hopefully reduce the need for further clinical intervention, and in particular, will be advantageous for the periodontal soft tissue regeneration.

.

7.3 Future prospective

The experimental work performed has achieved the initial project objectives outlined in Chapter 1. However, it is difficult to conclude that 1% fluoride containing bioactive glass (P6.33F1) is the 'optimal' composition to be applied as bone substitutes without conducting animal studies and further experimental work, although glass P6.33F1 has shown significant positive effects on apatite formation, pre-osteogenic and pro-angiogenic responses, oral soft tissues and pathogens growth *in vitro.* Due to the complexity of *in vivo* environment, an 'optimised' form also should be obtained to satisfy clinical requirements such as good handling characteristics, biomimetic compressive strength and proper degradable rate, since the bioactive glasses investigated in this project are in particles, which are difficult for *in vivo* applications. Therefore, the future work would focus on how to transfer those particles into clinical applied substitutes followed by proper animal studies.

Currently, granular bone graft materials, such as the Straumann® Bone Ceramic and Geistlich Bio-Oss®, are the common clinical available options when filling the alveolar socket or undertaking guided bone regeneration for fixation of an implant. Straumann® Bone Ceramic is a fully alloplastic biphasic calcium phosphate composed of hydroxylapatite and β-tricalcium phosphate, while Geistlich Bio-Oss® is derived from bovine bone. They are granules (i.e. 0.25 - 2 mm size) and have been used successfully offering a scaffolding and somewhat resorbable and osteoconductive bone substitute material. However, low resorption rate is a problem cannot be ignored. As hydroxyapatite is a stable crystalline phase may take many

years to be degraded, and in some instances may never occur, while it is desirable that after use of a bone substitute material rapid resorption and replacement with host bone will occur.

PerioGlas® from NovaBone is another granular bone graft material composed of bioactive glass 45S5. It has been demonstrated to form hydroxycarbonate apatite layer creating an ideal environment for cellular attachment and for protein and growth factor absorption, enhance cell signalling and upregulate the bone forming process. Most importantly, it is completely resorbable. Therefore, combining the advantages of bioactive glasses and high phosphate low fluoride effects, it is an option to prepare the bioactive glasses investigated in this project into granules prior to *in vivo* study.

As granules are the most common bone graft materials currently, there are still some noticeable disadvantages, such as, granular bone substitutes are typically wetted and mixed with patients' blood or saline solution prior to implantation, which lengthens the surgical time. By the nature of granules, they have no inherent bulk strength until they have been fully osseointegrated so that they can easily be deformed by the application of pressure and force which can cause potential granule migration from the implantation site and the formation of voids in the material, may result in incomplete guided bone regeneration.

Therefore, introduction of an injectable material that hardens in situ can be an alternative option to address the problems caused by granular bone substitutes and to avoid unnecessary discomfort for the patient, difficulty for the clinician, lengthening of surgical time and compromised *in vivo*

performance. Currently, vertebroplasty and kyphoplasty procedures use injectable polymethylmethacrylate (PMMA) cement that provides support within the vertebral body. The negative characteristics of PMMA-based bone cements are the strongly exothermic reaction, toxic effects of the monomer which leads to poor osteointegration and pain. In addition, the PMMA bulk does not 'mechanically integrate' with bone and will carry all the weight, effectively isolating the pre-existing bone to osteogenic stimuli. This will lead to further bone resorption and complications

Recently a novel injectable bone substitute material has been developed and patented at the Bart's and The London School of Medicine and Dentistry, Queen Mary University of London (Patent Number: PCT/EP2012/076844). The novel material is a mixture of bioactive glass and $Ca(H_2PO_4)_2$ powder which reacts when mixed with water to form hydroxyapatite through the following reaction:

Bioactive Glass + $Ca(H_2PO_4)_2 \rightarrow Ca_{10}(PO_4)_6(OH)_2$

After implantation the cement hardens *in vivo* in 15 minutes after initial mixing. As the cement sets to form hydroxyapatite, the mineral phase of bones and teeth, it is able to be osseointegrated, resorbed, and then replaced by host bone.

However, only four basic bioactive glass components (Ca, Na, P and Si) were included in the previous patent. The glass composition can be altered at will to change the properties of the cement including setting time, strength, resorption rate and influence on osteogenic rate. Thus the cement can be tailored to have the exact properties desired to give the

material an ideal setting time and strength for optimal bone remodelling to facilitate healing.

As the numerous positive effects from high phosphate and low fluoride addition investigated in this project, it is another option to develop a novel injectable bone graft material with those high phosphate and low fluoride addition bioactive glasses as a precursor. This new cement material will combine the benefits of high phosphate, fluoride, bioactive glass and cement, such as fast implantation by injection, mouldable to implant site, no implant migration, porous, yet resistant to force, osteoconductive, resorbable, antibacterial and positive effects on oral soft tissue regeneration.

For bone grafting substitutes, porous interconnecting structures with micro-pores or macro-pores can provide a higher surface area for cell attachment, and subsequently invading the scaffold to proliferate and form extra cellular matrix at early time points (Bonfield, 2006). Bonfield also suggested there was a particular requirement for the pore size of those porous scaffolds, greater than 100 μm in diameter was a key requirement both for ingression of cells and to develop associated vascularization to maintain viable bone (Bonfield, 2006). Therefore, to develop an injectable bone substitute with porous structure and proper strength, both fine (0-38 μm size) and coarse (i.e. 100-200 μm size) bioactive glass powder can be produced and used to react with $Ca(H_2PO_4)_2$ salt according to the above reaction, in which, the fine bioactive glass particles and $Ca(H_2PO_4)_2$ salt react on contact with aqueous solution to form the cement phase. Upon mixing the glass dissolves rapidly, releasing Ca^{2+} and PO_4^{3-} ions that react

with the $Ca(H_2PO_4)_2$ salt to form the hydroxyapatite cement phase. Incorporation of the coarse bioactive particles is not to react during the initial setting but will degrade rapidly leaving a network of pores, such as 100-200 μm, that will facilitate the ingrowth of cells and neovascularization. In this way, the bulk cement strength is maintained but the rate of remodelling is increased.

Therefore, the future plan for this project could be transferring the investigated novel high phosphate low fluoride bioactive glasses into injectable cements, then the cement properties including setting time, dissolution and compressive strength will be explored *in vitro*, followed by proper *in vivo* animal studies.

Chapter 8 References

AARON, J. E., DE VERNEJOUL, M. C. & KANIS, J. A. 1991. The effect of sodium fluoride on trabecular architecture. *Bone,* 12**,** 307-10.

AASETH, J., SHIMSHI, M., GABRILOVE, J. L. & BIRKETVEDT, G. S. 2004. Fluoride: A toxic or therapeutic agent in the treatment of osteoporosis? *The Journal of Trace Elements in Experimental Medicine,* 17**,** 83-92.

ABDULMAJEED, A. A., KOKKARI, A. K., KAPYLA, J., MASSERA, J., HUPA, L., VALLITTU, P. K. & NARHI, T. O. 2014. In vitro blood and fibroblast responses to BisGMA-TEGDMA/bioactive glass composite implants. *J Mater Sci Mater Med,* 25**,** 151-62.

AGUIAR, H., SOLLA, E. L., SERRA, J., GONZÁLEZ, P., LEÓN, B., ALMEIDA, N., CACHINHO, S., DAVIM, E. J. C., CORREIA, R., OLIVEIRA, J. M. & FERNANDES, M. H. V. 2008. Orthophosphate nanostructures in SiO2–P2O5–CaO–Na2O–MgO bioactive glasses. *Journal of Non-Crystalline Solids,* 354**,** 4075-4080.

AL-NOAMAN, A., KARPUKHINA, N., RAWLINSON, S. C. F. & HILL, R. G. 2013. Effect of FA on bioactivity of bioactive glass coating for titanium dental implant. Part I: Composite powder. *Journal of Non-Crystalline Solids,* 364**,** 92-98.

AL-NOAMAN, A., RAWLINSON, S. C. F. & HILL, R. G. 2012. The influence of CaF2 content on the physical properties and apatite formation of bioactive glass coatings for dental implants. *Journal of Non-Crystalline Solids,* 358**,** 1850-1858.

ALGATE, K., HAYNES, D. R., BARTOLD, P. M., CROTTI, T. N. & CANTLEY, M. D. 2015. The effects of tumour necrosis factor-alpha on bone cells involved in periodontal alveolar bone loss; osteoclasts, osteoblasts and osteocytes. *J Periodontal Res*.

ALLAN, I., NEWMAN, H. & WILSON, M. 2001. Antibacterial activity of particulate bioglass against supra- and subgingival bacteria. *Biomaterials,* 22**,** 1683-7.

AMADASI, A., MERLI, D., BRANDONE, A., POPPA, P., GIBELLI, D. & CATTANEO, C. 2013. The Survival of Gunshot Residues in Cremated Bone: An Inductively Coupled Plasma Optical Emission Spectrometry Study. *J Forensic Sci*.

AMEERAMJA, J., PANNEERSELVAM, L., GOVINDARAJAN, V., JEYACHANDRAN, S., BASKARALINGAM, V. & PERUMAL, E. 2015. Tamarind seed coat ameliorates fluoride induced cytotoxicity, oxidative stress, mitochondrial dysfunction and apoptosis in A549 cells. *J Hazard Mater,* 301**,** 554-565.

ANDERSON, H. C. 2003. Matrix vesicles and calcification. *Curr Rheumatol Rep,* 5**,** 222-6.

ANGELL, C. A. 1983. Fast ion motion in glassy and amorphous materials. *Solid State Ionics,* 9–10, Part 1**,** 3-16.

ANGELL, C. A. 1986. Recent developments in fast ion transport in glassy and amorphous materials. *Solid State Ionics,* 18–19, Part 1**,** 72-88.

ANURADHA, K. P., CHADRASHEKAR, J. & RAMESH, N. 2002. Prevalence of periodontal disease in endemically flourosed areas of Davangere Taluk, India. *Indian J Dent Res,* 13**,** 15-9.

AOBA, T. 1997. The effect of fluoride on apatite structure and growth. *Crit Rev Oral Biol Med,* 8**,** 136-53.

APELT, D., THEISS, F., EL-WARRAK, A. O., ZLINSZKY, K., BETTSCHART-WOLFISBERGER, R., BOHNER, M., MATTER, S., AUER, J. A. & VON RECHENBERG, B. 2004. In vivo behavior of three different injectable hydraulic calcium phosphate cements. *Biomaterials,* 25**,** 1439-51.

ARAKAWA, Y., BHAWAL, U. K., IKOMA, T., KIMOTO, K., KUROHA, K., KUBOTA, T., HAMADA, N., KUBOTA, E. & ARAKAWA, H. 2009. Low concentration fluoride stimulates cell motility of epithelial cells in vitro. *Biomed Res,* 30**,** 271-7.

ARMITAGE, G. C. 2004. Periodontal diagnoses and classification of periodontal diseases. *Periodontol 2000,* 34**,** 9-21.

ARTHUR, R. A., KOHARA, E. K., WAEISS, R. A., ECKERT, G. J., ZERO, D. & ANDO, M. 2014. Enamel Carious Lesion Development in Response to Sucrose and Fluoride Concentrations and to Time of Biofilm Formation: An Artificial-Mouth Study. *J Oral Dis,* 2014.

ATANASOVA, K. R. & YILMAZ, O. 2014. Looking in the Porphyromonas gingivalis cabinet of curiosities: the microbium, the host and cancer association. *Mol Oral Microbiol,* 29**,** 55-66.

BADET, C. & THEBAUD, N. B. 2008. Ecology of lactobacilli in the oral cavity: a review of literature. *Open Microbiol J,* 2**,** 38-48.

BARBATO, L., FRANCIONI, E., BIANCHI, M., MASCITELLI, E., MARCO, L. B. & TONELLI, D. P. 2015. Periodontitis and bone metabolism. *Clin Cases Miner Bone Metab,* 12**,** 174-7.

BARRERE, F., VAN, B. C., DE, G. K. & LAYROLLE, P. 2002. Nucleation of biomimetic Ca-P coatings on ti6A14V from a SBF x 5 solution: influence of magnesium. *Biomaterials,* 23**,** 2211-20.

BARTOLD, P. M., GRONTHOS, S., IVANOVSKI, S., FISHER, A. & HUTMACHER, D. W. 2016. Tissue engineered periodontal products. *J Periodontal Res,* 51**,** 1-15.

BARTOLD, P. M., WALSH, L. J. & NARAYANAN, A. S. 2000. Molecular and cell biology of the gingiva. *Periodontol 2000,* 24**,** 28-55.

BASHUTSKI, J. D. & WANG, H. L. 2009. Periodontal and endodontic regeneration. *J Endod,* 35**,** 321-8.

BEAR, R. S. & SELBY, C. C. 1956. The structure of paramyosin fibrils according to x-ray diffraction. *J Biophys Biochem Cytol,* 2**,** 55-69.

BECK, G. R., JR. 2003. Inorganic phosphate as a signaling molecule in osteoblast differentiation. *J Cell Biochem,* 90**,** 234-43.

BECK, G. R., JR., MORAN, E. & KNECHT, N. 2003. Inorganic phosphate regulates multiple genes during osteoblast differentiation, including Nrf2. *Exp Cell Res,* 288**,** 288-300.

BECK, G. R., JR., SULLIVAN, E. C., MORAN, E. & ZERLER, B. 1998. Relationship between alkaline phosphatase levels, osteopontin expression, and mineralization in differentiating MC3T3-E1 osteoblasts. *J Cell Biochem,* 68**,** 269-80.

BECK, G. R., JR., ZERLER, B. & MORAN, E. 2000. Phosphate is a specific signal for induction of osteopontin gene expression. *Proc Natl Acad Sci U S A,* 97**,** 8352-7.

BELLUCCI, D., SOLA, A., ANESI, A., SALVATORI, R., CHIARINI, L. & CANNILLO, V. 2015. Bioactive glass/hydroxyapatite composites: mechanical properties and biological evaluation. *Mater Sci Eng C Mater Biol Appl,* 51**,** 196-205.

BERNSTEIN, D. S. & COHEN, P. 1967. Use of sodium fluoride in the treatment of osteoporosis. *J Clin Endocrinol Metab,* 27**,** 197-210.

BERNSTEIN, D. S. & GURI, C. D. 1963. OSTEOPOROSIS: ETIOLOGY AND THERAPY. *Postgrad Med,* 34**,** 407-9.

BHATT, R. A. & ROZENTAL, T. D. 2012. Bone graft substitutes. *Hand Clin,* 28**,** 457-68.

BIO-RAD. 2015. *What is alamarBlue®* [Online]. Available: https://www.abdserotec.com/alamarblue-cell-viability-assay-resazurin.html [Accessed 8 Sep 2015.

BOHNER, M. & LEMAITRE, J. 2009. Can bioactivity be tested in vitro with SBF solution? *Biomaterials,* 30**,** 2175-9.

BOIVIN, G., CHAVASSIEUX, P., CHAPUY, M. C., BAUD, C. A. & MEUNIER, P. J. 1989. Skeletal fluorosis: histomorphometric analysis of bone changes and bone fluoride content in 29 patients. *Bone,* 10**,** 89-99.

BONEWALD, L. F. & JOHNSON, M. L. 2008. Osteocytes, mechanosensing and Wnt signaling. *Bone,* 42**,** 606-615.

BONFIELD, W. 2006. Designing porous scaffolds for tissue engineering. *Philos Trans A Math Phys Eng Sci,* 364**,** 227-32.

BOSE, S., FIELDING, G., TARAFDER, S. & BANDYOPADHYAY, A. 2013. Understanding of dopant-induced osteogenesis and angiogenesis in calcium phosphate ceramics. *Trends Biotechnol,* 31**,** 594-605.

BOSE, S., ROY, M. & BANDYOPADHYAY, A. 2012. Recent advances in bone tissue engineering scaffolds. *Trends Biotechnol,* 30**,** 546-54.

BOSSHARDT, D. D. & SELVIG, K. A. 1997. Dental cementum: the dynamic tissue covering of the root. *Periodontol 2000,* 13**,** 41-75.

BOSTANCI, N. & BELIBASAKIS, G. N. 2012. Porphyromonas gingivalis: an invasive and evasive opportunistic oral pathogen. *FEMS Microbiol Lett,* 333**,** 1-9.

BOYCE, B. F. 2013. Advances in the regulation of osteoclasts and osteoclast functions. *J Dent Res,* 92**,** 860-7.

BOYCE, B. F., ROSENBERG, E., DE PAPP, A. E. & DUONG LE, T. 2012. The osteoclast, bone remodelling and treatment of metabolic bone disease. *Eur J Clin Invest,* 42**,** 1332-41.

BOYCE, B. F., YAO, Z. & XING, L. 2009. Osteoclasts have multiple roles in bone in addition to bone resorption. *Crit Rev Eukaryot Gene Expr,* 19**,** 171-80.

BRADSHAW, D. J., MCKEE, A. S. & MARSH, P. D. 1990. Prevention of population shifts in oral microbial communities in vitro by low fluoride concentrations. *J Dent Res,* 69**,** 436-41.

BRAUER, D. S., ANJUM, M. N., MNEIMNE, M., WILSON, R. M., DOWEIDAR, H. & HILL, R. G. 2012. Fluoride-containing bioactive glass-ceramics. *Journal of Non-Crystalline Solids,* 358**,** 1438-1442.

BRAUER, D. S., KARPUKHINA, N., LAW, R. V. & HILL, R. G. 2009. Structure of fluoride-containing bioactive glasses. *Journal of Materials Chemistry,* 19**,** 5629-5636.

BRAUER, D. S., KARPUKHINA, N., O'DONNELL, M. D., LAW, R. V. & HILL, R. G. 2010. Fluoride-containing bioactive glasses: Effect of glass design and structure on degradation, pH and apatite formation in simulated body fluid. *Acta Biomaterialia,* 6**,** 3275-3282.

BRIGIDO, J. A., DA SILVEIRA, V. R., REGO, R. O. & NOGUEIRA, N. A. 2014. Serotypes of Aggregatibacter actinomycetemcomitans in relation to periodontal status and geographic origin of individuals-a review of the literature. *Med Oral Patol Oral Cir Bucal,* 19**,** e184-91.

BROWN, L., WASEEM, A., CRUZ, I. N., SZARY, J., GUNIC, E., MANNAN, T., UNADKAT, M., YANG, M., VALDERRAMA, F., O'TOOLE, E. A. & WAN, H. 2014. Desmoglein 3 promotes cancer cell migration and invasion by regulating activator protein 1 and protein kinase C-dependent-Ezrin activation. *Oncogene,* 33**,** 2363-74.

BRYDONE, A. S., MEEK, D. & MACLAINE, S. 2010. Bone grafting, orthopaedic biomaterials, and the clinical need for bone engineering. *Proc Inst Mech Eng H,* 224**,** 1329-43.

BUCK, D. W., 2ND & DUMANIAN, G. A. 2012. Bone biology and physiology: Part I. The fundamentals. *Plast Reconstr Surg,* 129**,** 1314-20.

BURKE, F. M., RAY, N. J. & MCCONNELL, R. J. 2006. Fluoride-containing restorative materials. *Int Dent J,* 56**,** 33-43.

BURSON, K. M., SCHLEXER, P., BÜCHNER, C., LICHTENSTEIN, L., HEYDE, M. & FREUND, H.-J. 2015. Characterizing Crystalline-Vitreous Structures: From Atomically Resolved Silica to Macroscopic Bubble Rafts. *Journal of Chemical Education,* 92**,** 1896-1902.

BYUN, R., NADKARNI, M. A., CHHOUR, K. L., MARTIN, F. E., JACQUES, N. A. & HUNTER, N. 2004. Quantitative analysis of diverse Lactobacillus species present in advanced dental caries. *J Clin Microbiol,* 42**,** 3128-36.

CALVO-GUIRADO, J. L., GARCES, M., DELGADO-RUIZ, R. A., RAMIREZ FERNANDEZ, M. P., FERRES-AMAT, E. & ROMANOS, G. E. 2014. Biphasic beta-TCP mixed with silicon increases bone formation in critical site defects in rabbit calvaria. *Clin Oral Implants Res*.

CARLSTROM, D. & ENGFELDT, B. 1954. Biophysical studies on bone tissue. IX. X-ray diffraction studies on bone tissue from osteogenic sarcoma. *Exp Cell Res,* 6**,** 535-6.

CARMICHAEL, J., MITCHELL, J. B., DEGRAFF, W. G., GAMSON, J., GAZDAR, A. F., JOHNSON, B. E., GLATSTEIN, E. & MINNA, J. D. 1988. Chemosensitivity testing of human lung cancer cell lines using the MTT assay. *Br J Cancer,* 57**,** 540-7.

CARPENTER, C. D., O'NEILL, T., PICOT, N., JOHNSON, J. A., ROBICHAUD, G. A., WEBSTER, D. & GRAY, C. A. 2012. Anti-mycobacterial natural products from the Canadian medicinal plant Juniperus communis. *J Ethnopharmacol,* 143**,** 695-700.

CARTER, D. R. & BEAUPRE, G. S. 1990. Effects of fluoride treatment on bone strength. *J Bone Miner Res,* 5 Suppl 1**,** S177-84.

CARVALHO, M. D., SUAID, F. F., SANTAMARIA, M. P., CASATI, M. Z., NOCITI, F. H., JR., SALLUM, A. W. & SALLUM, E. A. 2011. Platelet-rich plasma plus bioactive glass in the treatment of intra-bony defects: a study in dogs. *J Appl Oral Sci,* 19**,** 82-9.

CAVERZASIO, J., PALMER, G. & BONJOUR, J. P. 1998. Fluoride: mode of action. *Bone,* 22**,** 585-9.

CETINKAYA, B. O., KELES, G. C., AYAS, B., AYDIN, O., KIRTILOGLU, T. & ACIKGOZ, G. 2007. Comparison of the proliferative activity in gingival epithelium after surgical treatments of intrabony defects with bioactive glass and bioabsorbable membrane. *Clin Oral Investig,* 11**,** 61-8.

CHACHRA, D., VIEIRA, A. P. & GRYNPAS, M. D. 2008. Fluoride and mineralized tissues. *Crit Rev Biomed Eng,* 36**,** 183-223.

CHADWICK, E. G., CLARKIN, O. M., RAGHAVENDRA, R. & TANNER, D. A. 2014. A bioactive metallurgical grade porous silicon-polytetrafluoroethylene sheet for guided bone regeneration applications. *Biomed Mater Eng,* 24**,** 1563-74.

CHAVASSIEUX, P., CHENU, C., VALENTIN-OPRAN, A., DELMAS, P. D., BOIVIN, G., CHAPUY, M. C. & MEUNIER, P. J. 1993. In vitro exposure to sodium fluoride does not modify activity or proliferation of human osteoblastic cells in primary cultures. *J Bone Miner Res,* 8**,** 37-44.

CHAZOTTE, B. 2011. Labeling nuclear DNA using DAPI. *Cold Spring Harb Protoc,* 2011**,** pdb prot5556.

CHIEN, C. H., OTSUKI, S., CHOWDHURY, S. A., KOBAYASHI, M., TAKAHASHI, K., KANDA, Y., KUNII, S., SAKAGAMI, H. & KANEGAE, H. 2006. Enhancement of cytotoxic activity of sodium fluoride against human periodontal ligament fibroblasts by water pressure. *In Vivo,* 20**,** 849-56.

CHRISTENSON, R. H. 1997. Biochemical markers of bone metabolism: an overview. *Clin Biochem,* 30**,** 573-93.

CHRISTIE, J. K., PEDONE, A., MENZIANI, M. C. & TILOCCA, A. 2011. Fluorine Environment in Bioactive Glasses: ab Initio Molecular Dynamics Simulations. *The Journal of Physical Chemistry B,* 115**,** 2038-2045.

CIAPETTI, G., CENNI, E., PRATELLI, L. & PIZZOFERRATO, A. 1993. In vitro evaluation of cell/biomaterial interaction by MTT assay. *Biomaterials,* 14**,** 359-64.

CLARKE, B. 2008. Normal bone anatomy and physiology. *Clin J Am Soc Nephrol,* 3 Suppl 3**,** S131-9.

COLLINS, L. & FRANZBLAU, S. G. 1997. Microplate alamar blue assay versus BACTEC 460 system for high-throughput screening of compounds against Mycobacterium tuberculosis and Mycobacterium avium. *Antimicrob Agents Chemother,* 41**,** 1004-9.

CONRADS, K. A., YI, M., SIMPSON, K. A., LUCAS, D. A., CAMALIER, C. E., YU, L. R., VEENSTRA, T. D., STEPHENS, R. M., CONRADS, T. P. & BECK, G. R., JR. 2005. A combined proteome and microarray investigation of inorganic phosphate-induced pre-osteoblast cells. *Mol Cell Proteomics,* 4**,** 1284-96.

CONRADS, K. A., YU, L. R., LUCAS, D. A., ZHOU, M., CHAN, K. C., SIMPSON, K. A., SCHAEFER, C. F., ISSAQ, H. J., VEENSTRA, T. D., BECK, G. R., JR. & CONRADS, T. P. 2004. Quantitative proteomic analysis of inorganic phosphate-induced murine MC3T3-E1 osteoblast cells. *Electrophoresis,* 25**,** 1342-52.

COOPER, L. F., ZHOU, Y., TAKEBE, J., GUO, J., ABRON, A., HOLMEN, A. & ELLINGSEN, J. E. 2006. Fluoride modification effects on osteoblast behavior and bone formation at TiO2 grit-blasted c.p. titanium endosseous implants. *Biomaterials,* 27**,** 926-36.

CORACA-HUBER, D. C., FILLE, M., HAUSDORFER, J., PUTZER, D. & NOGLER, M. 2014. Efficacy of antibacterial bioactive glass S53P4 against S. aureus biofilms grown on titanium discs in vitro. *J Orthop Res,* 32**,** 175-7.

CULITY, B. D. 1956. *Elements Of X Ray Diffraction*, Addison-Wesley Publishing Company, Inc.

DA SILVA, N. B., ALEXANDRIA, A. K., DE LIMA, A. L., CLAUDINO, L. V., DE OLIVEIRA CARNEIRO, T. F., DA COSTA, A. C., VALENCA, A. M. & CAVALCANTI, A. L. 2012. In vitro antimicrobial activity of mouth washes and herbal products against dental biofilm-forming bacteria. *Contemp Clin Dent,* 3**,** 302-5.

DARBY, I. 2011. Periodontal materials. *Aust Dent J,* 56 Suppl 1**,** 107-18.

DARVEAU, R. P. 2009. The oral microbial consortium's interaction with the periodontal innate defense system. *DNA Cell Biol,* 28**,** 389-95.

DAS, S. & CROCKETT, J. C. 2013. Osteoporosis - a current view of pharmacological prevention and treatment. *Drug Des Devel Ther,* 7**,** 435-48.

DAY, R. M. 2005. Bioactive glass stimulates the secretion of angiogenic growth factors and angiogenesis in vitro. *Tissue Eng,* 11**,** 768-77.

DE PAULA E SILVA, A. C., OLIVEIRA, H. C., SILVA, J. F., SANGALLI-LEITE, F., SCORZONI, L., FUSCO-ALMEIDA, A. M. & MENDES-GIANNINI, M. J. 2013. Microplate alamarBlue assay for Paracoccidioides susceptibility testing. *J Clin Microbiol,* 51**,** 1250-2.

DELAISSE, J. M., ANDERSEN, T. L., ENGSIG, M. T., HENRIKSEN, K., TROEN, T. & BLAVIER, L. 2003. Matrix metalloproteinases (MMP) and cathepsin K contribute differently to osteoclastic activities. *Microsc Res Tech,* 61**,** 504-13.

DELIA S. BRAUER, N. K., DAPHNE SEAH, ROBERT V. LAW, ROBERT G. HILL 2008. Fluoride-Containing Bioactive Glasses. *Advanced Materials Research,* (Volumes 39 - 40**,** 299-304.

DELLINGER, M. & GEZE, M. 2001. Detection of mitochondrial DNA in living animal cells with fluorescence microscopy. *J Microsc,* 204**,** 196-202.

DENTINO, A., LEE, S., MAILHOT, J. & HEFTI, A. F. 2013. Principles of periodontology. *Periodontol 2000,* 61**,** 16-53.

DIBA, M., TAPIA, F., BOCCACCINI, A. R. & STROBEL, L. A. 2012. Magnesium-Containing Bioactive Glasses for Biomedical Applications. *International Journal of Applied Glass Science,* 3**,** 221-253.

DIETRICH, E., OUDADESSE, H., LUCAS-GIROT, A. & MAMI, M. 2009. In vitro bioactivity of melt-derived glass 46S6 doped with magnesium. *J Biomed Mater Res A,* 88**,** 1087-96.

DOBELIN, N., LUGINBUHL, R. & BOHNER, M. 2010. Synthetic calcium phosphate ceramics for treatment of bone fractures. *Chimia (Aarau),* 64**,** 723-9.

DOGAN, S., GUNAY, H., LEYHAUSEN, G. & GEURTSEN, W. 2002. Chemical-biological interactions of NaF with three different cell lines and the caries pathogen Streptococcus sobrinus. *Clin Oral Investig,* 6**,** 92-7.

DRAGO, L., ROMANO, D., DE VECCHI, E., VASSENA, C., LOGOLUSO, N., MATTINA, R. & ROMANO, C. L. 2013. Bioactive glass BAG-S53P4 for the adjunctive treatment of chronic osteomyelitis of the long bones: an in vitro and prospective clinical study. *BMC Infect Dis,* 13**,** 584.

DREXLER, H. G. & UPHOFF, C. C. 2002. Mycoplasma contamination of cell cultures: Incidence, sources, effects, detection, elimination, prevention. *Cytotechnology,* 39**,** 75-90.

DUAN, X., XU, H., WANG, Y., WANG, H., LI, G. & JING, L. 2014. Expression of core-binding factor alpha1 and osteocalcin in fluoride-treated fibroblasts and osteoblasts. *J Trace Elem Med Biol,* 28**,** 278-83.

DUNCAN, M. J. 2003. Genomics of oral bacteria. *Crit Rev Oral Biol Med,* 14**,** 175-87.

DVORAK, M. M., SIDDIQUA, A., WARD, D. T., CARTER, D. H., DALLAS, S. L., NEMETH, E. F. & RICCARDI, D. 2004. Physiological changes in extracellular calcium concentration directly control osteoblast function in the absence of calciotropic hormones. *Proc Natl Acad Sci U S A,* 101**,** 5140-5.

EANES, E. D. & MEYER, J. L. 1978. The influence of fluoride on apatite formation from unstable supersaturated solutions at pH 7.4. *J Dent Res,* 57**,** 617-624.

ECHEZARRETA-LOPEZ, M. M. & LANDIN, M. 2013. Using machine learning for improving knowledge on antibacterial effect of bioactive glass. *Int J Pharm,* 453**,** 641-7.

EDÉN, M. 2011. The split network analysis for exploring composition–structure correlations in multi-component glasses: I. Rationalizing bioactivity-composition trends of bioglasses. *Journal of Non-Crystalline Solids,* 357**,** 1595-1602.

ELGAYAR, I., ALIEV, A. E., BOCCACCINI, A. R. & HILL, R. G. 2005. Structural analysis of bioactive glasses. *Journal of Non-Crystalline Solids,* 351**,** 173-183.

EPKER, B. N. 1967. Effects of fluoride on bone remodeling and balance and its use in the treatment of osteoporosis. *Annu Meet Am Inst Oral Biol***,** 19-29.

EVERETT, E. T. 2011. Fluoride's effects on the formation of teeth and bones, and the influence of genetics. *J Dent Res,* 90**,** 552-60.

FAN, Y., SUN, Z. & MORADIAN-OLDAK, J. 2009. Effect of fluoride on the morphology of calcium phosphate crystals grown on acid-etched human enamel. *Caries Res,* 43**,** 132-6.

FAN, Y., SUN, Z., WANG, R., ABBOTT, C. & MORADIAN-OLDAK, J. 2007. Enamel inspired nanocomposite fabrication through amelogenin supramolecular assembly. *Biomaterials,* 28**,** 3034-42.

FARLEY, J. R., WERGEDAL, J. E. & BAYLINK, D. J. 1983. Fluoride directly stimulates proliferation and alkaline phosphatase activity of bone-forming cells. *Science,* 222**,** 330-2.

FEATHERSTONE, J. D. 2004. The continuum of dental caries--evidence for a dynamic disease process. *J Dent Res,* 83 Spec No C**,** C39-42.

FERNANDES, M. D., YANAI, M. M., MARTINS, G. M., IANO, F. G., LEITE, A. L., CESTARI, T. M., TAGA, R., BUZALAF, M. A. & DE OLIVEIRA, R. C. 2012. Effects of fluoride in bone repair: an evaluation of RANKL, OPG and TRAP expression. *Odontology*.

FERRARA, N. 2004. Vascular endothelial growth factor: basic science and clinical progress. *Endocr Rev,* 25**,** 581-611.

FERRARA, N. & DAVIS-SMYTH, T. 1997. The biology of vascular endothelial growth factor. *Endocr Rev,* 18**,** 4-25.

FIELDING, G. & BOSE, S. 2013. SiO2 and ZnO dopants in three-dimensionally printed tricalcium phosphate bone tissue engineering scaffolds enhance osteogenesis and angiogenesis in vivo. *Acta Biomater,* 9**,** 9137-48.

FINE, D. H., MARKOWITZ, K., FURGANG, D. & VELLIYAGOUNDER, K. 2010. Aggregatibacter actinomycetemcomitans as an early colonizer of oral tissues: epithelium as a reservoir? *J Clin Microbiol,* 48**,** 4464-73.

FITZGERALD, V., PICKUP, D. M., GREENSPAN, D., SARKAR, G., FITZGERALD, J. J., WETHERALL, K. M., MOSS, R. M., JONES, J. R. & NEWPORT, R. J. 2007. A Neutron and X-Ray Diffraction Study of Bioglass® with Reverse Monte Carlo Modelling. *Advanced Functional Materials,* 17**,** 3746-3753.

FIVES-TAYLOR, P. M., MEYER, D. H., MINTZ, K. P. & BRISSETTE, C. 1999. Virulence factors of Actinobacillus actinomycetemcomitans. *Periodontol 2000,* 20**,** 136-67.

FLORENCIO-SILVA, R., SASSO, G. R., SASSO-CERRI, E., SIMOES, M. J. & CERRI, P. S. 2015. Biology of Bone Tissue: Structure, Function, and Factors That Influence Bone Cells. *Biomed Res Int,* 2015**,** 421746.

FOOLADI, A. A., HOSSEINI, H. M., HAFEZI, F., HOSSEINNEJAD, F. & NOURANI, M. R. 2013. Sol-gel-derived bioactive glass containing SiO2-MgO-CaO-P2O5 as an antibacterial scaffold. *J Biomed Mater Res A,* 101**,** 1582-7.

FRIEDERICHS, R. J., BROOKS, R. A., UEDA, M. & BEST, S. M. 2015. In vitro osteoclast formation and resorption of silicon-substituted hydroxyapatite ceramics. *J Biomed Mater Res A*.

GARRETT, S. 1996. Periodontal regeneration around natural teeth. *Ann Periodontol,* 1**,** 621-66.

GEMECHU, A., GIDAY, M., WORKU, A. & AMENI, G. 2013. In vitro anti-mycobacterial activity of selected medicinal plants against Mycobacterium tuberculosis and Mycobacterium bovis strains. *BMC Complement Altern Med,* 13**,** 291.

GENTLEMAN, E., STEVENS, M. M., HILL, R. G. & BRAUER, D. S. 2013. Surface properties and ion release from fluoride-containing bioactive glasses promote osteoblast differentiation and mineralization in vitro. *Acta Biomater,* 9**,** 5771-9.

GERGELY, I., ZAZGYVA, A., MAN, A., ZUH, S. G. & POP, T. S. 2014. The in vitro antibacterial effect of S53P4 bioactive glass and gentamicin impregnated polymethylmethacrylate beads. *Acta Microbiol Immunol Hung,* 61**,** 145-60.

GERHARDT, L. C., WIDDOWS, K. L., EROL, M. M., NANDAKUMAR, A., ROQAN, I. S., ANSARI, T. & BOCCACCINI, A. R. 2013. Neocellularization and neovascularization of nanosized bioactive glass-coated decellularized trabecular bone scaffolds. *J Biomed Mater Res A,* 101**,** 827-41.

GILLETTE, R. L., SWAIM, S. F., SARTIN, E. A., BRADLEY, D. M. & COOLMAN, S. L. 2001. Effects of a bioactive glass on healing of closed skin wounds in dogs. *Am J Vet Res,* 62**,** 1149-53.

GOLUB, E. E. 2009. Role of matrix vesicles in biomineralization. *Biochim Biophys Acta,* 1790**,** 1592-8.

GORUSTOVICH, A. A., ROETHER, J. A. & BOCCACCINI, A. R. 2010. Effect of bioactive glasses on angiogenesis: a review of in vitro and in vivo evidences. *Tissue Eng Part B Rev,* 16**,** 199-207.

GREEN, R. J., USUI, M. L., HART, C. E., AMMONS, W. F. & NARAYANAN, A. S. 1997. Immunolocalization of platelet-derived growth factor A and B chains and PDGF-alpha and beta receptors in human gingival wounds. *J Periodontal Res,* 32**,** 209-14.

GRYNPAS, M. D. 1990. Fluoride effects on bone crystals. *Journal of Bone and Mineral Research,* 5**,** S169-S175.

GRZESIK, W. J. & NARAYANAN, A. S. 2002. Cementum and Periodontal Wound Healing and Regeneration. *Critical Reviews in Oral Biology & Medicine,* 13**,** 474-484.

HABEL, B. & GLASER, R. 1998. Human osteoblast-like cells respond not only to the extracellular calcium concentration but also to its changing rate. *Eur Biophys J,* 27**,** 411-6.

HACCHOU, Y., UEMATSU, T., UEDA, O., USUI, Y., UEMATSU, S., TAKAHASHI, M., UCHIHASHI, T., KAWAZOE, Y., SHIBA, T., KURIHARA, S., YAMAOKA, M. & FURUSAWA, K. 2007. Inorganic polyphosphate: a possible stimulant of bone formation. *J Dent Res,* 86**,** 893-7.

HAIKEL, Y., TURLOT, J. C., CAHEN, P. M. & FRANK, R. 1989. Periodontal treatment needs in populations of high- and low-fluoride areas of Morocco. *J Clin Periodontol,* 16**,** 596-600.

HAJISHENGALLIS, G. & LAMONT, R. J. 2014. Breaking bad: manipulation of the host response by Porphyromonas gingivalis. *Eur J Immunol,* 44**,** 328-38.

HARRISON, G., SHAPIRO, I. M. & GOLUB, E. E. 1995. The phosphatidylinositol-glycolipid anchor on alkaline phosphatase facilitates mineralization initiation in vitro. *J Bone Miner Res,* 10**,** 568-73.

HAUBEK, D. & JOHANSSON, A. 2014. Pathogenicity of the highly leukotoxic JP2 clone of Aggregatibacter actinomycetemcomitans and its geographic dissemination and role in aggressive periodontitis. *J Oral Microbiol,* 6.

HE, L. F. & CHEN, J. G. 2006. DNA damage, apoptosis and cell cycle changes induced by fluoride in rat oral mucosal cells and hepatocytes. *World J Gastroenterol,* 12**,** 1144-8.

HE, X. S. & SHI, W. Y. 2009. Oral microbiology: past, present and future. *Int J Oral Sci,* 1**,** 47-58.

HENCH, L. L. 1988. Bioactive ceramics. *Ann N Y Acad Sci,* 523**,** 54-71.

HENCH, L. L. 2006. The story of Bioglass. *J Mater Sci Mater Med,* 17**,** 967-78.

HENCH, L. L. 2015. The future of bioactive ceramics. *J Mater Sci Mater Med,* 26**,** 86.

HENCH, L. L. 2016. Bioglass: 10 milestones from concept to commerce. *Journal of Non-Crystalline Solids,* 432**,** 2-8.

HENCH, L. L. & JONES, J. R. 2015. Bioactive Glasses: Frontiers and Challenges. *Front Bioeng Biotechnol,* 3**,** 194.

HENCH, L. L., SPLINTER, R. J., ALLEN, W. C. & GREENLEE, T. K. 1971. Bonding mechanisms at the interface of ceramic prosthetic materials. *Journal of Biomedical Materials Research,* 5**,** 117-141.

HENCH, L. L. & THOMPSON, I. 2010. Twenty-first century challenges for biomaterials. *J R Soc Interface,* 7 Suppl 4**,** S379-91.

HENDERSON, B., NAIR, S. P., WARD, J. M. & WILSON, M. 2003. Molecular pathogenicity of the oral opportunistic pathogen Actinobacillus actinomycetemcomitans. *Annu Rev Microbiol,* 57**,** 29-55.

HENSTOCK, J. R., CANHAM, L. T. & ANDERSON, S. I. 2015. Silicon: the evolution of its use in biomaterials. *Acta Biomater,* 11**,** 17-26.

HILL, R. 1996. An alternative view of the degradation of bioglass. *Journal of Materials Science Letters,* 15**,** 1122-1125.

HILL, R. G. & BRAUER, D. S. 2011. Predicting the bioactivity of glasses using the network connectivity or split network models. *Journal of Non-Crystalline Solids,* 357**,** 3884-3887.

HILL, R. G., COSTA, N. D. & LAW, R. V. 2005. Characterization of a mould flux glass. *Journal of Non-Crystalline Solids,* 351**,** 69-74.

HOFER, A. M. 2005. Another dimension to calcium signaling: a look at extracellular calcium. *J Cell Sci,* 118**,** 855-62.

HOJO, K., NAGAOKA, S., OHSHIMA, T. & MAEDA, N. 2009. Bacterial interactions in dental biofilm development. *J Dent Res,* 88**,** 982-90.

HORCH, K. W., WHITEHORN, D. & BURGESS, P. R. 1974. Impulse generation in type I cutaneous mechanoreceptors. *J Neurophysiol,* 37**,** 267-81.

HOUGHTON, P. E., KEEFER, K. A., DIEGELMANN, R. F. & KRUMMEL, T. M. 1996. A simple method to assess the relative amount of collagen deposition in wounded fetal mouse limbs. *Wound Repair Regen,* 4**,** 489-95.

HU, S., CHANG, J., LIU, M. & NING, C. 2009. Study on antibacterial effect of 45S5 Bioglass. *J Mater Sci Mater Med,* 20**,** 281-6.

HUO, L., LIU, K., PEI, J., YANG, Y., YE, Y., LIU, Y., SUN, J., HAN, H., XU, W. & GAO, Y. 2013. Flouride Promotes Viability and Differentiation of Osteoblast-Like Saos-2 Cells Via BMP/Smads Signaling Pathway. *Biol Trace Elem Res*.

IIJIMA, M. 2001. Formation of octacalcium phosphate in vitro. *Monogr Oral Sci,* 18**,** 17-49.

IIJIMA, M. & MORADIAN-OLDAK, J. 2005. Control of apatite crystal growth in a fluoride containing amelogenin-rich matrix. *Biomaterials,* 26**,** 1595-603.

INKIELEWICZ-STEPNIAK, I., SANTOS-MARTINEZ, M. J., MEDINA, C. & RADOMSKI, M. W. 2014. Pharmacological and toxicological effects of co-exposure of human gingival fibroblasts to silver nanoparticles and sodium fluoride. *Int J Nanomedicine,* 9**,** 1677-87.

INVIVOGEN. 2012. *Mycoplasma Contamination of Cell Cultures - Review* [Online]. Available: http://www.invivogen.com/review-mycoplasma [Accessed 3 Dec 2015].

ITO, N., FINDLAY, D. M., ANDERSON, P. H., BONEWALD, L. F. & ATKINS, G. J. 2013. Extracellular phosphate modulates the effect of 1alpha,25-dihydroxy vitamin D3 (1,25D) on osteocyte like cells. *J Steroid Biochem Mol Biol,* 136**,** 183-6.

IVANOVSKI, S. 2009. Periodontal regeneration. *Aust Dent J,* 54 Suppl 1**,** S118-28.

IVANOVSKI, S., VAQUETTE, C., GRONTHOS, S., HUTMACHER, D. W. & BARTOLD, P. M. 2014. Multiphasic scaffolds for periodontal tissue engineering. *J Dent Res,* 93**,** 1212-21.

IZUAGIE, I. A., PELHAM, C. J. & AGRAWAL, D. K. 2015. Synergistic effect of angiotensin II on vascular endothelial growth factor-A-mediated differentiation of bone marrow-derived mesenchymal stem cells into endothelial cells. *Stem Cell Res Ther,* 6**,** 4.

JAKOB, M., SAXER, F., SCOTTI, C., SCHREINER, S., STUDER, P., SCHERBERICH, A., HEBERER, M. & MARTIN, I. 2012. Perspective on the evolution of cell-based bone tissue engineering strategies. *Eur Surg Res,* 49**,** 1-7.

JALLOT, E. 2003. Role of magnesium during spontaneous formation of a calcium phosphate layer at the periphery of a bioactive glass coating doped with MgO. *Applied Surface Science,* 211**,** 89-95.

JENG, J. H., HSIEH, C. C., LAN, W. H., CHANG, M. C., LIN, S. K., HAHN, L. J. & KUO, M. Y. 1998. Cytotoxicity of sodium fluoride on human oral mucosal fibroblasts and its mechanisms. *Cell Biol Toxicol,* 14**,** 383-9.

JEONG, S. J. & JEONG, M. J. 2016. Effect of Thymosin beta4 on the Differentiation and Mineralization of MC3T3-E1 Cell on a Titanium Surface. *J Nanosci Nanotechnol,* 16**,** 1979-83.

JOHANSSON, A. 2011. Aggregatibacter actinomycetemcomitans leukotoxin: a powerful tool with capacity to cause imbalance in the host inflammatory response. *Toxins (Basel),* 3**,** 242-59.

JOHNSSON, M. S. & NANCOLLAS, G. H. 1992. The role of brushite and octacalcium phosphate in apatite formation. *Crit Rev Oral Biol Med,* 3**,** 61-82.

JONASSON, G. & RYTHEN, M. 2016. Alveolar bone loss in osteoporosis: a loaded and cellular affair? *Clin Cosmet Investig Dent,* 8**,** 95-103.

JONES, J. R. 2013. Review of bioactive glass: from Hench to hybrids. *Acta Biomater,* 9**,** 4457-86.

JONES, J. R., GENTLEMAN, E. & POLAK, J. 2007. Bioactive Glass Scaffolds for Bone Regeneration. *Elements,* 3**,** 393-399.

JONES, J. R., LEE, P. D. & HENCH, L. L. 2006. Hierarchical porous materials for tissue engineering. *Philos Trans A Math Phys Eng Sci,* 364**,** 263-81.

JONES, J. R., SEPULVEDA, P. & HENCH, L. L. 2001. Dose-dependent behavior of bioactive glass dissolution. *J Biomed Mater Res,* 58**,** 720-6.

JUNQUEIRA, L. C., BIGNOLAS, G. & BRENTANI, R. R. 1979. Picrosirius staining plus polarization microscopy, a specific method for collagen detection in tissue sections. *Histochem J,* 11**,** 447-55.

KANATANI, M., SUGIMOTO, T., KANO, J., KANZAWA, M. & CHIHARA, K. 2003. Effect of high phosphate concentration on osteoclast differentiation as well as bone-resorbing activity. *J Cell Physiol,* 196**,** 180-9.

KARAGEORGIOU, V. & KAPLAN, D. 2005. Porosity of 3D biomaterial scaffolds and osteogenesis. *Biomaterials,* 26**,** 5474-91.

KARATZAS, S., ZAVRAS, A., GREENSPAN, D. & AMAR, S. 1999. Histologic observations of periodontal wound healing after treatment with PerioGlas in nonhuman primates. *Int J Periodontics Restorative Dent,* 19**,** 489-99.

KARRING, T. 2000. Regenerative periodontal therapy. *J Int Acad Periodontol,* 2**,** 101-9.

KASSEM, M., MOSEKILDE, L. & ERIKSEN, E. F. 1994. Effects of fluoride on human bone cells in vitro: differences in responsiveness between stromal osteoblast precursors and mature osteoblasts. *Eur J Endocrinol,* 130**,** 381-6.

KATAWERA, V., SIEDNER, M. & BOUM, Y., 2ND 2014. Evaluation of the modified colorimetric resazurin microtiter plate-based antibacterial assay for rapid and reliable tuberculosis drug susceptibility testing. *BMC Microbiol,* 14**,** 259.

KAVOURAS, P., KEHAGIAS, T., KOMNINOU, P., CHRISSAFIS, K., CHARITIDIS, C. & KARAKOSTAS, T. 2008. Interface controlled active fracture modes in glass-ceramics. *Journal of Materials Science,* 43**,** 3954-3959.

KAWASHIMA, J., NAKAJO, K., WASHIO, J., MAYANAGI, G., SHIMAUCHI, H. & TAKAHASHI, N. 2013. Fluoride-sensitivity of growth and acid production of oral Actinomyces: comparison with oral Streptococcus. *Microbiol Immunol,* 57**,** 797-804.

KAY, S. A., WISNER-LYNCH, L., MARXER, M. & LYNCH, S. E. 1997. Guided bone regeneration: integration of a resorbable membrane and a bone graft material. *Pract Periodontics Aesthet Dent,* 9**,** 185-94; quiz 196.

KESHAW, H., FORBES, A. & DAY, R. M. 2005. Release of angiogenic growth factors from cells encapsulated in alginate beads with bioactive glass. *Biomaterials,* 26**,** 4171-9.

KINI, U. & NANDEESH, B. N. 2012. Physiology of Bone Formation, Remodeling, and Metabolism. *In:* FOGELMAN, I., GNANASEGARAN, G. & WALL, H. (eds.)

Radionuclide and Hybrid Bone Imaging. Berlin, Heidelberg: Springer Berlin Heidelberg.

KIRSCH, T. 2012. Biomineralization--an active or passive process? *Connect Tissue Res,* 53**,** 438-45.

KLIMENT, C. R., ENGLERT, J. M., CRUM, L. P. & OURY, T. D. 2011. A novel method for accurate collagen and biochemical assessment of pulmonary tissue utilizing one animal. *Int J Clin Exp Pathol,* 4**,** 349-55.

KOKUBO, T., KUSHITANI, H., SAKKA, S., KITSUGI, T. & YAMAMURO, T. 1990. Solutions able to reproduce in vivo surface-structure changes in bioactive glass-ceramic A-W3. *Journal of Biomedical Materials Research,* 24**,** 721-734.

KOKUBO, T. & TAKADAMA, H. 2006. How useful is SBF in predicting in vivo bone bioactivity? *Biomaterials,* 27**,** 2907-15.

KONTONASAKI, E., SIVROPOULOU, A., PAPADOPOULOU, L., GAREFIS, P., PARASKEVOPOULOS, K. & KOIDIS, P. 2007. Attachment and proliferation of human periodontal ligament fibroblasts on bioactive glass modified ceramics. *J Oral Rehabil,* 34**,** 57-67.

KOPP, J. B. & ROBEY, P. G. 1990. Sodium fluoride does not increase human bone cell proliferation or protein synthesis in vitro. *Calcif Tissue Int,* 47**,** 221-9.

KORKMAZ, F. M., TUZUNER, T., BAYGIN, O., BURUK, C. K., DURKAN, R. & BAGIS, B. 2013. Antibacterial activity, surface roughness, flexural strength, and solubility of conventional luting cements containing chlorhexidine diacetate/cetrimide mixtures. *J Prosthet Dent,* 110**,** 107-15.

KUBO, K., KAKIMOTO, T., KANDA, C., TSUKASA, N., UEHARA, M., IZUMI, Y., KAMADA, T., KANEKO, N. & SUEDA, T. 1993. Bioactive glass promoted formation of nodules in periodontal-ligament fibroblasts in vitro. *J Biomed Mater Res,* 27**,** 1175-80.

KUBO, K., KAMADA, T., MATSUYAMA, T., TSUKASA, N., UEHARA, M., IZUMI, Y., KITANO, M., OGINO, M. & SUEDA, T. 1995. Characterization of nodules induced by bioactive glass on cultured periodontal-ligament fibroblasts. *J Biomed Mater Res,* 29**,** 503-9.

KUBO, K., TSUKASA, N., UEHARA, M., IZUMI, Y., OGINO, M., KITANO, M. & SUEDA, T. 1997. Calcium and silicon from bioactive glass concerned with formation of nodules in periodontal-ligament fibroblasts in vitro. *J Oral Rehabil,* 24**,** 70-5.

KUMAR, P. R. & JOHN, J. 2011. Assessment of periodontal status among dental fluorosis subjects using community periodontal index of treatment needs. *Indian J Dent Res,* 22**,** 248-51.

KURIEN, T., PEARSON, R. G. & SCAMMELL, B. E. 2013. Bone graft substitutes currently available in orthopaedic practice: the evidence for their use. *Bone Joint J,* 95-B**,** 583-97.

KUZYK, P. R. & SCHEMITSCH, E. H. 2011. The basic science of peri-implant bone healing. *Indian J Orthop,* 45**,** 108-15.

LABARCA, C. & PAIGEN, K. 1980. A simple, rapid, and sensitive DNA assay procedure. *Anal Biochem,* 102**,** 344-52.

LAHEIJ, A. M., DE SOET, J. J., VEERMAN, E. C., BOLSCHER, J. G. & VAN LOVEREN, C. 2013. The influence of oral bacteria on epithelial cell migration in vitro. *Mediators Inflamm,* 2013**,** 154532.

LALK, M., REIFENRATH, J., ANGRISANI, N., BONDARENKO, A., SEITZ, J. M., MUELLER, P. P. & MEYER-LINDENBERG, A. 2013. Fluoride and calcium-phosphate coated sponges of the magnesium alloy AX30 as bone grafts: a comparative study in rabbits. *J Mater Sci Mater Med,* 24**,** 417-36.

LAREAU, C. R., DEREN, M. E., FANTRY, A., DONAHUE, R. M. & DIGIOVANNI, C. W. 2015. Does autogenous bone graft work? A logistic regression analysis of data from 159 papers in the foot and ankle literature. *Foot Ankle Surg,* 21**,** 150-9.

LEBECQ, I., DÉSANGLOIS, F., LERICHE, A. & FOLLET-HOUTTEMANE, C. 2007. Compositional dependence on the in vitro bioactivity of invert or conventional bioglasses in the Si-Ca-Na-P system. *Journal of Biomedical Materials Research Part A,* 83A**,** 156-168.

LEE, H. J. & CHOI, C. H. 2015. Anti-inflammatory effects of bamboo salt and sodium fluoride in human gingival fibroblasts-An in vitro study. *Kaohsiung J Med Sci,* 31**,** 303-8.

LEE, J. H., RYU, M. Y., BAEK, H. R., LEE, K. M., SEO, J. H., LEE, H. K. & RYU, H. S. 2013. Effects of porous beta-tricalcium phosphate-based ceramics used as an E. coli-derived rhBMP-2 carrier for bone regeneration. *J Mater Sci Mater Med*.

LEGEROS, R. Z., DACULSI, G., ORLY, I., ABERGAS, T. & TORRES, W. 1989. Solution-mediated transformation of octacalcium phosphate (OCP) to apatite. *Scanning Microsc,* 3**,** 129-37; discussion 137-8.

LELLOUCHE, J., KAHANA, E., ELIAS, S., GEDANKEN, A. & BANIN, E. 2009. Antibiofilm activity of nanosized magnesium fluoride. *Biomaterials,* 30**,** 5969-78.

LEPPARANTA, O., VAAHTIO, M., PELTOLA, T., ZHANG, D., HUPA, L., HUPA, M., YLANEN, H., SALONEN, J. I., VILJANEN, M. K. & EEROLA, E. 2008. Antibacterial effect of bioactive glasses on clinically important anaerobic bacteria in vitro. *J Mater Sci Mater Med,* 19**,** 547-51.

LEU, A., STIEGER, S. M., DAYTON, P., FERRARA, K. W. & LEACH, J. K. 2009. Angiogenic response to bioactive glass promotes bone healing in an irradiated calvarial defect. *Tissue Eng Part A,* 15**,** 877-85.

LI, H. & CHANG, J. 2013. Bioactive silicate materials stimulate angiogenesis in fibroblast and endothelial cell co-culture system through paracrine effect. *Acta Biomater,* 9**,** 6981-91.

LIEVREMONT, M., POTUS, J. & GUILLOU, B. 1982. Use of alizarin red S for histochemical staining of Ca2+ in the mouse; some parameters of the chemical reaction in vitro. *Acta Anat (Basel),* 114**,** 268-80.

LIM, K. P., CIRILLO, N., HASSONA, Y., WEI, W., THURLOW, J. K., CHEONG, S. C., PITIYAGE, G., PARKINSON, E. K. & PRIME, S. S. 2011. Fibroblast gene expression profile reflects the stage of tumour progression in oral squamous cell carcinoma. *J Pathol,* 223**,** 459-69.

LIM, P. N., CHANG, L., TAY, B. Y., GUNETA, V., CHOONG, C., HO, B. & THIAN, E. S. 2014. Proposed mechanism of antibacterial action of chemically modified apatite for reduced bone infection. *ACS Appl Mater Interfaces,* 6**,** 17082-92.

LIU, G., ZHANG, W., JIANG, P., LI, X., LIU, C. & CHAI, C. 2012. Role of nitric oxide and vascular endothelial growth factor in fluoride-induced goitrogenesis in rats. *Environ Toxicol Pharmacol,* 34**,** 209-17.

LIU, Y. K., LU, Q. Z., PEI, R., JI, H. J., ZHOU, G. S., ZHAO, X. L., TANG, R. K. & ZHANG, M. 2009. The effect of extracellular calcium and inorganic phosphate on the growth and osteogenic differentiation of mesenchymal stem cells in vitro: implication for bone tissue engineering. *Biomed Mater,* 4**,** 025004.

LOCHAIWATANA, Y., POOLTHONG, S., HIRATA, I., OKAZAKI, M., SWASDISON, S. & VONGSAVAN, N. 2015. The synthesis and characterization of a novel potassium chloride-fluoridated hydroxyapatite varnish for treating dentin hypersensitivity. *Dent Mater J,* 34**,** 31-40.

LOCKYER, M. W. G., HOLLAND, D. & DUPREE, R. 1995. NMR investigation of the structure of some bioactive and related glasses. *Journal of Non-Crystalline Solids,* 188**,** 207-219.

LOZANO, R. M., PEREZ-MACEDA, B. T., CARBONERAS, M., ONOFRE-BUSTAMANTE, E., GARCIA-ALONSO, M. C. & ESCUDERO, M. L. 2013. Response of MC3T3-E1 osteoblasts, L929 fibroblasts, and J774 macrophages to fluoride surface-modified AZ31 magnesium alloy. *J Biomed Mater Res A,* 101**,** 2753-62.

LU, X. & LENG, Y. 2005a. Theoretical analysis of calcium phosphate precipitation in simulated body fluid. *Biomaterials,* 26**,** 1097-108.

LU, X. & LENG, Y. 2005b. Theoretical analysis of calcium phosphate precipitation in simulated body fluid. *Biomaterials,* 26**,** 1097-1108.

LUSVARDI, G., MALAVASI, G., CORTADA, M., MENABUE, L., MENZIANI, M. C., PEDONE, A. & SEGRE, U. 2008. Elucidation of the Structural Role of Fluorine in Potentially Bioactive Glasses by Experimental and Computational Investigation. *The Journal of Physical Chemistry B,* 112**,** 12730-12739.

LUSVARDI, G., MALAVASI, G., MENABUE, L., AINA, V. & MORTERRA, C. 2009. Fluoride-containing bioactive glasses: Surface reactivity in simulated body fluids solutions. *Acta Biomaterialia,* 5**,** 3548-3562.

LUTFIOGLU, M., SAKALLIOGLU, E. E., SAKALLIOGLU, U., GULBAHAR, M. Y., MUGLALI, M., BAS, B. & AKSOY, A. 2012. Excessive fluoride intake alters the MMP-2, TIMP-1 and TGF-beta levels of periodontal soft tissues: an experimental study in rabbits. *Clin Oral Investig,* 16**,** 1563-70.

LYNCH, E., BRAUER, D. S., KARPUKHINA, N., GILLAM, D. G. & HILL, R. G. 2012. Multi-component bioactive glasses of varying fluoride content for treating dentin hypersensitivity. *Dental Materials,* 28**,** 168-178.

MA, A. N., GONG, N., LU, J. M., HUANG, J. L., HAO, B., GUO, Y., ZHONG, J., XU, Y., CHANG, J. & WANG, Y. X. 2013a. Local protective effects of oral 45S5 bioactive glass on gastric ulcers in experimental animals. *J Mater Sci Mater Med,* 24**,** 803-9.

MA, J., CHEN, C. Z., WANG, D. G. & HU, J. H. 2011. Effect of magnesia on structure, degradability and in vitro bioactivity of CaO–MgO–P2O5–SiO2 system ceramics. *Materials Letters,* 65**,** 130-133.

MA, J., CHEN, C. Z., WANG, D. G., JIAO, Y. & SHI, J. Z. 2010. Effect of magnesia on the degradability and bioactivity of sol-gel derived SiO2-CaO-MgO-P2O5 system glasses. *Colloids Surf B Biointerfaces,* 81**,** 87-95.

MA, W., ZHANG, X., SHI, S. & ZHANG, Y. 2013b. Neuropeptides stimulate human osteoblast activity and promote gap junctional intercellular communication. *Neuropeptides,* 47**,** 179-86.

MAES, C. & CLEMENS, T. L. 2014. Angiogenic-osteogenic coupling: the endothelial perspective. *Bonekey Rep,* 3**,** 578.

MANCHON, A., ALKHRAISAT, M., RUEDA-RODRIGUEZ, C., TORRES, J., PRADOS-FRUTOS, J. C., EWALD, A., GBURECK, U., CABREJOS-AZAMA, J., RODRIGUEZ-GONZALEZ, A. & LOPEZ-CABARCOS, E. 2015. Silicon calcium phosphate ceramic as novel biomaterial to simulate the bone regenerative properties of autologous bone. *J Biomed Mater Res A,* 103**,** 479-88.

MARCZUK-KOLADA, G., JAKONIUK, P., MYSTKOWSKA, J., LUCZAJ-CEPOWICZ, E., WASZKIEL, D., DABROWSKI, J. R. & LESZCZYNSKA, K. 2006. Fluoride release and antibacterial activity of selected dental materials. *Postepy Hig Med Dosw (Online),* 60**,** 416-20.

MARKS, D. C., BELOV, L., DAVEY, M. W., DAVEY, R. A. & KIDMAN, A. D. 1992. The MTT cell viability assay for cytotoxicity testing in multidrug-resistant human leukemic cells. *Leuk Res,* 16**,** 1165-73.

MARQUIS, R. E. 1995. Antimicrobial actions of fluoride for oral bacteria. *Can J Microbiol,* 41**,** 955-64.

MARQUIS, R. E., CLOCK, S. A. & MOTA-MEIRA, M. 2003. Fluoride and organic weak acids as modulators of microbial physiology. *FEMS Microbiol Rev,* 26**,** 493-510.

MCANDREW, J., EFRIMESCU, C., SHEEHAN, E. & NIALL, D. 2013. Through the looking glass; bioactive glass S53P4 (BonAlive(R)) in the treatment of chronic osteomyelitis. *Ir J Med Sci,* 182**,** 509-11.

MEFFERT, R. M. 1996. Periodontitis vs. peri-implantitis: the same disease? The same treatment? *Crit Rev Oral Biol Med,* 7**,** 278-91.

MELCHER, A. H. 1976. On the repair potential of periodontal tissues. *J Periodontol,* 47**,** 256-60.

MENCZEL, J. 1964. THE EFFECT OF FLUORIDE ON BONE STRUCTURE AND ITS POSSIBLE CLINICAL APPLICATION. *Isr Med J,* 23**,** 45-52.

MENGEL, R., SCHREIBER, D. & FLORES-DE-JACOBY, L. 2006. Bioabsorbable membrane and bioactive glass in the treatment of intrabony defects in patients with generalized aggressive periodontitis: results of a 5-year clinical and radiological study. *J Periodontol,* 77**,** 1781-7.

MENGEL, R., SOFFNER, M. & FLORES-DE-JACOBY, L. 2003. Bioabsorbable membrane and bioactive glass in the treatment of intrabony defects in patients with generalized aggressive periodontitis: results of a 12-month clinical and radiological study. *J Periodontol,* 74**,** 899-908.

MERCIER, C., FOLLET-HOUTTEMANE, C., PARDINI, A. & REVEL, B. 2011. Influence of P2O5 content on the structure of SiO2-Na2O-CaO-P2O5 bioglasses by 29Si and 31P MAS-NMR. *Journal of Non-Crystalline Solids,* 357**,** 3901-3909.

MICHALEK, S. M., HIRASAWA, M., KIYONO, H., OCHIAI, K. & MCGHEE, J. R. 1981. Oral ecology and virulence of Lactobacillus casei and Streptococcus mutans in gnotobiotic rats. *Infect Immun,* 33**,** 690-6.

MICHIGAMI, T. 2013. Extracellular phosphate as a signaling molecule. *Contrib Nephrol,* 180**,** 14-24.

MILLER, C. J., KASSEM, H. S., PEPPER, S. D., HEY, Y., WARD, T. H. & MARGISON, G. P. 2003. Mycoplasma infection significantly alters microarray gene expression profiles. *Biotechniques,* 35**,** 812-4.

MITCHELL, J. 2011. Streptococcus mitis: walking the line between commensalism and pathogenesis. *Mol Oral Microbiol,* 26**,** 89-98.

MLADENOVIC, Z., JOHANSSON, A., WILLMAN, B., SHAHABI, K., BJORN, E. & RANSJO, M. 2014. Soluble silica inhibits osteoclast formation and bone resorption in vitro. *Acta Biomater,* 10**,** 406-18.

MNEIMNE, M., HILL, R. G., BUSHBY, A. J. & BRAUER, D. S. 2011. High phosphate content significantly increases apatite formation of fluoride-containing bioactive glasses. *Acta Biomater,* 7**,** 1827-34.

MOJUMDAR, S., KOZÁNKOVÁ, J., CHOCHOLOUŠEK, J., MAJLING, J. & FÁBRYOVÁ, D. 2004. Fluoroapatite - material for medicine, Growth, morphology and thermoanalytical properties. *Journal of Thermal Analysis and Calorimetry,* 78**,** 73-82.

MONFOULET, L. E., BECQUART, P., MARCHAT, D., VANDAMME, K., BOURGUIGNON, M., PACARD, E., VIATEAU, V., PETITE, H. & LOGEART-AVRAMOGLOU, D. 2014. The pH in the microenvironment of human mesenchymal stem cells is a critical factor for optimal osteogenesis in tissue engineered constructs. *Tissue Eng Part A*.

MONJO, M., LAMOLLE, S. F., LYNGSTADAAS, S. P., RONOLD, H. J. & ELLINGSEN, J. E. 2008. In vivo expression of osteogenic markers and bone mineral density at the surface of fluoride-modified titanium implants. *Biomaterials,* 29**,** 3771-80.

MOOSVI, S. R. & DAY, R. M. 2009. Bioactive glass modulation of intestinal epithelial cell restitution. *Acta Biomater,* 5**,** 76-83.

MORENO, E. C., KRESAK, M. & ZAHRADNIK, R. T. 1977. Physicochemical aspects of fluoride-apatite systems relevant to the study of dental caries. *Caries Res,* 11 Suppl 1**,** 142-71.

MORENO, S. & CONTRERAS, A. 2013. Functional differences of Porphyromonas gingivalis Fimbriae in determining periodontal disease pathogenesis: a literature review. *Colomb Med (Cali),* 44**,** 48-56.

MORTAZAVI, V., NAHRKHALAJI, M. M., FATHI, M. H., MOUSAVI, S. B. & ESFAHANI, B. N. 2010. Antibacterial effects of sol-gel-derived bioactive glass nanoparticle on aerobic bacteria. *J Biomed Mater Res A,* 94**,** 160-8.

MOSMANN, T. 1983. Rapid colorimetric assay for cellular growth and survival: application to proliferation and cytotoxicity assays. *J Immunol Methods,* 65**,** 55-63.

MOTA, J., YU, N., CARIDADE, S. G., LUZ, G. M., GOMES, M. E., REIS, R. L., JANSEN, J. A., WALBOOMERS, X. F. & MANO, J. F. 2012. Chitosan/bioactive glass nanoparticle composite membranes for periodontal regeneration. *Acta Biomater,* 8**,** 4173-80.

MULLER, W. E., WANG, X., DIEHL-SEIFERT, B., KROPF, K., SCHLOSSMACHER, U., LIEBERWIRTH, I., GLASSER, G., WIENS, M. & SCHRODER, H. C. 2011. Inorganic polymeric phosphate/polyphosphate as an inducer of alkaline phosphatase and a modulator of intracellular Ca2+ level in osteoblasts (SaOS-2 cells) in vitro. *Acta Biomater,* 7**,** 2661-71.

MUNUKKA, E., LEPPARANTA, O., KORKEAMAKI, M., VAAHTIO, M., PELTOLA, T., ZHANG, D., HUPA, L., YLANEN, H., SALONEN, J. I., VILJANEN, M. K. & EEROLA, E. 2008. Bactericidal effects of bioactive glasses on clinically important aerobic bacteria. *J Mater Sci Mater Med,* 19**,** 27-32.

MURRAY J. FAVUS, D. A. B., AND JACOB LEMANN JR. 2006. Regulation of calcium, magnesium, and phosphate metabolism. *Primers on the Metabolic Bone Diseases and Disorders of the Mineral Metabolism*.

MYSAK, J., PODZIMEK, S., SOMMEROVA, P., LYUYA-MI, Y., BARTOVA, J., JANATOVA, T., PROCHAZKOVA, J. & DUSKOVA, J. 2014. Porphyromonas gingivalis: major periodontopathic pathogen overview. *J Immunol Res,* 2014**,** 476068.

NAGAYAMA, M., SATO, M., YAMAGUCHI, R., TOKUDA, C. & TAKEUCHI, H. 2001. Evaluation of co-aggregation among Streptococcus mitis, Fusobacterium nucleatum and Porphyromonas gingivalis. *Lett Appl Microbiol,* 33**,** 122-5.

NANCI, A. & BOSSHARDT, D. D. 2006. Structure of periodontal tissues in health and disease. *Periodontol 2000,* 40**,** 11-28.

NANDI, S. K., ROY, S., MUKHERJEE, P., KUNDU, B., DE, D. K. & BASU, D. 2010. Orthopaedic applications of bone graft & graft substitutes: a review. *Indian J Med Res,* 132**,** 15-30.

NAORUNGROJ, S., WEI, H. H., ARNOLD, R. R., SWIFT, E. J., JR. & WALTER, R. 2010. Antibacterial surface properties of fluoride-containing resin-based sealants. *J Dent,* 38**,** 387-91.

NEVINS, M. L., CAMELO, M., NEVINS, M., KING, C. J., ORINGER, R. J., SCHENK, R. K. & FIORELLINI, J. P. 2000. Human histologic evaluation of bioactive ceramic in the treatment of periodontal osseous defects. *Int J Periodontics Restorative Dent,* 20**,** 458-67.

NEWMAN, M. G., TAKEI, H., KLOKKEVOLD, P. R. & CARRANZA, F. A. 2011. *Carranza's Clinical Periodontology*, Elsevier Health Sciences.

NOBLE, B. S. 2008. The osteocyte lineage. *Archives of Biochemistry and Biophysics,* 473**,** 106-111.

NOMI, M., ATALA, A., COPPI, P. D. & SOKER, S. 2002. Principals of neovascularization for tissue engineering. *Molecular Aspects of Medicine,* 23**,** 463-483.

NOROWSKI, P. A., JR. & BUMGARDNER, J. D. 2009. Biomaterial and antibiotic strategies for peri-implantitis: a review. *J Biomed Mater Res B Appl Biomater,* 88**,** 530-43.

NOVOSEL, E. C., KLEINHANS, C. & KLUGER, P. J. 2011. Vascularization is the key challenge in tissue engineering. *Advanced Drug Delivery Reviews,* 63**,** 300-311.

NRAS. 2014. *Gum Disease* [Online]. Available: http://www.nras.org.uk/gum-disease [Accessed 3 Nov 2015].

NUSS, K. M. & VON RECHENBERG, B. 2008. Biocompatibility issues with modern implants in bone - a review for clinical orthopedics. *Open Orthop J,* 2**,** 66-78.

O'DONNELL, M. D., WATTS, S. J., HILL, R. G. & LAW, R. V. 2009. The effect of phosphate content on the bioactivity of soda-lime-phosphosilicate glasses. *J Mater Sci Mater Med,* 20**,** 1611-8.

O'DONNELL, M. D., WATTS, S. J., LAW, R. V. & HILL, R. G. 2008a. Effect of P2O5 content in two series of soda lime phosphosilicate glasses on structure and properties – Part I: NMR. *Journal of Non-Crystalline Solids,* 354**,** 3554-3560.

O'DONNELL, M. D., WATTS, S. J., LAW, R. V. & HILL, R. G. 2008b. Effect of P2O5 content in two series of soda lime phosphosilicate glasses on structure and properties – Part II: Physical properties. *Journal of Non-Crystalline Solids,* 354**,** 3561-3566.

ODATSU, T., AZIMAIE, T., VELTEN, M. F., VU, M., LYLES, M. B., KIM, H. K., ASWATH, P. B. & VARANASI, V. G. 2015. Human periosteum cell osteogenic differentiation enhanced by ionic silicon release from porous amorphous silica fibrous scaffolds. *J Biomed Mater Res A*.

OGAARD, B., LARSSON, E., HENRIKSSON, T., BIRKHED, D. & BISHARA, S. E. 2001. Effects of combined application of antimicrobial and fluoride varnishes in orthodontic patients. *Am J Orthod Dentofacial Orthop,* 120**,** 28-35.

OKUDA, A., KANEHISA, J. & HEERSCHE, J. N. 1990. The effects of sodium fluoride on the resorptive activity of isolated osteoclasts. *J Bone Miner Res,* 5 Suppl 1**,** S115-20.

PAGE, R. C., OFFENBACHER, S., SCHROEDER, H. E., SEYMOUR, G. J. & KORNMAN, K. S. 1997. Advances in the pathogenesis of periodontitis: summary of developments, clinical implications and future directions. *Periodontol 2000,* 14**,** 216-48.

PALMER, R. M. & CORTELLINI, P. 2008. Periodontal tissue engineering and regeneration: Consensus Report of the Sixth European Workshop on Periodontology. *J Clin Periodontol,* 35**,** 83-6.

PARIROKH, M., FORGHANI, F. R., PASEBAN, H., ASGARY, S., ASKARIFARD, S. & ESMAEELI MAHANI, S. 2015. Cytotoxicity of two resin-based sealers and a fluoride varnish on human gingival fibroblasts. *Iran Endod J,* 10**,** 89-92.

PASTER, B. J., OLSEN, I., AAS, J. A. & DEWHIRST, F. E. 2006. The breadth of bacterial diversity in the human periodontal pocket and other oral sites. *Periodontol 2000,* 42**,** 80-7.

PEDONE, A., CHARPENTIER, T., MALAVASI, G. & MENZIANI, M. C. 2010. New Insights into the Atomic Structure of 45S5 Bioglass by Means of Solid-State NMR Spectroscopy and Accurate First-Principles Simulations. *Chemistry of Materials,* 22**,** 5644-5652.

PEDONE, A., CHARPENTIER, T. & MENZIANI, M. C. 2012. The structure of fluoride-containing bioactive glasses: new insights from first-principles calculations and solid state NMR spectroscopy. *Journal of Materials Chemistry,* 22**,** 12599-12608.

PEI, J., LI, B., GAO, Y., WEI, Y., ZHOU, L., YAO, H., WANG, J. & SUN, D. 2012. Fluoride decreased osteoclastic bone resorption through the inhibition of NFATc1 gene expression. *Environ Toxicol*.

PEITL, O., DUTRA ZANOTTO, E. & HENCH, L. L. 2001. Highly bioactive P2O5–Na2O–CaO–SiO2 glass-ceramics. *Journal of Non-Crystalline Solids,* 292**,** 115-126.

PINAR ERDEM, A., SEPET, E., KULEKCI, G., TROSOLA, S. C. & GUVEN, Y. 2012. Effects of two fluoride varnishes and one fluoride/chlorhexidine varnish on Streptococcus mutans and Streptococcus sobrinus biofilm formation in vitro. *Int J Med Sci,* 9**,** 129-36.

PIWAT, S., SOPHATHA, B. & TEANPAISAN, R. 2015. An assessment of adhesion, aggregation and surface charges of Lactobacillus strains derived from the human oral cavity. *Lett Appl Microbiol,* 61**,** 98-105.

PLUMB, J. A. 2004. Cell sensitivity assays: the MTT assay. *Methods Mol Med,* 88**,** 165-9.

POLIMENI, G., XIROPAIDIS, A. V. & WIKESJO, U. M. 2006. Biology and principles of periodontal wound healing/regeneration. *Periodontol 2000,* 41**,** 30-47.

POSNER, A. S. & BEEBE, R. A. 1975. The surface chemistry of bone mineral and related calcium phosphates. *Semin Arthritis Rheum,* 4**,** 267-91.

PRADO, E., WURTZ, T., FERBUS, D., SHABANA EL, H., FOREST, N. & BERDAL, A. 2011. Sodium fluoride influences the expression of keratins in cultured keratinocytes. *Cell Biol Toxicol,* 27**,** 69-81.

PROBIOTIC. 2010. *Lactobacillus Casei* [Online]. Available: http://www.probiotic.org/lactobacillus-casei.htm [Accessed 6 Feb 2016].

PUPO, Y. M., FARAGO, P. V., NADAL, J. M., SIMAO, L. C., ESMERINO, L. A., GOMES, O. M. & GOMES, J. C. 2014. Effect of a novel quaternary ammonium methacrylate polymer (QAMP) on adhesion and antibacterial properties of dental adhesives. *Int J Mol Sci,* 15**,** 8998-9015.

PYE, A. D., LOCKHART, D. E., DAWSON, M. P., MURRAY, C. A. & SMITH, A. J. 2009. A review of dental implants and infection. *J Hosp Infect,* 72**,** 104-10.

QU, W. J., ZHONG, D. B., WU, P. F., WANG, J. F. & HAN, B. 2008. Sodium fluoride modulates caprine osteoblast proliferation and differentiation. *J Bone Miner Metab,* 26**,** 328-34.

QUIRYNEN, M., DE SOETE, M. & VAN STEENBERGHE, D. 2002. Infectious risks for oral implants: a review of the literature. *Clin Oral Implants Res,* 13**,** 1-19.

RAGO, R., MITCHEN, J. & WILDING, G. 1990. DNA fluorometric assay in 96-well tissue culture plates using Hoechst 33258 after cell lysis by freezing in distilled water. *Anal Biochem,* 191**,** 31-4.

RAHAMAN, M. N., BAL, B. S. & HUANG, W. 2014. Review: emerging developments in the use of bioactive glasses for treating infected prosthetic joints. *Mater Sci Eng C Mater Biol Appl,* 41**,** 224-31.

RAJA, M., UMMER, F. & DHIVAKAR, C. P. 2014. Aggregatibacter actinomycetemcomitans - a tooth killer? *J Clin Diagn Res,* 8**,** ZE13-6.

RANDALL, J., SEOW, W. & WALSH, L. 2014. Antibacterial activity of fluoride compounds and herbal toothpastes on Streptococcus mutans: An in vitro study. *Aust Dent J*.

RECTENWALD, J. E., MINTER, R. M., ROSENBERG, J. J., GAINES, G. C., LEE, S. & MOLDAWER, L. L. 2002. Bioglass attenuates a proinflammatory response in mouse peritoneal endotoxicosis. *Shock,* 17**,** 135-8.

REDDY, J. & GROBLER, S. R. 1988. The relationship of the periodontal status to fluoride levels of alveolar bone and tooth roots. *J Clin Periodontol,* 15**,** 217-21.

REFSNES, M., KERSTEN, H., SCHWARZE, P. E. & LAG, M. 2002. Involvement of protein kinase C in fluoride-induced apoptosis in different types of lung cells. *Ann N Y Acad Sci,* 973**,** 218-20.

REFSNES, M., SCHWARZE, P. E., HOLME, J. A. & LAG, M. 2003. Fluoride-induced apoptosis in human epithelial lung cells (A549 cells): role of different G protein-linked signal systems. *Hum Exp Toxicol,* 22**,** 111-23.

REGARD, J. B., ZHONG, Z., WILLIAMS, B. O. & YANG, Y. 2012. Wnt signaling in bone development and disease: making stronger bone with Wnts. *Cold Spring Harb Perspect Biol,* 4.

REN, G., WANG, K., CHANG, R., SU, Y., WANG, J., SU, J. & HAN, B. 2011. Simultaneous administration of fluoride and selenite regulates proliferation and apoptosis in murine osteoblast-like MC3T3-E1 cells by altering osteoprotegerin. *Biol Trace Elem Res,* 144**,** 1437-48.

RIBEIRO, D. A., ALVES DE LIMA, P. L., MARQUES, M. E. & SALVADORI, D. M. 2006. Lack of DNA damage induced by fluoride on mouse lymphoma and human fibroblast cells by single cell gel (comet) assay. *Braz Dent J,* 17**,** 91-4.

RIGGS, B. L., HODGSON, S. F., O'FALLON, W. M., CHAO, E. Y., WAHNER, H. W., MUHS, J. M., CEDEL, S. L. & MELTON, L. J., 3RD 1990. Effect of fluoride treatment on the fracture rate in postmenopausal women with osteoporosis. *N Engl J Med,* 322**,** 802-9.

RISS, T. L., MORAVEC, R. A., NILES, A. L., BENINK, H. A., WORZELLA, T. J. & MINOR, L. 2004. Cell Viability Assays. *In:* SITTAMPALAM, G. S., GAL-EDD, N., ARKIN, M., AULD, D., AUSTIN, C., BEJCEK, B., GLICKSMAN, M., INGLESE, J., LEMMON, V., LI, Z., MCGEE, J., MCMANUS, O., MINOR, L., NAPPER, A., RISS, T., TRASK, O. J. & WEIDNER, J. (eds.) *Assay Guidance Manual.* Bethesda MD.

ROMANO, C. L., LOGOLUSO, N., MEANI, E., ROMANO, D., DE VECCHI, E., VASSENA, C. & DRAGO, L. 2014. A comparative study of the use of bioactive glass S53P4 and antibiotic-loaded calcium-based bone substitutes in the treatment of chronic osteomyelitis: a retrospective comparative study. *Bone Joint J,* 96-B**,** 845-50.

ROSTAMI, A., MOZAFARI, M., GHOLIPOURMALEKABADI, M., CAICEDO, H. H., LASJERDI, Z., SAMENI, M. & SAMADIKUCHAKSARAEI, A. 2015. Optimization of fluoride-containing bioactive glasses as a novel scolicidal agent adjunct to hydatid surgery. *Acta Trop*.

ROUWKEMA, J., RIVRON, N. C. & VAN BLITTERSWIJK, C. A. 2008. Vascularization in tissue engineering. *Trends in Biotechnology,* 26**,** 434-441.

SAJJAN, P. G., NAGESH, L., SAJJANAR, M., REDDY, S. K. & VENKTESH, U. G. 2013. Comparative evaluation of chlorhexidine varnish and fluoride varnish on plaque Streptococcus mutans count--an in vivo study. *Int J Dent Hyg,* 11**,** 191-7.

SAM, G. & PILLAI, B. R. 2014. Evolution of Barrier Membranes in Periodontal Regeneration-"Are the third Generation Membranes really here?". *J Clin Diagn Res,* 8**,** ZE14-7.

SANCHEZ-TORRES, A., SANCHEZ-GARCES, M. A. & GAY-ESCODA, C. 2014. Materials and prognostic factors of bone regeneration in periapical surgery: a systematic review. *Med Oral Patol Oral Cir Bucal,* 19**,** e419-25.

SATO, M. & WEBSTER, T. J. 2004. Nanobiotechnology: implications for the future of nanotechnology in orthopedic applications. *Expert Rev Med Devices,* 1**,** 105-14.

SAYGIN, N. E., GIANNOBILE, W. V. & SOMERMAN, M. J. 2000. Molecular and cell biology of cementum. *Periodontol 2000,* 24**,** 73-98.

SCHERR, N., ROLTGEN, K., WITSCHEL, M. & PLUSCHKE, G. 2012. Screening of antifungal azole drugs and agrochemicals with an adapted alamarBlue-based assay demonstrates antibacterial activity of croconazole against Mycobacterium ulcerans. *Antimicrob Agents Chemother,* 56**,** 6410-3.

SCHIPANI, E., MAES, C., CARMELIET, G. & SEMENZA, G. L. 2009. Regulation of osteogenesis-angiogenesis coupling by HIFs and VEGF. *J Bone Miner Res,* 24**,** 1347-53.

SCHLIEPHAKE, H., RUBLACK, J., FORSTER, A., SCHWENZER, B., REICHERT, J. & SCHARNWEBER, D. 2015. Functionalization of titanium implants using a modular system for binding and release of VEGF enhances bone implant contact in a rodent model. *J Clin Periodontol*.

SCHUPBACH, P. & GLAUSER, R. 2007. The defense architecture of the human periimplant mucosa: a histological study. *J Prosthet Dent,* 97**,** S15-25.

SEEMAN, E. & DELMAS, P. D. 2006. Bone quality--the material and structural basis of bone strength and fragility. *N Engl J Med,* 354**,** 2250-61.

SEPULVEDA, P., JONES, J. R. & HENCH, L. L. 2002. In vitro dissolution of melt-derived 45S5 and sol-gel derived 58S bioactive glasses. *J Biomed Mater Res,* 61**,** 301-11.

SHAH, F. A., BRAUER, D. S., DESAI, N., HILL, R. G. & HING, K. A. 2014a. Fluoride-containing bioactive glasses and Bioglass® 45S5 form apatite in low pH cell culture medium. *Materials Letters,* 119**,** 96-99.

SHAH, F. A., BRAUER, D. S., HILL, R. G. & HING, K. A. 2015. Apatite formation of bioactive glasses is enhanced by low additions of fluoride but delayed in the presence of serum proteins. *Materials Letters,* 153**,** 143-147.

SHAH, F. A., BRAUER, D. S., WILSON, R. M., HILL, R. G. & HING, K. A. 2014b. Influence of cell culture medium composition on in vitro dissolution behavior of a fluoride-containing bioactive glass. *J Biomed Mater Res A,* 102**,** 647-54.

SHELBURNE, S. A., SAHASRABHOJANE, P., SALDANA, M., YAO, H., SU, X., HORSTMANN, N., THOMPSON, E. & FLORES, A. R. 2014. Streptococcus mitis strains causing severe clinical disease in cancer patients. *Emerg Infect Dis,* 20**,** 762-71.

SHIBUYA, N. & JUPITER, D. C. 2015. Bone graft substitute: allograft and xenograft. *Clin Podiatr Med Surg,* 32**,** 21-34.

SHIMOGISHI, M., TSUTSUMI, Y., KURODA, S., MUNAKATA, M., HANAWA, T. & KASUGAI, S. 2014. Effects of acidic sodium fluoride-treated, commercially pure titanium on periodontal pathogens and rat bone marrow cells. *Dent Mater J,* 33**,** 70-8.

SHINONAGA, Y., ARITA, K., NISHIMURA, T., CHIU, S. Y., CHIU, H. H., ABE, Y., SONOMOTO, M., HARADA, K. & NAGAOKA, N. 2015. Effects of porous-hydroxyapatite incorporated into glass-ionomer sealants. *Dent Mater J*.

SIEW, C., GRUNINGER, S. E., CHOW, L. C. & BROWN, W. E. 1992. Procedure for the study of acidic calcium phosphate precursor phases in enamel mineral formation. *Calcif Tissue Int,* 50**,** 144-8.

SILVER, I. A., MURRILLS, R. J. & ETHERINGTON, D. J. 1988. Microelectrode studies on the acid microenvironment beneath adherent macrophages and osteoclasts. *Exp Cell Res,* 175**,** 266-76.

SIMON-SORO, A., BELDA-FERRE, P., CABRERA-RUBIO, R., ALCARAZ, L. D. & MIRA, A. 2013. A tissue-dependent hypothesis of dental caries. *Caries Res,* 47**,** 591-600.

SLUTZKY, H., FEUERSTEIN, O., NAMUZ, K., SHPACK, N., LEWINSTEIN, I. & MATALON, S. 2014. The effects of in vitro fluoride mouth rinse on the antibacterial properties of orthodontic cements. *Orthod Craniofac Res,* 17**,** 150-7.

SOGAARD, C. H., MOSEKILDE, L., RICHARDS, A. & MOSEKILDE, L. 1994. Marked decrease in trabecular bone quality after five years of sodium fluoride therapy--assessed by biomechanical testing of iliac crest bone biopsies in osteoporotic patients. *Bone,* 15**,** 393-9.

SOGAARD, C. H., MOSEKILDE, L., SCHWARTZ, W., LEIDIG, G., MINNE, H. W. & ZIEGLER, R. 1995. Effects of fluoride on rat vertebral body biomechanical competence and bone mass. *Bone,* 16**,** 163-9.

SONG, S., DU, L., YU, J., AI, Q., PAN, Y., FU, Y. & WANG, Z. 2015. Does Streptococcus mitis, a neonatal oropharyngeal bacterium, influence the pathogenicity of Pseudomonas aeruginosa? *Microbes Infect,* 17**,** 710-6.

SPECTOR, J. A., MEHRARA, B. J., GREENWALD, J. A., SAADEH, P. B., STEINBRECH, D. S., BOULETREAU, P. J., SMITH, L. P. & LONGAKER, M. T. 2001. Osteoblast expression of vascular endothelial growth factor is modulated by the extracellular microenvironment. *Am J Physiol Cell Physiol,* 280**,** C72-80.

SREENIVASAN, P. K., VERED, Y., ZINI, A., MANN, J., KOLOG, H., STEINBERG, D., ZAMBON, J. J., HARASZTHY, V. I., DA SILVA, M. P. & DE VIZIO, W. 2011. A 6-month study of the effects of 0.3% triclosan/copolymer dentifrice on dental implants. *J Clin Periodontol,* 38**,** 33-42.

STAIGER, M. P., PIETAK, A. M., HUADMAI, J. & DIAS, G. 2006. Magnesium and its alloys as orthopedic biomaterials: a review. *Biomaterials,* 27**,** 1728-34.

STANFORD, C. M., JACOBSON, P. A., EANES, E. D., LEMBKE, L. A. & MIDURA, R. J. 1995. Rapidly forming apatitic mineral in an osteoblastic cell line (UMR 106-01 BSP). *J Biol Chem,* 270**,** 9420-8.

STEBBINS, J. F. & ZENG, Q. 2000. Cation ordering at fluoride sites in silicate glasses: a high-resolution 19F NMR study. *Journal of Non-Crystalline Solids,* 262**,** 1-5.

STEFFENSEN, B., DUONG, A. H., MILAM, S. B., POTEMPA, C. L., WINBORN, W. B., MAGNUSON, V. L., CHEN, D., ZARDENETA, G. & KLEBE, R. J. 1992. Immunohistological localization of cell adhesion proteins and integrins in the periodontium. *J Periodontol,* 63**,** 584-92.

STOOR, P., SODERLING, E. & SALONEN, J. I. 1998. Antibacterial effects of a bioactive glass paste on oral microorganisms. *Acta Odontol Scand,* 56**,** 161-5.

STRUZYCKA, I. 2014. The oral microbiome in dental caries. *Pol J Microbiol,* 63**,** 127-35.

SUN, N., YANG, L., LI, Y., ZHANG, H., CHEN, H., LIU, D., LI, Q. & CAI, D. 2013. Effect of advanced oxidation protein products on the proliferation and osteogenic differentiation of rat mesenchymal stem cells. *Int J Mol Med*.

TABUCHI, Y., YUNOKI, T., HOSHI, N., SUZUKI, N. & KONDO, T. 2014. Genes and gene networks involved in sodium fluoride-elicited cell death accompanying endoplasmic reticulum stress in oral epithelial cells. *Int J Mol Sci,* 15**,** 8959-78.

TAYLOR, M. L., BOYDE, A. & JONES, S. J. 1989. The effect of fluoride on the patterns of adherence of osteoclasts cultured on and resorbing dentine: a 3-D assessment of vinculin-labelled cells using confocal optical microscopy. *Anat Embryol (Berl),* 180**,** 427-35.

TAYLOR, M. L., MACONNACHIE, E., FRANK, K., BOYDE, A. & JONES, S. J. 1990. The effect of fluoride on the resorption of dentine by osteoclasts in vitro. *J Bone Miner Res,* 5 Suppl 1**,** S121-30.

TEANPAISAN, R., PIWAT, S. & DAHLEN, G. 2011. Inhibitory effect of oral Lactobacillus against oral pathogens. *Lett Appl Microbiol,* 53**,** 452-9.

THEISS, F., APELT, D., BRAND, B., KUTTER, A., ZLINSZKY, K., BOHNER, M., MATTER, S., FREI, C., AUER, J. A. & VON RECHENBERG, B. 2005. Biocompatibility and resorption of a brushite calcium phosphate cement. *Biomaterials,* 26**,** 4383-94.

TILOCCA, A. & CORMACK, A. N. 2007. Structural effects of phosphorus inclusion in bioactive silicate glasses. *J Phys Chem B,* 111**,** 14256-64.

TOWLER, M. R., STANTON, K. T., MOONEY, P., HILL, R. G., MORENO, N. & QUEROL, X. 2002. Modelling of the glass phase in fly ashes using network connectivity theory. *Journal of Chemical Technology & Biotechnology,* 77**,** 240-245.

TRAUTZ, O. R. 1955. X-ray diffraction of biological and synthetic apatites. *Ann N Y Acad Sci,* 60**,** 696-712.

TRIBBLE, G. D., KERR, J. E. & WANG, B. Y. 2013. Genetic diversity in the oral pathogen Porphyromonas gingivalis: molecular mechanisms and biological consequences. *Future Microbiol,* 8**,** 607-20.

TSENG, Y. H., MOU, C. Y. & CHAN, J. C. 2006. Solid-state NMR study of the transformation of octacalcium phosphate to hydroxyapatite: a mechanistic model for central dark line formation. *J Am Chem Soc,* 128**,** 6909-18.

TURNER, C. H., HASEGAWA, K., ZHANG, W., WILSON, M., LI, Y. & DUNIPACE, A. J. 1995. Fluoride reduces bone strength in older rats. *J Dent Res,* 74**,** 1475-81.

USUI, Y., UEMATSU, T., UCHIHASHI, T., TAKAHASHI, M., ISHIZUKA, M., DOTO, R., TANAKA, H., KOMAZAKI, Y., OSAWA, M., YAMADA, K., YAMAOKA, M. & FURUSAWA, K. 2010. Inorganic polyphosphate induces osteoblastic differentiation. *J Dent Res,* 89**,** 504-9.

VALERIO, P., PEREIRA, M. M., GOES, A. M. & LEITE, M. F. 2004. The effect of ionic products from bioactive glass dissolution on osteoblast proliferation and collagen production. *Biomaterials,* 25**,** 2941-8.

VALERIO, P., PEREIRA, M. M., GOES, A. M. & LEITE, M. F. 2009. Effects of extracellular calcium concentration on the glutamate release by bioactive glass (BG60S) preincubated osteoblasts. *Biomed Mater,* 4**,** 045011.

VALÉRIO, P., PEREIRA, M. M., GOES, A. M. & LEITE, M. F. 2007. BG60S dissolution interferes with osteoblast calcium signals. *Journal of Materials Science: Materials in Medicine,* 18**,** 265-271.

VALLET-REGI, M., J. SALINAS, A., ROMAN, J. & GIL, M. 1999. Effect of magnesium content on the in vitro bioactivity of CaO-MgO-SiO2-P2O5 sol-gel glasses. *Journal of Materials Chemistry,* 9**,** 515-518.

VAN LOVEREN, C. 2001. Antimicrobial activity of fluoride and its in vivo importance: identification of research questions. *Caries Res,* 35 Suppl 1**,** 65-70.

VAN MEERLOO, J., KASPERS, G. J. & CLOOS, J. 2011. Cell sensitivity assays: the MTT assay. *Methods Mol Biol,* 731**,** 237-45.

VAN WINKELHOFF, A. J., GOENE, R. J., BENSCHOP, C. & FOLMER, T. 2000. Early colonization of dental implants by putative periodontal pathogens in partially edentulous patients. *Clin Oral Implants Res,* 11**,** 511-20.

VARANASI, V. G., OWYOUNG, J. B., SAIZ, E., MARSHALL, S. J., MARSHALL, G. W. & LOOMER, P. M. 2011. The ionic products of bioactive glass particle dissolution enhance periodontal ligament fibroblast osteocalcin expression and enhance early mineralized tissue development. *J Biomed Mater Res A,* 98**,** 177-84.

VESTERGAARD, P., JORGENSEN, N. R., SCHWARZ, P. & MOSEKILDE, L. 2008. Effects of treatment with fluoride on bone mineral density and fracture risk--a meta-analysis. *Osteoporos Int,* 19**,** 257-68.

VIGNOLETTI, F., NUNEZ, J. & SANZ, M. 2014. Soft tissue wound healing at teeth, dental implants and the edentulous ridge when using barrier membranes, growth and differentiation factors and soft tissue substitutes. *J Clin Periodontol,* 41 Suppl 15**,** S23-35.

VILLACA, J. H., NOVAES, A. B., JR., SOUZA, S. L., TABA, M., JR., MOLINA, G. O. & CARVALHO, T. L. 2005. Bioactive glass efficacy in the periodontal healing of intrabony defects in monkeys. *Braz Dent J,* 16**,** 67-74.

VOGEL, W., KREIDL, N. & BARRETO, M. L. 2012. *Glass Chemistry*, Springer Berlin Heidelberg.

WALSH, W. R., MORBERG, P., YU, Y., YANG, J. L., HAGGARD, W., SHEATH, P. C., SVEHLA, M. & BRUCE, W. J. 2003. Response of a calcium sulfate bone graft substitute in a confined cancellous defect. *Clin Orthop Relat Res***,** 228-36.

WANG, C., LIN, K., CHANG, J. & SUN, J. 2013a. Osteogenesis and angiogenesis induced by porous beta-CaSiO(3)/PDLGA composite scaffold via activation of AMPK/ERK1/2 and PI3K/Akt pathways. *Biomaterials,* 34**,** 64-77.

WANG, C., ZHAO, Y., ZHENG, S., XUE, J., ZHOU, J., TANG, Y., JIANG, L. & LI, W. 2015. Effect of enamel morphology on nanoscale adhesion forces of streptococcal bacteria : An AFM study. *Scanning,* 37**,** 313-21.

WANG, D., CHRISTENSEN, K., CHAWLA, K., XIAO, G., KREBSBACH, P. H. & FRANCESCHI, R. T. 1999. Isolation and characterization of MC3T3-E1 preosteoblast subclones with distinct in vitro and in vivo differentiation/mineralization potential. *J Bone Miner Res,* 14**,** 893-903.

WANG, Y., SAMOEI, G. K., LALLIER, T. E. & XU, X. 2012. Synthesis and Characterization of New Antibacterial Fluoride-Releasing Monomer and Dental Composite. *ACS Macro Lett,* 2**,** 59-62.

WANG, Z., YANG, X., YANG, S., REN, G., FERRERI, M., SU, Y., CHEN, L. & HAN, B. 2011. Sodium fluoride suppress proliferation and induce apoptosis through decreased insulin-like growth factor-I expression and oxidative stress in primary cultured mouse osteoblasts. *Arch Toxicol,* 85**,** 1407-17.

WANG, Z., ZHANG, J., ZOU, H., DONG, M., QIU, D. & YANG, P. 2013b. Model and experimental investigations of aluminum oxide slurry transportation and vaporization behavior for nebulization inductively coupled plasma optical emission spectrometry. *Talanta,* 107**,** 338-43.

WATTS, S. J., HILL, R. G., O'DONNELL, M. D. & LAW, R. V. 2010. Influence of magnesia on the structure and properties of bioactive glasses. *Journal of Non-Crystalline Solids,* 356**,** 517-524.

WEIBING, Z. & WANG, L. 2014. [Correlation between vascular endothelial growth factor temporal expression and new bone formation in midpalatal suture during rapid maxillary expansion]. *Hua Xi Kou Qiang Yi Xue Za Zhi,* 32**,** 561-5.

WEITZMANN, M. N. 2013. The Role of Inflammatory Cytokines, the RANKL/OPG Axis, and the Immunoskeletal Interface in Physiological Bone Turnover and Osteoporosis. *Scientifica (Cairo),* 2013**,** 125705.

WERGEDAL, J. E., LAU, K. H. & BAYLINK, D. J. 1988. Fluoride and bovine bone extract influence cell proliferation and phosphatase activities in human bone cell cultures. *Clin Orthop Relat Res***,** 274-82.

WEST, J. K. & HENCH, L. L. 1995. Molecular Orbital Models of Silica Rings and Their Vibrational Spectra. *Journal of the American Ceramic Society,* 78**,** 1093-1096.

WHYTE, M. P. 1994. Hypophosphatasia and the role of alkaline phosphatase in skeletal mineralization. *Endocr Rev,* 15**,** 439-61.

WIEGAND, A., BUCHALLA, W. & ATTIN, T. 2007. Review on fluoride-releasing restorative materials--fluoride release and uptake characteristics, antibacterial activity and influence on caries formation. *Dent Mater,* 23**,** 343-62.

WILSON, J. & LOW, S. B. 1992. Bioactive ceramics for periodontal treatment: comparative studies in the Patus monkey. *J Appl Biomater,* 3**,** 123-9.

WILSON, J., PIGOTT, G. H., SCHOEN, F. J. & HENCH, L. L. 1981. Toxicology and biocompatibility of bioglasses. *Journal of Biomedical Materials Research,* 15**,** 805-817.

WOLFF, L. F. & MULLALLY, B. 2000. New clinical materials and techniques in guided tissue regeneration. *Int Dent J,* 50**,** 235-44.

YAN, X., FENG, C., CHEN, Q., LI, W., WANG, H., LV, L., SMITH, G. W. & WANG, J. 2009. Effects of sodium fluoride treatment in vitro on cell proliferation, apoptosis and caspase-3 and caspase-9 mRNA expression by neonatal rat osteoblasts. *Arch Toxicol,* 83**,** 451-8.

YANG, S., WANG, Z., FARQUHARSON, C., ALKASIR, R., ZAHRA, M., REN, G. & HAN, B. 2011. Sodium fluoride induces apoptosis and alters bcl-2 family protein expression in MC3T3-E1 osteoblastic cells. *Biochem Biophys Res Commun,* 410**,** 910-5.

YOSHIHARA, A., SAKUMA, S., KOBAYASHI, S. & MIYAZAKI, H. 2001. Antimicrobial effect of fluoride mouthrinse on mutans streptococci and lactobacilli in saliva. *Pediatr Dent,* 23**,** 113-7.

YOSHIKO, Y., CANDELIERE, G. A., MAEDA, N. & AUBIN, J. E. 2007. Osteoblast autonomous Pi regulation via Pit1 plays a role in bone mineralization. *Mol Cell Biol,* 27**,** 4465-74.

YOSHINARI, M., ODA, Y., KATO, T. & OKUDA, K. 2001. Influence of surface modifications to titanium on antibacterial activity in vitro. *Biomaterials,* 22**,** 2043-8.

YUAN, K., CHAN, Y. J., KUNG, K. C. & LEE, T. M. 2014. Comparison of osseointegration on various implant surfaces after bacterial contamination and cleaning: a rabbit study. *Int J Oral Maxillofac Implants,* 29**,** 32-40.

ZACHARIASEN, W. H. 1932. THE ATOMIC ARRANGEMENT IN GLASS. *Journal of the American Chemical Society,* 54**,** 3841-3851.

ZEHNDER, M., WALTIMO, T., SENER, B. & SODERLING, E. 2006. Dentin enhances the effectiveness of bioactive glass S53P4 against a strain of Enterococcus faecalis. *Oral Surg Oral Med Oral Pathol Oral Radiol Endod,* 101**,** 530-5.

ZELZER, E. & OLSEN, B. R. 2005. Multiple roles of vascular endothelial growth factor (VEGF) in skeletal development, growth, and repair. *Curr Top Dev Biol,* 65**,** 169-87.

ZHAI, W., LU, H., CHEN, L., LIN, X., HUANG, Y., DAI, K., NAOKI, K., CHEN, G. & CHANG, J. 2012. Silicate bioceramics induce angiogenesis during bone regeneration. *Acta Biomater,* 8**,** 341-9.

ZHANG, D., LEPPARANTA, O., MUNUKKA, E., YLANEN, H., VILJANEN, M. K., EEROLA, E., HUPA, M. & HUPA, L. 2010. Antibacterial effects and dissolution behavior of six bioactive glasses. *J Biomed Mater Res A,* 93**,** 475-83.

ZHANG, J. F., WU, R., FAN, Y., LIAO, S., WANG, Y., WEN, Z. T. & XU, X. 2014. Antibacterial dental composites with chlorhexidine and mesoporous silica. *J Dent Res,* 93**,** 1283-9.

ZIMMERMANN, G. & MOGHADDAM, A. 2011. Allograft bone matrix versus synthetic bone graft substitutes. *Injury,* 42, Supplement 2**,** S16-S21.

ZUCKERBRAUN, H. L., BABICH, H., MAY, R. & SINENSKY, M. C. 1998. Triclosan: cytotoxicity, mode of action, and induction of apoptosis in human gingival cells in vitro. *Eur J Oral Sci,* 106**,** 628-36.

Chapter 9 Appendix

9.1 Bone biology

Bone tissue is highly organized, dynamic and vascularized, extremely specialized and able to regenerate and remodel.

9.1.1 Bone structure

The macrostructure of bone can be thought as central marrow space and endosteum surrounded by bone matrix and periosteum (Fig. 9.1 below). There are two types of mature bone, cortical, also known as compact bone, and cancellous, referred as trabecular or spongy bone.

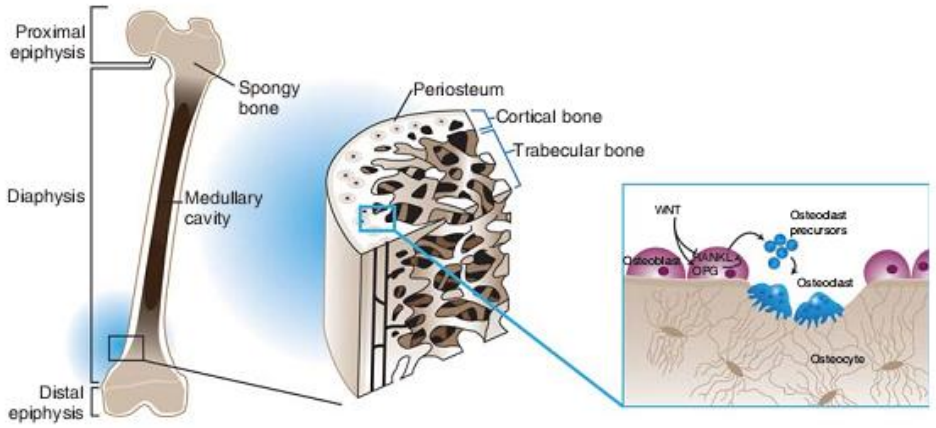

Figure 9.1 Anatomy of bone (Regard et al., 2012)

Cortical bone is dense, forms the outer layer of most bones with a porosity of 5-10% (Buck and Dumanian, 2012). As the low ratio of surface to volume, it provides protection and support for the inner regions and, gives resistance to torsion and bending and provides compressive strength.

Cancellous bone is located inside of cortical bone in long bones (in epiphysis and prox/distal diaphysis) and with a porosity up to 50-90% (Buck and Dumanian, 2012). It exhibits macro-sized pores with large surface area, which is thought to facilitate the metabolic activity of bones mediated by osteoblasts and osteoclasts (Regard et al., 2012). Cancellous bone and diaphysis shaft provides storage space for bone marrow, which contains stem cells are essential for the growth of tissues and blood cell production (Brydone et al., 2010).

Periosteum, a fibrous connective membrane, covers the external surface of bone and is tightly attached via thick collagenous fibres. It provides attachment site for ligaments, contributes to an additional vascular supply and is the main storage for osteoprogenitor cells and osteoblasts, thus being particularly vital in fracture repair.

For the bone microstructure as shown in Fig. 9.2 A, cortical bone is consisted of precisely organized osteons, known as Haversian systems. Osteons are typically microscopic cylinders running roughly parallel to the long axis of bone (Buck and Dumanian, 2012). At their centre are osteonic (Haversian) canals containing vessels and nerves. Surrounding these canals are concentric rings (lamellae) of matrix. Spaces between the lamellae are called lacunae, where mature bone cells and osteocytes are resident. Neighbouring lacunae are connected by small channels named canaliculi, which allows osteocyte connectivity (Florencio-Silva et al., 2015). Communication between osteons is maintained by canals, also known as Volkmann canals, which contain blood vessels and nerves.

As shown in Fig. 9.2 B, cancellous bone forms a honeycomb-like network of trabeculae with irregular cavities between, which contain bone marrow. Blood vessels are embedded in the bone marrow to provide nutrients to osteoblasts, osteocytes and osteoclasts resident in the trabeculae (Buck and Dumanian, 2012).

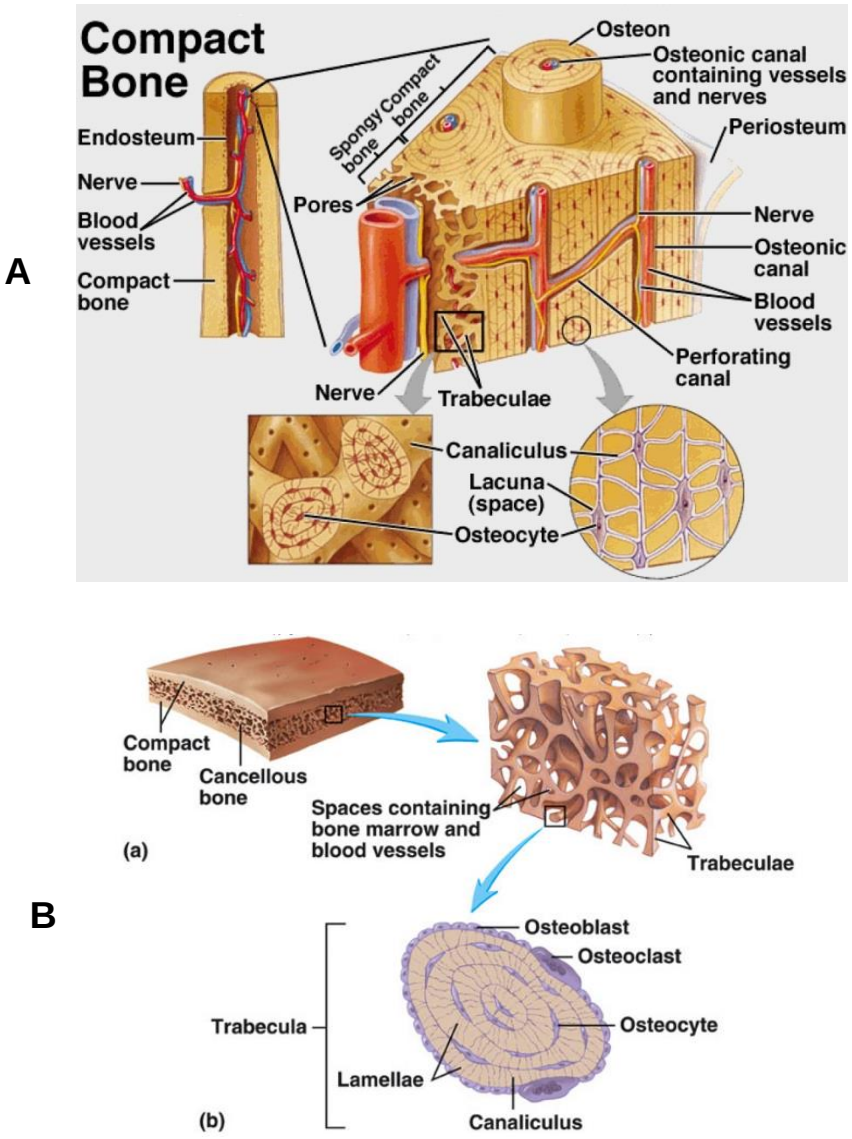

Figure 9.2 A, B Microstructure of cortical and cancellous bone

(Taken from: http://faculty.southwest.tn.edu/rburkett/A&P1_bone_tissue_lab.htm and http://www.rci.rutgers.edu/~uzwiak/AnatPhys/APFallLect8.html)

As shown in Fig. 9.3 below, collagen fibrils are the predominant components of nanoscale osteons. Inorganic bone apatite crystals are trapped within collagen fibrils in the form of plates or needles (Sato and Webster, 2004).

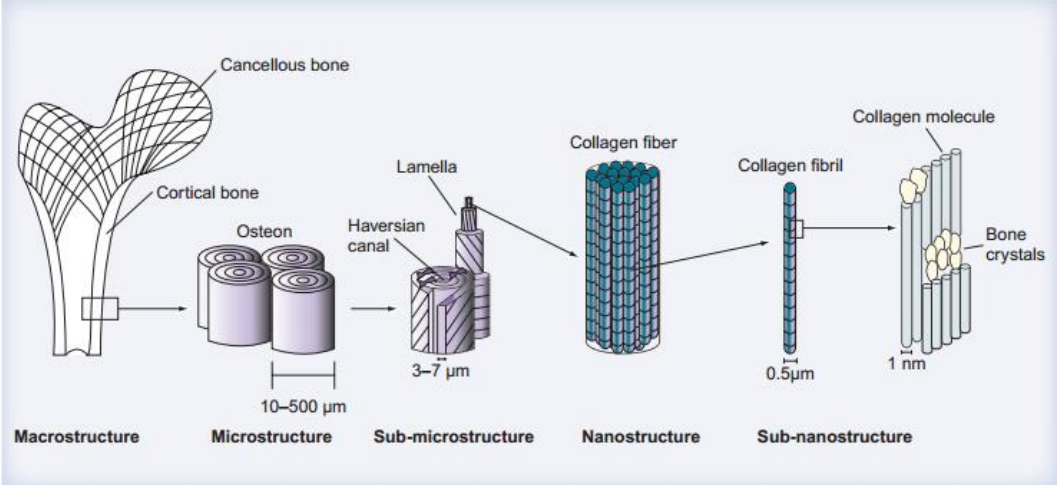

Figure 9.3 Macro- to nanostructures of bone (Sato and Webster, 2004)

9.1.2 Bone blood supply

Bone is highly vascularized with complex blood vessel networks as shown in Fig. 9.4. In tubular bones, for example, they have a dual blood supply (Buck and Dumanian, 2012). The predominant supply is the nutrient artery penetrating the diaphysis supplying the medullary cavity and providing nutrients to cells resided in the cortical bone through countless micro-canals. There are also numerous smaller metaphyseal and epiphyseal arteries that generally arise from the arteries that provide oxygen and nutrients to the cancellous bone and the adjacent joint and anastomose with the diaphyseal capillaries.

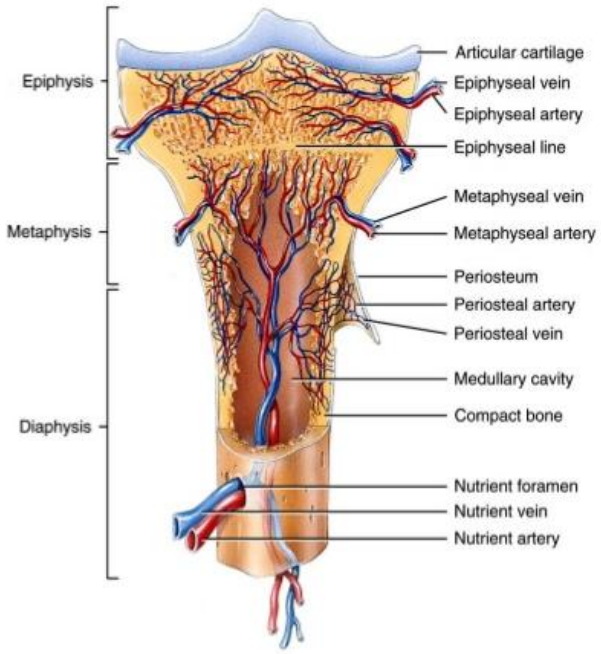

Figure 9.4 Schematic view of blood supply to a long bone

(Taken from: https://quizlet.com/20960701/bone-001-flash-cards/)

Bone with high metabolic activity relies on a branched blood vessel system with an optimal distance less than 200 µm (Rouwkema et al., 2008, Novosel et al., 2011). Therefore, the construction of new bones by graft substitutes for reparative purposes relies on angiogenesis for the vascularisation within these new grafts to supply oxygen and nutrients. Skeletal development and repair can be considered as an angiogenic–osteogenic coupling mechanism mediated by osteoblast lineage cells and endothelial cells (Maes and Clemens, 2014).

Angiogenic phenomena are governed by many interacting signalling pathways, among which the vascular endothelial growth factor (VEGF) pathway is considered as the most crucial (Nomi et al., 2002). VEGF, a heparin-binding homodimeric glycoprotein of 45 kDa, is a potent mitogen

for macro- and microvascular endothelial cells and considered as a major regulator of neovascularization under physiological and pathological conditions (Ferrara and Davis-Smyth, 1997, Ferrara, 2004). It is widely expressed in different tissues by a variety of cell types including osteoblasts, in which the VEGF expression levels are influenced in response to a variety of extracellular stimuli (Spector et al., 2001). Fig. 9.5 below represents the regulation of osteogenesis-angiogenesis coupling by VEGF. Mature osteoblasts located on the bone surface express VEGF, which is induced in response to extracellular stimuli such as hypoxia. VEGF acts through its receptors (VEGFR) on endothelial cells to induce angiogenesis and thus indirectly promote the supply of oxygen and nutrients required for osteogenesis. Increased vascularization also leads to a higher input of pre-osteoblasts and increased levels of osteogenic growth factors. In addition, it is also found that VEGF can affect osteogenesis directly as an autocrine regulator of osteoblastic differentiation and activity (Zelzer and Olsen, 2005).

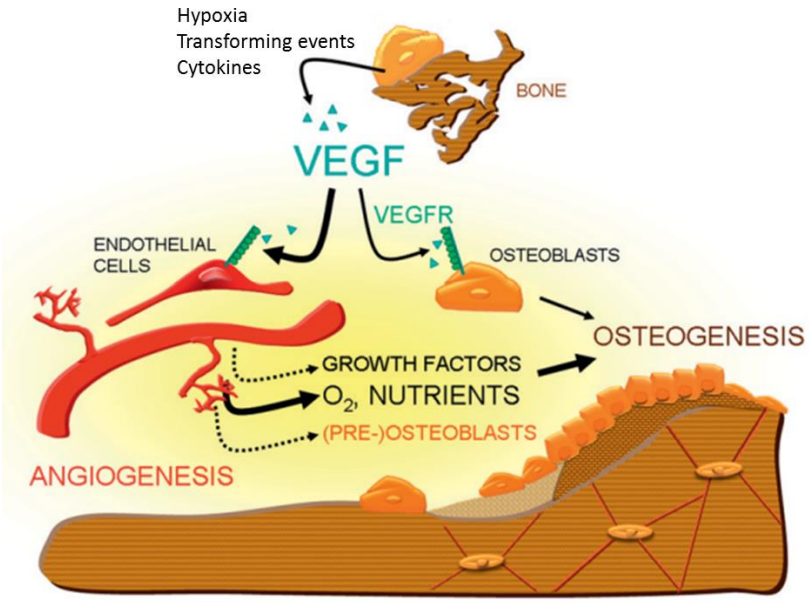

Figure 9.5 Schematic view of osteogenesis-angiogenesis coupling regulation by VEGF (Adapted from (Schipani et al., 2009, Ferrara and Davis-Smyth, 1997))

9.1.3 Bone cells

There are three distinct types of bone cells: the matrix producing osteoblasts, tissue resorbing osteoclasts and osteocytes.

Osteoblasts, responsible for the synthesis and secretion of bone matrix, are developed from pre-osteoblasts, which are generated from osteoprogenitor cells and, further from mesenchymal stem cells. Generally, osteoblasts are 10 - 20 μm in size with characteristic morphology of protein synthesizing cells, including abundant rough endoplasmic reticulum and prominent Golgi apparatus, as well as various secretory vesicles (Florencio-Silva et al., 2015). Thus, they can regulate the mineralization process, for instance, by synthesizing tightly packed collagen to provide lattices for the growth of hydroxyapatite crystals (Kirsch, 2012). Osteoblasts are rich in alkaline phosphatase (ALP), an

enzyme involved in calcification. They also secrete a number of proteins such as osteocalcin, osteopotin and bone sialoprotein linked to the mineralization and maturation of bone matrix (Florencio-Silva et al., 2015).

Osteocytes are non-proliferative, terminally differentiated cells of the osteoblast lineage and reside within the bone matrix and in newly formed osteoid (Noble, 2008). They are smaller and less active than osteoblasts. Due to their distribution throughout the bone matrix and extensive interconnectivity, osteocytes probably sense bone deformation, regulate osteoclast and osteoblast functions through mechanosensor action and thereby signalling the need for adaptive remodelling of bone size, shape, and distribution to accommodate prevailing loads (Seeman and Delmas, 2006, Bonewald and Johnson, 2008).

Osteoclasts are derived from a monocyte lineage cells, which are formed in the bone marrow and attracted to bone surfaces to fuse and form multinucleated cells (20-100 μm) to complete bone resorption (Boyce, 2013). The formation and functions of osteoclasts are centred on receptor activator of NF-κB ligand (RANKL) and macrophage-colony-stimulating factor (M-CSF), which are now considered to be the main cytokines that drive osteoclastogenesis and regulate osteoclastic bone resorption (Weitzmann, 2013, Boyce et al., 2012). RANKL, regulated by osteoprotegerin (OPG) from osteoblasts, belongs to the TNF super-family and, M-CSF is crucial for the proliferation, survival, and differentiation of osteoclast precursors, which are both produced mainly by marrow stromal cells and osteoblasts (Clarke, 2008). Besides the main function of bone resorption, osteoclasts also play other roles, such as, they can regulate

osteoblast precursors differentiation and, drive the hematopoietic stem cells move from the bone marrow to the bloodstream; they are also involved in immune responses including cytokine secretion to affect their own functions and other cells in inflammatory and neoplastic processes affecting bone (Boyce et al., 2009).

9.1.4 Bone matrix

Organic component:

The organic matrix of bone, gives tensile strength, is secreted by osteoblasts and constitutes about 10% bone volume (Posner and Beebe, 1975). It mainly consists of collagenous proteins (up to 85-90%), which are predominantly type I collagen and some type III and V collagens that may play roles in determining collagen fibril diameter at certain stages of bone formation (Clarke, 2008). The organic matrix also contains some non-collagenous proteins including proteoglycans, glycosylated proteins and other growth factors such as bone morphogenic proteins, osteocalcin, osteonectin, and bone sialoprotein, which contribute in bone mineralization, and remodelling (Buck and Dumanian, 2012). ALP, the main glycosylated protein in bone, is bound to osteoblast surfaces and also found free in mineralized matrix. It is considered to be involved in pre-osteoblast differentiation and bone mineralization (Whyte, 1994).

Inorganic component:

The inorganic bone matrix, constitutes 90% of overall bone volume and is mainly composed by inorganic material (up to 90%). It gives stiffness to resist compression and, is considered to be the main mineral store in

humans and animals. Inorganic bone matrix contains 99% of the body's calcium, 85% of the phosphorous and 40-60% of the magnesium and sodium (Buck and Dumanian, 2012). Hydroxyapatite [$Ca_{10}(PO_4)_6(OH)_2$] is the main component in inorganic matrix, with small amounts of carbonate, magnesium and acid phosphate (Clarke, 2008). Bone hydroxyapatite is very small (200Å in dimension at most), poorly crystallized (more soluble than geologic hydroxyapatite crystals), which makes it reactive and allows to participate in metabolism (Clarke, 2008).

9.1.5 Bio-mineralization

Bio-mineralization is a cell-mediated process, through which living organisms use biomolecular pathways to control deposition of inorganic chemical compounds within and outside the cells (Kirsch, 2012).

Bone matrix synthesis starts from the secretion of collagen proteins by osteoblasts, followed by matrix mineralization, which takes place in two phases: the vesicular and the fibrillary phases (Yoshiko et al., 2007). Matrix vesicles (MVs), small (20–200 nm) spherical bodies located in the pre-mineralized matrix of dentin, cartilage and bone, are considered as the initial site in bio-mineralization (Anderson, 2003). During the vesicular phase, calcium is absorbed into MVs via an annexin channel and phosphate enters through a type III Na^+ dependent phosphate transporter to form apatite inside of MVs (Golub, 2009). Acidic phospholipids and other MV constituents are thought to regulate the nucleation of these nanocrystals. The fibrillary phase occurs when these apatite crystals grow, become bigger, protrude through the MV membrane and are finally

exposed to the extracellular environment, resulting in the further growth of these hydroxyapatite crystals (Florencio-Silva et al., 2015).

9.1.6 Bone remodelling

Bone remodelling is a dynamic process involving continuous removal of discrete packets of old bone, replacement of these packets with newly synthesized matrix, and subsequent mineralization of the matrix to form new bone (Kini and Nandeesh, 2012). It is dominated by osteoclasts and osteoblasts to maintain normal physiological structure and mineral content (Das and Crockett, 2013). The bone remodelling process is composed of four sequential phases, named osteoclast activation, bone resorption, reversal phase and new bone formation, in which the remodelling sites may develop randomly but also are targeted to areas that require repair (Clarke, 2008).

Osteoclast activation involves recruitment and activation of mononuclear monocyte-macrophage osteoclast precursors from the circulation which fuse to form multi-nucleated osteoclasts. After binding to the bone matrix, these giant resorbing cells secrete hydrogen ions into the resorbing sites to lower the pH (as low as 4.5), which helps mobilize bone minerals (Silver et al., 1988). Some enzymes like tartrate-resistant acid phosphatase (TRAP) and matrix metalloproteinase 9 (MMP9) are secreted by activated osteoclasts to digest the organic matrix (Delaisse et al., 2003). Reversal phase follows the completion of bone resorption. Osteoblast precursors are recruited, proliferate and differentiate into mature osteoblasts. They synthesize new collagenous organic matrix and regulate mineralization of

matrix by releasing small, membrane-bound matrix vesicles that concentrate calcium and phosphate and enzymatically destroy mineralization inhibitors such as pyrophosphate or proteoglycans (Clarke, 2008). Then, osteoblasts change into osteocytes as they are surrounded by (and buried within) matrix, which completes the bone remodelling cycle (Dobelin et al., 2010). Fig. 9.6 represents the bone remodelling process.

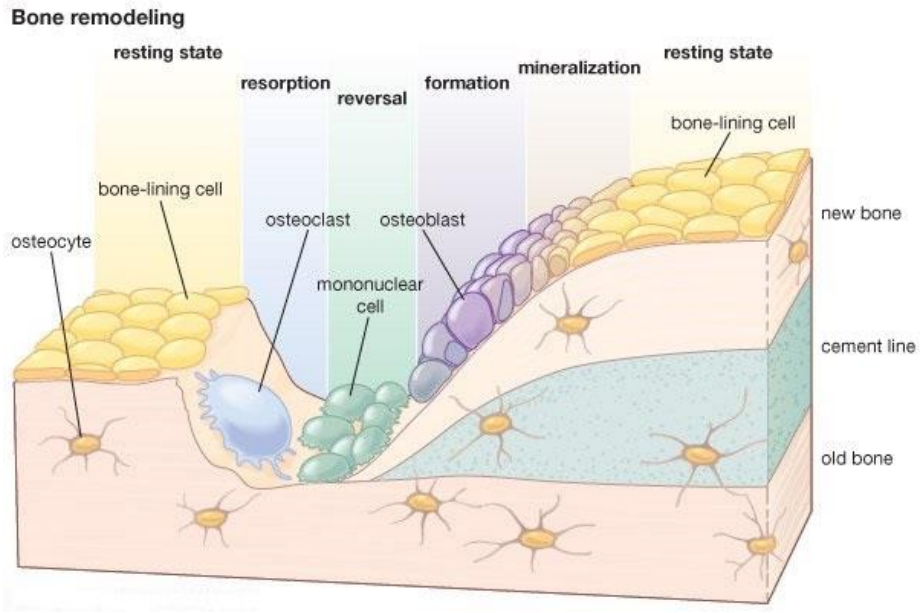

Figure 9.6 Schematic representation of bone remodelling

(Taken from: http://www.britannica.com/science/bone-remodeling)

9.2 Oral microorganism

The oral cavity is a complex and dynamic ecosystem covered with epithelium, with grooves as well as hollows in the teeth and around the gingival margin, these sites promote the development of microorganisms (Struzycka, 2014). Commonly known as 'dental plaque', oral microbial communities colonizing the oral hard and soft tissues profoundly affect oral health. In the periodontal pocket, over 400 bacteria species have been identified, demonstrating diversity and complexity (Paster et al., 2006). Extensive clinical research and animal studies have demonstrated that the oral microbial flora is responsible for two major human oral diseases: dental caries and gum disease (He and Shi, 2009). The cause of dental caries is usually the supra-gingival microbiome dominated by Gram-positive aerobic bacteria, such as *Streptococcus sanguinis*, *Streptococcus mutans*, *Streptococcus mitis*, *Streptococcus salivarius*, and *lactobacilli*, while the sub-gingival microbiome associated with gingivitis and periodontal disease is made up primarily by Gram-negative anaerobic bacteria, such as *Aggregatibacter (Actinobacillus) actinomycetemcomitans*, *Fusobacterium nucleatum* and *Porphyromonas gingivalis* (He and Shi, 2009) .

An oral microbial biofilm, also known as dental plaque, is a group of microorganisms on the surfaces between the teeth and along the gingival margins. It initiates and develops in three main steps as represented in Fig. 9.10 below: attachment and colonization of the pioneer bacterial species, co-adhesion and co-aggregation of other microorganism species, followed by the biofilm development including the metabolic

communication and competitive interactions among microorganisms, and most noticeable, the production and accumulation of deleterious bacterial metabolites such as extracellular polysaccharides to influence the host. In addition, the matured biofilm may function as a barrier against antibiotics (Struzycka, 2014, Hojo et al., 2009).

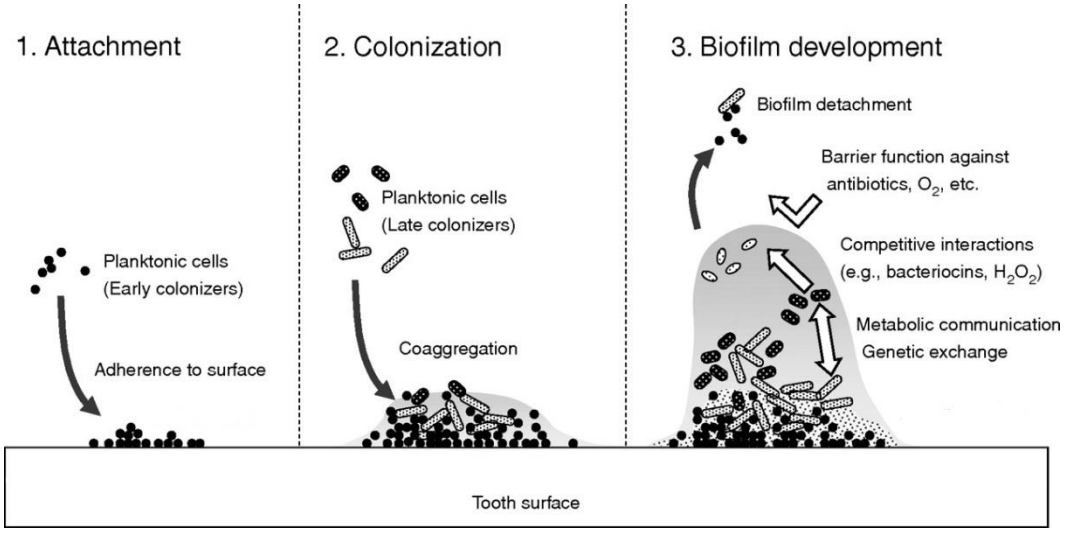

Figure 9.7 A diagrammatic representation of biofilm formation on the tooth surface (Hojo et al., 2009)

Streptococcus mitis (*S. mitis*) is a Gram-positive bacteria species that predominantly colonizes human oral teeth, tongue, cheeks and subgingival sites. More importantly, it is considered to be a representative 'pioneer colonizer' of oral cavity (Nagayama et al., 2001). During the formation and development of the bacterial biofilm, the initial attachment is critical since all other bacteria species (especially pathogenic species) rely on the initial colonizers as the base structure of the biofilm to adhere. Therefore, *S. mitis* plays an important role in the establishment of dental plaque (Wang et al., 2015, Nagayama et al., 2001). Song *et al*. observed that *S. mitis* enhanced the adhesion and biofilm formation of pathogenic

species *pseudomonas aeruginosa* (Song et al., 2015). A wide range of strategies have been used by *S. mitis* to effectively colonize the human cavity, including the expression of adhesins, immunoglobulin A proteases and toxins, and modulation of the host immune system (Mitchell, 2011). Furthermore, in vulnerable immune-compromised patients, *S. mitis* may use the same colonization and immune modulation factors as virulence factors promoting its opportunistic pathogenesis. Shelburne *et al.* reported that *S. mitis* caused a disproportionate percentage of serious infections in cancer patients (Shelburne et al., 2014). Thus, *S. mitis* is also considered as an infrequent opportunistic pathogen in healthy infants and adults implicated in a variety of diseases from dental caries, to bacterial infective endocarditis, bacteraemia, meningitis, eye infections and pneumonia. However, very little is understood about how exactly it causes these various diseases (Mitchell, 2011). Therefore, the role of traditionally viewed non-pathogenic bacteria *S. mitis* in biofilms should not be ignored.

Dental caries, a multifactorial disease that induces demineralization and destruction of the teeth, is determined by the coexistence of three main factors: microorganisms, carbohydrates derived from the dietary, and host immune system (Struzycka, 2014). When cariogenic microorganisms accumulate in dental plaque and ferment dietary carbohydrates over sufficient time, their metabolism products such as lactic, formic, acetic and propionic acids will locally decrease pH level below 5.5, resulting in demineralization and proteolytic breakdown of teeth. (Simon-Soro et al., 2013, Struzycka, 2014). Dental caries progress can also affect the tooth

pulp and spreads to the periodontal tissues and even the jaws (Featherstone, 2004).

Historically, *Lactobacilli* are the first microorganisms implicated in dental caries development although they comprise only a small percentage (<1%) of the human normal oral microbial flora. A strong correlation has been established between saliva *Lactobacillus* count and the presence of carious decay. In addition, *Lactobacilli* are found in root caries especially in deep dentinal caries associated with pulpitis (Badet and Thebaud, 2008, Byun et al., 2004, Michalek et al., 1981, Piwat et al., 2015). *Lactobacillus casei (L. casei),* one of the bacteria species belonging in the genus *Lactobacilli*, is a Gram-positive, rod shaped, facultative anaerobic non-spore-forming and catalase-negative bacteria (Teanpaisan et al., 2011). *L. casei* resides in the human oral cavity, intestinal tracts and reproductive systems, and also naturally found in various environments such as raw and fermented dairy products. The effects of *L. casei*, however, are disputed. Commercially, it can serve as probiotics to promote and support a beneficial balance of microorganisms living in the human gastrointestinal tract (Probiotic, 2010). In addition, Teanpaisan *et al.* reported that *L. casei* was able to inhibit the growth of both periodontitis- and caries-related pathogens (Teanpaisan et al., 2011). However, in numerous antibacterial studies, *L. casei* is considered as dental cariogenic bacteria species (Da Silva et al., 2012, Korkmaz et al., 2013, Pupo et al., 2014, Zhang et al., 2014). By using real-time PCR, Byun *et al.* demonstrated that *L. casei* was the most prevalent species of *lactobacilli* in carious dentine samples (Byun et al., 2004)

Periodontal disease has been recognized as one of the most common bacterially induced inflammatory diseases resulting in the destruction of the periodontal tissues, leading to oral alveolar bone and tooth loss (Bostanci and Belibasakis, 2012). Among the factors that contribute to periodontal disease, bacteria are essential and the major pathogens have been identified, however, host factors such as oral hygiene together with environmental factors such as smoking also play important roles to regulate the disease occurrence and severity (Page et al., 1997).

For the treatment of periodontitis induced tooth loss, dental implants have become a highly successful and routine procedure. However, early failures caused by bacterial infection and late plaque-induced peri-implantitis are still observed clinically (Norowski and Bumgardner, 2009). Peri-implantitis is a periodontitis-like process, since untreated periodontitis can result in the loss of natural teeth, while peri-implantitis may ultimately lead to the dental implants loss (Meffert, 1996, Pye et al., 2009, Quirynen et al., 2002). Substantial evidence indicates that bacterial plaque is the primary etiologic factor to stimulate the host immune responses and induce the production of pro-inflammatory cytokines, resulting in the loss of both teeth and implants. In addition, pathogens associated with periodontal disease have also been associated with dental implant and defect repair failure (van Winkelhoff et al., 2000). Furthermore, active periodontitis also has been linked to increased morbidity of certain systemic conditions including cardiovascular disease, preeclampsia, low birth weight and rheumatoid arthritis (Moreno and Contreras, 2013, Tribble et al., 2013, Atanasova and Yilmaz, 2014).

A strong correlation has been established between *Porphyromonas gingivalis (P. gingivalis)* and periodontal disease activity in adults (Duncan, 2003). As a keystone pathogen for periodontitis, this Gram-negative anaerobe species is a late colonizer in bacterial plaque, however, it can rapidly and actively invade gingival sulcus epithelial cells, and potentially the underlying soft and hard tissues. Firstly, *P. gingivalis* can survive, replicate and disseminate from cell to cell through actin cytoskeleton bridges, and affect cell-cycle pathways after intracellular invasion (Bostanci and Belibasakis, 2012). There are four main virulence factors in *P. gingivalis* including lipopolysaccharide (LPS), capsular polysaccharide (CPS), fimbriae and gingipains, which contribute to *P. gingivalis* colonization, invasion, establishment, and persistence within the host, induce pro-inflammatory cytokines evasion by destructing host immune system mechanisms and damage to protective periodontal tissues (Bostanci and Belibasakis, 2012, Moreno and Contreras, 2013, Mysak et al., 2014). Secondly, after invading the protective barrier gingival epithelial cells, *P. gingivalis* blocks the epithelial cell interleukin-8 (IL-8) response to other oral bacteria, suggesting that the host may not detect the presence of local bacterial colonization and cannot direct leukocytes to remove them (Darveau, 2009), resulting in the rapid establishment and growth of other species found in subgingival biofilms. These properties may be among the reasons that *P. gingivalis* is so frequently associated with active tissue destruction (Page et al., 1997). In addition, it is also found that the destructed tissue can release peptides and heme-containing compounds, which in turn stimulate the growth of *P. gingivalis* (Hajishengallis and

Lamont, 2014). The clinical attachment loss and ongoing periodontal inflammation generates a periodontal pocket, which is deep, protected from disturbance and, more likely to be anaerobic, and has a stable, slightly alkaline pH, providing ideal conditions for *P. gingivalis* propagation (Tribble et al., 2013). An *in vitro* study demonstrated that *P. gingivalis* inhibited the migration of oral epithelial cells and this may be involved in delayed wound healing (Laheij et al., 2013).

Localized, aggressive periodontitis occurs in a severe and rapidly progressing form and most often affects young adults aged 25-30 years old. It particularly affects first molars and incisors (Brigido et al., 2014). *Aggregatibacter actinomycetemcomitans* (*A. actinomycetemcomitans*), previously known as *Actinobacillus actinomycetemcomitans*, has been frequently associated with the initiation and progression of aggressive periodontitis from longitudinal studies of both humans and animals (Fine et al., 2010). It is found in 90% of localised aggressive periodontitis and 30-50% of severe adult periodontitis (Raja et al., 2014). *A. actinomycetemcomitans* is a Gram-negative, non-motile, facultative anaerobic coccobacillus bacterium and considered as an early colonizer of the human oral cavity. It may use buccal cells as a reservoir for initial attachment and eventual movement to non-shedding tooth surfaces (Fine et al., 2010).

A. actinomycetemcomitans produces a variety of virulence factors to modulate the host immune system, induce tissue destruction and inhibit tissue repair. Firstly, surface proteins such as adhesins and invasins, promote colonization by binding with specific receptors in the saliva, tooth,

extra cellular matrix and epithelial cells. The surface ultrastructure entities of *A. actinomycetemcomitans* including extracellular amorphous material and vesicles mediate the aggregation. In addition, the bacterium fimbriae enhances adhesion by three to four fold (Raja et al., 2014). Secondly, *A. actinomyctemcomitans* produces two important exotoxins named cytolethal distending toxin (CDT) and leukotoxin. CDT is demonstrated to cause death of the host tissues by blocking cell proliferation (Johansson, 2011). While leukotoxin activates the immune cells in the periodontal pocket and the surrounding tissues (Haubek and Johansson, 2014), it selectively causes the death of cells of hematopoietic origin, by binding to the specific target cell receptor named lymphocyte function associated receptor 1 (LFA-1), which is only expressed on leukocytes. In the monocytes and macrophages, leukotoxin activates caspase-1, a cysteine proteinase that causes a pro-inflammatory response by activating and secreting IL-1β and IL-18. This results in an imbalance of the host response and promotes the degenerative processes in the tooth-supporting tissues (Johansson, 2011). In addition, leukotoxin is demonstrated to induce a substantial pro-inflammatory effect in human endothelial cells (Haubek and Johansson, 2014). Taken together, the mechanisms by which leukotoxin kills leukocytes and promotes inflammatory responses are closely related to the pathogenic mechanisms of periodontitis. *A. actinomyctemcomitans* also can produce lipopolysaccharide (LPS) to induce the expression of membrane IL-1 in macrophages, enabling them to promote bone resorption *in vitro* (Henderson et al., 2003). In addition, *A. actinomyctemcomitans* has been

reported to produce a number of, as yet unidentified, proteins with cell cycle-inhibitory activity to cause T cell apoptosis and to inhibit osteoblast proliferation and bone collagen synthesis (Raja et al., 2014, Fives-Taylor et al., 1999).

Therefore, during the periodontal defect regeneration, therapeutic strategies targeting the elimination of plaque pioneer colonizer *S. mitis*, cariogenic microorganism *L. casei* and periodontal disease pathogens including *P. gingivalis* and *A. actinomyctemcomitans* should be considered, to maintain tissue of oral cavity and to reduce incidence of systemic conditions.